

Faculty of Biology

University of Gdańsk

Anne Norbertine Maria Andrea Ausems

Reconstructing important phases of the annual cycle of four species of storm-petrels using stable isotope analyses and ptilochronology

Thesis presented to the
Biological Sciences Discipline Board of the University of Gdańsk
in order to obtain a doctoral degree
in the field of natural sciences
in the discipline of biological sciences

Promotor/Supervisor: prof. dr hab. Dariusz Jakubas,
the Department of Vertebrate Zoology and Ecology

GDAŃSK 2021

Wydział Biologii

Uniwersytetu Gdańskiego

Anne Norbertine Maria Andrea Ausems

Rekonstrukcja istotnych faz cyklu życiowego czterech gatunków oceanników i nawalników przy wykorzystaniu analizy stabilnych izotopów oraz ptilochronologii

Praca przedstawiona
Radzie Dyscypliny Nauki biologiczne Uniwersytetu Gdańskiego
celem uzyskania stopnia doktora
w dziedzinie nauk ścisłych i przyrodniczych
w dyscyplinie nauki biologiczne

Promotor/Supervisor: prof. dr hab. Dariusz Jakubas,
Katedra Ekologii i Zoologii Kręgowców

GDAŃSK 2021

Table of Contents

Table of Contents.....	1
1. Summaries.....	2
1.1. English summary	2
1.2. Streszczenie po polsku.....	6
1.3. References.....	10
2. Authorship statements.....	12
2.1. Candidate statement.....	12
2.2. Co-authorship statements.....	14
3. Research Paper no. 1.....	18
Ausems, A.N.M.A., Wojczulanis-Jakubas, K., Jakubas, D. 2019 Differences in tail feather growth rate in storm-petrels breeding in the Northern and Southern hemisphere: a ptilochronological approach, PeerJ 7:e7807 http://doi.org/10.7717/peerj.7807	18
4. Research Paper no. 2.....	51
Ausems, A.N.M.A., Skrzypek, G., Wojczulanis-Jakubas, K., Jakubas, D. 2020 Sharing menus and kids' specials: Inter- and intraspecific differences in stable isotope niches between sympatrically breeding storm-petrels, Science of the Total Environment, 728, 138768, https://doi.org/10.1016/j.scitotenv.2020.138768	51
5. Research Paper no. 3.....	75
Ausems, A.N.M.A., Skrzypek, G., Wojczulanis-Jakubas, K., Jakubas, D. 2021 Birds of a feather moult together: differences in moulting distribution of four species of storm-petrels, PLOS ONE 16(1):e0245756. https://doi.org/10.1371/journal.pone.0245756	75
6. Other publications in the project.....	110
7. Acknowledgements.....	114

1. Summaries

1.1. English summary

Introduction

Seabirds being a part of the marine food chains¹ and transporting nutrients and contaminants between habitats², link marine, coastal and terrestrial ecosystems³. Currently, seabirds are under threat from several processes (e.g. invasive species, overfishing, climate change⁴). Environmental changes affect the productivity of all trophic levels of the food chain, including seabirds⁵, through changing the composition and phenology of small phytoplankton⁶. Changes in seabird population dynamics directly influence nutrient flows^{7,8} and may thus have unexpected ramifications for coastal ecosystems. Therefore, seabirds can be used as sentinels for marine ecosystem health and productivity^{9,10}. To be able to translate fluctuations in seabird abundance and breeding success to a proxy for marine ecosystem health, we need to understand the challenges they face throughout all stages of their life.

The annual cycle of seabirds can be divided into several important phases, which may partially overlap. In pelagic seabirds, which spend the majority of the year at open sea, the annual cycle can be separated into the breeding period, the only time they return to land, and the non-breeding period, often spanning most of the year. Aside from the energetically demanding breeding period (especially through incubation and chick provisioning^{11,12}), other important and energetically costly phases of the avian annual cycle are the moulting period (due to plumage gaps decreasing flight efficiency^{13,14}), and in several pelagic seabirds, migration away from the breeding grounds. Knowledge about the ecology of the different stages of the avian annual cycle is crucial to understand the challenges species face throughout the year, especially given the fact that the events during one stage may cause carry-over effects into subsequent stages¹⁵⁻¹⁸.

For this dissertation four species of storm-petrels breeding sympatrically were studied; two species from the family *Hydrobatidae* on the Northern hemisphere (European storm-petrel, *Hydrobates pelagicus*, ESP; Leach's storm-petrel, *Oceanodroma leucorhoa*, LSP) and two species from the family *Oceanobatidae* on the Southern hemisphere (black-bellied storm-petrel, *Fregetta tropica*, BBSP; Wilson's storm-petrel, *Oceanites oceanicus*, WSP). The studied storm-petrels are typical pelagic seabirds and thus should be highly mobile throughout the year¹⁹. Therefore, they shed a limited number of feathers at once during moult and feather growth takes them up to several weeks^{20,21}. Due to their abundance²², they serve as integral parts of marine ecosystems both as predator and prey²³. However, studying their foraging, breeding and movement ecology throughout the year remains challenging, as they mostly to breed in hard-to-reach burrows or crevices and after the hatching of the egg adults only visit the colonies at night^{24,25}. Storm-petrels, similarly to other petrel species, may convert part of their stomach contents into nutrient rich oil^{26,27}, complicating diet composition studies further. Due to the small size of storm-petrels, tracking devices have only very recently become miniaturised enough to use for fine-scale movement studies^{19,28-31}. As such, alternate methods are necessary to study the ecology of the storm-petrels.

Stable isotope analyses have been used extensively to study seabird ecology³²⁻³⁴. Stable carbon isotope ratios ($\delta^{13}\text{C}$) vary little between trophic levels and can thus be used to determine foraging habitats³⁵. The trophic component of stable oxygen isotope ratios ($\delta^{18}\text{O}$) is less well known and varies depending on diet and location³⁶, but the trophic enrichment factor between seawater and feathers can be calculated from recent water samples and feather material (e.g. from regrowing feathers). In contrast, stable nitrogen isotope ratios ($\delta^{15}\text{N}$) do differ strongly and predictably between predator and prey in food webs (3 – 4 ‰)³⁷, and can thus be used to provide information on consumer trophic level³⁸. The stable isotope compositions of different tissues reflect the foraging ecology at different stages and time scales; blood stable isotopes reflect the trophic position and foraging area during the last weeks³⁹, while feathers remain inert after formation and thus reflect the foraging ecology at the time of feather synthesis⁴⁰.

Ptilochronology can be used to reconstruct energy availability during moult. This method uses feather growth bar width as a proxy for feather growth rate^{41,42}. During the formation of feathers alternating light and dark bands are formed, which correlate with periods of activity and rest (e.g. day – night rhythms⁴³; activity linked to twilight periods⁴⁴). Individuals with relatively larger growth bars are assumed to have more energy available for feather synthesis than individuals with relatively smaller growth bars^{41,45}.

Aims and hypotheses

The aim of this doctoral project was to reconstruct the foraging and movement ecology of storm-petrels at different annual phases, using stable isotope and ptilochronology methods.

Firstly, energy availability during moult between the four species of storm-petrels was compared. It has been hypothesised that, as ESP and LSP are known to partially overlap the end of the breeding period with the start of tail feather (i.e. right outer rectrix) moult^{46–49} while BBSP and WSP fully moult during the non-breeding period²⁵, the Northern species would have a lower energy availability during moult (i.e. smaller growth bars) than the Southern species.

Secondly, stable isotopic niche partitioning during breeding in the Southern species was studied, and the effect of parents foraging at different trophic levels on chick growth was examined. The expectation was to find that BBSP foraged at a higher trophic level than WSP, as BBSP diets are known to contain a larger proportion of fish than WSP diets, which consist mostly of crustaceans^{24,50–52}. Additionally, chicks were expected to be fed at a higher trophic level than adults ingested themselves^{53–55}, but see ⁵⁶.

Lastly, differences in moult distribution between all four species (i.e. ESP, LSP, BBSP, WSP) were studied and correlated to variation in body morphology, feather growth rate and $\delta^{15}\text{N}$. Differences in moult distribution between the species within each hemisphere were expected (as the timing of the breeding and non-breeding periods is mirrored between the hemispheres and the non-breeding periods thus only partially overlap, species were not compared between hemispheres). Additionally, intra-specific variation in moult distribution linked to body morphology with larger individuals migrating to farther moulting grounds than smaller individuals³⁴ was expected. Moreover, differences in moult distribution were expected to affect feather growth rate and $\delta^{15}\text{N}$ as moulting areas may differ in food availability.

Methods

The field work for this project was carried out in two locations, during two consecutive breeding seasons. During the austral summer of 2017 and 2018 (January – April) BBSP and WSP adults were captured using mist-nets set up at night, and by taking incubating adults from nests in breeding colonies around the Henryk Arctowski Polish Polar Station on King George Island, South Shetland Islands, Antarctica (62°09'S, 58°27'W). Each captured individual was weighed to the nearest 0.1 g, its tarsus length was measured to the nearest 0.1 mm and its wing length to the nearest 1 mm. Tissue samples (feather and blood) were taken for stable isotope and ptilochronological analyses from each individual. Additionally, chick growth rate (i.e. body weight, tarsus length and wing length) of both species was measured every three days, weather permitting, and feather samples for stable isotope analyses were collected. In August of 2018 and 2019 adult ESP and LSP were captured at night using mist-nets set up in a mixed breeding colony on Mykines, Faroe Islands (62°05'N, 07°39'W). Each individual was weighed, and measured (tarsus length and wing length), and tissue samples for stable isotope and ptilochronological analyses were collected.

Stable isotopes ($\delta^{15}\text{N}$, $\delta^{13}\text{C}$ and $\delta^{18}\text{O}$) compositions of the feather and blood samples were analysed using a mass spectrometer. Feather length was measured from the tip to the base of the calamus with callipers to the nearest 0.1 mm. Growth bar width was measured to the nearest 0.1 mm, following Grubb 1989⁴¹. Mean growth bar width per feather was treated as a proxy for feather growth rate.

All statistical analyses were performed in R⁵⁷. Statistical methods differed per tested hypothesis and are fully detailed in particular papers.

Results and discussion

Paper no. 1 – Feather growth rate differences: Distinct differences in feather growth rate between species in both hemispheres were found. Part of these differences could be related to size differences, as larger species generally have higher feather growth rates. The expected feather growth rate for each storm-petrel species was estimated based on the feather growth rates of a large set of species from different avian families, reported in literature. Feather growth rate does not linearly increase with body feather length, such that larger species have relatively lower feather growth rates compared to feather length. The expected feather growth rates differed significantly from the observed feather growth rates in both hemispheres, but in opposite directions. Both Northern species had significantly lower observed feather growth rates than expected, while both Southern species had significantly higher feather growth rates than expected. This implies that the Northern species had less energy available for feather synthesis than the Southern species. It suggests that these differences are caused by the partial overlap of breeding and moult in the Northern species, forcing them to allocate their energy between both processes, while moulting Southern species are free from the costs of breeding and can allocate more energy to moulting.

Paper no. 2 – Niche partitioning during the breeding period: Analyses showed that chicks of both WSP and BBSP were fed at a higher trophic level than the adults ingested themselves, likely to compensate for the higher nutritional demands of the growing chick. However, while BBSP chicks were provisioned at a higher trophic level than the other studied groups, the isotopic niches of the adults of both species and the WSP chicks showed considerable overlap. Additionally, pre-laying females (as indicated by chick down isotope compositions) had wider stable isotope niches than chick and adults during the chick-rearing period. Pre-laying females are free roaming while chick-rearing adults are central-place foragers forced to return to the nest for chick-provisioning. In both species, chick growth rate was negatively correlated with $\delta^{15}\text{N}$ values, indicating nutritional stress. Nutritional stress may cause the use of endogenous instead of dietary amino acids in protein synthesis, thus inflating $\delta^{15}\text{N}$ values. The higher trophic level of the larger BBSP chicks may be due to a higher nutritional demand caused by a longer stay in the nest and relatively larger body mass gain, despite chick growth rates being similar to the smaller WSP chicks. The sympatric breeding of BBSP and WSP should lead to niche partitioning to avoid competition over resources. The apparent overlap in foraging niches as implied by the overlapping isotopic niches, may be caused by sharing main prey species and the relative simplicity of the Antarctic food chain. Only few species (e.g. krill and myctophid fish)⁵⁸⁻⁶⁰ take key positions in the diet compositions of many predators, thus reducing the detectability of foraging niche partitioning through stable isotope analyses.

Paper no. 3 – Moulting distribution: Moulting distribution as implied by different $\delta^{13}\text{C}$ and $\delta^{18}\text{O}$ compositions differed between species in both the Northern and Southern hemisphere. In three out of the four studied species (i.e. ESP, LSP and WSP), individuals could be separated into groups with different moulting distributions based on several variables. In all three mentioned species $\delta^{13}\text{C}$ and $\delta^{18}\text{O}$ compositions differed between years, implying either inter-annual differences in moulting grounds locations or inter-annual differences in the $\delta^{13}\text{C}$ and $\delta^{18}\text{O}$ compositions at the moulting grounds. Additionally, ESP and WSP could be further separated based on morphological variation, implying either an effect of morphology on migration strategy (e.g. distance to the breeding ground) or foraging behaviour (e.g. foraging in different oceanic zones). Furthermore, WSP showed $\delta^{15}\text{N}$ differences between moulting groups, caused either by differences in moulting area affecting $\delta^{15}\text{N}$ composition at the base of the food chain, or by differences in diet and thus trophic level. By implementing a geographical distribution prediction model based on oceanic $\delta^{13}\text{C}$ and $\delta^{18}\text{O}$ isoscapes, combined with chlorophyll-*a* concentrations (a proxy for primary production) and observations of birds at sea, potential moulting areas of the studied species were predicted. The Northern species were predicted to moult in temperate and tropical Atlantic zones, while BBSP was predicted to moult on

the Southern hemisphere north of the Subtropical Front, and WSP showed more variation in moulting distribution including groups predicted to moult south of the Subtropical front and as far north as the Arctic and northern Pacific.

Conclusions

The results of my PhD dissertation show that (1) indirect techniques such as stable isotope analyses and ptilochronology may provide valuable insights into the different stages of the avian annual cycle of elusive seabirds that are otherwise hard to study; (2) that distinct differences in moulting strategies and distribution exist between storm-petrels breeding on both hemispheres; and (3) that distinct differences exist between sympatrically breeding species in foraging, chick provisioning and moulting strategies. Different moult-breeding schedules may affect energy allocation into feather synthesis, and variation in moulting distribution may be affected by different aspects within each species.

Additionally, the amount of variation in moulting distribution may differ between species. Lastly, the results of this dissertation show that, in contrast to expectations that sympatrically breeding species should show niche partitioning to avoid interspecific competition, the high productivity of the Antarctic marine ecosystem may facilitate foraging niche overlap of sympatrically living species. This study forms the basis for further research into the foraging and movement ecology of storm-petrels at more fine-scale analyses, made possible by ongoing technical advances in animal tracking and stable isotope methods. Furthermore, the results can be used to properly delineate key conservation areas, to decide where to direct protection efforts, and to form conservation planning in the vast ocean.

1.2. Streszczenie po polsku

Wstęp

Ptaki morskie, stanowiące istotną część morskich sieci troficznych¹ oraz transportujące biogeny i zanieczyszczania pomiędzy siedliskami², łączą ekosystemy morza, wybrzeża i lądu³. Obecnie, populacje ptaków morskich są zagrożone przez szereg czynników (m.in., przełowienie zasobów w morzach, zmiany klimatu, pojawienie się gatunków inwazyjnych⁴). Zmiany w środowisku wywierają wpływ na produktywność na wszystkich poziomach troficznych łańcucha pokarmowego, z ptakami morskimi włącznie⁵, poprzez zmiany w składzie i fenologii fitoplanktonu⁶. Zmiany w dynamice liczebności populacji ptaków morskich wywierające bezpośredni wpływ na przepływ biogenów^{7,8}, mogą mieć nieoczekiwane konsekwencje dla ekosystemów wybrzeżowych. Z tego powodu ptaki morskie mogą być wykorzystywane jako wskaźniki kondycji i produktywności ekosystemu morskiego^{9,10}. Dla przełożenia fluktuacji liczebności oraz sukcesu reprodukcyjnego ptaków morskich na wskaźniki stanu ekosystemu morskiego, potrzeba jednak zrozumieć jakim wyzwaniom ptaki morskie muszą sprostać na wszystkich etapach swojego życia.

Roczny cykl życiowy ptaków można podzielić na kilka ważnych etapów, które częściowo zachodzą na siebie. U pelagicznych ptaków morskich cykl roczny można podzielić na dwie części: sezon lęgowy (jedyny okres kiedy ptaki powracają na ląd), oraz sezon pozalęgowy, najczęściej wypełniający większość cyklu rocznego. Oprócz energetycznie wymagającego sezonu lęgowego (szczególnie na etapach inkubacji i opieki nad pisklętami^{11,12}), kolejną ważną i kosztowną fazą cyklu rocznego ptaków jest okres pierzenia (obniżającą sprawność lotu z powodu ubytków w upierzeniu^{13,14}), a u niektórych ptaków morskich również migracja. Wiedza na temat ekologii ptaków w czasie kolejnych etapów rocznego cyklu życiowego jest kluczowa dla zrozumienia wyzwań, jakim muszą sprostać w czasie roku, szczególnie zważywszy na fakt, że efekty zdarzeń podczas jednego etapu mogą przenosić się (ang. *carry-over effect*) na kolejne etapy¹⁵⁻¹⁸.

W niniejszej rozprawie badano cztery gatunki ptaków rurkonosych gniazdujących sympatrycznie – dwa gatunki na półkuli północnej z rodziny *Hydrobatidae* (nawałnik burzowy, *Hydrobates pelagicus*, NBU oraz nawałnik duży, inaczej nawałnik Leacha, *Oceanodroma leucorhoa*, NLE) oraz dwa gatunki z półkuli południowej z rodziny *Oceanitidae* (oceannik czarnobrzuchy, *Fregetta tropica*, OCB; oraz oceannik żółtopłetwy, *Oceanites oceanicus*, OZP). Badane gatunki jako typowe pelagiczne ptaki morskie powinny być wysoce mobilne w ciągu całego roku¹⁹. W związku z tym podczas pierzenia zrzucają jednorazowo ograniczoną liczbę piór, a ich wzrost zajmuje do kilku tygodni^{20,21}. Ze względu na ich wysoką liczebność²², badane gatunki stanowią integralną część ekosystemów morskich zarówno jako drapieżniki jak i ofiary²³. Badania ekologii żerowania, rozrodu i przemieszczania się w ciągu roku pozostaje badawczym wyzwaniem u wszystkich czterech gatunków, ponieważ najczęściej gniazdują one w trudno dostępnych norach lub szczelinach i po wykluciu piskląt ptaki dorosłe odwiedzają kolonię tylko nocą^{24,25}. Ponadto, badane gatunki, podobnie jak inne rurkonose, mogą przekształcać część zawartości żołądka w bogaty w pierwiastki biogenne olej^{26,27}, komplikując tym samym analizy składu diety. Ze względu na niewielkie rozmiary nawałników i oceanników, urządzenia pozycjonujące dopiero od niedawna stały się na tyle zminiaturyzowane aby umożliwić badania przemieszeń tych ptaków w skali lokalnej^{19,28-31}. Tak więc do zbadania ekologii tej grupy ptaków morskich konieczne jest zastosowanie alternatywnych metod.

Analiza stabilnych izotopów jest szeroko wykorzystywana w badaniach ekologicznych ptaków morskich³²⁻³⁴. Proporcje stabilnych izotopów węgla ($\delta^{13}\text{C}$) wahają się nieznacznie pomiędzy poziomami troficznymi dzięki czemu mogą być użyte do rekonstrukcji siedlisk żerowiskowych³⁵. Implikacje troficzne zmienności proporcji stabilnych izotopów tlenu ($\delta^{18}\text{O}$) są mniej poznane, ale wiadomo, że zależą od diety i lokalizacji geograficznej³⁶, a stopień wzbogacenia troficznego (ang. *trophic enrichment factor*) pomiędzy wodą morską i piórami może być obliczony bazując na różnicach pomiędzy próbkami wody oraz piór (np. świeżo odrośniętych po usunięciu). W odróżnieniu od dwóch wspomnianych izotopów, wartości stabilnych izotopów azotu ($\delta^{15}\text{N}$) różnią się znacząco i przewidywalnie pomiędzy drapieżcami i ofiarami (o 3 – 4 ‰)³⁷, i w związku z tym mogą być użyte

do uzyskania informacji na temat poziomu troficznego konsumuentów³⁸. Skład izotopów stabilnych w różnych tkankach odzwierciedla ekologię żerowania na różnych etapach życia i skalach czasowych; stabilne izotopy we krwi odzwierciedlają poziomy troficzne oraz obszary żerowiskowe eksplorowane w ciągu ostatnich kilku tygodni³⁹, podczas gdy pióra odzwierciedlają ekologię żerowania tylko w okresie wzrostu pióra⁴⁰.

Ptilochronologia może być użyta do rekonstrukcji dostępności energii dla ptaków w czasie wzrostu piór. Metoda ta wykorzystuje prążki wzrostu piór jako wskaźnik tempa ich wzrostu^{41,42}. W czasie wzrostu piór formują się naprzemiennie jasne i ciemne prążki, których powstawanie skorelowane jest z okresami aktywności i spoczynku (np. cyklu dnia i nocy⁴³; aktywność związana z okresami ciemności i jasności⁴⁴). Zakłada się, że osobniki z relatywnie szerszymi prążkami wzrostu piór mają więcej energii dostępnej do syntezy piór w porównaniu z osobnikami z węższymi prążkami^{41,45}.

Cele i hipotezy

Celem niniejszej rozprawy była rekonstrukcja ekologii żerowania oraz przemieszczeń oceaników i nawałników w różnych fazach cyklu rocznego, z wykorzystaniem analizy stabilnych izotopów oraz ptilochronologii.

Po pierwsze, porównano dostępność energii w czasie pierzenia dla badanych gatunków nawałników i oceaników. Ponieważ wiadomo, że u NBU i NLE koniec okresu lęgowego częściowo pokrywa się z początkiem pierzenia piór ogona (tj. skrajnej sterówki)⁴⁶⁻⁴⁹ a OCB i OZP pierzą się w okresie pozalęgowym²⁵, można oczekiwać, że nawałniki będą miały mniej dostępnej energii na pierzenie (co będzie odzwierciedlone w węższych prążkach wzrostu piór) w porównaniu z oceanikami.

Po drugie, zbadano rozdział nisz izotopowych w okresie lęgowym u oceaników z półkuli południowej, oraz sprawdzono jak żerowanie na różnych poziomach troficznych wpływa na ptaki dorosłe oraz na wzrost piskląt. Ponieważ w diecie OCB stwierdzono większą proporcję ryb niż u OZP (którego dieta składa się głównie z skorupiaków)^{24,50-52}, można oczekiwać, że sygnatury izotopowe prób od OCB będą charakterystyczne dla wyższego poziomu troficznego niż u OZP. Co więcej, można oczekiwać, że pisklęta będą karmione pokarmem z wyższego poziomu troficznego niż ptaki dorosłe żerujące na własne potrzeby⁵³⁻⁵⁵, ale zobacz też⁵⁶.

Po trzecie, zbadano różnice w rozmieszczeniu pierzowisk nawałników i oceaników w powiązaniu ze zróżnicowaniem w ich morfologii, tempie wzrostu piór oraz zawartości $\delta^{15}\text{N}$. Oczekiwano znaleźć różnice w rozmieszczeniu pierzowisk w obrębie par gatunków gniazdujących na poszczególnych półkulach (jako że sezony lęgowy i pozalęgowy na obydwóch półkulach czasowo są wzajemnym lustrzanym odbiciem i w konsekwencji okresy pozalęgowe tylko częściowo zachodzą na siebie, nie porównano par gatunków między półkulami). Dodatkowo oczekiwano znaleźć zróżnicowanie wewnątrzgatunkowe w rozmieszczeniu pierzowisk powiązane z morfologią ciała z większymi osobnikami migrującymi na pierzowiska na dalsze dystanse w porównaniu z mniejszymi osobnikami³⁴. Ponadto spodziewano się, że różnice w rozmieszczeniu pierzowisk, i co za tym idzie w dostępności pokarmu, będą wpływać na tempo wzrostu piór oraz sygnatury izotopowe $\delta^{15}\text{N}$.

Metody

Prace terenowe były prowadzone w dwóch lokalizacjach w ciągu dwóch kolejnych sezonów lęgowych. W czasie antarktycznego lata w 2017 i 2018 roku (styczeń – kwiecień) chwymano dorosłe osobniki OCB i OZP w sieci ornitologiczne bądź wysiadujące w norach gniazdowych w koloniach lęgowych w pobliżu Polskiej Stacji Polarnej im. Arctowskiego na Wyspie Króla Jerzego na Szetlandach Południowych w Antarktyce (62°09'S, 58°27'W). Każdy schwyty osobnik został zważony z dokładnością do 0,1 g i zmierzony (długość skoku z dokładnością do 0.1 mm oraz długość skrzydła z dokładnością do 1 mm). Od każdego osobnika pobrano próbki tkanek (pióra i krew) na potrzeby badań stabilnych izotopów oraz ptilochronologii. Ponadto mierzono tempo wzrostu piskląt (tj. masę ciała, długość skoku oraz długość skrzydła) obydwu gatunków oceaników co około trzy dni (działania terenowe były pogodo-zależne), oraz zebrano próbki piór do analiz izotopowych. W

sierpniu 2018 i 2019 chwymano w sieci ornitologiczne dorosłe osobniki NBU i NLE, w mieszanej kolonii lęgowej na wyspie Mykines na Wyspach Owczych (62°05'N, 07°39'W). Schwymane osobniki były ważone i mierzone (długość skoku i skrzydła) oraz pobrano od nich próbki krwi oraz piór, na analizy izotopowe i ptilochronologiczne.

Skład izotopowy ($\delta^{15}\text{N}$, $\delta^{13}\text{C}$ i $\delta^{18}\text{O}$) próbek piór i krwi był analizowany przy pomocy spektrometru masowego. Długość piór była mierzona od szczytu do nasady za pomocą suwmiarki z dokładnością do 0.1 mm. Szerokość prążków wzrostu była mierzona z dokładnością do 0.1 mm (według zaleceń literaturowych⁴¹). Przyjęto średnią szerokość prążka wzrostu jako wskaźnik tempa wzrostu pióra.

Wszystkie analizy statystyczne wykonano w programie R⁵⁷. Metody statystyczne były odpowiednio dobrane dla testowanych hipotez i są dokładnie opisane w poszczególnych pracach.

Wyniki i dyskusja

Artykuł nr 1 – Różnice w tempie wzrostu piór: Analizy wykazały wyraźne różnice w tempie wzrostu piór pomiędzy gatunkami gniazdującymi na obydwu półkulach. Część tych różnic może być związana z wielkością ciała ponieważ większe gatunki charakteryzują się generalnie szybszym tempem wzrostu piór. Oceniono spodziewane tempo wzrostu piór u oceanników i nawałników bazując na danych literaturowych na ten temat, pochodzących od wielu gatunków ptaków z różnych rodzin. Nie stwierdzono liniowej zależności pomiędzy tempem wzrostu piór i długością piór; tak więc większe gatunki miały relatywnie niższe tempo wzrostu piór w odniesieniu do długości pióra. Stwierdzono, że spodziewane tempo wzrostu piór u nawałników i oceanników było różne od faktycznie obserwowanego. Nawałniki charakteryzowały się istotnie niższym od spodziewanego obserwowanym tempem wzrostu piór, podczas gdy oceanniki miały istotnie wyższe tempo od oczekiwanego. Te wyniki sugerują, że nawałniki w porównaniu z oceannikami mają mniej energii dostępnej do syntezy piór. Te różnice mogą być spowodowane częściowym zachodzeniem w czasie okresów lęgowego i pierzenia u nawałników, co zmusza je do alokacji energii pomiędzy obydwie procesy, podczas gdy pierzące się oceanniki są wolne od wydatków na rozród i mogą alokować więcej energii na pierzenie.

Artykuł nr. 2 – Rozdział nisz w czasie sezonu lęgowego: Praca wykazała, że pokarm piskląt, zarówno OZP jak i OCB, pochodził z wyższego poziomu troficznego w porównaniu z pokarmem ptaków dorosłych; wynikało to prawdopodobnie z konieczności zaspokojenia wysokich potrzeb energetycznych u rozwijających się piskląt. Jednakże podczas gdy pisklęta OCB były karmione pokarmem z wyższego poziomu troficznego niż pozostałe badane grupy ptaków, nisz izotopowe ptaków dorosłych obydwu gatunków oceanników i piskląt OZP w znacznym stopniu się pokrywały. Co więcej, wykazano, że samice w okresie przed złożeniem jaja (na podstawie sygnatur izotopowych puchu piskląt) miały szersze nisz izotopowe niż pisklęta czy ptaki dorosłe w czasie okresu opieki nad pisklętami. Samice w okresie przed złożeniem jaja swobodnie eksplorują ocean podczas gdy osobniki dorosłe w okresie opieki nad pisklętami są zmuszone do regularnego powracania do gniazda w celu nakarmienia piskląt. U obydwu gatunków oceanników, tempo wzrostu piskląt malało wraz z rosnącymi wartościami sygnatur izotopowych $\delta^{15}\text{N}$ wskazując na możliwość wystąpienia stresu żywieniowego. Ów stres może wynikać z użycia nie dieto-pochodnych lecz endogennych aminokwasów w procesie syntezy białek, wpływając na obniżenie wartości sygnatur $\delta^{15}\text{N}$. Sygnatury izotopowe piór piskląt OCB wskazujące na wyższy poziom troficzny mogą wynikać z wyższych wymagań żywieniowych w związku z dłuższym przebywaniem w gnieździe i relatywnie większymi rozmiarami ciała w porównaniu z OZP, pomimo podobnego tempa wzrostu piskląt u obydwu oceanników. Sympatryczne gniazdowanie obydwu oceanników powinno prowadzić do rozdzielenia nisz w celu uniknięcia konkurencji o zasoby. Istotne zachodzenie nisz pokarmowych, na co wskazuje zachodzenie nisz izotopowych, może wynikać ze wspólnego korzystania przez obydwie gatunki oceanników z tego samego gatunku ofiar oraz z relatywnie uproszczonej struktury sieci troficznych Antarktyki, gdzie zaledwie kilka gatunków ofiar (np. kryl oraz ryby świetlikowate)⁵⁸⁻⁶⁰ zajmuje kluczową pozycję w diecie wielu drapieżników, tym samym ograniczając wykrywalność rozdziału nisz metodą analizy stabilnych izotopów.

Artykuł nr 3 – Rozmieszczenie pierzowisk nawałników i oceanników: Praca wykazała różnice w rozmieszczeniu pierzowisk oceanników i nawałników bazując na różnicach w sygnaturach izotopowych $\delta^{13}\text{C}$ and $\delta^{18}\text{O}$. Pokazano, że u trzech spośród czterech badanych gatunków (tj. u NBU, NLE i OZP), osobniki można rozdzielić na grupy o różnym rozmieszczeniu pierzowisk bazując na szeregu zmiennych. U wszystkich wspomnianych trzech gatunków sygnatury izotopowe $\delta^{13}\text{C}$ i $\delta^{18}\text{O}$ różniły się między latami wskazując na różnice w lokalizacji pierzowisk lub w wartościach sygnatur izotopowych $\delta^{13}\text{C}$ oraz $\delta^{18}\text{O}$ na pierzowiskach. Co więcej, u NBU i OZP można było wydzielić grupy bazując na cechach morfologicznych, co wskazuje na wpływ morfologii na strategię migracyjną (tj. dystans do lęgowisk) lub na zachowania żerowiskowe (np. żerowanie w różnych strefach oceanicznych). Dodatkowo, u OZP stwierdzono różnice w sygnaturach $\delta^{15}\text{N}$ spowodowane przez różnice w lokalizacji pierzowisk wpływające na sygnatury izotopowe $\delta^{15}\text{N}$ u podstawy łańcucha pokarmowego, lub przez różnice w poziomie troficznym ofiar. Dzięki zastosowaniu modeli predykcyjnych przewidujących rozmieszczenie geograficzne bazujących na oceanicznych krajobrazach izotopowych (ang. *isoscapes*) $\delta^{13}\text{C}$ oraz $\delta^{18}\text{O}$ w połączeniu z mapami koncentracji chlorofilu *a* (wskaźnik, produkcji pierwotnej) oraz danymi o obserwacjach ptaków na morzu przewidziano rozmieszczenie potencjalnych pierzowisk badanych gatunków. Analizy wykazały, że spodziewane tereny pierzowiskowe nawałników zlokalizowane są w umiarkowanej i tropikalnej strefie Atlantyku, podczas gdy spodziewane pierzowiska OCB leżą na półkuli południowej, na północ od Frontu Subtropikalnego. OZP wykazywały większe zróżnicowanie w rozmieszczeniu pierzowisk, z grupami pierzającymi się na południe od Frontu Subtropikalnego jak i grupami pierzającymi się daleko na północy globu – aż w Arktyce i północnym Pacyfiku.

Podsumowanie

Niniejsza praca doktorska pokazała: (1) że metody pośrednie takie jak analiza stabilnych izotopów i ptilochronologia mogą dostarczyć istotnych informacji na temat różnych etapów rocznego cyklu życiowego ptaków morskich, trudnych do zbadania innymi metodami; (2) istnienie znaczących różnic w strategiach pierzenia i lokalizacji pierzowisk pomiędzy ptakami gniazdującymi na przeciwnych półkulach (3) obecność znaczących różnic w żerowaniu, karmieniu piskląt oraz strategiach pierzenia pomiędzy sympatrycznie gniazdującymi gatunkami. Wykazano, że odmienne wzorce czasowe pierzenia i rozrodu mogą wpływać na alokację energii na syntezę piór, a na zmienność w rozmieszczeniu pierzowisk mogą wpływać różne czynniki wewnątrzgatunkowe. Dodatkowo, wykazano, że zakres zmienności w rozmieszczeniu pierzających się ptaków może różnić się między gatunkami. Pokazano, że wbrew oczekiwanej konieczności rozdziału nisz pomiędzy sympatrycznie gniazdującymi gatunkami w celu uniknięcia konkurencji międzygatunkowej, wysoce produktywne ekosystemy morskie Antarktyki mogą umożliwić zachodzenie nisz sympatrycznie występujących gatunków. Niniejsza praca stanowi podstawę do dalszych badań ekologii żerowania i przemieszczeń nawałników i oceanników w mniejszej skali, możliwych dzięki aktualnemu rozwojowi metod pozycjonowania zwierząt oraz analiz stabilnych izotopów. Co więcej, wyniki pracy mogą być wykorzystane w celu odpowiedniego wyznaczenia kluczowych obszarów chronionych, podejmowania decyzji o miejscach podjęcia konkretnych zabiegów ochronnych i do efektywnego planowania ochrony rozległych obszarów morskich.

1.3. References

1. Mancini, P. L. & Bugoni, L. Resources partitioning by seabirds and their relationship with other consumers at and around a small tropical archipelago. *ICES J. Mar. Sci.* **71**, 2599–2607 (2014).
2. Blais, J. M. *et al.* Arctic seabirds transport marine-derived contaminants. *Science* **309**, 445 (2005).
3. Culhane, F. E., Frid, C. L. J., Royo Gelabert, E., White, L. & Robinson, L. A. Linking marine ecosystems with the services they supply: what are the relevant service providing units? *Ecol. Appl.* **28**, 1740–1751 (2018).
4. Dias, M. P. *et al.* Threats to seabirds: A global assessment. *Biol. Conserv.* **237**, 525–537 (2019).
5. Ballerini, T. *et al.* Productivity and linkages of the food web of the southern region of the western Antarctic Peninsula continental shelf. *Prog. Oceanogr.* **122**, 10–29 (2014).
6. Bers, A. V., Momo, F., Schloss, I. R. & Abele, D. Analysis of trends and sudden changes in long-term environmental data from King George Island (Antarctica): Relationships between global climatic oscillations and local system response. *Clim. Change* **116**, 789–803 (2013).
7. Duda, M. P. *et al.* Long-term changes in terrestrial vegetation linked to shifts in a colonial seabird population. *Ecosystems* (2020). doi:10.1007/s10021-020-00494-8
8. Michelutti, N. *et al.* Seabird-driven shifts in Arctic pond ecosystems. *Proc. R. Soc. B Biol. Sci.* **276**, 591–596 (2009).
9. Furness, R. W. & Camphuysen, C. J. Seabirds as monitors of the marine environment. *ICES J. Mar. Sci.* **54**, 726–737 (1997).
10. Cairns, D. K. Seabirds as indicators of marine food supplies. *Biol. Oceanogr.* **5**, 261–271 (1988).
11. Green, J. A. *et al.* An increase in minimum metabolic rate and not activity explains field metabolic rate changes in a breeding seabird. *J. Exp. Biol.* **216**, 1726–1735 (2013).
12. Crossin, G. T., Phillips, R. A., Lattin, C. R., Romero, L. M. & Williams, T. D. Corticosterone mediated costs of reproduction link current to future breeding. *Gen. Comp. Endocrinol.* **193**, 112–120 (2013).
13. Hedenström, A. & Sunada, S. On the aerodynamics of moult gaps in birds. *J. Exp. Biol.* **202**, 67–76 (1999).
14. Edwards, A. E. Large-scale variation in flight feather molt as a mechanism enabling biennial breeding in albatrosses. *J. Avian Biol.* **39**, 144–151 (2008).
15. Reiertsen, T. K. *et al.* Prey density in non-breeding areas affects adult survival of black-legged kittiwakes *Rissa tridactyla*. *Mar. Ecol. Prog. Ser.* **509**, 289–302 (2014).
16. Bogdanova, M. I. *et al.* Multi-colony tracking reveals spatio-temporal variation in carry-over effects between breeding success and winter movements in a pelagic seabird. *Mar. Ecol. Prog. Ser.* **578**, 167–181 (2017).
17. Pacyna, A. D. *et al.* Storm petrels as indicators of pelagic seabird exposure to chemical elements in the Antarctic marine ecosystem. *Sci. Total Environ.* **692**, 382–392 (2019).
18. Pacyna-Kuchta, A. D., Jakubas, D., Frankowski, M., Polkowska, Ż. & Wojczulanis-Jakubas, K. Exposure of a small Arctic seabird, the little auk (*Alle alle*) breeding in Svalbard, to selected elements throughout the course of a year. *Sci. Total Environ.* **732**, 139103 (2020).
19. Halpin, L. R., Pollet, I. L., Lee, C., Morgan, K. H. & Carter, H. R. Year-round movements of sympatric Fork-tailed (*Oceanodroma furcata*) and Leach’s (*O. leucorhoa*) storm-petrels. *J. F. Ornithol.* **89**, 207–220 (2018).
20. Rohwer, S., Ricklefs, R. E., Rohwer, V. G. & Copple, M. M. Allometry of the duration of flight feather molt in birds. *PLoS Biol.* **7**, e1000132 (2009).
21. Aulsems, A. N. M. A., Wojczulanis-Jakubas, K. & Jakubas, D. Differences in tail feather growth rate in storm-petrels breeding in the Northern and Southern hemisphere: a ptilochronological approach. *PeerJ* **7**, e7807 (2019).
22. BirdLife International. IUCN Red List for birds. (2020). Available at: <http://www.birdlife.org>. (Accessed: 30th September 2020)
23. Büßer, C., Hahn, S., Gladbach, A. & Lorenz, S. A decade of fundamental ecological research on storm-petrels at the Tres Hermanos colony, Potter Peninsula, King George Island. *Reports Polar Mar. Res.* **571**, 168–175 (2008).
24. Beck, J. R. & Brown, D. W. Breeding biology of the black-bellied storm-petrel. *Ibis (Lond. 1859)*. **113**, 73–90 (1971).
25. Beck, J. R. & Brown, D. W. The biology of Wilson’s storm petrel, *Oceanites oceanicus* (Kuhl), at Signy Island, South Orkney Islands. *Br. Antarct. Surv. Sci. Reports* **69**, 1–54 (1972).
26. Warham, J., Watts, R. & Dainty, R. J. The composition, energy content and function of the stomach oils of petrels (order, Procellariiformes). *J. Exp. Mar. Bio. Ecol.* **23**, 1–13 (1976).
27. Obst, B. S. & Nagy, K. A. Stomach oil and the energy budget of Wilson’s storm-petrel nestlings. *Condor* **95**, 792–805 (1993).
28. Pollet, I. L., Hedd, A., Taylor, P. D., Montevecchi, W. A. & Shutler, D. Migratory movements and wintering areas of Leach’s storm-petrels tracked using geolocators. *J. F. Ornithol.* **85**, 321–328 (2014).
29. Pollet, I. L., Ronconi, R. A., Leonard, M. L. & Shutler, D. Migration routes and stopover areas of Leach’s storm petrels *Oceanodroma leucorhoa*. *Mar. Ornithol.* **47**, 53–63 (2019).
30. Pollet, I. L. *et al.* Foraging movements of Leach’s storm-petrels *Oceanodroma leucorhoa* during incubation. *J. Avian Biol.* **45**, 001–010 (2014).
31. Bolton, M. GPS tracking reveals highly consistent use of restricted foraging areas by European Storm-petrels *Hydrobates pelagicus* breeding at the largest UK colony: implications for conservation management. *Bird Conserv. Int.* 1–18 (2020). doi:10.1017/S0959270920000374
32. Hobson, K. A., Piatt, J. F. & Pitocchelli, J. Using stable isotopes to determine seabird trophic relationships. *J. Anim. Ecol.* **63**, 786–798 (1994).
33. Newsome, S. D., Rio, Martinez del, C., Bearhop, S. & Phillips, D. L. A niche for isotope ecology. *Front. Ecol. Environ.* **5**, 429–436 (2007).

34. Phillips, R. A., Bearhop, S., McGill, R. A. R. & Dawson, D. A. Stable isotopes reveal individual variation in migration strategies and habitat preferences in a suite of seabirds during the nonbreeding period. *Oecologia* **160**, 795–806 (2009).
35. Michener, R. H. & Schell, D. M. Stable isotopes as tracers in marine aquatic food webs. in *Stable isotopes in ecology and environmental science* (eds. Lajtha, K. & Michener, R. H.) 138–157 (Blackwell Scientific Publications, 1994).
36. Magozzi, S., Vander Zanden, H. B., Wunder, M. B. & Bowen, G. J. Mechanistic model predicts tissue–environment relationships and trophic shifts in animal hydrogen and oxygen isotope ratios. *Oecologia* **191**, 777–789 (2019).
37. Minagawa, M. & Wada, E. Stepwise enrichment of ^{15}N along food chains: Further evidence and the relation between $\delta^{15}\text{N}$ and animal age. *Geochim. Cosmochim. Acta* **48**, 1135–1140 (1984).
38. Deniro, M. J. & Epstein, S. Influence of diet on the distribution of nitrogen isotopes in animals. *Geochim. Cosmochim. Acta* **45**, 341–351 (1981).
39. Bearhop, S., Waldron, S., Votier, S. C. & Furness, R. W. Factors that influence assimilation rates and fractionation of nitrogen and carbon stable isotopes in avian blood and feathers. *Physiol. Biochem. Zool.* **75**, 451–458 (2002).
40. Mizutani, H., Fukuda, M. & Kabaya, Y. ^{13}C and ^{15}N enrichment factors of feathers of 11 species of adult birds. *Ecology* **73**, 1391–1395 (1992).
41. Grubb, T. C. Ptilochronology: feather growth bars as indicators of nutritional-status. *Auk* **106**, 314–320 (1989).
42. Grubb, T. C. *Ptilochronology*. (Oxford University Press, 2006).
43. Jovani, R., Blas, J., Navarro, C. & Mougeot, F. Feather growth bands and photoperiod. *J. Avian Biol.* **42**, 1–4 (2011).
44. Langston, N. E. & Rohwer, S. Molt-breeding tradeoffs in albatrosses: life history implications for big birds. *Oikos* **76**, 498–510 (1996).
45. Hill, G. E. & Montgomerie, R. Plumage colour signals nutritional condition in the house finch. *Proc. Biol. Sci.* **258**, 47–52 (1994).
46. Ainley, D. G., Lewis, J. & Morrell, S. Molt in Leach’s and Ashy storm-petrels. *Wilson Bull.* **88**, 76–95 (1976).
47. Amengual, J. F. *et al.* The Mediterranean storm petrel *Hydrobates pelagicus melitensis* at Cabrera archipelago (Balearic Islands, Spain): Breeding moult, biometry and evaluation of the population size by mark and recapture techniques. *Ringing Migr.* **19**, 181–190 (1999).
48. Arroyo, B., Mínguez, E., Palomares, L. & Pinilla, J. The timing and pattern of moult of flight feathers of European storm-petrel *Hydrobates pelagicus* in Atlantic and Mediterranean breeding areas. *Ardeola* **51**, 365–373 (2004).
49. Bolton, M. & Thomas, R. Molt and ageing of storm petrels *Hydrobates pelagicus*. *Ringing Migr.* **20**, 193–201 (2001).
50. Hahn, S. The food and chick feeding of blackbellied stormpetrel (*Fregatta tropica*) at King George Island, South Shetlands. *Polar Biol.* **19**, 354–357 (1998).
51. Ridoux, V. The diets and dietary segregation of seabirds at the subantarctic Crozet Islands. *Mar. Ornithol.* **22**, 1–192 (1994).
52. Quillfeldt, P. Seasonal and annual variation in the diet of breeding and non-breeding Wilson’s storm-petrels on King George Island, South Shetland Islands. *Polar Biol.* **25**, 216–221 (2002).
53. Forero, M. G. *et al.* Food resource utilisation by the Magellanic penguin evaluated through stable-isotope analysis: segregation by sex and age and influence on offspring quality. *Mar. Ecol. Prog. Ser.* **234**, 289–299 (2002).
54. Hodum, P. J. & Hobson, K. A. Trophic relationships among Antarctic fulmarine petrels: Insights into dietary overlap and chick provisioning strategies inferred from stable-isotope ($\delta^{15}\text{N}$ and $\delta^{13}\text{C}$) analyses. *Mar. Ecol. Prog. Ser.* **198**, 273–281 (2000).
55. Rosciano, N. G., Polito, M. J. & Raya Rey, A. What’s for dinner mom? Selective provisioning in southern rockhopper penguins (*Eudyptes chrysocome*). *Polar Biol.* **42**, 1529–1535 (2019).
56. Booth, J. M. & McQuaid, C. D. Northern rockhopper penguins prioritise future reproduction over chick provisioning. *Mar. Ecol. Prog. Ser.* **486**, 289–304 (2013).
57. R Core Team. R: A language and environment for statistical computing. (2020).
58. Murphy, E. J. *et al.* Understanding the structure and functioning of polar pelagic ecosystems to predict the impacts of change. *Proc. R. Soc. B Biol. Sci.* **283**, 20161646 (2016).
59. Trathan, P. N. & Hill, S. The Importance of krill predation in the Southern Ocean. in *Biology and Ecology of Antarctic Krill. Advances in Polar Ecology* (ed. Siegel, V.) (Springer, Cham, 2016). doi:10.1007/978-3-319-29279-3
60. Saunders, R. A., Hill, S. L., Tarling, G. A. & Murphy, E. J. Myctophid fish (family Myctophidae) are central consumers in the food web of the Scotia Sea (Southern Ocean). *Front. Mar. Sci.* **6**, 1–22 (2019).

2. Authorship statements

2.1. Candidate statement

2.2. Co-authorship statements

3. Research Paper no. 1

Ausems, A.N.M.A., Wojczulanis-Jakubas, K, Jakubas, D. 2019 Differences in tail feather growth rate in storm-petrels breeding in the Northern and Southern hemisphere: a ptilochronological approach, PeerJ 7:e7807

<http://doi.org/10.7717/peerj.7807>

Differences in tail feather growth rate in storm-petrels breeding in the Northern and Southern hemisphere: a ptilochronological approach

Anne N.M.A. Ausems, Katarzyna Wojczulanis-Jakubas and Dariusz Jakubas

Department of Vertebrate Ecology and Zoology, Faculty of Biology, University of Gdańsk, Gdańsk, Poland

ABSTRACT

Moulting and breeding are costly stages in the avian annual cycle and may impose trade-offs in energy allocation between both stages or in their timing. Here, we compared feather growth rates (FGR) of rectrices in adults between two pairs of small pelagic Procellariiformes species differing in moult-breeding strategies: the European storm-petrel *Hydrobates pelagicus* and Leach's storm-petrel *Oceanodroma leucorhoa* breeding in the Northern Hemisphere (Faroe Islands), showing moult-breeding overlap in tail feathers; and the Wilson's storm-petrel *Oceanites oceanicus* and black-bellied storm-petrel *Fregetta tropica*, breeding in the Southern Hemisphere (South Shetlands), temporally separating moult and breeding. We used ptilochronology (i.e., feather growth bar width) to reconstruct FGR reflecting relative energy availability during moult. Based on previous research, we expected positive correlations between feather length (FL) and FGR. Additionally, we expected to find differences in FGR relative to FL between the moult-breeding strategies, where a relatively higher FGR to FL indicates a higher energy availability for moult. To investigate if energy availability during moult in the studied species is similar to species from other avian orders, we used FGR and FL found in literature ($n = 164$) and this study. We fitted a phylogenetic generalized least squares (PGLS) model to FGR with FL, group (i.e., Procellariiformes vs. non-Procellariiformes) and the interaction FL * group as predictors. As it has been suggested that Procellariiformes may form two growth bars per 24 h, we fitted the same model but with doubled FGR for Procellariiformes (PGLSadj). The group term was significant in the PGLS model, but was not in the PGLSadj model, confirming this suggestion. Individually predicted FGR by the PGLSadj model based on FL, showed that the Southern species have a significantly higher FGR relative to FL compared to the Northern species. Additionally, we found no correlation between FL and FGR in the Northern species, and a positive correlation between FL and FGR in the Southern species, suggesting differences in the trade-off between feather growth and size between species from both hemispheres. The observed differences between the Northern and Southern species may be caused by different moult-breeding strategies. The Southern species may have had more energy available for moult as they are free from breeding duties during moult, while the Northern species may have had less free energy due to a trade-off in energy allocation between breeding and moulting. Our study shows how different moult-breeding strategies may affect relative nutritional condition or energy allocation during moult of migratory pelagic seabirds.

Submitted 16 April 2019
Accepted 31 August 2019
Published 15 October 2019

Corresponding author
Anne N.M.A. Ausems,
anne.ausems@gmail.com

Academic editor
Ginger Rebstock

Additional Information and
Declarations can be found on
page 16

DOI 10.7717/peerj.7807

© Copyright
2019 Ausems et al.

Distributed under
Creative Commons CC-BY 4.0

OPEN ACCESS

Subjects Ecology, Zoology

Keywords Ptilochronology, Storm-petrels, Growth bar width, Moulting-breeding overlap, Feather growth rate

INTRODUCTION

Moulting and breeding are energetically costly stages of the annual cycle of birds. The costs of feather synthesis can be illustrated by the fact that metabolic rate during moult increases by more than 100% compared to pre-moulting (Lindström, Visser & Daan, 1993). Feather production costs are linked with body mass in a way that moult is relatively more demanding for smaller birds (Lindström, Visser & Daan, 1993). Additionally, moult gaps in the remiges and/or rectrices formed after losing old feathers reduce aerodynamic performance, mostly through affecting manoeuvrability (Hedenström & Sunada, 1999; Slagsvold & Dale, 1996) and less so through increased flight costs (Hedenström & Sunada, 1999).

The costs of breeding (e.g., incubation and chick provisioning) are apparent in the increased field metabolic rates (e.g., 11% from incubation to chick rearing in Australasian gannets, *Morus serrator*) (Green et al., 2013) and increased stress levels (e.g., higher feather corticosterone concentrations in giant petrels, *Macronectes* spp.) in successful compared to failed breeders (Crossin et al., 2013). Increased reproductive costs negatively affected the breeding success in the following year, and birds may even forego breeding if the costs are too high (Crossin et al., 2013; Minguéz, 1998; Pratte et al., 2018).

Due to the high energetic costs of moulting and breeding, trade-offs may emerge regarding energy allocation between them, e.g., as shown by decreasing chick quality when artificially increasing parental flight costs (Mauck & Grubb, 1995; Navarro & González-Solís, 2007). Indeed, in many avian species these two life-stages are temporally separated, with complete moult following the breeding period. Failed breeders and non-breeders often take advantage of the absence of breeding duties by advancing moult (Alonso et al., 2009; Barbraud & Chastel, 1998; Crossin et al., 2013; Hemborg, Sanz & Lundberg, 2001; Mumme, 2018; Ramos et al., 2018). In contrast, individuals that breed relatively late in the season (Stutchbury et al., 2011), or that have higher foraging costs during the breeding period (Alonso et al., 2009), moult later in the season. Moreover, individuals of some species may suspend moult until they arrive at the wintering areas (Catry et al., 2013; Ramos et al., 2009), providing some flexibility in allocation of energy between moulting, breeding and migration. The extent of this flexibility partially depends on environmental circumstances (e.g., day-length linked to latitude or food availability) (Hemborg, Sanz & Lundberg, 2001; Terrill, 2018), and the trade-off between moulting and breeding may even differ strongly between closely related species (e.g., in Northern, *Fulmarus glacialis*, and Southern, *F. glacialisoides*, fulmars; Barbraud & Chastel, 1998). For instance, some seabird species overlap breeding and moulting, although populations with higher foraging costs show less overlap than populations with lower costs (e.g., in Cory's shearwaters, *Calonectris diomedea borealis*; Alonso et al., 2009). Moulting-breeding overlap may therefore only be possible when energetic demands can be met, e.g., when food availability is high (Alonso et al., 2009; Barbraud & Chastel, 1998). Likewise, moulting-breeding overlap seems more

prevalent in sedentary than migratory species (*Bridge, 2006*), though several migratory species adopt this strategy as well (*Alonso et al., 2009; Barbraud & Chastel, 1998; Ramos et al., 2009*).

Investigating the trade-off in energy allocation between moulting and breeding may be challenging in pelagic seabirds as they are only available for researchers when they come to land for breeding. As at least part of the moulting period is often completed away from the breeding colony, studying their energy management during feather growth may prove difficult. Ptilochronology may offer a way to retrospectively determine the relative amount of energy available during moulting in seabirds, and so evaluate their energy allocation towards feather production. The method is based on feather growth rate, which is determined by the mean feather growth bar width (*Grubb, 1989; Grubb, 2006*). Growth bars are alternating light and dark bands formed during feather growth. It is generally assumed that one growth bar is formed over a period of 24 h (*Grubb, 2006; Jovani et al., 2011; White & Kennedy, 1992*), making it a convenient measure for feather growth rate.

Mean growth bar width is linked with nutritional status, with birds foraging in areas with higher food availability having relatively larger growth bars (*Grubb, 1989; Hill & Montgomerie, 1994*). However, within species, growth bar width has also been related to other feather traits (i.e., positively to feather size (*De la Hera, Pérez-Tris & Tellería, 2009; Hargitai et al., 2014; Le Tortorec et al., 2012; Pérez-Tris, Carbonell & Tellería, 2002*), though not in all species (*De la Hera, Pérez-Tris & Tellería, 2009; Pérez-Tris, Carbonell & Tellería, 2002*), and negatively to feather quality (*Marzal et al., 2013*). Inter-species comparisons have shown that growth bar width is positively correlated with feather length and mass. This correlation is negatively allometric, such that species with larger feathers have relatively lower growth rates per unit of feather length (*De la Hera, DeSante & Milá, 2012*). A similar correlation has been found between feather growth rate and body size, with larger species having higher absolute feather growth rates, but lower relative growth rates per unit of body size (*Rohwer et al., 2009*).

The aim of our study was to compare relative energy availability during moult between pelagic storm-petrel species with contrasting moult-breeding strategies, i.e., moult-breeding overlap or non-breeding moult. In order to understand the inter- and intra-specific differences in energy availability during moult we compared feather growth rates with feather length. Additionally, to infer the relative energy allocation for each of the species towards moulting, we compared their observed feather growth rate with feather growth rate data for other species found in literature. This study is the first to compare differences in expected feather growth rates between similar species breeding in both hemispheres. Due to their small size and pelagic life-style the non-breeding period of storm-petrels can be hard to study but thanks to recent developments in technology specific migration routes of some species are being discovered (*Pollet et al., 2014; Halpin et al., 2018; Martínez et al., 2019; Lago, Austad & Metzger, 2019*). Our study adds to the understanding of storm-petrel migratory, moulting and breeding strategies by giving some, admittedly indirect, insights into their energy management.

Since larger feathers have been linked to a higher growth rate both within (*De la Hera, Pérez-Tris & Tellería, 2009; Hargitai et al., 2014; Le Tortorec et al., 2012; Pérez-Tris, Carbonell & Tellería, 2002*) and between species (*De la Hera et al., 2011*), we expected to find positive correlations between feather length and growth bar width both within and between the four storm-petrel species. Since the studied species adopt contrasting moult-breeding strategies, we expected to find differences in feather growth rate relative to feather length between the two strategies, indicating differences in relative energy allocation towards moult.

MATERIALS AND METHODS

Studied species

We studied European storm-petrels, *Hydrobates pelagicus* (hereafter also ESP), and Leach's storm-petrels, *Oceanodroma leucorhoa* (hereafter also LSP), breeding sympatrically in the Northern Atlantic, and Wilson's storm-petrels, *Oceanites oceanicus* (hereafter also WSP), and black-bellied storm-petrels, *Fregatta tropica* (hereafter also BBSP), breeding sympatrically in the Maritime Antarctic. The European storm-petrel is the world's smallest pelagic seabird, while the Wilson's storm-petrel is the smallest endotherm breeding in the Antarctic. Black-bellied and Leach's storm-petrels are similar in body morphology, apart from tarsus length, and both are significantly larger than the European and Wilson's storm-petrels (*Carboneras et al., 2017*). All four species are migratory, and move towards and sometimes beyond the equator, during the non-breeding season. Though morphologically similar (*Flood & Thomas, 2007*), storm-petrels are divided into two families: the Northern *Hydrobatidae* and the Southern *Oceanitidae* (*Penhallurick & Wink, 2004; Rheindt & Austin, 2005; Robertson et al., 2016*).

The breeding season for all species takes several months from first arrival at the colony to fledging and takes place during summer (boreal and austral in Northern and Southern hemispheres respectively), with chicks fledging in late summer (egg laying until fledging takes on average 3,5 months for all species) (*Carboneras et al., 2017; Cramp et al., 1977; Wasilewski, 1986*). The diets of the studied storm-petrel species consist mostly of crustaceans and myctophid fish, though the Northern species eat relatively more fish than crustaceans compared to the Southern species (*Ainley, O'Connor & Boekelheide, 1984; Ainslie & Atkinson, 1936; Büfser, Kahles & Quillfeldt, 2004; Croxall & North, 1988; Croxall & Prince, 1980; D'Elbée & Hémerly, 1998; Hahn et al., 1998; Hedd & Montevecchi, 2006; Quillfeldt, 2002; Ridoux, 1994; Wasilewski, 1986*). Wilson's and black-bellied storm-petrels start moulting after the breeding period (*Beck & Brown, 1972*) while European and Leach's storm-petrels start moulting during the breeding period, exhibiting moult-breeding overlap (*Ainley, Lewis & Morrell, 1976; Amengual et al., 1999; Arroyo et al., 2004; Bolton & Thomas, 2001*).

Sample collection

We sampled European ($n = 52$) and Leach's storm-petrels ($n = 55$) in the Northern Hemisphere (hereafter Northern species) on the island of Mykines, Faroe Islands ($62^{\circ}05'N$, $07^{\circ}39'W$). During the breeding period of 2018 we captured adults in mist nets at night,

placed in a mixed colony. We studied Wilson's ($n = 228$) and black-bellied storm-petrels ($n = 32$) in the Southern Hemisphere (hereafter Southern species), on King George Island, South Shetland Islands, Antarctica ($62^{\circ}09'S$, $58^{\circ}27'W$). During the breeding periods of 2017 and 2018 we captured adults in mist nets placed in the colonies and took parents from the nests.

We collected the right outermost rectrix from adults of the four species of storm-petrels. In 2018 32 adults were recaptured that were previously caught in 2017, with fully formed rectrices. Additionally, one Wilson's storm-petrel was recaptured within 2018 with a fully regrown rectrix, though the regrown feather has not been used for the statistical analyses. We did not notice anything untoward in their tail feathers, or during the analyses (e.g., obvious outliers), which leads us to assume that our plucking of the feathers did not cause long-term harm to the birds. See below for pseudo-replication management.

All individuals of the Northern species and some individuals of the Southern species were captured in mist-nets, which could lead to uncertainty in the breeding stage of the adults. By capturing birds in a mist-net it becomes harder to determine the breeding status of the sampled adults, as sub-adults may be caught while prospecting the colony (floaters) (Sanz-Aguilar *et al.*, 2010). Especially when using tape-lures, prospecting birds may be attracted to the net (Furness & Baillie, 1981; Amengual *et al.*, 1999). However, breeding birds can be identified by their readiness to regurgitate and the presence of a brood patch (Furness & Baillie, 1981). We did not use tape-lures for the European storm-petrels, or either of the Southern species, during capturing events, decreasing the likelihood of catching floaters. We did use tape-lures for the Leach's storm-petrels, which could have increased the chances of attracting floaters. However, almost all Leach's storm-petrels were observed to readily regurgitate, and all had either fully bare brood patches, or brood patches with only few feathers present. This leads us to assume that at least the vast majority of the sampled birds were breeders.

Birds were handled under licence of the Statens Naturhistoriske Museum, Københavns Universitet C 1012 and with permission of the Polish National SCAR, Institute of Biochemistry and Biophysics (Permit for entering the Antarctic Specially Protected Area No. 3/2016 & No. 08/2017, Permit for taking or harmful interference of Antarctic fauna and flora No. 6/2017 & No. 7/2016). Permission to enter the study site on Mykines was sought through local land-owners.

Feather measurements

We measured feather length (FL) from the tip to the base of the calamus with calipers to the nearest 0.1 mm. We measured growth bar width by placing the feather on a white paper background and marking the tip and the base of the calamus, and each visible growth bar in the vane area of the feather before rounding of the tip and above the white area, with a pinprick. We then used calipers to measure the distances between each pinprick on the background to the nearest 0.1 mm, following Grubb (1989). A new piece of paper was used for each feather. We used mean growth bar width per feather as a proxy for feather growth rate (FGR).

Statistical analyses

Since we sampled the Southern species during two field seasons, we investigated the inter-annual differences in FGR and FL using a Welch t -test (*t.test*, package *stats* in R version 3.6.1 (R Core Team, 2018)). FGR was significantly higher in 2017 compared to 2018 for the Wilson's but did not differ significantly for black-bellied storm-petrels (Welch t -test; WSP: $t_{163.69} = 3.192$, $p = 0.002$; BBSP: $t_{29.343} = -0.901$, $p = 0.375$). However, although significant for the Wilson's storm-petrels, we deemed the absolute differences in FGR between the years small enough (high overlap of the 95% confidence ellipses, Fig. S1) to justify pooling the data. FL did not differ significantly between the years for either species (Welch t -test; WSP: $t_{216.29} = -0.549$, $p = 0.584$; BBSP: $t_{29.706} = -0.519$, $p = 0.608$), and therefore we also pooled these data.

Since some individuals were caught in both years ($n = 28$ for WSP, $n = 3$ for BBSP) we assessed the effect of pseudo-replication by comparing the mean values of FL and FGR between the seasons of 2017 and 2018 for the Wilson's and black-bellied storm-petrels individuals captured in both years. We found no significant differences between the means of both seasons for either species (Paired t -test; FL: WSP: $t_{27} = -0.993$, $p = 0.330$; BBSP: $t_2 = 0.096$, $p = 0.932$; FGR: WSP: $t_{27} = 1.469$, $p = 0.153$; BBSP: $t_2 = -1.023$, $p = 0.414$). Thus, in further analyses based on individuals, to avoid pseudo-replication, we used the mean values per individual instead of repeated measurements which reduced the sample size to $n = 200$ unique individuals for the Wilson's storm-petrels and to $n = 29$ unique individuals for the black-bellied storm-petrels.

To compare FL and FGR among species we used univariate tests. Due to inequality of variances (Fligner-Killeen test, *fligner.test*, package *stats*) of FL ($\chi^2 = 10.87$, $df=3$, $p = 0.012$) we used non-parametric Kruskal-Wallis and *post-hoc* Dunn tests (*dunn.test*, package *dunn.test*) for all inter-species comparisons. To examine the relationships between FL and FGR for each species, we used Spearman's rho correlation (*cor.test*, package *stats*) because we did not necessarily expect linear relationships after plotting FGR and FL data for multiple species found in literature (Fig. S2). Additionally, we chose not to transform the data to make them linear as the transformations needed differed between the species and would inhibit inter-specific comparisons.

To investigate if the observed FGR of the studied species was higher or lower than expected (i.e., what their energy availability was) we fitted a phylogenetic generalized least square (PGLS) model (*gls*, package *nlme*) with Pagel's λ (*corPagel*, package *ape*) to multi-species data. The full model contained FGR as response variable with FL, group [group 1: non-Procellariiformes ($n = 162$); group 2: Procellariiformes ($n = 6$)] and the interaction FL * group as predictor variables (PGLS model). We used ΔAIC to determine if the updated model had a better fit, and dropped terms that did not improve the model.

For the PGLS model we used FGR and FL data found in literature ($n = 164$ species, 194 observations) and from this study ($n = 4$ species) (Table S1). For species with multiple records of FGR and FL, we averaged the values per species. We searched for suitable studies in the Web of Science Database (<https://www.webofknowledge.com>; 05-11-2018) using *ptilochronology*, *growth bars* and *feather growth rate* as keywords. We then only selected papers if they contained FGR and FL measurements in SI units.

We reconstructed the phylogeny based on the most recent complete avian time-calibrated phylogeny (Jetz *et al.*, 2012) with a backbone tree developed by Ericson *et al.* (2006). To account for phylogenetic uncertainty we calculated the consensus tree, based on 100 alternative trees, downloaded from the BirdTree database (<http://www.birdtree.org>; Jetz *et al.*, 2012). We corrected for FGR and FL left-skewed data by log10 transformation of the data.

The feather types (rectrix or primary) used to determine FGR differed between studies, but FGR is highly correlated between both types (Saino *et al.*, 2012). A comparison of correlation coefficients for a PGLS model with only rectrices ($n = 129$) and a PGLS model with only primaries ($n = 44$), using Fisher's Z (*cocor.indep.groups*, package *cocor*) showed no significant difference ($z = 1.91$, $p = 0.056$) (Table S2). Feather type was thus not used as a predictor in the PGLS models.

Langston & Rohwer (1996) suggested that in the Procellariiformes the relationship between FGR and FL may differ from that of other species, i.e., they may form two growth bars per 24 h due to foraging on prey that show diel migration. To test this possibility we firstly ran the PGLS model with raw data. Then, we fitted identical PGLS models (i.e., $FGR \sim FL$, $FGR \sim FL + Group$ and $FGR \sim FL * Group$) but doubled the FGR values for the Procellariiformes (PGLSadj), and again dropped terms that did not improve the model. We could not compare the models with the raw and adjusted data directly with each other, as they have different data sets, but with this approach we could show the effect of Group on the model fit for both data sets.

We predicted FGR based on individual FL inserted into the PGLSadj model, and then calculated the residual difference with observed FGR doubled. As Fligner-Killeen tests showed variance inequality in the residuals between the species ($\chi^2 = 24.339$, $df = 3$, $p < 0.001$) and hemispheres ($\chi^2 = 26.077$, $df = 3$, $p < 0.001$) we used non-parametric Kruskal–Wallis and Dunn post-hoc tests to compare the differences between the species. To compare the residuals between the two hemispheres, and thus moult-breeding strategies, we used Welch two-sample *t*-tests as they are robust for variance differences (*t.test*, package *stats*). To determine whether the residuals were positively or negatively different from zero, and thus if energy availability was relatively high or low, we used one-sample Student's *t*-tests for each species (*t.test*, package *stats*).

RESULTS

Feather characteristics

We found significant differences between the species in FGR and FL (Kruskal–Wallis test, FGR: $\chi^2 = 214.35$, $p < 0.001$; FL: $\chi^2 = 248.35$, $p < 0.001$). Post-hoc tests (Dunn test, $p < 0.001$) revealed that black-bellied storm-petrels had a higher FGR than Wilson's storm-petrels and the Southern species had a higher FGR than the Northern species (Table 1). FL differed significantly between all species pairs (Dunn-test, $p < 0.001$) except between black-bellied and Leach's storm-petrels (Table 1). Only the Southern species showed a significant positive correlation between FGR and FL, with Wilson's storm-petrels showing a weak positive correlation (Spearman correlation, $r_s = 0.215$, $p = 0.002$) and

Table 1 Results of the *post-hoc* Dunn test for inter-specific differences in feather length (FL) and feather growth rate (FGR) for each studied species.

Species	Var	Black-bellied storm-petrel (Z, <i>p</i>)		European storm-petrel (Z, <i>p</i>)		Leach's storm-petrel (Z, <i>p</i>)	
European storm-petrel	FL	12.177,	<0.001				
	FGR	10.363,	<0.001				
Leach's storm-petrel	FL	0.698,	0.243	−13.763,	<0.001		
	FGR	9.438,	<0.001	−1.218,	0.111		
Wilson's storm-petrel	FL	7.587,	<0.001	−8.446,	<0.001	8.850,	<0.001
	FGR	3.602,	<0.001	−10.831,	<0.001	−9.528,	<0.001

Notes.

Var, variable, *p*-values $\leq \alpha/2$ ($\alpha = 0.05$) are bolded.

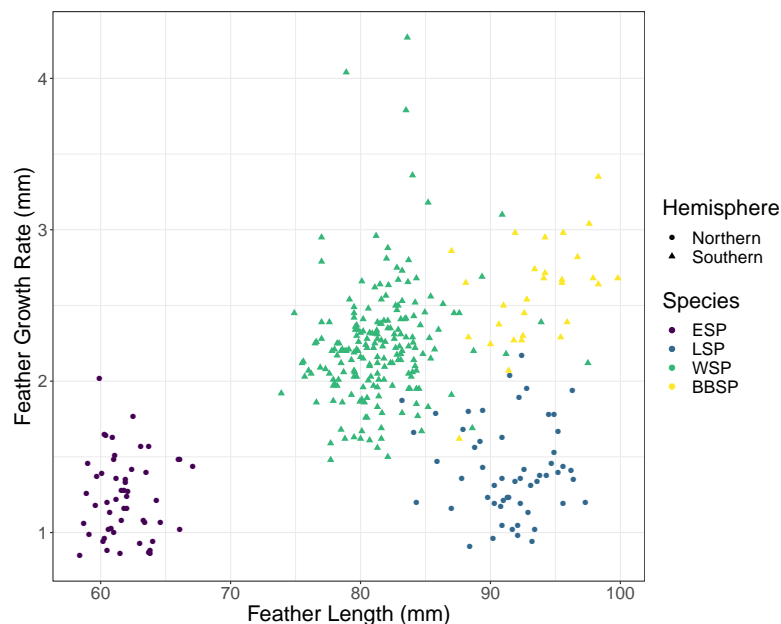


Figure 1 Correlation between feather growth rate (FGR) and feather length (FL) for all four studied storm-petrel species. European storm-petrels (ESP) are shown in purple; Leach's storm-petrels (LSP) in blue; Wilson's storm-petrels (WSP) in green; black-bellied storm-petrels (BBSP) in yellow. Species from the Northern Hemisphere are shown with dots, species from the Southern Hemisphere with triangles. See Tables 1 and 2 for statistical analyses.

Full-size DOI: 10.7717/peerj.7807/fig-1

black-bellied storm-petrels a moderately positive correlation ($r_s = 0.513$, $p = 0.04$) (Fig. 1, Table 2). For the Northern species we found no correlation between FGR and FL ($p > 0.05$) (Table 2).

Relative energy availability

In the full PGLS model ($AIC = -497.59$), FL ($p < 0.001$) and group (i.e., Procellariiformes vs. non-Procellariiformes) had a significant effect ($p < 0.001$) on FGR but the interaction FL * group did not ($p = 0.729$) (Fig. 2A, Table 3). The PGLS model with group as a predictor (hereafter optimised PGLS model) was better ($AIC = -499.47$) than the PGLS

Table 2 Spearman's Rank Correlation output for correlations between feather growth rate (FGR) and feather length (FL) for each studied species.

Species	S	rho	p-value
European storm-petrel	2,3327	0.004	0.976
Leach's storm-petrel	27,756	-0.001	0.993
Wilson's storm-petrel	1,046,299	0.215	0.002
black-bellied storm-petrel	1,977.7	0.513	0.004

Notes.

S, sum of squared rank differences; rho, Spearman's rank correlation rho.
P-values ≤ 0.05 are bolded.

model without group (AIC = -484.99, Δ AIC = 14.48) (Table 4). The model with group and interaction did not differ from the model without the interaction (AIC = -497.59, Δ AIC = 1.88). After multiplying Procellariiformes' FGR by two (i.e., PGLSadj), FL still had a significant effect on FGR ($p < 0.001$) (Fig. 2B, Table 3). Neither group ($p = 0.912$) nor the interaction FL * group was significant ($p = 0.729$) (Table 3). The PGLSadj model without the group predictor (AIC = -501.46) was not different from the PGLSadj model including group (AIC = -499.47, Δ AIC = 1.99) nor was the PGLSadj model including group different from the model including group and interaction (AIC = -497.59, Δ AIC = 1.88) (Fig. 2B, Table 4).

The individual residuals of predicted FGR based on the optimized PGLS model differed significantly between the studied storm-petrel species (Kruskal-Wallis; $\chi^2 = 198.92$, $df = 3$, $p < 0.001$) (Table 5) and hemispheres (Welch t -test, $p < 0.001$) (Fig. 3). The residuals for the Southern species were significantly higher than those of the Northern species (mean Southern = 0.126, mean Northern = -0.091, $t_{158,56} = -21.371$). The residuals differed significantly from zero for all four species. Both Northern species had negative residuals, while both Southern species had positive residuals (Student's t -test, ESP: $t_{51} = -5.847$, $p < 0.001$; LSP: $t_{54} = -8.367$, $p < 0.001$; WSP: $t_{199} = 25.310$, $p < 0.001$; BBSP $t_{28} = 14.460$, $p < 0.001$) (Fig. 3, Table 6).

DISCUSSION

The Spearman's rho correlations showed significant, positive relationships between mean growth bar width and feather length for the Southern storm-petrel species, but not for the Northern species. Additionally, using the PGLS model, we found that the Southern species had a higher feather growth rate than predicted while the Northern species had a lower feather growth rate than predicted.

The difference in residual length between the studied species, and between the hemispheres may be associated with a difference in relative energy availability during moulting between species of both hemispheres, possibly caused by their different moult-breeding strategy. The Southern species, both moulting during the non-breeding period (Beck & Brown, 1972), are free from breeding duties during moult and may use all available energy for feather synthesis, while the Northern species, showing moult-breeding overlap (Amengual et al., 1999; Arroyo et al., 2004; Bolton & Thomas, 2001), have to allocate that energy between moulting and breeding. The differences between storm-petrels from both

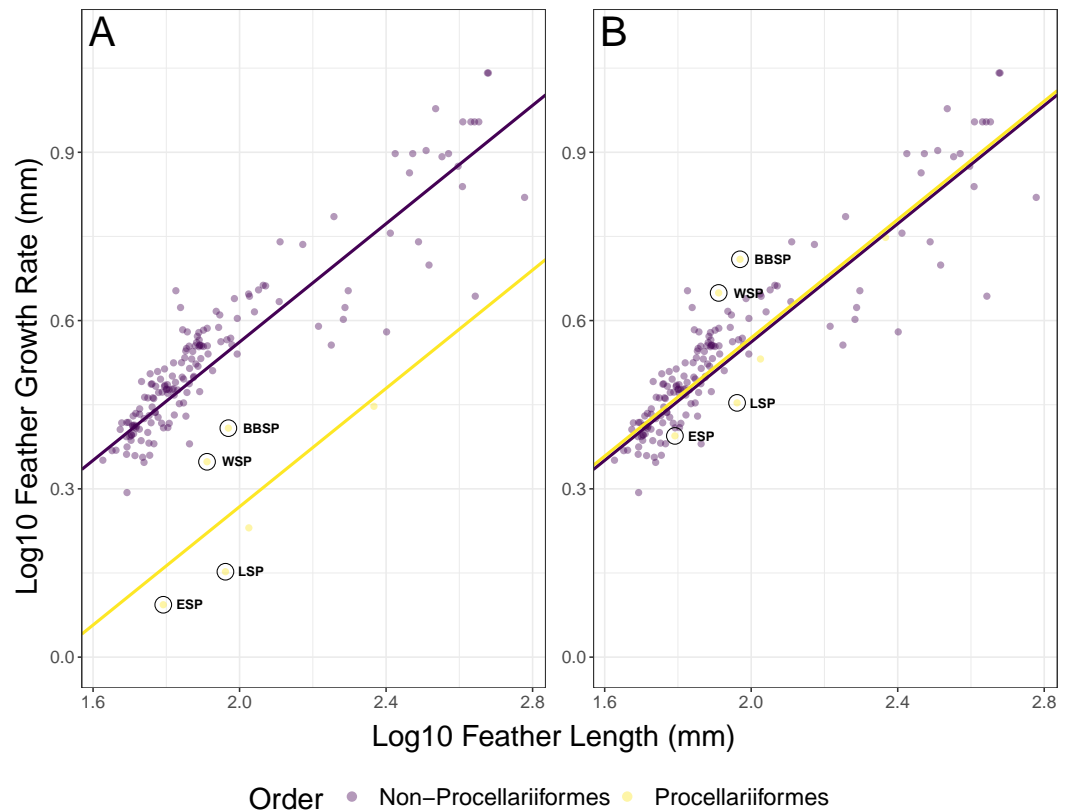


Figure 2 Phylogenetic generalized least squares (PGLS) models for feather growth rate (FGR) based on feather length (FL). (A) The optimized PGLS model, with Pagel's λ , based on the phylogenetic tree, was fitted to log₁₀ FGR as response variable, and log₁₀ FL and group as predictors, for data found in literature ($n = 164$ species) and this study ($n = 4$ species). The groups were defined as non-Procariiformes and Procariiformes, to determine whether the Procariiformes behaved differently from the other reported species. The data used for this model were not adjusted. (B) The PGLS model with group as predictor and with Procariiformes FGR doubled (PGLSadj model), following *Langston & Rohwer's (1996)* suggestion that Procariiformes might form two GBs per 24 h. The group term was not significant in this model, indicating that the aforementioned suggestion was likely correct. Procariiformes are shown in yellow, non-Procariiformes in purple. The studied species are circled in black (ESP, European storm-petrel; LSP, Leach's storm-petrel; WSP, Wilson's storm-petrel; BBSP, black-bellied storm-petrel). See also [Table 3](#) for model description and [Table 4](#) for model comparison.

Full-size DOI: [10.7717/peerj.7807/fig-2](https://doi.org/10.7717/peerj.7807/fig-2)

hemispheres in trade-offs in energy allocation between moulting and breeding may affect the correlations between feather length and feather growth rate, resulting in a lack of significant correlations between feather length and mean growth bar width in the Northern species in contrast to significant relationships between feather length and mean growth bar width in the Southern species.

Moult-breeding overlap in the Northern species has so far only been shown in the Mediterranean subspecies of the European storm-petrel (*Hydrobates pelagicus melitensis*) (*Amengual et al., 1999; Arroyo et al., 2004*), in a British population of European storm-petrels (Scott 1970 in *Cramp et al., 1977*), in Canadian populations of the Leach's storm-petrel (*Ainley, Lewis & Morrell, 1976*), but the overlap extend is not (yet) generally accepted

Table 3 Phylogenetic generalized least squares (PGLS) models for feather growth rate (FGR) based on feather length (FL). PGLS models, with Pagel's λ based on the phylogenetic tree, were fitted to log10 FGR as response variable and log10 FL as predictor, for data found in literature ($n = 164$ species) and this study ($n = 4$ species). To determine whether the Procellariiform species considered ($n = 6$ species) differed in number of growth bars (GB) formed per 24 h, we added a group term (group 1 = non-Procellariiformes, group 2 = Procellariiformes) and its interaction to the full PGLS model (no. 1). Terms were dropped based on significance and improvement of AIC (no. 2 & 3). To test whether Langston and Rohwer's (1996) suggestion that Procellariiformes might form two GBs per 24 h was true, Procellariiformes FGR was doubled (PGLSadj model) and an analogous set of models were tried. Pagel's λ is the phylogenetic signal, with values between 0 and 1.

Model	No.	Predictor	AIC	Pagel's λ	Estimate	SE	t-value	Pr(> t)	
PGLS	1	Intercept			-0.500	0.107	-4.669	<0.001	
		Log10(FL)	-497.59	0.935	0.531	0.043	12.320	<0.001	
		Group			-0.156	0.402	-0.388	0.699	
			Log10(FL):Group			-0.067	0.194	-0.347	0.729
	2	Intercept			-0.493	0.105	-4.708	<0.001	
		Log10(FL)	-499.47	0.935	0.527	0.042	12.588	<0.001	
Group				-0.294	0.068	-4.309	<0.001		
3	Intercept			-0.590	0.112	-5.288	<0.001		
	Log10(FL)	-484.99	0.962	0.554	0.045	12.374	<0.001		
	Intercept			-0.500	0.107	-4.669	<0.001		
PGLSadj	1	Log10(FL)	-497.59	0.935	0.531	0.043	12.320	<0.001	
		Group			0.145	0.402	0.361	0.719	
		Log10(FL):Group			-0.067	0.194	0.347	0.729	
	2	Intercept			-0.493	0.105	-4.708	<0.001	
		Log10(FL)	-499.47	0.935	0.527	0.042	12.588	<0.001	
		Group			0.008	0.068	0.110	0.912	
3	Intercept			-0.490	0.102	-4.814	<0.001		
	Log10(FL)	-501.46	0.935	0.527	0.041	12.760	<0.001		

Notes.

All p -values ≤ 0.05 are bolded.

Table 4 AIC and Δ AIC values of phylogenetic generalized least squares (PGLS) models. A PGLS model with Pagel's λ was fitted to log10 feather growth rate (FGR) with feather length (FL) and Group (non-Procellariiformes vs. Procellariiformes). No 1 is the full model, 2 & 3 with the interaction, and the interaction and group dropped respectively. Models were fitted to raw data (PGLS model) and data with Procellariiformes feather growth rate doubled (PGLSadj). Model selection was based on AIC and delta, but properly as I can't seem to add it to acrobat reader AIC values.

Model	No.	df	AIC	Δ AIC
PGLS	1	6	-497.59	1.88
	2	5	-499.47	0.00
	3	4	-484.99	14.48
PGLSadj	1	6	-497.59	1.88
	2	5	-499.47	1.99
	3	4	-501.46	0.00

in Northern populations. However, preliminary stable-isotope analyses show that tail feather isotopes of the Northern species are more closely matched with blood isotopes collected during the breeding season, than those of the Southern species (Ausems et al., in prep.). This seems to indicate that both the feathers and blood were synthesised under more

Table 5 Results of non-parametric post-hoc Dunn test for the residuals of the storm-petrel species from the optimized phylogenetic generalized least squares (PGLS) model. For the multi-species model, PGLS models were fitted to log₁₀ feather growth rate (FGR) found in literature as response variable with log₁₀ feather length (FL) as predictor. To test whether the Procellariiformes behaved differently from other species, a group variable was added with group 1 being all non-Procellariiformes and group 2 being the Procellariiformes. The residuals of the predicted log₁₀ FGR of the individuals per storm-petrel species were obtained by inserting individual FL into the model with group set to Procellariiformes, and comparing the predicted log₁₀ FGR with log₁₀ observed FGR. *P*-values $\leq \alpha/2$ ($\alpha = 0.05$) are bolded. For plots see Fig. 3.

Species	Dunn's multiple comparisons test					
	black-bellied storm-petrel (Z, p)		European storm-petrel (Z, p)		Leach's storm-petrel (Z, p)	
European storm-petrel	8.389,	<0.001				
Leach's storm-petrel	9.075,	<0.001	0.715,	0.237		
Wilson's storm-petrel	2.228,	0.013	-9.646,	<0.001	-10.770,	<0.001

Table 6 One-sample Student's *t*-test output of the residuals of feather growth rate (FGR) of each studied species predicted by the optimized phylogenetic generalized least squares (PGLS) model. For the multi-species model, PGLS models were fitted to log₁₀ feather growth rate (FGR) found in literature as response variable with log₁₀ feather length (FL) as predictor. To test whether the Procellariiformes behaved differently from results reported for other species, a group variable was added with group 1 being all non-Procellariiformes and group 2 being the Procellariiformes. The residuals of the predicted log₁₀ FGR of the individuals per storm-petrel species were obtained by inserting individual FL into the model with group set to Procellariiformes, and comparing the predicted log₁₀ FGR with log₁₀ observed FGR. *P*-values $\leq \alpha/2$ ($\alpha = 0.05$) are bolded. For plots see Fig. 3.

Species	Residuals			Residuals difference		
	Mean residuals	95% CI lower	95% CI upper	<i>t</i>	df	<i>p</i>
European storm-petrel	-0.076	-0.102	-0.050	-5.847	51	<0.001
Leach's storm-petrel	-0.106	-0.132	-0.081	-8.367	54	<0.001
Wilson's storm-petrel	0.122	0.113	0.132	25.310	199	<0.001
black-bellied storm-petrel	0.154	0.132	0.176	14.460	28	<0.001

similar foraging conditions and in similar foraging areas, strengthening our conviction that the Northern species at least partially overlap their tail moult and breeding.

Austral summer is short and primary production is highest only in favourable conditions (i.e., longer daylight hours and retreating sea ice) (Arrigo, Van Dijken & Bushinsky, 2008; Murphy et al., 2016). The peak abundance of the main prey of the Southern storm-petrels, Antarctic krill, *Euphausia superba*, usually lasts from December to February (Food and Agriculture Organization of the United Nations, 2019; Ross & Quetin, 2014). The relatively short period of high food abundance and possible competition over it e.g., from penguins, whales and krill fisheries (Barlow et al., 2002; Descamps et al., 2016; Ratcliffe et al., 2015), could inhibit the Southern storm-petrels from overlapping moult and breeding as there is no longer enough food available at the end of the breeding season. Additionally, compared to the North Atlantic and Arctic ocean, the highly productive oceanographic features in the Southern Ocean, such as ocean fronts and eddies, occur over larger spatial scales and are usually farther away from the breeding colonies, forcing the birds to take longer foraging trips (Bost et al., 2009). During the non-breeding period birds free from the constraint of central-place foraging may exploit these highly productive areas freely, which may explain the relatively higher than predicted daily feather growth rate of the Southern species.

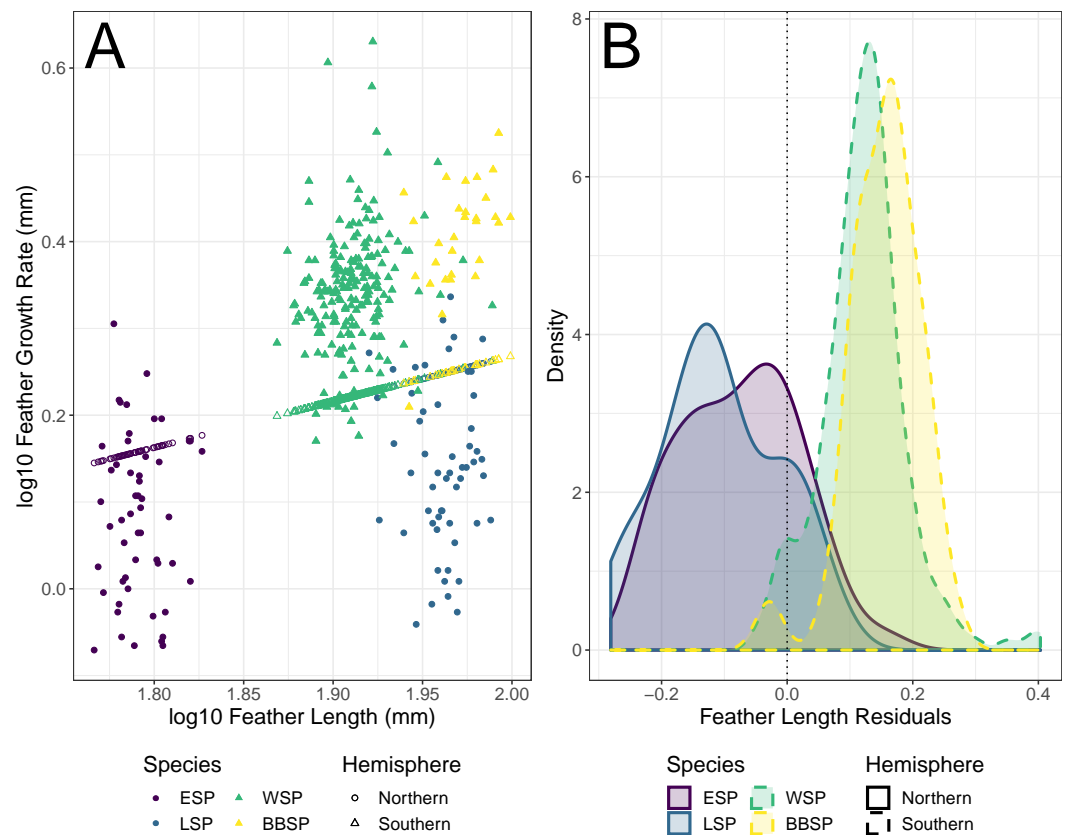


Figure 3 Predicted feather growth rates (FGR) and their residuals based on the optimized phylogenetic generalized least squares (PGLS) model for individual storm-petrels. (A) Individual FGR was predicted (open points) using the optimized PGLS model (i.e., \log_{10} FGR \log_{10} FL + group, where FL is feather length and groups were specified as non-Procellariiformes vs. Procellariiformes), and residuals were calculated based on the distance to the observed values (closed points). Individual FL was used for model prediction and group was set to Procellariiformes. The Northern species are represented by dots, the Southern by triangles. European storm-petrels (ESP) are shown in purple; Leach's storm-petrels (LSP) in blue; Wilson's storm-petrels (WSP) in green; black-bellied storm-petrels (BBSP) in yellow. (B) The density plot shows residual distribution from the optimized PGLS model. The dotted line shows a residual length of 0.0. The Northern species are represented by solid lines, the Southern species by dashed lines. The colour codes are the same as in panel A. For statistical comparisons between the species and hemispheres see Table 5 & main text, and for species mean deviation from zero see Table 6.

Full-size [DOI: 10.7717/peerj.7807/fig-3](https://doi.org/10.7717/peerj.7807/fig-3)

In contrast, both Northern storm-petrels have been reported to show moult-breeding overlap, including the moult of tail feathers (*Ainley, Lewis & Morrell, 1976; Amengual et al., 1999; Arroyo et al., 2004; Bolton & Thomas, 2001*), though Leach's storm-petrels seem to start moulting relatively earlier in the breeding season than European storm-petrels. In the North Atlantic, around the Faroe Islands, primary production peaks over a longer period (*Eliassen, 2017*) as it is not linked to sea ice cover. Thus, food abundance might still be sufficient for moulting at the end of the breeding season for the Northern species. However, primary production varies strongly between years, which could lead to distinct inter-annual differences in food abundance for the storm-petrels (*Bonitz et al., 2018; ICES,*

2005; ICES, 2008). As food availability may thus be unpredictable for the Northern species during breeding, individuals may make different choices in prioritising either moult or reproduction, leading to obscured relationships between mean growth bar width and feather length.

Langston & Rohwer (1996) suggested that Laysan albatrosses (*Phoebastria immutabilis*) may form two growth bars per 24 h because their main prey (i.e., various squid species) is active at night and the albatrosses forage for them at dawn and dusk. This would result in two activity-rest cycles per 24 h, which would explain the formation of two growth bars daily as growth bar formation has been linked to sleep or rest rhythms (*Jovani et al., 2011*). Indeed, after doubling the feather growth rate of the Procellariiformes, their correlation between feather growth rate and feather length was very similar to that of the other orders (Fig. 2B), as shown by the lack of a significant group effect in the PGLSadj model. This seems to confirm *Langston & Rohwer's (1996)* suggestion that Procellariiformes form two growth bars per 24 h. The four studied storm-petrel species may also have two activity-rest cycles per 24 h, which is consistent with the main prey activity of the studied storm-petrels during the breeding season, myctophid fish and krill. These prey species have a nocturnal activity similar to the prey of the albatrosses (*Hedd & Montevecchi, 2006; Siegel, 2012*), and several seabirds, including storm-petrels, forage in more oceanic habitats during the non-breeding period where they seem to increase their intake of myctophid fish (*Watanuki & Thiebot, 2018*).

We are aware of several possible limitations of the present study. Although growth bar widths have originally been linked to relative nutritional condition (*Grubb, 1989; Hill & Montgomerie, 1994*), it is not a direct measurement of food availability and the results should be interpreted with caution in that regard (*Murphy & King, 1991*). In this study we used feather growth rate as a way to retrospectively infer energy availability during moulting, as direct examinations of diet and food availability during moulting were impossible due to the pelagic nature and small body size of our study species. In order to put the feather growth rates observed in our study species into perspective, we compared their growth rates with data found in literature. However, while the reported measuring methods were similar between the studies, sampling techniques may have differed. In some studies samples were taken from museum specimens (e.g., *De la Hera, DeSante & Milá, 2012; Rohwer et al., 2009*) while others collected samples from live birds (e.g., *De la Hera et al., 2011*). This could lead to a bias in the condition of the birds sampled, as museum specimens may come from individuals in relatively poor health, or from relatively young individuals. Sample sizes per species ranged between 1 and 54 (*De la Hera, DeSante & Milá, 2012*) and for some species multiple sources were found (e.g., *Sitta carolinensis: De la Hera, DeSante & Milá, 2012; Dolby & Grubb, 1998; Grubb & Cimprich, 1990*). Especially Passeriformes were highly represented ($n = 160$ observations) in the model, while orders with larger species were under-represented. The model may therefore be less appropriate for larger species, but since the four storm-petrel species studied fall in a highly represented body size category in the model we feel it is appropriate to use here. Due to differences in the studied species' availability, large differences in sample sizes in our research occurred: the Northern species were comparatively abundant during mist-netting sessions, while

the Southern species were not. Additionally, nests of Wilson's storm-petrels were more accessible and concentrated than black-bellied storm-petrel nests, which were spread out over larger areas and more often located on inaccessible cliffs and ledges. Nevertheless, our study provides the first comparison of relative energy availability during tail-feather moult of storm-petrels differing in moult-breeding strategies and breeding in different hemispheres.

Our results suggest that for many pelagic seabirds ptilochronology may be a useful, non-invasive, and often only feasible, tool to study their relative energy allocation to feather growth during the non-breeding period when they are hardly accessible to researchers. Due to their specific life-history traits, pelagic seabirds may be especially interesting for ptilochronology studies as one may expect different patterns of feather growth compared to other species.

CONCLUSIONS

We expected to find positive correlations between feather length and feather growth rate both within and between species, and to find differences in relative energy availability during moulting between species with differing moult-breeding strategies. The results of our analyses showed distinct differences in relative energy availability between four species of storm-petrels. The Southern species had a higher feather growth rate than predicted by a model based on data from multiple species and orders, while the Northern species had a lower feather growth rate than predicted. We suggest that all these differences can be attributed to the different moult-breeding strategies the species adopt, as the Southern storm-petrel species show no moult-breeding overlap while the Northern species do overlap both stages of the annual cycle. The better relative energy availability of the Southern species during moult may be explained by the fact that they change their feathers during the non-breeding period and can thus use all free energy for feather synthesis. In contrast, the Northern species have to allocate their energy between breeding and moulting. Our study shows how different moult-breeding strategies may affect the relative energy availability or energy allocation during moult of migratory pelagic seabirds. Additionally, we showed that at least a subset of the Procellariiformes likely forms two growth bars per 24 h instead of one, probably associated with the diel migration of their main prey species.

ACKNOWLEDGEMENTS

We would like to thank the Henryk Arctowski Polish Antarctic Station and the Department of Antarctic Biology of the Polish Academy of Sciences for their hospitality and logistic support during our stay on King George Island. We are indebted to Jens-Kjeld Jensen and Marita Gulkkett for their hospitality and help on the Faroe Islands. We are grateful also to the three anonymous reviewers of our paper that helped us improve its quality. Lastly, we would like to thank Rosanne Michielsen, Rachel Shepherd and Jessica Hey for their support in the field.

ADDITIONAL INFORMATION AND DECLARATIONS

Funding

This work was supported by a grant from the National Science Centre, Poland (2015/19/B/NZ8/01981). The funders had no role in study design, data collection and analysis, decision to publish, or preparation of the manuscript.

Grant Disclosures

The following grant information was disclosed by the authors:
National Science Centre, Poland: 2015/19/B/NZ8/01981.

Competing Interests

The authors declare there are no competing interests.

Author Contributions

- Anne N.M.A. Ausems and Katarzyna Wojczulanis-Jakubas analyzed the data, contributed reagents/materials/analysis tools, prepared figures and/or tables, authored or reviewed drafts of the paper, approved the final draft.
- Katarzyna Wojczulanis-Jakubas analyzed the data, contributed reagents/materials/analysis tools, authored or reviewed drafts of the paper, approved the final draft.
- Dariusz Jakubas analyzed the data, contributed reagents/materials/analysis tools, authored or reviewed drafts of the paper, approved the final draft.

Animal Ethics

The following information was supplied relating to ethical approvals (i.e., approving body and any reference numbers):

The Polish National SCAR, Institute of Biochemistry and Biophysics approved any harmful interference of Antarctic fauna (permit for taking or harmful interference of Antarctic flora and fauna: No. 7/2016 & No. 6/2017). On the Faroe Islands, birds were handled under license of the Statens Naturhistoriske Museum, Københavns Universitet (C 1012).

Field Study Permissions

The following information was supplied relating to field study approvals (i.e., approving body and any reference numbers):

The Antarctic part of the study was performed under the permission of the Polish National SCAR, Institute of Biochemistry and Biophysics (permit for entering the Antarctic Specially Protected Area No. 3/2016 & No. 08/2017). On the Faroe Islands permission to enter the study site was sought through local land owners.

Data Availability

The following information was supplied regarding data availability:

The raw data are available in the [Supplemental File](#).

Supplemental Information

Supplemental information for this article can be found online at <http://dx.doi.org/10.7717/peerj.7807#supplemental-information>.

REFERENCES

- Ainley DG, Lewis J, Morrell S. 1976. Molt in Leach's and Ashy storm-petrels. *The Wilson Bulletin* 88(1):76–95.
- Ainley DG, O'Connor EF, Boekelheide RJ. 1984. The marine ecology of birds in the Ross Sea, Antarctica. *Ornithological monographs* 32: pp. iii-x, 1-97 DOI 10.2307/40166773.
- Ainslie JA, Atkinson R. 1936. On the breeding habits of Leach's fork-tailed petrel. *British Birds* 30:234–249.
- Alonso H, Matias R, Granadeiro JP, Catry P. 2009. Moulting strategies of Cory's shearwaters *Calonectris diomedea borealis*: the influence of colony location, sex and individual breeding status. *Journal of Ornithology* 150(2):329–337 DOI 10.1007/s10336-008-0354-2.
- Amengual JF, Gargallo G, Suárez M, Bonnín J, González JM, Rebassa M, McMinn M. 1999. The Mediterranean storm petrel *Hydrobates pelagicus melitensis* at Cabrera archipelago (Balearic Islands, Spain): breeding moult, biometry and evaluation of the population size by mark and recapture techniques. *Ringed and Migration* 19(3):181–190 DOI 10.1080/03078698.1999.9674180.
- Arrigo KR, Van Dijken GL, Bushinsky S. 2008. Primary production in the Southern ocean, 1997–2006. *Journal of Geophysical Research: Oceans* 113(C8):1997–2006 DOI 10.1029/2007JC004551.
- Arroyo B, Mínguez E, Palomares L, Pinilla J. 2004. The timing and pattern of moult of flight feathers of European storm-petrel *Hydrobates pelagicus* in Atlantic and Mediterranean breeding areas. *Ardeola* 51(2):365–373.
- Barbraud C, Chastel O. 1998. Southern fulmars molt their primary feathers while incubating. *The Condor* 100(3):563–566 DOI 10.2307/1369726.
- Barlow KE, Boyd IL, Croxall JP, Reid K, Staniland IJ, Brierley AS. 2002. Are penguins and seals in competition for Antarctic krill at South Georgia? *Marine Biology* 140(2):205–213 DOI 10.1007/s00227-001-0691-7.
- Beck JR, Brown DW. 1972. The biology of Wilson's storm petrel, *Oceanites oceanicus* (Kuhl), at Signy Island, South Orkney Islands. *British Antarctic Survey Scientific Reports* 69:1–54.
- Bolton M, Thomas R. 2001. Moulting and ageing of storm petrels *Hydrobates pelagicus*. *Ringed and Migration* 20(3):193–201 DOI 10.1080/03078698.2001.9674244.
- Bonitz FGW, Andersson C, Trofimova T, Hátún H. 2018. Links between phytoplankton dynamics and shell growth of *Arctica islandica* on the Faroe Shelf. *Journal of Marine Systems* 179:72–87 DOI 10.1016/j.jmarsys.2017.11.005.
- Bost CA, Cotté C, Bailleul F, Cherel Y, Charrassin JB, Guinet C, Ainley DG, Weimerskirch H. 2009. The importance of oceanographic fronts to marine birds and

- mammals of the Southern oceans. *Journal of Marine Systems* **78**(3):363–376
DOI [10.1016/j.jmarsys.2008.11.022](https://doi.org/10.1016/j.jmarsys.2008.11.022).
- Bridge ES. 2006.** Influences of morphology and behavior on wing-molt strategies in seabirds. *Marine Ornithology* **34**(1):7–19 DOI [10.1111/j.1472-4642.2007.0034.x](https://doi.org/10.1111/j.1472-4642.2007.0034.x).
- Büßer C, Kahles A, Quillfeldt P. 2004.** Breeding success and chick provisioning in Wilson’s storm-petrels *Oceanites oceanicus* over seven years: frequent failures due to food shortage and entombment. *Polar Biology* **27**(10):613–622
DOI [10.1007/s00300-004-0627-z](https://doi.org/10.1007/s00300-004-0627-z).
- Carboneras C, Jutglar F, Kirwan GM, Christie DA, Jutglar F, Kirwan GM, Sharpe CJ. 2017.** Order Procellariiformes. In: Del Hoyo J, Elliot A, Sargatal J, Christie DA, De Juana E, eds. *Handbook of the birds of the world alive*. Barcelona: Lynx Edicions, 197–278.
- Catry P, Lemos RT, Brickle P, Phillips RA, Matias R, Granadeiro J. 2013.** Predicting the distribution of a threatened albatross: the importance of competition, fisheries and annual variability. *Progress in Oceanography* **110**:1–10
DOI [10.1016/j.pocean.2013.01.005](https://doi.org/10.1016/j.pocean.2013.01.005).
- Cramp S, Simmons KEL, Ferguson-Lees IJ, Gillmor R, Hollom PAD, Hudson R, Nicholson EM, Ogilvie MA, Olney PJS, Voous KH, Wattel J. 1977.** Family *Hydrobatidae* storm-petrels. In: *Handbook of the birds of Europe and the Middle East and North Africa the birds of the Western Palearctic Volume I.* Oxford: Oxford University Press, 155–178.
- Crossin GT, Phillips RA, Lattin CR, Romero LM, Williams TD. 2013.** Corticosterone mediated costs of reproduction link current to future breeding. *General and Comparative Endocrinology* **193**:112–120 DOI [10.1016/j.ygcen.2013.07.011](https://doi.org/10.1016/j.ygcen.2013.07.011).
- Croxall JP, North AW. 1988.** Fish prey of Wilson’s storm petrel *Oceanites oceanicus* at South Georgia. *British Antarctic Survey Bulletin* **78**:37–42.
- Croxall JP, Prince PA. 1980.** Food, feeding ecology and segregation of seabirds at South Georgia. *Biological Journal of the Linnean Society* **14**:103–131
DOI [10.1111/j.1095-8312.1980.tb00101.x](https://doi.org/10.1111/j.1095-8312.1980.tb00101.x).
- De la Hera I, DeSante DF, Milá B. 2012.** Feather growth rate and mass in Nearctic passerines with variable migratory behavior and molt pattern. *The Auk* **129**(2):222–230 DOI [10.1525/auk.2012.11212](https://doi.org/10.1525/auk.2012.11212).
- De la Hera I, Pérez-Tris J, Tellería JL. 2009.** Migratory behaviour affects the trade-off between feather growth rate and feather quality in a passerine bird. *Biological Journal of the Linnean Society* **97**(1):98–105 DOI [10.1111/j.1095-8312.2008.01189.x](https://doi.org/10.1111/j.1095-8312.2008.01189.x).
- De la Hera I, Schaper SV, Díaz JA, Pérez-Tris J, Bensch S, Tellería JL. 2011.** How much variation in the molt duration of passerines can be explained by the growth rate of tail feathers? *The Auk* **128**(2):321–329 DOI [10.1525/auk.2011.10181](https://doi.org/10.1525/auk.2011.10181).
- D’Elbée J, Hémery G. 1998.** Diet and foraging behaviour of the British storm petrel *Hydrobates pelagicus* in the Bay of Biscay during summer. *Ardea* **86**:1–10.
- Descamps S, Tarroux A, Cherel Y, Delord K, Godø OR, Kato A, Krafft BA, Lorentsen SH, Ropert-Coudert Y, Skaret G, Varpe Ø. 2016.** At-sea distribution and prey

- selection of Antarctic petrels and commercial krill fisheries. *PLOS ONE* **11**(8):1–18 DOI 10.1371/journal.pone.0156968.
- Dolby AS, Grubb TC. 1998.** Benefits to satellite members in mixed-species foraging groups: an experimental analysis. *Animal Behaviour* **56**(2):501–509 DOI 10.1006/anbe.1998.0808.
- Eliassen SK. 2017.** Primary production on the Faroe shelf—spatial and temporal variations with links to hydrography. PhD thesis, Faculty of Science and Technology University of the Faroe Islands. Available at <http://www.hav.fo/PDF/Ritgerdir/SolvaPhD.pdf>.
- Ericson PG, Anderson CL, Britton T, Elzanowski A, Johansson US, Källersjö M, Ohlson JI, Parsons TJ, Zuccon D, Mayr G. 2006.** Diversification of Neoaves: integration of molecular sequence data and fossils. *Biology Letters* **2**:543–547 DOI 10.1098/rsbl.2006.0523.
- Flood RL, Thomas B. 2007.** Identification of “black-and-white” storm-petrels of the North Atlantic. *British Birds* **100**:407–442.
- Food and Agriculture Organization of the United Nations (FAO). 2019.** Species fact sheets *Euphausia superba*. Available at <http://www.fao.org/fishery/species/3393/en> (accessed on 11 December 2018).
- Furness RW, Baillie SR. 1981.** Factors affecting capture rate and biometrics of storm petrels on St Kilda. *Ringing & Migration* **3**(3):137–148 DOI 10.1080/03078698.1981.9673772.
- Green JA, Aitken-Simpson EJ, White CR, Bunce A, Butler PJ, Frappell PB. 2013.** An increase in minimum metabolic rate and not activity explains field metabolic rate changes in a breeding seabird. *Journal of Experimental Biology* **216**(9):1726–1735 DOI 10.1242/jeb.085092.
- Grubb TC. 1989.** Ptilochronology—feather growth bars as indicators of nutritional status. *AUK* **106**(2):314–320.
- Grubb TC. 2006.** *Ptilochronology*. Oxford: Oxford University Press.
- Grubb TC, Cimprich DA. 1990.** Supplementary food improves the nutritional condition of wintering woodland birds: evidence from ptilochronology. *Ornis Scandinavica* **21**(4):277–281 DOI 10.2307/3676392.
- Hahn S, Peter H, Quillfeldt P, Reinhardt K. 1998.** The birds of the Potter Peninsula, King George Island, South Shetland Islands, Antarctica, 1965–1998. *Marine Ornithology* **26**(1995):1–6.
- Halpin LR, Pollet IL, Lee C, Morgan KH, Carter HR. 2018.** Year-round movements of sympatric Fork-tailed (*Oceanodroma furcata*) and Leach’s (*O. leucorhoa*) storm-petrels. *Journal of Field Ornithology* **89**(3):207–220 DOI 10.1111/jof.12255.
- Hargitai R, Hegyi G, Herényi M, Laczi M, Nagy G, Rosivall B, Szöllösi E, Török J. 2014.** Winter body condition in the Collared Flycatcher: determinants and carryover effects on future breeding parameters. *The Auk* **131**:257–264 DOI 10.1642/AUK-13-158.1.

- Hedd A, Montevecchi WA. 2006.** Diet and trophic position of Leach's storm-petrel *Oceanodroma leucorhoa* during breeding and moult, inferred from stable isotope analysis of feathers. *Marine Ecology Progress Series* **322**:291–301 DOI [10.3354/meps322291](https://doi.org/10.3354/meps322291).
- Hedenström A, Sunada S. 1999.** On the aerodynamics of moult gaps in birds. *Journal of Experimental Biology* **202**:67–76.
- Hemborg C, Sanz J, Lundberg A. 2001.** Effects of latitude on the trade-off between reproduction and moult: a long-term study with pied flycatcher. *Oecologia* **129**(2):206–212 DOI [10.1007/s004420100710](https://doi.org/10.1007/s004420100710).
- Hill GE, Montgomerie R. 1994.** Plumage colour signals nutritional condition in the house finch. *Proceedings: Biological Sciences* **258**(1351):47–52.
- International Council for the Exploration of the Sea (ICES). 2005.** Report of the ICES advisory committee on fishery management, advisory committee on the marine environment and advisory committee on ecosystems, 2005. In: *ICES advice*. Vol. 1. Copenhagen: International Council for the Exploration of the Sea.
- International Council for the Exploration of the Sea (ICES). 2008.** Report of the ICES advisory committee 2008. In: *ICES advice, Book 4*. Copenhagen: International Council for the Exploration of the Sea.
- Jetz W, Thomas GH, Joy JB, Hartmann K, Mooers AO. 2012.** The global diversity of birds in space and time. *Nature* **491**:444–448 DOI [10.1038/nature11631](https://doi.org/10.1038/nature11631).
- Jovani R, Blas J, Navarro C, Mougeot F. 2011.** Feather growth bands and photoperiod. *Journal of Avian Biology* **42**(1):1–4 DOI [10.1111/j.1600-048X.2010.05175.x](https://doi.org/10.1111/j.1600-048X.2010.05175.x).
- Lago P, Austad M, Metzger BJ. 2019.** Partial migration in the Mediterranean Storm Petrel (*Hydrobates pelagicus melitensis*). *Marine Ornithology* **47**:105–113.
- Langston NE, Rohwer S. 1996.** Molt-breeding tradeoffs in albatrosses: life history implications for big birds. *Oikos* **76**(3):498–510 DOI [10.2307/3546343](https://doi.org/10.2307/3546343).
- Le Tortorec E, Helle S, Suorsa P, Sirkiä P, Huhta E, Nivala V, Hakkarainen H. 2012.** Feather growth bars as a biomarker of habitat fragmentation in the Eurasian treecreeper. *Ecological Indicators* **15**(1):72–75 DOI [10.1016/j.ecolind.2011.09.013](https://doi.org/10.1016/j.ecolind.2011.09.013).
- Lindström Å, Visser GH, Daan S. 1993.** The energetic cost of feather synthesis to basal metabolic rate is proportional. *Physiological Zoology* **66**(4):490–510 DOI [10.2307/30163805](https://doi.org/10.2307/30163805).
- Martínez C, Roscales JL, Sanz-Aguilar A, González-Solís J. 2019.** Inferring the wintering distribution of the mediterranean populations of european storm-petrels hydrobates pelagicus melitensis from stable isotope analysis and observational field data. *Ardeola* **66**(1):13–32 DOI [10.13157/arla.66.1.2019.ra2](https://doi.org/10.13157/arla.66.1.2019.ra2).
- Marzal A, Asghar M, Rodríguez L, Reviriego M, Hermosell IG, Balbontín J, Garcia-Longoria L, De Lope F, Bensch S. 2013.** Co-infections by malaria parasites decrease feather growth but not feather quality in house martin. *Journal of Avian Biology* **44**(5):437–444 DOI [10.1111/j.1600-048X.2013.00178.x](https://doi.org/10.1111/j.1600-048X.2013.00178.x).
- Mauck RA, Grubb TC. 1995.** Petrel parents shunt all experimentally increased reproductive costs to their offspring. *Animal Behaviour* **49**(4):999–1008 DOI [10.1006/anbe.1995.0129](https://doi.org/10.1006/anbe.1995.0129).

- Minguez E. 1998.** The costs of incubation in the British Storm-Petrel: an experimental study in a single- egg layer. *Journal of Avian Biology* **29**(2):183–189 DOI [10.2307/3677197](https://doi.org/10.2307/3677197).
- Mumme RL. 2018.** The trade-off between molt and parental care in hooded warblers: simultaneous rectrix molt and uniparental desertion of late-season young. *The Auk* **135**(3):427–438 DOI [10.1642/AUK-17-240.1](https://doi.org/10.1642/AUK-17-240.1).
- Murphy EJ, Cavanagh RD, Drinkwater KE, Grant SM, Heymans JJ, Hofmann , Hunt Jr GL, Johnston NM. 2016.** Understanding the structure and functioning of polar pelagic ecosystems to predict the impacts of change. *Proceedings of the Royal Society B: Biological Sciences* **283**:20161646 DOI [10.1098/rspb.2016.1646](https://doi.org/10.1098/rspb.2016.1646).
- Murphy ME, King JR. 1991.** Ptilochronology: a critical evaluation of assumptions and utilities. *The Auk* **108**:695–704 DOI [10.2307/4088109](https://doi.org/10.2307/4088109).
- Navarro J, González-Solís J. 2007.** Experimental increase of flying costs in a pelagic seabird: effects on foraging strategies, nutritional state and chick condition. *Oecologia* **151**(1):150–160 DOI [10.1007/s00442-006-0559-0](https://doi.org/10.1007/s00442-006-0559-0).
- Penhallurick J, Wink M. 2004.** Analysis of the taxonomy and nomenclature of the Procellariiformes based on complete nucleotide sequences of the mitochondrial cytochrome b gene. *Emu* **72**(2):249–266.
- Pérez-Tris J, Carbonell R, Tellería JL. 2002.** Parasites and the blackcap’s tail: implications for the evolution of feather ornaments. *Biological Journal of the Linnean Society* **76**(4):481–492 DOI [10.1046/j.1095-8312.2002.00083.x](https://doi.org/10.1046/j.1095-8312.2002.00083.x).
- Pollet IL, Hedd A, Taylor PD, Montevecchi WA, Shutler D. 2014.** Migratory movements and wintering areas of Leach’s storm-petrels tracked using geolocators. *Journal of Field Ornithology* **85**(3):321–328 DOI [10.1111/jfo.12071](https://doi.org/10.1111/jfo.12071).
- Pratte I, Boadway KA, Diamond AW, Mallory ML. 2018.** Changes in isotopic niches across stages of the annual cycle in the Arctic tern (*Sterna paradisaea*). *Arctic* **71**(3):259–268.
- Quillfeldt P. 2002.** Seasonal and annual variation in the diet of breeding and non-breeding Wilson’s storm-petrels on King George Island, South Shetland Islands. *Polar Biology* **25**:216–221 DOI [10.1007/s00300-001-0332-0](https://doi.org/10.1007/s00300-001-0332-0).
- R Core Team. 2018.** R: a language and environment for statistical computing. Vienna: R Foundation for Statistical Computing. Available at <https://www.r-project.org>.
- Ramos R, Llabrés V, Monclús L, López-Béjar M, González-Solís J. 2018.** Costs of breeding are rapidly buffered and do not affect migratory behavior in a long-lived bird species. *Ecology* **99**(9):2010–2024 DOI [10.1002/ecy.2435](https://doi.org/10.1002/ecy.2435).
- Ramos R, Militão T, González-Solís J, Ruiz X. 2009.** Moulting strategies of a long-distance migratory seabird, the Mediterranean Cory’s shearwater *Calonectris diomedea diomedea*. *Ibis* **151**(1):151–159 DOI [10.1111/j.1474-919X.2008.00877.x](https://doi.org/10.1111/j.1474-919X.2008.00877.x).
- Ratcliffe N, Hill SL, Staniland IJ, Brown R, Adlard S, Horswill C, Trathan PN. 2015.** Do krill fisheries compete with macaroni penguins? Spatial overlap in prey consumption and catches during winter. *Diversity and Distributions* **21**(11):1339–1348 DOI [10.1111/ddi.12366](https://doi.org/10.1111/ddi.12366).

- Rheindt FE, Austin JJ. 2005.** Major analytical and conceptual shortcomings in a recent taxonomic revision of the Procellariiformes—a reply to Penhallurick and Wink (2004). *Emu* **105**(2):181–186 DOI [10.1071/MU04039](https://doi.org/10.1071/MU04039).
- Ridoux V. 1994.** The diets and dietary segregation of seabirds at the subantarctic Crozet Islands. *Marine Ornithology* **22**(1):1–192.
- Robertson BC, Stephenson BM, Ronconi RA, Goldstien SJ, Shepherd L, Tennyson A, Carlile N, Ryan PG. 2016.** Phylogenetic affinities of the *Fregatta* storm-petrels are not black and white. *Molecular Phylogenetics and Evolution* **97**:170–176 DOI [10.1016/j.ympev.2016.01.004](https://doi.org/10.1016/j.ympev.2016.01.004).
- Rohwer S, Ricklefs RE, Rohwer VG, Copple MM. 2009.** Allometry of the duration of flight feather molt in birds. *PLOS Biology* **7**(6):1–9 DOI [10.1371/journal.pbio.1000132](https://doi.org/10.1371/journal.pbio.1000132).
- Ross RM, Quetin LB. 2014.** How productive are Antarctic krill? Recent research is challenging some long-held assumptions about the fecundity and development of *Euphausia superba*. *BioScience* **36**(4):264–269.
- Saino N, Romano M, Caprioli M, Ambrosini R, Rubolini D, Scandolara C, Romano A. 2012.** A ptilochronological study of carry-over effects of conditions during wintering on breeding performance in the barn swallow *Hirundo rustica*. *Journal of Avian Biology* **43**:513–524 DOI [10.1111/j.1600-048X.2012.05622.x](https://doi.org/10.1111/j.1600-048X.2012.05622.x).
- Sanz-Aguilar A, Tavecchia G, Minguéz E, Massa B, Lo Valvo F, Ballesteros GA, Barberá GG, Amengual JF, Rodríguez A, McMinn M, Oro D. 2010.** Recapture processes and biological inference in monitoring burrow-nesting seabirds. *Journal of Ornithology* **151**(1):133–146 DOI [10.1007/s10336-009-0435-x](https://doi.org/10.1007/s10336-009-0435-x).
- Siegel V. 2012.** Krill stocks in high latitudes of the Antarctic Lazarev sea: seasonal and interannual variation in distribution, abundance and demography. *Polar Biology* **35**(8):1151–1177 DOI [10.1007/s00300-012-1162-y](https://doi.org/10.1007/s00300-012-1162-y).
- Slagsvold T, Dale S. 1996.** Disappearance of female pied flycatchers in relation to breeding stage and experimentally induced molt. *Ecology* **77**(2):461–471.
- Stutchbury BJM, Gow EA, Done T, MacPherson M, Fox JW, Afanasyev V. 2011.** Effects of post-breeding moult and energetic condition on timing of songbird migration into the tropics. *Proceedings of the Royal Society B: Biological Sciences* **278**(1702):131–137 DOI [10.1098/rspb.2010.1220](https://doi.org/10.1098/rspb.2010.1220).
- Terrill RS. 2018.** Feather growth rate increases with latitude in four species of widespread resident Neotropical birds. *The Auk* **135**(4):1055–1063 DOI [10.1642/AUK-17-176.1](https://doi.org/10.1642/AUK-17-176.1).
- Wasilewski A. 1986.** Ecological aspects of the breeding cycle in the Wilson's storm petrel, *Oceanites oceanicus* (Kuhl), at King George Island (South Shetland Islands, Antarctica). *Polish Polar Research* **7**(3):173–216.
- Watanuki Y, Thiebot JB. 2018.** Factors affecting the importance of myctophids in the diet of the world's seabirds. *Marine Biology* **165**:1–14 DOI [10.1007/s00227-017-3259-x](https://doi.org/10.1007/s00227-017-3259-x).
- White DW, Kennedy ED. 1992.** Growth of induced feathers in photostimulated American tree sparrows. *The Condor* **94**(2):543–545 DOI [10.2307/1369230](https://doi.org/10.2307/1369230).

Differences in tail feather growth rate in storm-petrels breeding in the Northern and Southern hemisphere: a ptilochronological approach

Anne N.M.A. Ausems, Katarzyna Wojczulanis-Jakubas and Dariusz Jakubas

Department of Vertebrate Ecology and Zoology, Faculty of Biology, University of Gdańsk, Gdańsk, Poland

Fig. S1 Inter-annual differences in feather length (FL) and feather growth rate (FGR) for the Southern storm-petrel species.

(A) Boxplots showing the inter-annual differences in FL for the Wilson's (WSP) and black-bellied (BBSP) storm-petrels. 2017 is shown in purple, 2018 in yellow. Student's t-tests showed significant differences for WSP but not for BBSP (see Materials and Methods), probably because of differences in sample size. (B) Boxplots showing the inter-annual differences in FGR. Student's t-tests showed significant differences for WSP but not for BBSP (see Materials and Methods), probably because of differences in sample size. (C) Scatterplot showing the overlap between years in FL and FGR for WSP. Ellipses show the 95% confidence level. (D) Scatterplot showing the overlap between years in FL and FGR for BBSP.

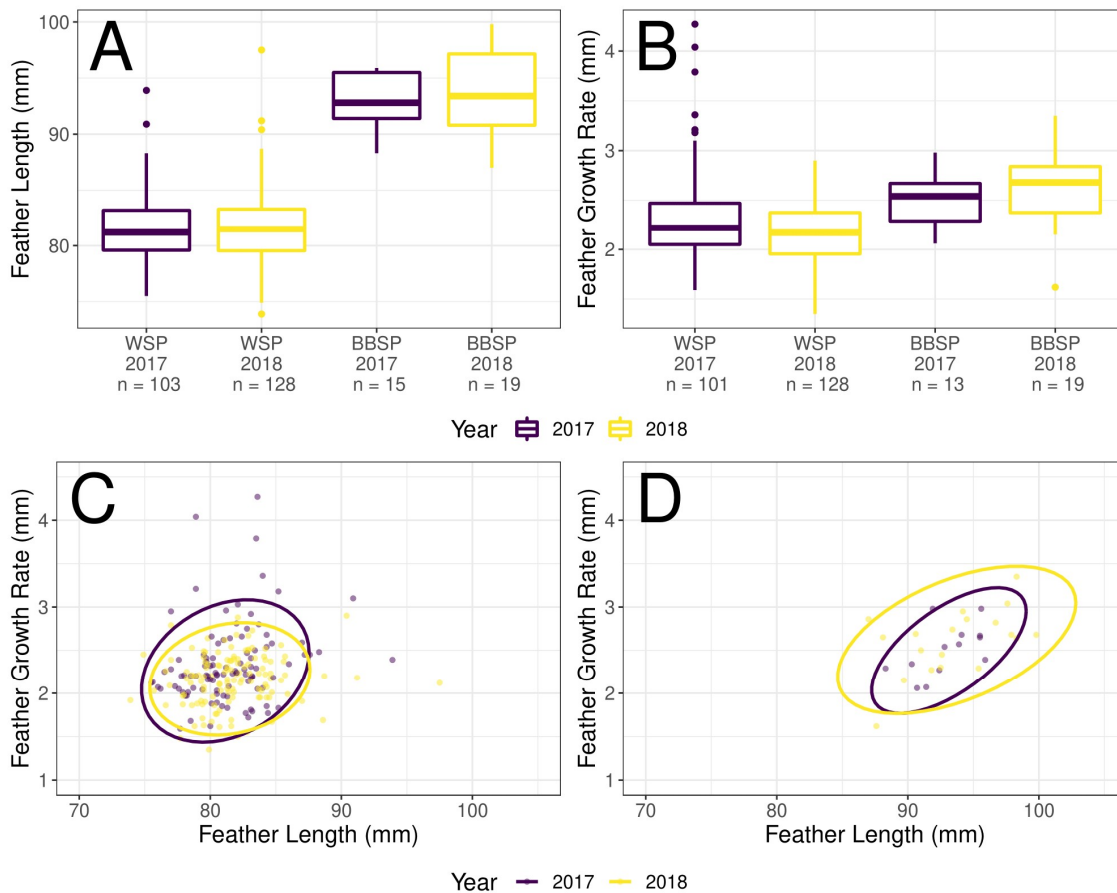


Fig. S2 Relationship between daily feather growth rate (FGR) and feather length (FL) for non-Procellariiformes reported in literature

A scatterplot showing the relationship between FGR and FL. Each dot represents the average reported value for a single species (see Table S2, and Materials and Methods for details). The dotted line shows a linear correlation as generated by ggplot (*geom_smooth, method = "lm"*, package *ggplot2*) and the dashed line a loess regression.

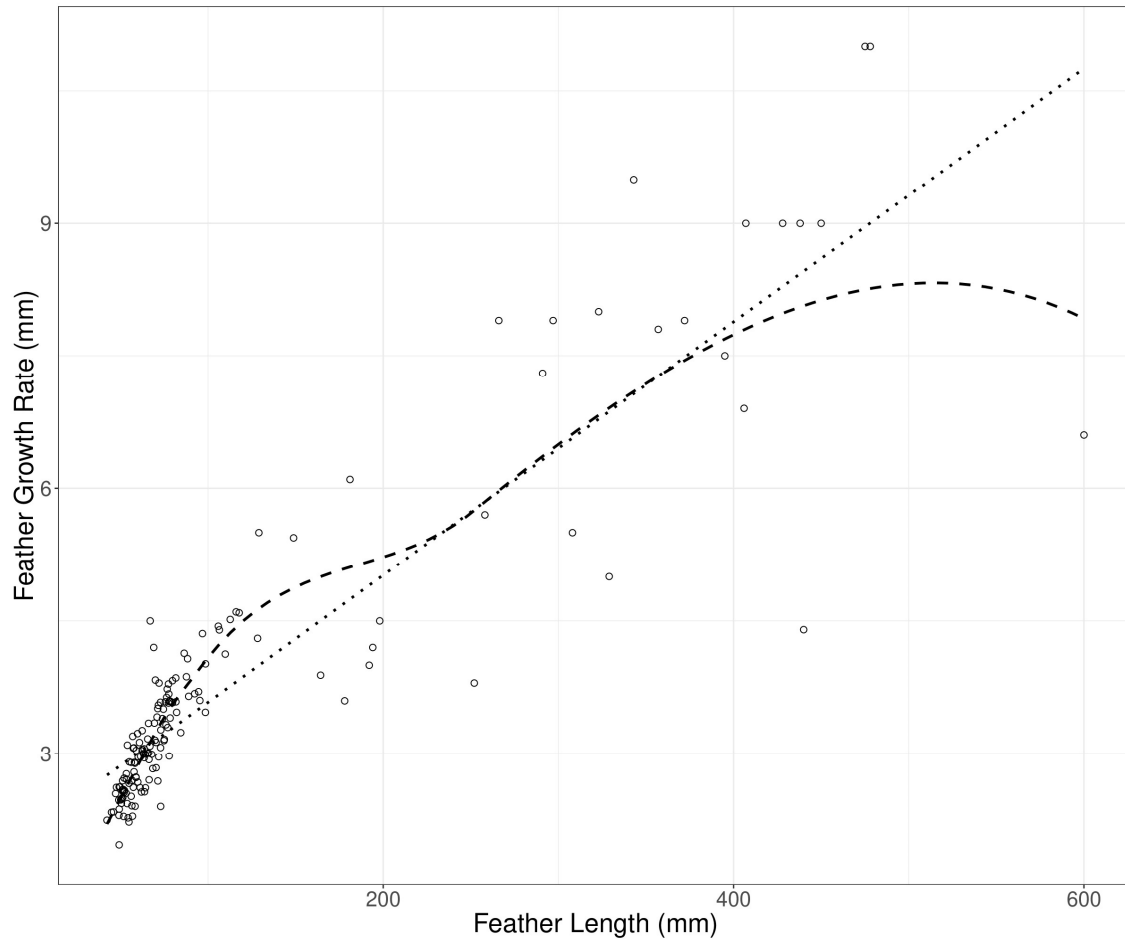


Table S1 Data used for the literature based phylogenetic generalized least squares (PGLS) model with Pagel's λ .

Feather growth rate (FGR) as inferred from measuring mean growth bar widths and feather length (FL) as found in literature and determined in this study were used in the PGLS models described in the materials and methods. Flight feathers were taken from different tracts (FT): P = primary; R = rectrix. FGR between P and R is highly correlated (Saino et al., 2012) and did not significantly affect the PGLS model (see materials and methods, and supplementary table S2). Species are ordered phylogenetically, based on the tree used (see materials and methods).

Species	FGR (mm)	FL (mm)	FT	Source
<i>Chen caerulescens</i>	7.9	297	P	Rohwer et al., 2009
<i>Chen rossii</i>	7.9	266	P	Rohwer et al., 2009
<i>Anser anser</i>	5.5	308	P	Rohwer et al., 2009
<i>Branta canadensis</i>	7.8	357	P	Rohwer et al., 2009
<i>Branta leucopsis</i>	7.3	291	P	Rohwer et al., 2009
<i>Branta bernicla</i>	5.7	258	P	Rohwer et al., 2009
<i>Cygnus cygnus</i>	9	407	P	Rohwer et al., 2009
<i>Cygnus olor</i>	6.9	406	P	Rohwer et al., 2009
<i>Coscoroba coscoroba</i>	5	329	P	Rohwer et al., 2009
<i>Anas platyrhynchos</i>	4.5	198	P	Rohwer et al., 2009
<i>Gallus gallus</i>	4	192	P	Rohwer et al., 2009
<i>Meleagris gallopavo</i>	7.5	395	P	Rohwer et al., 2009
<i>Phasianus colchicus</i>	6.1	181	P	Rohwer et al., 2009
<i>Oceanites oceanicus</i>	2.23	81.5	R	This study
<i>Fregetta tropica</i>	2.56	93.2	R	This study
<i>Phoebastria immutabilis</i>	2.8	232.7	P	Langston & Rohwer, 1996
<i>Hydrobates pelagicus</i>	1.24	61.9	R	This study
<i>Oceanodroma leucorhoa</i>	1.42	91.5	R	This study
<i>Oceanodroma homochroa</i>	1.7	106	P	Rohwer et al., 2009
<i>Grus leucogeranus</i>	9	450	P	Rohwer et al., 2009
<i>Grus carunculatus</i>	11	475	P	Rohwer et al., 2009
<i>Grus japonensis</i>	11	478	P	Rohwer et al., 2009
<i>Grus grus</i>	9	438	P	Rohwer et al., 2009
<i>Grus vipio</i>	9	428	P	Rohwer et al., 2009
<i>Larus hyperboreus</i>	8	323	P	Rohwer et al., 2009
<i>Larus marinus</i>	9.5	343	P	Rohwer et al., 2009
<i>Falco tinnunculus</i>	4.2	194	P	Rohwer et al., 2009
<i>Empidonax difficilis</i>	2.61	61.26	R	de la Hera, DeSante, & Milá, 2012

<i>Empidonax occidentalis</i>	2.7	66.35	R	de la Hera, DeSante, & Milá, 2012
<i>Empidonax fulvifrons</i>	2.41	56.56	R	de la Hera, DeSante, & Milá, 2012
<i>Empidonax wrightii</i>	3.17	65.55	R	de la Hera, DeSante, & Milá, 2012
<i>Empidonax oberholseri</i>	2.61	64.27	R	de la Hera, DeSante, & Milá, 2012
<i>Empidonax virescens</i>	2.96	60.11	R	de la Hera, DeSante, & Milá, 2012
<i>Contopus virens</i>	2.84	70.32	R	de la Hera, DeSante, & Milá, 2012
<i>Contopus sordidulus</i>	2.69	71.37	R	de la Hera, DeSante, & Milá, 2012
<i>Contopus cooperi</i>	2.97	77.83	R	de la Hera, DeSante, & Milá, 2012
<i>Sayornis phoebe</i>	3.17	75.03	R	de la Hera, DeSante, & Milá, 2012
<i>Myiarchus crinitus</i>	4.36	96.8	R	de la Hera, DeSante, & Milá, 2012
<i>Vireo griseus</i>	2.47	50.16	R	de la Hera, DeSante, & Milá, 2012
<i>Vireo huttoni</i>	2.22	54.85	R	de la Hera, DeSante, & Milá, 2012
<i>Vireo olivaceus</i>	2.79	57.72	R	de la Hera, DeSante, & Milá, 2012
<i>Lanius senator</i>	3.3	77	P	Rohwer et al., 2009
<i>Lanius ludovicianus</i>	3.28	97.51	R	Grubb & Yosef, 1994
<i>Lanius ludovicianus</i>	3.45	97.93	R	Grubb & Yosef, 1994
<i>Lanius ludovicianus</i>	3.5	98.54	R	Grubb & Yosef, 1994
<i>Lanius ludovicianus</i>	3.65	100.09	R	Grubb & Yosef, 1994
<i>Corvus monedula</i>	3.6	178	P	Rohwer et al., 2009
<i>Corvus frugilegus</i>	3.8	252	P	Rohwer et al., 2009
<i>Pica pica</i>	5.18	156.5	R	de la Hera et al., 2011
<i>Pica pica</i>	2.6	172	P	Rohwer et al., 2009
<i>Garrulus glandarius</i>	5.44	148.8	R	de la Hera et al., 2011
<i>Cyanocitta cristata</i>	4.52	112.66	R	de la Hera, DeSante, & Milá, 2012
<i>Cyanocitta stelleri</i>	4.3	128.29	R	de la Hera, DeSante, & Milá, 2012
<i>Perisoreus canadensis</i>	4.58	116.5	R	Waite, 1990
<i>Perisoreus canadensis</i>	4.6	119.1	R	Waite, 1990
<i>Baeolophus bicolor</i>	3.01	71.2	R	de la Hera, DeSante, & Milá, 2012
<i>Baeolophus bicolor</i>	2.88	70.25	R	Grubb & Cimprich, 1990
<i>Baeolophus bicolor</i>	2.94	71.9	R	Grubb & Cimprich, 1990
<i>Baeolophus bicolor</i>	3.02	74.04	R	Grubb & Cimprich, 1990
<i>Parus atricapillus</i>	2.68	59.92	R	de la Hera, DeSante, & Milá, 2012
<i>Parus carolinensis</i>	2.34	52.84	R	de la Hera, DeSante, & Milá, 2012
<i>Parus carolinensis</i>	2.18	52.51	R	Grubb & Cimprich, 1990
<i>Parus carolinensis</i>	2.28	57.14	R	Grubb & Cimprich, 1990
<i>Parus carolinensis</i>	2.29	54.99	R	Grubb & Cimprich, 1990
<i>Parus major</i>	2.99	66.71	R	de la Hera et al., 2011

<i>Parus major</i>	2.87	65.9	R	Matysioková & Remeš, 2010
<i>Parus caeruleus</i>	2.43	53.86	R	de la Hera et al., 2011
<i>Phylloscopus trochilus</i>	3.1	54	P	Rohwer et al., 2009
<i>Phylloscopus collybita</i>	2.37	49.29	R	de la Hera et al., 2011
<i>Psaltriparus minimus</i>	1.97	49.28	R	de la Hera, DeSante, & Milá, 2012
<i>Aegithalos caudatus</i>	2.4	58.36	R	de la Hera et al., 2011
<i>Acrocephalus scirpaceus</i>	2.66	54.91	R	de la Hera et al., 2011
<i>Acrocephalus schoenobaenus</i>	2.38	48.28	R	de la Hera et al., 2011
<i>Acrocephalus schoenobaenus</i>	2.6	53	P	Rohwer et al., 2009
<i>Acrocephalus arundinaceus</i>	3.4	74	P	Rohwer et al., 2009
<i>Sylvia atricapilla</i>	2.95	62.87	R	Carbonell & Tellería, 1999
<i>Sylvia atricapilla</i>	2.99	63.31	R	Carbonell & Tellería, 1999
<i>Sylvia atricapilla</i>	3.01	63.04	R	Carbonell & Tellería, 1999
<i>Sylvia atricapilla</i>	3.08	63.95	R	de la Hera et al., 2011
<i>Sylvia borin</i>	3.04	59.04	R	de la Hera et al., 2011
<i>Sylvia communis</i>	3.35	66.03	R	de la Hera et al., 2011
<i>Prinia gracilis</i>	2.25	56.5	R	Yosef, 1997
<i>Prinia gracilis</i>	2.33	57.2	R	Yosef, 1997
<i>Toxostoma rufum</i>	4.13	109.81	R	de la Hera, DeSante, & Milá, 2012
<i>Mimus polyglottos</i>	4.4	106.45	R	de la Hera, DeSante, & Milá, 2012
<i>Dumetella carolinensis</i>	3.87	87.67	R	de la Hera, DeSante, & Milá, 2012
<i>Sturnus vulgaris</i>	3.8	70	R	White, Kennedy, & Stouffer, 1991
<i>Sturnus vulgaris</i>	3.8	69.4	R	White, Kennedy, & Stouffer, 1991
<i>Sturnus vulgaris</i>	3.9	70.4	R	White, Kennedy, & Stouffer, 1991
<i>Zoothera naevia</i>	3.6	95.3	R	de la Hera, DeSante, & Milá, 2012
<i>Hylocichla mustelina</i>	3.41	78.37	R	de la Hera, DeSante, & Milá, 2012
<i>Catharus ustulatus</i>	3.59	75.67	R	de la Hera, DeSante, & Milá, 2012
<i>Catharus guttatus</i>	3.51	74.49	R	de la Hera, DeSante, & Milá, 2012
<i>Catharus fuscescens</i>	3.64	76.31	R	de la Hera, DeSante, & Milá, 2012
<i>Catharus minimus</i>	3.86	81.59	R	de la Hera, DeSante, & Milá, 2012
<i>Turdus migratorius</i>	4.44	105.84	R	de la Hera, DeSante, & Milá, 2012
<i>Turdus merula</i>	4.6	116	R	de la Hera et al., 2011
<i>Turdus philomelos</i>	4.07	88.31	R	de la Hera et al., 2011
<i>Sialia sialis</i>	3.13	70.34	R	de la Hera, DeSante, & Milá, 2012
<i>Sialia mexicana</i>	3.15	74.84	R	de la Hera, DeSante, & Milá, 2012
<i>Luscinia megarhynchos</i>	3.35	69.42	R	de la Hera et al., 2011
<i>Luscinia luscinia</i>	4.2	69	P	Rohwer et al., 2009

<i>Luscinia svecica</i>	3.2	57	P	Rohwer et al., 2009
<i>Oenanthe oenanthe</i>	3.8	72	P	Rohwer et al., 2009
<i>Phoenicurus phoenicurus</i>	3.04	62.38	R	de la Hera et al., 2011
<i>Erithacus rubecula</i>	2.56	61.98	R	de la Hera et al., 2011
<i>Sitta carolinensis</i>	2.51	52.36	R	de la Hera, DeSante, & Milá, 2012
<i>Sitta carolinensis</i>	1.98	51.32	R	Dolby & Grubb, 1998
<i>Sitta carolinensis</i>	2.37	51.73	R	Grubb & Cimprich, 1990
<i>Bombycilla cedrorum</i>	3.06	63.53	R	de la Hera, DeSante, & Milá, 2012
<i>Regulus calendula</i>	2.3	49.14	R	de la Hera, DeSante, & Milá, 2012
<i>Carduelis carduelis</i>	2.69	51.22	R	de la Hera et al., 2011
<i>Carduelis tristis</i>	2.55	53.26	R	de la Hera, DeSante, & Milá, 2012
<i>Carduelis psaltria</i>	2.34	45.99	R	de la Hera, DeSante, & Milá, 2012
<i>Carduelis pinus</i>	2.5	51.37	R	de la Hera, DeSante, & Milá, 2012
<i>Carduelis flammea</i>	2.9	58	P	Rohwer et al., 2009
<i>Carduelis chloris</i>	2.73	57.45	R	de la Hera et al., 2011
<i>Carduelis chloris</i>	2.4	70	P	Rohwer et al., 2009
<i>Carpodacus purpureus</i>	3	64.21	R	de la Hera, DeSante, & Milá, 2012
<i>Carpodacus cassinii</i>	2.99	67.83	R	de la Hera, DeSante, & Milá, 2012
<i>Carpodacus mexicanus</i>	3.01	66.99	R	de la Hera, DeSante, & Milá, 2012
<i>Carpodacus mexicanus</i>	3	64	P	Rohwer et al., 2009
<i>Pyrrhula pyrrhula</i>	2.4	73	P	Rohwer et al., 2009
<i>Coccothraustes vespertinus</i>	3.16	69.71	R	de la Hera, DeSante, & Milá, 2012
<i>Fringilla coelebs</i>	3.42	70.85	R	de la Hera et al., 2011
<i>Miliaria calandra</i>	3.59	81.69	R	de la Hera et al., 2011
<i>Amphispiza bilineata</i>	3.26	62.4	R	de la Hera, DeSante, & Milá, 2012
<i>Spizella breweri</i>	3.05	62.53	R	de la Hera, DeSante, & Milá, 2012
<i>Spizella pusilla</i>	3.01	66.08	R	de la Hera, DeSante, & Milá, 2012
<i>Spizella passerina</i>	3	63.1	R	de la Hera, DeSante, & Milá, 2012
<i>Passerella iliaca</i>	3.6	77.78	R	de la Hera, DeSante, & Milá, 2012
<i>Spizella arborea</i>	2.83	68.48	R	White & Kennedy, 1992
<i>Junco hyemalis</i>	3.09	66.84	R	de la Hera, DeSante, & Milá, 2012
<i>Junco phaeonotus</i>	3.07	72.89	R	de la Hera, DeSante, & Milá, 2012
<i>Zonotrichia atricapilla</i>	3.58	79.69	R	de la Hera, DeSante, & Milá, 2012
<i>Zonotrichia leucophrys</i>	3.27	73.04	R	de la Hera, DeSante, & Milá, 2012
<i>Zonotrichia albicollis</i>	3.33	76	R	de la Hera, DeSante, & Milá, 2012
<i>Pipilo erythrophthalmus</i>	3.65	88.91	R	de la Hera, DeSante, & Milá, 2012
<i>Pipilo fuscus</i>	3.68	92.36	R	de la Hera, DeSante, & Milá, 2012

<i>Pipilo crissalis</i>	3.7	94.58	R	de la Hera, DeSante, & Milá, 2012
<i>Melospiza lincolnii</i>	2.52	56.15	R	de la Hera, DeSante, & Milá, 2012
<i>Melospiza georgiana</i>	2.73	58.79	R	de la Hera, DeSante, & Milá, 2012
<i>Melospiza melodia</i>	2.95	63.62	R	de la Hera, DeSante, & Milá, 2012
<i>Icterus galbula</i>	3.51	71.29	R	de la Hera, DeSante, & Milá, 2012
<i>Icterus bullockii</i>	3.59	78.81	R	de la Hera, DeSante, & Milá, 2012
<i>Molothrus ater</i>	3.79	77.4	R	de la Hera, DeSante, & Milá, 2012
<i>Agelaius phoeniceus</i>	4.14	86.34	R	de la Hera, DeSante, & Milá, 2012
<i>Seiurus aurocapilla</i>	2.89	58.3	R	de la Hera, DeSante, & Milá, 2012
<i>Vermivora celata</i>	2.57	51.41	R	de la Hera, DeSante, & Milá, 2012
<i>Vermivora virginiae</i>	2.59	51.66	R	de la Hera, DeSante, & Milá, 2012
<i>Vermivora pinus</i>	2.55	47.21	R	de la Hera, DeSante, & Milá, 2012
<i>Mniotilta varia</i>	2.77	53.37	R	de la Hera, DeSante, & Milá, 2012
<i>Seiurus motacilla</i>	2.9	56.17	R	de la Hera, DeSante, & Milá, 2012
<i>Seiurus noveboracensis</i>	3.07	57.37	R	de la Hera, DeSante, & Milá, 2012
<i>Protonotaria citrea</i>	2.62	47.67	R	de la Hera, DeSante, & Milá, 2012
<i>Limnothlypis swainsonii</i>	2.58	52.26	R	de la Hera, DeSante, & Milá, 2012
<i>Oporornis formosus</i>	2.59	51.12	R	de la Hera, DeSante, & Milá, 2012
<i>Oporornis tolmiei</i>	2.62	57.33	R	de la Hera, DeSante, & Milá, 2012
<i>Oporornis philadelphia</i>	2.47	49.08	R	de la Hera, DeSante, & Milá, 2012
<i>Geothlypis trichas</i>	2.49	50.74	R	de la Hera, DeSante, & Milá, 2012
<i>Dendroica pensylvanica</i>	2.62	49.75	R	de la Hera, DeSante, & Milá, 2012
<i>Dendroica petechia</i>	2.62	49.23	R	de la Hera, DeSante, & Milá, 2012
<i>Dendroica pinus</i>	2.73	58.87	R	de la Hera, DeSante, & Milá, 2012
<i>Parula americana</i>	2.24	42.34	R	de la Hera, DeSante, & Milá, 2012
<i>Dendroica magnolia</i>	2.56	52.12	R	de la Hera, DeSante, & Milá, 2012
<i>Wilsonia citrina</i>	2.7	56.63	R	de la Hera, DeSante, & Milá, 2012
<i>Wilsonia pusilla</i>	2.58	51.03	R	de la Hera, DeSante, & Milá, 2012
<i>Ergaticus ruber</i>	4.02	98.58	R	de la Hera, DeSante, & Milá, 2012
<i>Wilsonia canadensis</i>	2.71	53.35	R	de la Hera, DeSante, & Milá, 2012
<i>Helmitheros vermivorum</i>	2.72	52.08	R	de la Hera, DeSante, & Milá, 2012
<i>Icteria virens</i>	3.73	76.69	R	de la Hera, DeSante, & Milá, 2012
<i>Passerina caerulea</i>	3.55	71.62	R	de la Hera, DeSante, & Milá, 2012
<i>Passerina amoena</i>	3.23	59.73	R	de la Hera, DeSante, & Milá, 2012
<i>Passerina cyanea</i>	2.91	55.04	R	de la Hera, DeSante, & Milá, 2012
<i>Passerina ciris</i>	3.13	60.84	R	de la Hera, DeSante, & Milá, 2012
<i>Piranga rubra</i>	3.83	79.68	R	de la Hera, DeSante, & Milá, 2012

<i>Piranga olivacea</i>	3.58	72.82	R	de la Hera, DeSante, & Milá, 2012
<i>Piranga ludoviciana</i>	3.58	77.42	R	de la Hera, DeSante, & Milá, 2012
<i>Piranga flava</i>	3.24	84.42	R	de la Hera, DeSante, & Milá, 2012
<i>Pheucticus melanocephalus</i>	3.47	82.03	R	de la Hera, DeSante, & Milá, 2012
<i>Pheucticus ludovicianus</i>	3.68	77.59	R	de la Hera, DeSante, & Milá, 2012
<i>Sporophila torqueola</i>	2.33	44.87	R	de la Hera, DeSante, & Milá, 2012
<i>Motacilla alba</i>	4.5	67	P	Rohwer et al., 2009
<i>Passer domesticus</i>	3.17	64.51	R	de la Hera et al., 2011
<i>Passer domesticus</i>	3.03	62.93	R	de la Hera, DeSante, & Milá, 2012
<i>Passer domesticus</i>	2.7	57	P	Rohwer et al., 2009
<i>Passer montanus</i>	3.07	57.68	R	de la Hera et al., 2011
<i>Pandion haliaetus</i>	7.9	372	P	Rohwer et al., 2009
<i>Gypaetus barbatus</i>	6.6	600	P	Rohwer et al., 2009
<i>Gyps africanus</i>	4.4	440	P	Rohwer et al., 2009
<i>Picoides pubescens</i>	2.39	50.04	R	Grubb & Cimprich, 1990
<i>Picoides pubescens</i>	2.45	49.71	R	Grubb & Cimprich, 1990
<i>Picoides pubescens</i>	2.34	50.07	R	Grubb, 1989
<i>Picoides pubescens</i>	2.35	50.16	R	Grubb, 1989
<i>Picoides pubescens</i>	2.48	52.64	R	Grubb, 1989
<i>Picoides pubescens</i>	2.6	50.74	R	Grubb, 1989
<i>Halcyon leucocephala</i>	3.6	78	P	Rohwer et al., 2009
<i>Streptopelia roseogrisea</i>	5.5	129	P	Rohwer et al., 2009

References

- Carbonell, R., & Tellería, J. L. (1999). Feather traits and ptilochronology as indicators of stress in Iberian blackcaps *Sylvia atricapilla*. *Bird Study*, 46(2), 243–248. <https://doi.org/10.1080/00063659909461136>
- de la Hera, I., DeSante, D. F., & Milá, B. (2012). Feather growth rate and mass in Nearctic passerines with variable migratory behavior and molt pattern. *The Auk*, 129(2), 222–230. <https://doi.org/10.1525/auk.2012.11212>
- de la Hera, I., Schaper, S. V., Díaz, J. A., Pérez-Tris, J., Bensch, S., & Tellería, J. L. (2011). How much variation in the molt duration of passerines can be explained by the growth rate of tail feathers? *The Auk*, 128(2), 321–329. <https://doi.org/10.1525/auk.2011.10181>
- Dolby, A. S., & Grubb, T. C. (1998). Benefits to satellite members in mixed-species foraging groups: An experimental analysis. *Animal Behaviour*, 56(2), 501–509. <https://doi.org/10.1006/anbe.1998.0808>
- Grubb, T. C. (1989). Ptilochronology - feather growth bars as indicators of nutritional-status. *The Auk*, 106(2), 314–320.
- Grubb, T. C., & Cimprich, D. A. (1990). Supplementary food improves the nutritional condition of wintering woodland birds: evidence from ptilochronology. *Ornis Scandinavica*, 21(4), 277–281.
- Grubb, T. C., & Yosef, R. (1994). Habitat-specific nutritional condition in loggerhead shrikes (*Lanius ludovicianus*): Evidence from ptilochronology. *The Auk*, 111(3), 756–759.
- Langston, N. E., & Rohwer, S. (1996). Molt-breeding trade-offs in albatrosses: life history implications for big birds. *Oikos*, 76(3), 498–510.

- Matysioková, B., & Remeš, V. (2010). Assessing the usefulness of ptilochronology in the study of melanin- and carotenoid-based ornaments in the great tit *Parus major*. *Ibis*, 152(2), 397–401. <https://doi.org/10.1111/j.1474-919X.2009.01002.x>
- Rohwer, S., Ricklefs, R. E., Rohwer, V. G., & Copple, M. M. (2009). Allometry of the duration of flight feather molt in birds. *PLoS Biology*, 7(6). <https://doi.org/10.1371/journal.pbio.1000132>
- Saino, N., Romano, M., Caprioli, M., Ambrosini, R., Rubolini, D., Scandolara, C. and Romano, A. (2012). A ptilochronological study of carry-over effects of conditions during wintering on breeding performance in the barn swallow *Hirundo rustica*. *Journal of Avian Biology* 43, 513–524
- Waite, T. A. (1990). Effects of caching supplemental food on induced feather regeneration in wintering gray jays *Perisoreus canadensis*: a ptilochronology study. *Ornis Scandinavica*, 21(2), 122–128. <https://doi.org/10.2307/3676807>
- White, D. W., & Kennedy, E. D. (1992). Growth of induced feathers in photostimulated American tree sparrows. *The Condor*, 94(2), 543–545. <https://doi.org/10.2307/1369230>
- White, D. W., Kennedy, E. D., & Stouffer, P. C. (1991). Feather regrowth in female European starlings rearing broods of different sizes. *The Auk*, 108(4), 889–895. <https://doi.org/10.1016/j.res.2016.07.018>
- Yosef, R. (1997). On habitat-specific nutritional condition in graceful warblers *Prinia gracilis*: Evidence from ptilochronology. *Journal für Ornithologie*, 138(3), 309–313. <https://doi.org/10.1007/BF01651556>

Table S2 Phylogenetic generalized least squares (PGLS) models for feather growth rate (FGR) based on feather length (FL) per feather type

PGLS models, with Pagel's λ based on the phylogenetic tree, were fitted to log₁₀ FGR as response variable and log₁₀ FL as predictor, for data found in literature ($n = 164$ species) and this study ($n = 4$ species). To determine if feather type had an effect, both models were compared using Fisher's z (see methods). Pagel's λ is the phylogenetic signal, with values between 0 and 1. All p -values ≤ 0.05 are **bolded**.

Feather type	Predictor	Pagel's λ	Value	SE	t-value	Pr(> t)
Rectrices	Intercept	0.987	-0.828	0.080	-10.345	< 0.001
	Log ₁₀ FL		0.658	0.040	16.576	< 0.001
Primaries	Intercept	0.903	-0.276	0.241	-1.145	0.259
	Log ₁₀ FL		0.419	0.100	4.187	< 0.001

4. Research Paper no. 2

Ausems, A.N.M.A., Skrzypek, G., Wojczulanis-Jakubas, K., Jakubas, D. 2020
Sharing menus and kids' specials: Inter- and intraspecific differences in stable
isotope niches between sympatrically breeding storm-petrels, *Science of the
Total Environment*, 728, 138768,
<https://doi.org/10.1016/j.scitotenv.2020.138768>



Sharing menus and kids' specials: Inter- and intraspecific differences in stable isotope niches between sympatrically breeding storm-petrels

Anne N.M.A. Ausems^{a,*}, Grzegorz Skrzypek^b, Katarzyna Wojczulanis-Jakubas^a, Dariusz Jakubas^a

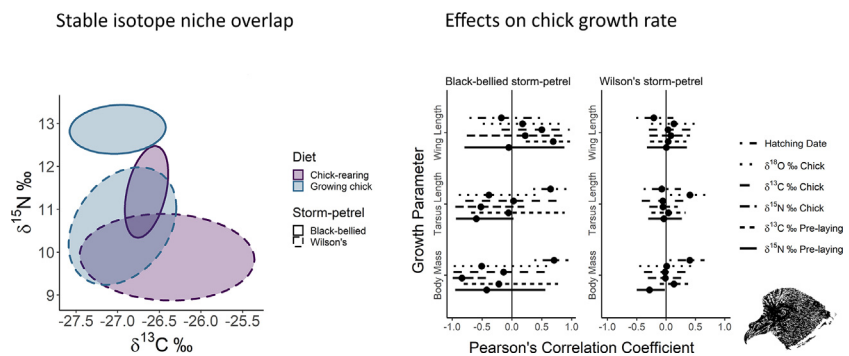
^a The University of Gdańsk, Faculty of Biology, Department of Vertebrate Ecology and Zoology, ul. Wita Stwosza 59, 80-308 Gdańsk, Poland

^b The University of Western Australia, School of Biological Sciences, West Australian Biogeochemistry Centre, 35 Stirling Highway, Crawley, WA 6009, Australia

HIGHLIGHTS

- 2 species of sympatrically breeding storm-petrels show considerable niche overlap.
- Black-bellied storm-petrel chick diet represents higher trophic level than adults.
- Wilson's storm-petrel chick and adult diet overlap considerably.
- Chick growth is mainly correlated with hatching date and $\delta^{15}\text{N}$ of the chick diet.
- Highly productive ecosystems may facilitate considerable foraging niche overlap.

GRAPHICAL ABSTRACT



ARTICLE INFO

Article history:

Received 9 March 2020

Received in revised form 15 April 2020

Accepted 15 April 2020

Available online 19 April 2020

Editor: Frederic Coulon

Keywords:

Stable isotopes

Niche partitioning

Chick growth rate

Wilson's storm-petrel

Black-bellied storm-petrel

Antarctica

ABSTRACT

Species sharing resources are predicted to compete, but co-occurring species can avoid competition through niche partitioning. Here, we investigated the inter- and intra-specific differences using stable isotope analyses in the black-bellied storm-petrel (*Fregatta tropica*) and the Wilson's storm-petrel (*Oceanites oceanicus*), breeding sympatrically in maritime Antarctica. We analysed stable carbon, nitrogen and oxygen isotopes in samples representing different life stages; chick down (pre-laying females), chick feather (chick), and adult blood (chick-rearing adults). Pre-laying females had wider stable isotope niches than chicks or chick-rearing adults, due to pre-laying females being free roaming while chick-rearing adults were central-place-foragers. Chicks were fed at a higher trophic level than the adults (higher $\delta^{15}\text{N}$), likely to compensate for the high nutritional demands of the growing chicks. Wilson's storm-petrels showed substantial overlap in stable isotope niches between all life stages, while the black-bellied storm-petrel chicks showed very little overlap. Wilson's storm-petrel niches significantly overlapped with those of pre-laying and chick-rearing black-bellied storm-petrels, suggesting negligible niche partitioning. Chick growth rate was negatively correlated with chick $\delta^{15}\text{N}$ values, suggesting nutritional stress resulting in the use endogenous instead of dietary amino acids in protein synthesis. The higher trophic level of the relatively larger black-bellied storm-petrel chicks may be due to their longer stay in the nest, and relatively larger body mass gain, despite chick growth rates being similar to the smaller Wilson's storm-petrel chicks. Despite breeding sympatrically, the studied storm-petrel species showed considerable overlap in isotopic niches, which may be explained by sharing the same main prey species, reducing the detectability of foraging niche partitioning through stable isotope analyses. We found dietary shifts in black-bellied storm-petrels that are absent in Wilson's, showing different chick provisioning strategies, and shows that the high productivity of the Antarctic marine ecosystem may facilitate foraging niche overlap of sympatrically living species.

© 2020 The Authors. Published by Elsevier B.V. This is an open access article under the CC BY license (<http://creativecommons.org/licenses/by/4.0/>).

* Corresponding author.

E-mail address: anne.ausems@gmail.com (A.N.M.A. Ausems).

1. Introduction

According to the niche theory, two or more species cannot permanently and simultaneously occupy exactly the same foraging niche if resources are limited, as interspecific competition would lead to one of them outcompeting the other (Hutchinson, 1957). Therefore, to avoid competition, sympatric species are expected to show foraging niche partitioning through spatial or temporal separation, or through foraging specialisation (Robertson et al., 2014). In sympatric seabird species, spatial foraging niche segregation can manifest, for example, in species foraging at different distances from a shared breeding ground (Barger et al., 2016; Robertson et al., 2014), at different depths in the water column (Masello et al., 2010; Wilson, 2010), or in different front areas (Force et al., 2015). Temporal segregation can occur through alternating foraging areas between species over the season (Clewlow et al., 2019) or day (Wilson, 2010), or staggered breeding (Croxall and Prince, 1980; Hatch and Hatch, 1990). Species with overlapping diets may avoid competition through prey selection, e.g., prey size preferences (Marinao et al., 2019) or generalist vs. specialist foraging (Polito et al., 2015). These preferences can manifest, for example, in differences in morphology, such as in bill shape (Pol et al., 2009) or hunting behaviours (Warham, 1996).

Consequently, niche partitioning results in differences in the size and shape of species' foraging niches, also described as their niche width (Roughgarden, 1972). Within species, niche widths can vary between colonies (Corman et al., 2016), age cohorts (Pelletier et al., 2014) and the sexes (Miller et al., 2018), and many species show differences in foraging niches between seasons (Cherel et al., 2007; Jaeger et al., 2010). When the availability of a preferred food decreases species may increase the width of their foraging niches (Carvalho and Davoren, 2019), switching to other food sources. Additionally, niche widths may change due to competition; niche widths can increase as the preferred prey becomes unavailable and individuals switch to a wider range of prey (Namgail et al., 2009; Svanbäck and Bolnick, 2007) or decrease as prey availability decreases for the focal species if the preferred prey becomes monopolised by more specialised species with better competitive abilities (Namgail et al., 2009).

The diet of a species determines its place in the food web, or trophic level (Lindeman, 1942). Trophic levels in relatively uncomplicated food webs, such as polar food networks, generally increases from invertebrates to fish, and from short-lived to long-lived prey species, although there is an overlap on species level (Hobson and Welch, 1992; Pauly et al., 1998). Within and between years seabird trophic levels can differ depending on seasonal prey availability, weather conditions or energetic demands (Davies et al., 2009; Moody et al., 2012). Additionally, parents and offspring can differ in trophic level (Davies et al., 2009), as can the sexes (Phillips et al., 2004) due to differing nutritional requirements.

Stable isotope analyses are currently widely used to study animal foraging niches (Newsome et al., 2007; Quillfeldt et al., 2005). They are particularly useful for pelagic seabirds that are important ecosystem components (Furness and Camphuysen, 1997) but challenging to study due to their often inaccessible foraging and breeding locations. Stable carbon and nitrogen isotopic signatures ($\delta^{13}\text{C}$ and $\delta^{15}\text{N}$) are most commonly used (Quillfeldt et al., 2005), because of their link with the food web. $\delta^{15}\text{N}$ increases stepwise with trophic level (Minagawa and Wada, 1984). $\delta^{13}\text{C}$ is linked to foraging areas: in the Southern Ocean $\delta^{13}\text{C}$ of particulate organic matter predictably decreases with latitude (Quillfeldt et al., 2005), related to different water masses (Cherel and Hobson, 2007), and can thus be used to identify foraging areas of seabirds in the Southern hemisphere. In this study, we also analysed $\delta^{18}\text{O}$ which like $\delta^{13}\text{C}$ differs between water masses but is mainly correlated with temperature (LeGrande and Schmidt, 2006) and freshwater input (Bigg and Rohling, 2000). Thus, including $\delta^{18}\text{O}$ allows identifying foraging areas more precisely.

Using stable isotope analyses of the three elements ($\delta^{15}\text{N}$, $\delta^{13}\text{C}$, $\delta^{18}\text{O}$), we aimed to study the extent of isotopic niche partitioning during the breeding season between two species of small, pelagic seabirds breeding sympatrically in maritime Antarctica (Jabłoński, 1986; Sierakowski, 1991; Sierakowski et al., 2017); the black-bellied storm-petrel (*Fregetta tropica*; hereafter BBSP) and the Wilson's storm-petrel (*Oceanites oceanicus*; hereafter WSP). Considering niche theory predictions, the fact that the species share the same guild and overlap in breeding areas, but are of different body size, we expected them to show differences in foraging niches. Previous research (Beck and Brown, 1971; Hahn, 1998a; Quillfeldt, 2002; Ridoux, 1994), although limited, indicated a higher proportion of fish in BBSP than in WSP diets. Following the results of these studies, we expected BBSP to forage at a higher trophic level than WSP, but to show considerable overlap. Further, given documented differences in diet composition, with the diet of the BBSP being more diverse (Beck and Brown, 1971; Hahn, 1998a; Ridoux, 1994), we expected its niche widths to be larger than those of WSP.

Additionally, we investigated the within-species differences in isotopic niches between samples representing different life stages (i.e. chick down representing pre-laying females, adult blood representing chick-rearing adults and chick feathers representing growing chicks), and the correlations between isotopic signatures and chick growth rates (i.e. body mass, tarsus length and wing length). During the pre-laying period, the storm-petrels are free to roam further away from the colony to forage than they are during the chick rearing period, when they have to return to the nest for chick provisioning. Therefore, we expected isotopic niches to be wider during the pre-laying period than during the chick-rearing period, as has also been observed in Arctic Terns (*Sterna paradisaea*) (Pratte et al., 2018). As $\delta^{15}\text{N}$ is often linked to trophic level (Minagawa and Wada, 1984) and thus diet and possibly caloric values, we expected to find the strongest correlation between $\delta^{15}\text{N}$ in chick feathers and chick growth rates, compared to $\delta^{13}\text{C}$ or $\delta^{18}\text{O}$. Furthermore, we expected chicks to be fed at a higher trophic level than adults to meet their high nutritional demands during growth, as has been observed in other seabirds foraging on krill and fish [(Forero et al., 2002; Hodum and Hobson, 2000; Rosciano et al., 2019), but see Booth and McQuaid, 2013].

Since we performed the study for two breeding seasons, due to potential inter-annual differences in storm-petrel prey availability driven by environmental conditions (Siegel, 2012), the inter-annual differences in diet composition should be reflected by differences in isotopic signatures of the sampled tissues (Moody et al., 2012). To control for this inter-annual variability in environmental conditions affecting foraging storm-petrels we compared sea surface temperature and chlorophyll-*a* (Santora et al., 2017) in potential foraging areas between the studied breeding seasons.

The results of our study are important to understand the functioning of the Antarctic food web that is currently experiencing rapidly occurring changes due to global climate change (Henley et al., 2019) and intensive harvesting of marine living resources (Krüger, 2019). WSP is considered one of the most abundant seabirds worldwide (Warham, 1990), and plays a significant role in the food web of the Southern Ocean and nutrients cycling. BBSP is one of the least studied storm petrels in the sub Antarctic and Antarctic region (e.g., 10 and 15 results total in Web of Science for "*black-bellied storm-petrel*" and "*Fregetta tropica*", respectively). It has only been a subject of a few studies of breeding and foraging ecology, with limited sample sizes ($n = 2-6$) for chicks (Beck and Brown, 1971; Hahn, 1998b), hence basic studies considering the birds foraging ecology are still needed (Büßer et al., 2008). These features underline the importance of fundamental knowledge of foraging ecology of these two species and their use as model organisms for questions regarding the adaptation to environmental variability in the maritime Antarctic (Büßer et al., 2008).

Table 1

Means and standard deviations of the isotopic values for both studied storm-petrel species:

BBSP – black-bellied storm-petrel; WSP – Wilson’s storm-petrel; n – sample size; chick-rearing – adult blood; Pre-laying – chick down; chick – chick feather (under-tail covert); blood was only collected in 2018; $\delta^{18}\text{O}$ was only analysed for chick feathers, and not determined separately per year for WSP due to low sample sizes in 2017.

Pooled values between years for both species						
Species	Life stage	n ($\delta^{13}\text{C}$ & $\delta^{15}\text{N}$)	$\delta^{13}\text{C}$ (‰ VPDB) Mean ± SD	$\delta^{15}\text{N}$ (‰ AIR) Mean ± SD	n ($\delta^{18}\text{O}$)	$\delta^{18}\text{O}$ (‰ VSMOW) Mean ± SD
BBSP	Chick-rearing	20	-26.65 ± 0.12	11.42 ± 0.49	-	-
	Pre-laying	10	-26.54 ± 0.39	10.80 ± 0.47	-	-
	Chick	8	-27.00 ± 0.20	12.87 ± 0.21	7	13.03 ± 1.29
WSP	Chick-rearing	32	-26.40 ± 0.47	9.92 ± 0.47	-	-
	Pre-laying	64	-26.36 ± 0.73	9.73 ± 0.55	-	-
	Chick	56	-26.94 ± 0.36	10.64 ± 0.65	31	11.94 ± 1.08
Values per year for WSP						
Year	Life stage	n	$\delta^{13}\text{C}$ (‰ VPDB) Mean ± SD	$\delta^{15}\text{N}$ (‰ AIR) Mean ± SD		
2017	Pre-laying	34	-26.20 ± 0.59	9.91 ± 0.62		
	Chick	30	-26.85 ± 0.36	10.60 ± 0.61		
2018	Pre-laying	30	-26.52 ± 0.86	9.52 ± 0.36		
	Chick	26	-26.86 ± 0.39	10.68 ± 0.71		

2. Materials and methods

2.1. Study area

In the Austral summer of 2017 and 2018 we studied BBSP and WSP breeding around the Henryk Arctowski Polish Antarctic Station on King George Island, South Shetland Islands, Antarctica (62°09’S, 58°27’W) (Fig. A1). The study area is one of the main breeding aggregations of

both storm-petrel species in the Admiralty Bay area (Jabłoński, 1986). The majority of the nests of both studied species were located in separate colonies. Most WSP nests were located in a colony at Rakusa Point [see Sierakowski et al. (2017) for maps]. However, the BBSP colony at Point Thomas was mixed with some WSP nests. Compared to historical research (WSP n = 140) (Jabłoński, 1986), we found a similar number of accessible nest burrows but less active nests (WSP n = 44), suggesting relatively low competition over burrows.

Table 2

Bayesian Standard Ellipse Area Overlap for $\delta^{13}\text{C}$ and $\delta^{15}\text{N}$ for both studied storm-petrel species: Inter- and intra-specific Bayesian Standard Ellipse Area Overlap between the sampled tissue types for both years pooled; inter-annual overlap for WSP. Overlap was calculated as the percentage of shared area of each individual ellipse with each relevant other ellipse. CI – credible interval of 95%; Chick-rearing – adult blood; Pre-laying – chick down; Chick – chick feather (under-tail covert); BBSP – black-bellied storm-petrel; WSP – Wilson’s storm-petrel. Combinations with a mean overlap of <5% are bolded and with a mean overlap between 5 and 10% are in italics.

Interspecific overlap					
Life stage	Species	Versus	Mean (%)	Lower CI (%)	Upper CI (%)
Chick-rearing	BBSP	WSP	31.0	4.93	65.7
	WSP	BBSP	7.96	1.12	19.4
Pre-laying	BBSP	WSP	54.6	20.0	92.1
	WSP	BBSP	25.6	8.37	51.1
Chick	BBSP	WSP	5.88	0.00	56.9
	WSP	BBSP	1.24	0.00	10.3
Intraspecific overlap					
Species	Life stage	Versus	Mean (%)	Lower CI (%)	Upper CI (%)
BBSP	Chick-rearing	Pre-laying	59.5	2.77	100
	Chick-rearing	Chick	4.71	0.00	28.8
	Pre-laying	Chick-rearing	19.1	0.91	39.7
	Pre-laying	Chick	0.59	0.00	7.45
	Chick	Chick-rearing	5.34	0.00	31.6
	Chick	Pre-laying	2.76	0.00	35.6
WSP	Chick-rearing	Pre-laying	93.8	76.3	100
	Chick-rearing	Chick	49.8	76.3	100
	Pre-laying	Chick-rearing	54.0	35.8	76.6
	Pre-laying	Chick	36.8	25.3	50.5
	Chick	Chick-rearing	49.1	28.5	71.5
	Chick	Pre-laying	63.2	47.4	71.5
Inter-annual overlap WSP					
Life stage	Year	Versus	Mean (%)	Lower CI (%)	Upper CI (%)
Pre-laying	2017	2018	42.8	26.0	62.2
	2018	2017	67.7	37.6	94.4
Chick	2017	2018	32.8	14.7	53.0
	2018	2017	37.1	20.2	55.4

2.2. Study species

In both BBSP and WSP, the partners share parental duties during the breeding season (Wasilewski, 1986). WSP adults arrive at the colony from September (Sierakowski, 1991) to October (Wasilewski, 1986), and egg-laying occurs from December to February (Wasilewski, 1986). BBSPs breeding on Signy Island have been reported to return to the colony in November, and egg-laying to occur from December to January (Beck and Brown, 1971). Like the other storm-petrel species, they lay a single egg (Carboneras et al., 2017), which is incubated for 38–59 days in WSP and 38–44 days in BBSP. The egg may be left unattended for several days at a time, increasing the time between egg laying and chick hatching (Beck and Brown, 1972, 1971). Fledgling takes place after about 60 days (54–69 days) in WSP (Beck and Brown, 1972) and after 65–71 days in BBSP (Carboneras et al., 2017). Fledging during our study period had finished by mid-April (authors' unpublished data).

The exact ranges of foraging flights during the breeding period are unknown for the studied species, although for WSP they have been estimated to be up to around 200–250 km from the colony (Croxall and Prince, 1980; Pennycuik et al., 1984). Storm-petrels, like other Procellariiformes, may provision their chicks with stomach oil assimilated from ingested prey during longer foraging trips (Obst and Nagy, 1993; Warham et al., 1976).

2.3. Data collection

For the collection of blood/feather samples of adults, we captured individuals by hand while they were incubating in the nest and using mist-nets spread in the colony at night, throughout the chick-rearing period. We collected samples for stable isotope analyses representing three life-stages from adults and chicks. We collected a small amount of blood from adults' wing veins (BBSP $n = 20$, WSP $n = 32$), representing the adult diet during chick-rearing. During the late chick-rearing phase in both studied years, we collected a down sample from each chick (BBSP $n = 10$, WSP $n = 64$), representing the maternal, pre-laying diet, and a chick feather sample (i.e. an under-tail-covert; BBSP $n = 9$, WSP $n = 56$), representing the chick diet, from each surviving chick, except one BBSP chick that fledged before feather collection. All samples were stored in $-20\text{ }^{\circ}\text{C}$ until further processing.

To record chick growth, we performed regular nest checks every three days starting from hatching, weather permitting. We measured chick body mass to the nearest 0.1 g using a digital scale (Pesola PTS3000, Switzerland) and tarsus length to the nearest 0.1 mm using callipers. We started measuring wing length to the nearest 0.1 mm using callipers once pin feathers became visible.

If nests were blocked by snow, we postponed chick measurements until the next check when the nest was open. This was in order to prevent affecting breeding success by damaging the natural insulation

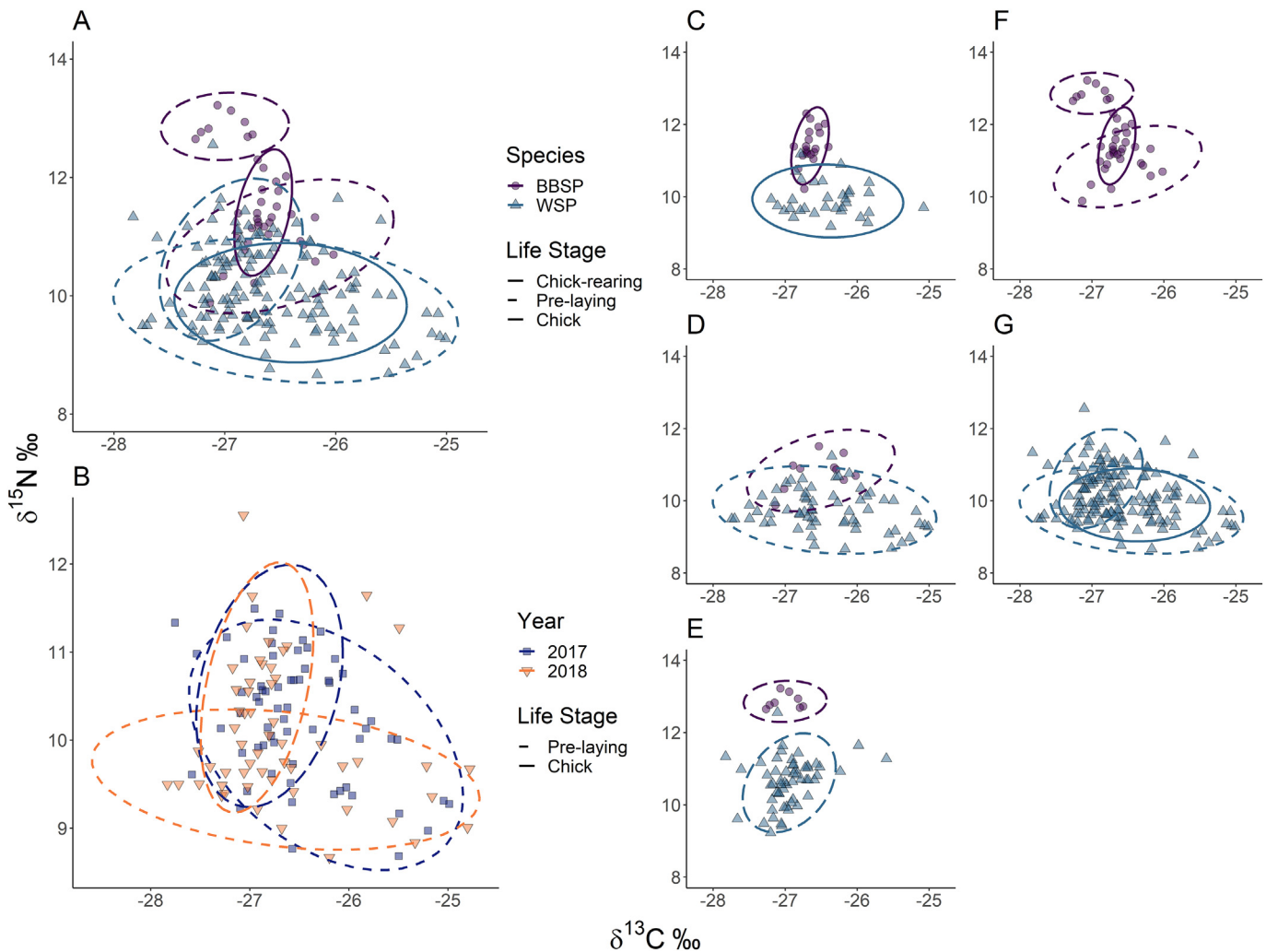


Fig. 1. Ellipse area overlap for $\delta^{13}\text{C}$ and $\delta^{15}\text{N}$ for both studied storm-petrels: Ellipse Areas encompass approximately 95% of the data. A – ellipses for both species in both studied years; B – ellipses for the Wilson's storm-petrels for 2017 and 2018 (blood was not collected in 2017); C–E – ellipses per life stage; F&G – ellipses per species. BBSP – black-bellied storm-petrels; WSP – Wilson's storm-petrels; chick-rearing – adult blood, collected throughout the breeding season; pre-laying – chick down; chick – chick feathers (under-tail coverts). See also Table 1 for overlap percentages.

Table 3

Bayesian Standard Ellipse Area Widths for $\delta^{13}\text{C}$ and $\delta^{15}\text{N}$ for both studied storm-petrel species: The Bayesian Standard Ellipse Areas based on data pooled between both years for both studied species of storm-petrels, and per year for WSP. CI – credible interval of 95%; chick-rearing – adult blood; pre-laying – chick down; chick – chick feather (under-tail covert); BBSP – black-bellied storm-petrel; WSP – Wilson's storm-petrel.

Species		BBSP		WSP	
Life stage	CI (%)	Lower ($\%^{2}$)	Upper ($\%^{2}$)	Lower ($\%^{2}$)	Upper ($\%^{2}$)
Chick-rearing	99	0.092	0.301	0.420	1.062
	95	0.104	0.258	0.467	0.949
	50	0.138	0.189	0.588	0.746
	Mode	0.159		0.663	
Pre-laying	99	0.189	1.279	0.856	1.690
	95	0.253	0.980	0.940	1.550
	50	0.385	0.610	1.109	1.312
	Mode	0.478		1.208	
Chick	99	0.047	0.353	0.478	1.000
	95	0.060	0.265	0.527	0.907
	50	0.093	0.154	0.628	0.754
	Mode	0.120		0.688	
Year		WSP ₂₀₁₇		WSP ₂₀₁₈	
Life stage	CI (%)	Lower ($\%^{2}$)	Upper ($\%^{2}$)	Lower ($\%^{2}$)	Upper ($\%^{2}$)
Pre-laying	99	0.638	1.615	0.546	1.491
	95	0.720	1.447	0.616	1.320
	50	0.917	1.623	0.795	1.018
	Mode	1.036		0.902	
Chick	99	0.386	1.066	0.433	1.344
	95	0.446	0.943	0.515	1.164
	50	0.580	0.745	0.684	0.897
	Mode	0.661		0.786	

properties of the snow, accidentally getting the chick wet or disturbing it's hypothermic state (Kuepper et al., 2018).

2.4. Stable isotope analyses

We freeze dried the blood samples for 48 h to prepare them for stable isotope analyses. The feather samples were washed in a 2:1 chloroform:methanol solution and twice in methanol, then air dried for 24 h and cut up into sub-millimetre sections using stainless steel scalpel blades. Stable nitrogen and carbon isotope compositions ($\delta^{15}\text{N}$ and $\delta^{13}\text{C}$) were analysed using a continuous flow system consisting of a Delta V Plus mass spectrometer connected with a Thermo Flush 1112 Elemental Analyzer via ConFlo IV (Thermo-Finnigan/Germany) (Skrzypek and Paul, 2006). We used multi-point normalisation to reduce raw values to the international scale (Skrzypek, 2013), based on international standards provided by IAEA: $\delta^{13}\text{C}$ – NBS22, USGS24, NBS19, LSVEC (Coplen, 1996); and for $\delta^{15}\text{N}$ – N1, N2, USGS32 and laboratory standards. Stable oxygen isotope composition ($\delta^{18}\text{O}$) of chick feather samples was analysed using a TC/EA coupled with Delta XL Mass Spectrometer in continuous flow mode (Thermo-Fisher Scientific). The $\delta^{18}\text{O}$ results were normalised to the VSMOW scale based on USGS42 and USGS43 and the equilibration method (Coplen and Qi, 2012). All $\delta^{13}\text{C}$ results are reported in ‰ on VPDB, $\delta^{15}\text{N}$ in ‰ on Air and $\delta^{18}\text{O}$ in ‰ on VSMOW scale (Skrzypek, 2013), with an external analytical uncertainty (one standard deviation) of 0.10‰ for $\delta^{13}\text{C}$ and $\delta^{15}\text{N}$, and 0.5‰ for $\delta^{18}\text{O}$. As we did not lipid-extract the samples, we mathematically corrected the $\delta^{13}\text{C}$ measurements for lipid-associated biases using the following equation (Cherel et al., 2014; Post et al., 2007):

$$\delta^{13}\text{C}_{\text{corrected}} = \delta^{13}\text{C} - 3.32 + (0.99 \times \text{C} : \text{N})$$

Additionally, due to differences in isotopic discrimination between tissues blood isotopic signatures should not be directly compared with feather isotopic signatures without controlling for the differences in discrimination factors (Quillfeldt et al., 2008). To calculate the difference in enrichment factors, we used three recaptured individuals in 2018 (1 BBSP, 2 WSPs) with feathers regrown over the season, for which we could calculate the enrichment factors between blood and feathers

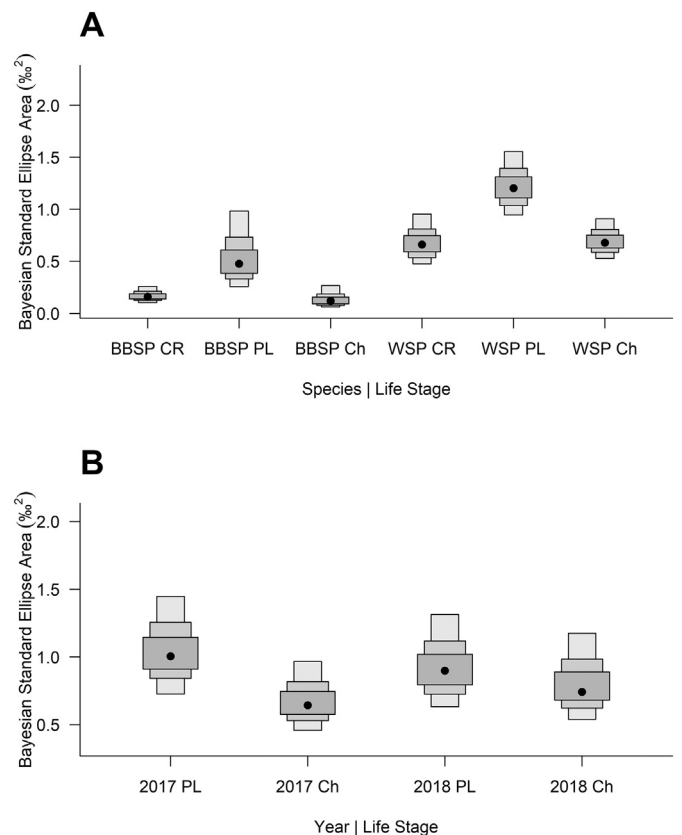


Fig. 2. Bayesian Standard Ellipse Areas (BSEA) for $\delta^{13}\text{C}$ and $\delta^{15}\text{N}$ for both studied storm-petrels: A – BSEAs for both species per tissue for both years; B – BSEAs for the Wilson's storm-petrels for each year per tissue (blood was not collected in 2017); box width and colour denote credible intervals (thick, dark grey – 50%, medium – 75%, narrow, light grey – 95%); black dots – median. BBSP – black-bellied storm-petrel; WSP – Wilson's storm-petrel; CR – chick-rearing adult, blood collected throughout the breeding season; PL – pre-laying female, chick down; Ch – chick, chick feathers (under-tail coverts). See also Table 2 for BSEA values.

isotopic signatures synthesised during the same time period (i.e. feather value minus blood value; BBSP: $\delta^{13}\text{C} + 0.64\text{‰}$, $\delta^{15}\text{N} + 0.84\text{‰}$; WSP: $\delta^{13}\text{C} + 0.55\text{‰}$, $\delta^{15}\text{N} + 0.46\text{‰}$). We then added these differences to the blood isotopic values to correct for the differences in isotopic discrimination before continuing with the statistical analyses.

2.5. Statistical analyses

We performed all statistical analyses in R version 3.6.1 (R Core Team, 2019). When comparing both species, we pooled the data between the years, as we did not have a large enough sample size for BBSP to analyse both years separately. Likewise, we had a too small sample size of $\delta^{18}\text{O}$ in 2017 for WSP. For $\delta^{13}\text{C}$ and $\delta^{15}\text{N}$ we did perform inter-annual comparisons in WSP. For growth rate analyses, we only considered fledged chicks and thus excluded the dead WSP chicks (8 in 2017 and 5 in 2018; no monitored BBSP chicks died).

2.5.1. Stable isotope niches

Due to the fact that $\delta^{18}\text{O}$ was only analysed in chick feathers (BBSP $n = 8$, WSP $n = 31$), and only for a subset of the WSPs in 2017 ($n = 5$), and the difference in sample sizes between $\delta^{13}\text{C}$ and $\delta^{15}\text{N}$, and $\delta^{18}\text{O}$, we decided to analyse isotopic niches both including and excluding $\delta^{18}\text{O}$. We started with a MANOVA with a Wilk's Lambda test (*manova*, package *stats*) to determine if the isotopic signatures differed

between the species (BBSP, WSP) and life stages (chick-rearing adult, pre-laying female, growing chick), (i.e. $\delta^{13}\text{C} + \delta^{15}\text{N} \sim \text{species} + \text{life stage} + \text{species}:\text{life stage}$). We removed the interaction if not significant. Then if we found significant results, we ran another MANOVA between species for each life stage separately (i.e. $\delta^{13}\text{C} + \delta^{15}\text{N} \sim \text{species}$) and within the species between life stages (i.e. $\delta^{13}\text{C} + \delta^{15}\text{N} \sim \text{life stage}$). For WSP we also added year as a factor (i.e. $\delta^{13}\text{C} + \delta^{15}\text{N} \sim \text{life stage} + \text{year}$) to test for inter-annual variability. If we found significant differences between the species, we used a Welch's two-sample *t*-test (*t.test*, package *stats*) to determine the extent of the difference for each significant isotope. If we found significant differences within species, we used a univariate ANOVA (*aov*, package *stats*) with a Tukey HSD *post hoc* test (*TukeyHSD*, package *stats*) for each isotope and the three life stages. WSP inter-annual variability was further explored during the chick growth rate analyses, described below.

We determined niche widths and overlap for $\delta^{13}\text{C}$ and $\delta^{15}\text{N}$ using the Stable Isotope Bayesian Ellipses in R (SIBER) package (Jackson et al., 2011). As a measure of foraging niches, we calculated posterior ellipses (*siberMVN*) for $\delta^{13}\text{C}$ and $\delta^{15}\text{N}$ in all three life stages for both species with 2×10^4 iterations, a 1×10^3 burnin, thinned by 10 and over 2 chains. We used uninformed priors, as we had no prior knowledge of our expected results. We determined the size of the niche width of each group using Bayesian Standard Ellipse Areas (BSEA, *siberEllipses*) and then used *bayesianOverlap* to calculate the niche overlap area

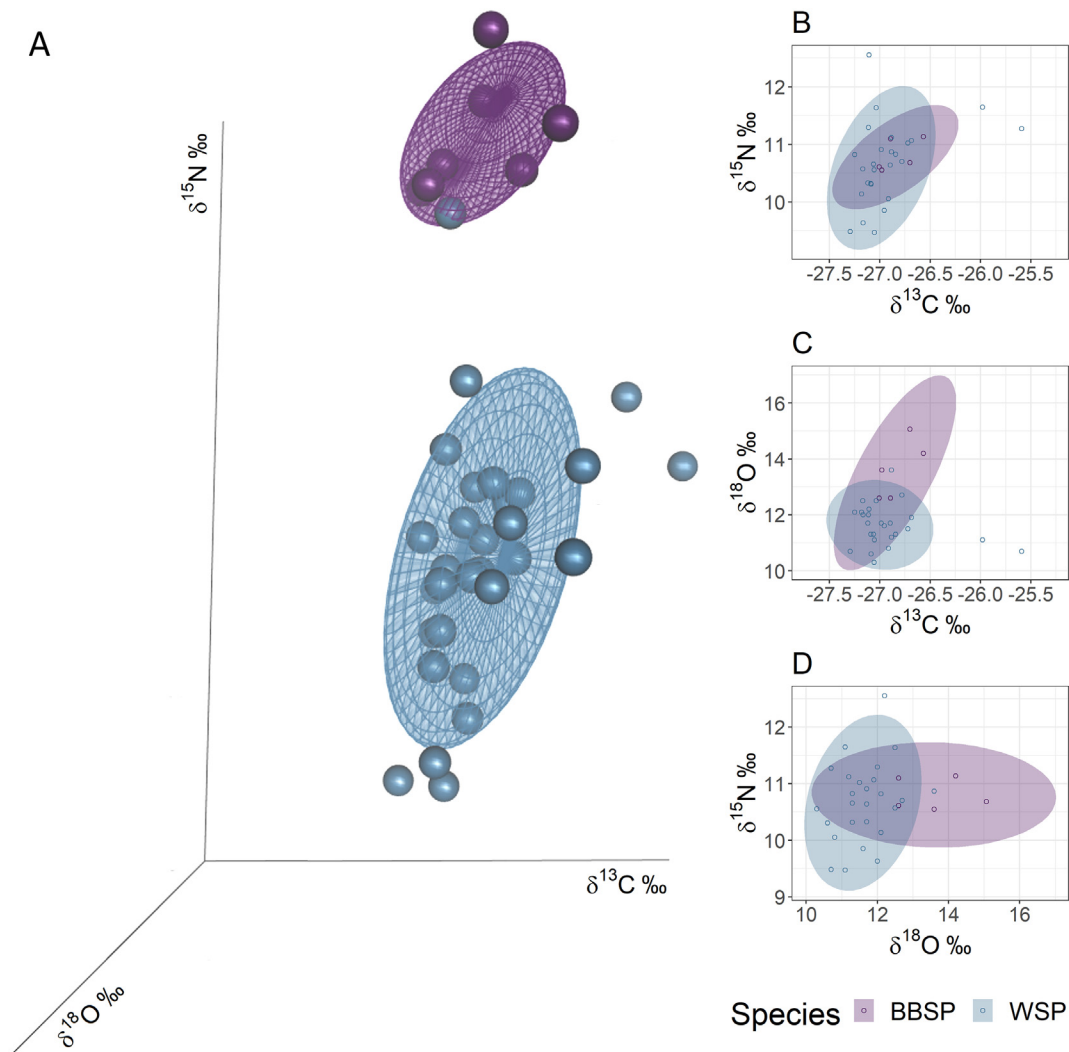


Fig. 3. Ellipsoid volume overlap for $\delta^{13}\text{C}$, $\delta^{15}\text{N}$ and $\delta^{18}\text{O}$ for chicks of both studied storm-petrels: A – ellipsoids containing ~50% of the data for both studied species in 3D; B–D – ellipse areas containing ~95% of the data for each isotope pair. BBSP – black-bellied storm-petrels; WSP – Wilson's storm-petrels.

between the corresponding Bayesian Estimates for the 95% Prediction Ellipse (BEPEA). In contrast to the suggested approach in SIBER, where niche overlap percentage is specified as the proportion of overlapping BEPEA relative to the non-overlapping BEPEA of both groups combined [i.e. overlapping BEPEA/(BEPEA group A + BEPEA group B — overlapping BEPEA)], we calculated niche overlap as the proportion of overlapping BEPE relative to the BEPE of each group separately (i.e. overlapping BEPE/BEPE group A or B). We did so because we were not interested in how much of the area overlapped, but rather in how much of each individual niche (i.e. species:life stage) overlapped with others.

Additionally, for both species we calculated chick niche widths and overlap including all three isotopes (i.e. $\delta^{13}\text{C}$, $\delta^{15}\text{N}$ and $\delta^{18}\text{O}$), following Rossman et al. (2016). We calculated the posterior ellipsoids for all three stable isotopes for chick feathers with 5×10^3 iterations, a burnin and adaptation of 1×10^3 , over three chains. We determined the niche width based on the Bayesian Standard Ellipsoid Volume (BSEV) and calculated niche overlap volume of the Bayesian Estimates for the 95% Prediction Ellipsoids (BEPEV), and calculated the percentage niche overlap as the proportion of overlapping BEPEV relative to the BEPEV of each group separately.

2.5.2. Chick growth

Due to logistic reasons and the extended period of egg-laying, we did not find all nests before hatching. In the first field work season (2017) we found five WSP nests before hatching, out of 25 nests followed that year, and one BBSP nest out of six in total. In 2018 we found 16 WSP nests before hatching out of 19 nests in total. We found all three BBSP nests followed in 2018 before hatching.

In order to determine chick growth rates, we calculated the predicted hatching date based on tarsus length (Quillfeldt and Peter, 2000). Firstly, we fitted a Non-linear Least Squares model (NLS) to the tarsus growth data from the chicks with known hatching dates (Fig. A2; Table A1), as tarsus growth follows an S-curve (Fig. A2) (Quillfeldt and Peter, 2000). We did this for both years separately for WSP but pooled the data for BBSP due to low sample sizes ($n = 8$). Then, we used the inverted NLS model to predict the age based on the tarsus measurement closest to the mid-point between minimum and maximum tarsus length, as an NLS model is most accurate at the linear growth phase. Since the chicks are not born with a tarsus length of zero, we used the following equation to calculate the mid-point for each chick:

$$mid = \left[TL_{max} \times \left(TL_{min} \times TL_{max}^{-1} \right) \right] + \left[TL_{max} \times \left(TL_{min} \times TL_{max}^{-1} \right)^2 \right]$$

where *mid* is the mathematical mid-point, and TL_{max} and TL_{min} are the maximum and minimum tarsus lengths measured for the known-age chicks, respectively. From the predicted age, we determined the predicted hatching date (*lm*, package *stats*; predicted hatching date ~ observed hatching date). This method was highly accurate for both species (BBSP $\beta \pm SE = 1.79 \pm 0.130$, $t = 13.83$, $p < 0.001$, adj. $R^2 = 0.745$, Fig. A3A; WSP $\beta \pm SE = 0.955 \pm 0.031$, $t = 31.09$, $p < 0.001$, adj. $R^2 = 0.780$, Fig. A3B). For comparability, in further analyses we used the predicted hatching date for all chicks.

To examine chick growth rates, we first plotted each parameter (i.e. tarsus growth, wing growth and log transformed body mass growth) against the predicted hatching date. Then, we visually determined the period of linear growth for each growth parameter per species, and per year for WSP (Table A2; Fig. A4). For each individual we selected all measurements within this period, and calculated the growth rate as the slope of a linear model (*lm*, package *stats*). We used Welch's *t*-tests to find inter-specific differences in the slope (*t.test*, package *stats*), with pooled data for both species. We calculated the variance inflation factor (VIF) (*vif*, package *car*) (Fox and Weisberg, 2011) to determine the level of multicollinearity for the growth parameters for both species and the datasets including and excluding $\delta^{18}\text{O}$. For BBSP VIF

Table 4

Bayesian Standard Ellipsoid Volumes for $\delta^{13}\text{C}$, $\delta^{15}\text{N}$ and $\delta^{18}\text{O}$ for chick feathers for both studied storm-petrel species: CI – credible interval; BBSP – black-bellied storm-petrel; WSP – Wilson's storm-petrel; n – sample size.

CI (%)	BBSP (n = 7)	WSP (n = 31)
2.5	0.971	0.919
50	2.127	1.375
97.5	5.345	2.163
Mode	1.679	1.272

ranged from 1.05 to 2.76 for the data excluding $\delta^{18}\text{O}$, and from 1.24 to 3.31 for the data including $\delta^{18}\text{O}$. For WSP VIF ranged from 1.02 to 1.42 when excluding $\delta^{18}\text{O}$, and from 1.06 to 2.54 when including $\delta^{18}\text{O}$. We deemed these values low enough to treat the growth parameters as independent (Neter et al., 1989; Rogerson, 2001).

Because the variance in growth rates (slope of regression for the period of linear growth) was relatively low within species (BBSP tarsus = 0.003, wing = 0.005, body mass = 0.022; WSP tarsus = 0.013, wing = 0.053, body mass = 0.010), and because of the relatively low sample sizes, we bootstrapped (1000 iterations) all analyses considering the effects on growth rates. We used Welch's two-sample *t*-tests to determine the inter-annual effects on the slope of each growth parameter for WSP, and each continuous predictor (i.e. $\delta^{13}\text{C}_{pre-laying}$, $\delta^{13}\text{C}_{chick}$, $\delta^{15}\text{N}_{pre-laying}$, $\delta^{15}\text{N}_{chick}$, predicted hatching date) except $\delta^{18}\text{O}_{chick}$. We used a series of Pearson's correlations to find the effects of each continuous predictor (i.e. $\delta^{13}\text{C}_{pre-laying}$, $\delta^{13}\text{C}_{chick}$, $\delta^{15}\text{N}_{pre-laying}$, $\delta^{15}\text{N}_{chick}$, $\delta^{18}\text{O}_{chick}$, predicted hatching date) on the slope of each growth parameter for both species. For BBSP we pooled the data from both years due to the low sample size, but for WSP we analysed the data both pooled between the years and for each year separately. If we found more than one predictor to have significant effect on a growth parameter we bootstrapped a linear model with all significant predictors as main effects, and determined the relative importance of each significant predictor using the *lmg* metric, which is based on R^2 partitioning by averaging over orders as introduced by Lindeman et al. (1980) (*calc.relimp*, package *relaimpo*) (Grömpig, 2006).

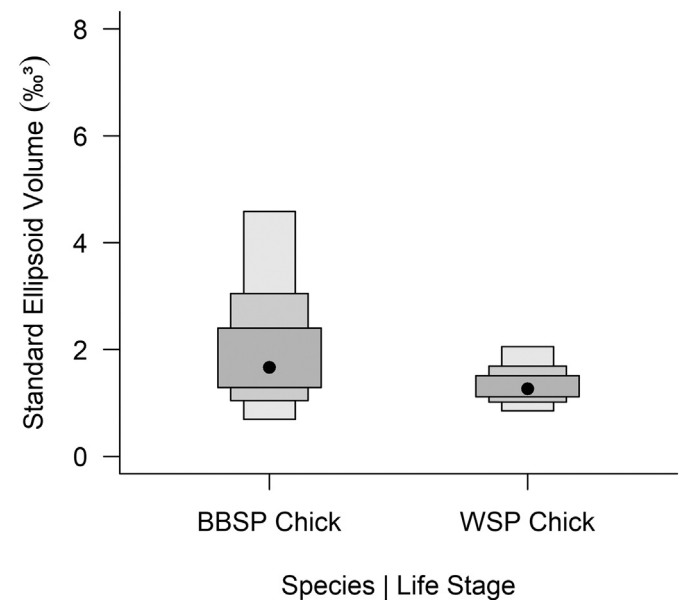


Fig. 4. Bayesian Standard Ellipsoid Volume for $\delta^{13}\text{C}$, $\delta^{15}\text{N}$ and $\delta^{18}\text{O}$ for chick feathers of both studied storm-petrels: Box width and colour denote credible intervals (thick, dark grey – 50%, medium – 75%, narrow, light grey – 95%); black dots – median. BBSP – black-bellied storm-petrel; WSP – Wilson's storm-petrel; chick – chick feathers (undertail coverts). See also Table 3 for values.

2.5.3. Environmental conditions in potential foraging areas

To assess inter-annual differences in environmental conditions, we used sea surface temperature [SST4; a night-time algorithm using two bands in the 4 μm atmospheric window, which shows markedly less scatter than the 11–12 μm SST (Minnett, 2010) ; we used SST4 because of better usable data coverage in the studied buffer zone compared to SST] and chlorophyll-*a* concentration (chl-*a*) at the surface layer. We used remote sensing MODIS Aqua satellite data (NASA Ocean Color Web, <https://oceancolor.gsfc.nasa.gov/>). To establish the environmental parameters, we randomly selected 500 points in the ocean within a 200 km buffer around the studied storm-petrel colonies (Fig. A1B), using ArcMap 10.3.1 (ESRI, 2014) . Then, we extracted the SST4 and chl-*a* values for these points for both studied seasons with a 4 km resolution of monthly composites from November until April (i.e. November 2016 until April 2017 and November 2017 until April 2018), however, due to missing data caused by high cloudiness the sample sizes differed between years and months (see Results). We determined inter-annual differences using a paired Wilcoxon Signed Rank test with continuity correction (*wilcox.test*, package *stats*).

Additionally, in 2018, to visualise local $\delta^{18}\text{O}$ isoscapes (due to a lack of published data from this region), we collected water samples ($n = 20$) at the end of the storm-petrel nesting period around Admiralty Bay (Fig. A1D), where the studied colonies are situated. All water samples were analysed using an Isotopic Liquid Water and Continuous

Water Vapor Analyzer (Picarro 2130) (Skrzypek and Ford, 2014), and results are shown in ‰ VSMOW according to the delta notation (Coplen, 1996) , with an external uncertainty for saline water samples (one standard deviation) of 0.10‰. Multi-points normalisation was used in order to reduce the raw values to the international scale (Skrzypek, 2013) . Normalisation was done based on three laboratory standards, each repeated twice, calibrated against international standards provided by IAEA: VSMOW2, SLAP2 and GISP (Coplen, 1996) . We prepared an isoscape map using inverse distance weighted (IDW) interpolation in ArcMap 10.3.1 (ESRI, 2014) .

3. Results

3.1. Stable isotopic niches

To determine how the isotopic values differed between the life stages (i.e. adult blood as a proxy for chick-rearing adults, chick down for pre-laying female diet and chick feathers for chick diet) between the species we first considered the full MANOVA model with interaction (Wilk's Lambda, $\delta^{13}\text{C} + \delta^{15}\text{N} \sim \text{species} + \text{life stage} + \text{species}:\text{life stage}$). Since the interaction was not significant ($F_{2, 185} = 1.493, p = 0.228$), we removed the interaction term. The results of the model without interaction showed differences in isotopic signatures between the species ($F_{2,186} = 75.68, p < 0.001$) and between the life stages ($F_{2, 186} =$

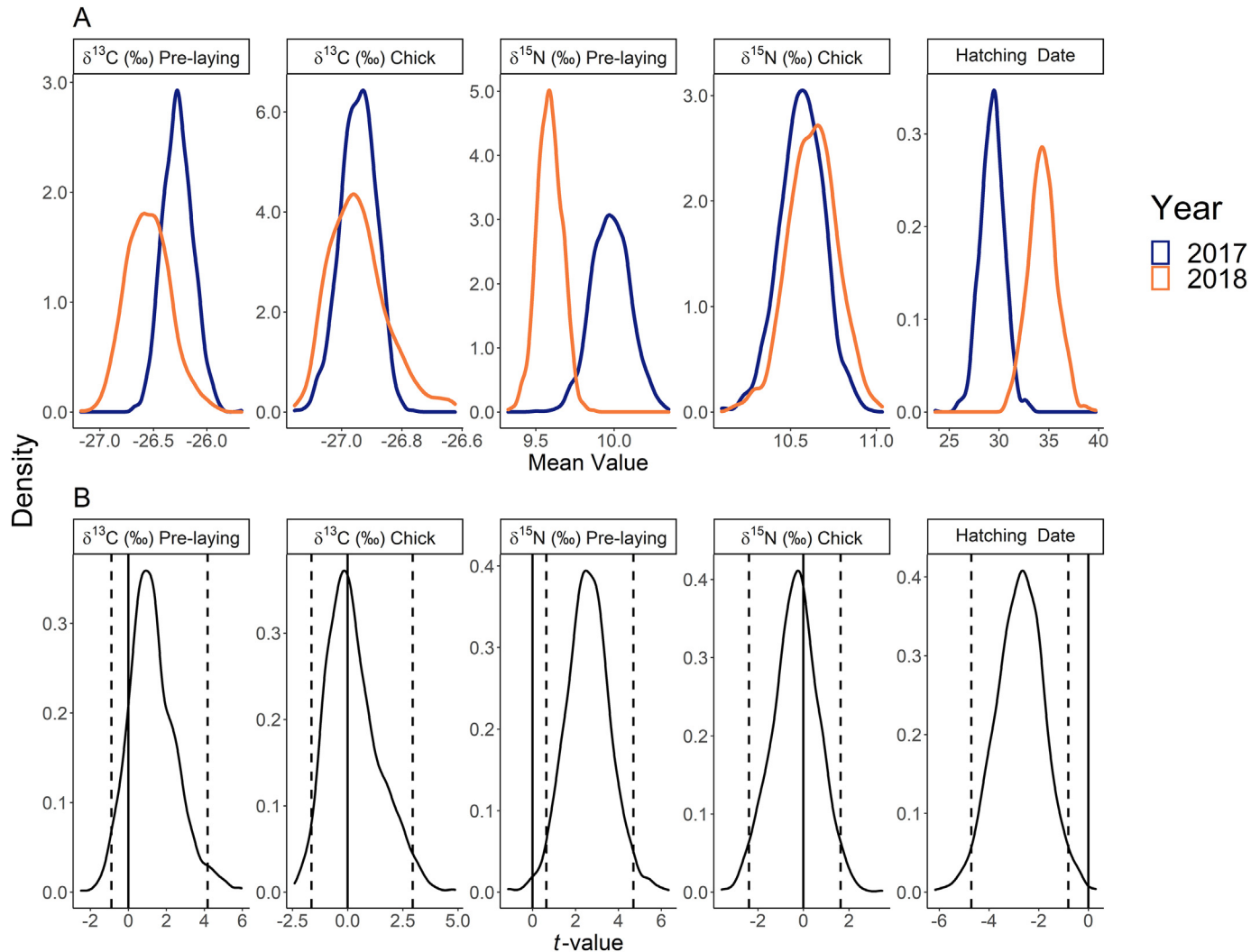


Fig. 5. Bootstrapped ($N = 1000$) chick growth predictors for the Wilson's storm-petrels: Mean and t -values for the chick growth predictors were extracted from Welch's two-sample t -tests comparing 2017 and 2018. A – mean chick growth predictor values between the years; B – t -values inter-annual differences in chick growth predictors. The dashed vertical lines show the 95% range (i.e. 2.5% and 97.5% quantiles); the solid vertical lines $t = 0.0$. We assumed significance if $t = 0.0$ fell outside of the 95% range.

34.17, $p < 0.001$). Further analyses showed significantly higher $\delta^{15}\text{N}$ values for BBSP compared to WSP for all three life stages (Welch's t -test, pre-laying females $t_{13,17} = 6.571$, $p < 0.001$; chick-rearing adults $t_{38,98} = 10.93$, $p < 0.001$; chicks $t_{31,54} = 19.47$, $p < 0.001$) (Table 1). We found no significant difference in $\delta^{13}\text{C}$ between the species (ANOVA, $F_{1,187} = 1.30$, $p = 0.255$), but did between the life stages ($F_{1,187} = 26.76$, $p < 0.001$) (Table 1).

Within BBSP we found significant differences between the life stages (MANOVA, $F_{2,35} = 8.15$, $p = 0.001$) in $\delta^{15}\text{N}$ values (ANOVA, $F_{1,36} = 13.57$, $p = 0.001$) and $\delta^{13}\text{C}$ values ($F_{1,36} = 6.47$, $p = 0.015$). A Tukey's HSD test showed that chicks had higher $\delta^{15}\text{N}$ values than both chick-rearing adults (difference = 1.45%, $p < 0.001$) and pre-laying females (difference = 2.07%, $p < 0.001$), and that pre-laying females had lower $\delta^{15}\text{N}$ values than chick-rearing adults (difference = -0.62%, $p = 0.002$) (Table 1). Chick-rearing adults and pre-laying females did not differ in $\delta^{13}\text{C}$ values (difference = -0.12%, $p = 0.426$), chicks had lower $\delta^{13}\text{C}$ values than both chick-rearing adults (difference = -0.35, $p = 0.003$), and pre-laying females (difference = -0.46, $p < 0.001$) (Table 1). Within WSP we found significant differences between the life stages (MANOVA, $F_{2,149} = 26.06$, $p < 0.001$) in $\delta^{15}\text{N}$ (ANOVA, $F_{1,150} = 38.09$, $p < 0.001$) and $\delta^{13}\text{C}$ ($F_{1,150} = 22.98$, $p < 0.001$) (Table 1). We found no significant difference in stable isotope signatures between the years for WSP (MANOVA, $F_{2,116} = 2.693$, $p = 0.072$). Chick-rearing adults and pre-laying females did not have

significantly different $\delta^{15}\text{N}$ values (Tukey's HSD, difference = 0.20%, $p = 0.257$) or $\delta^{13}\text{C}$ values (difference = -0.04%, $p = 0.936$), but chicks had higher $\delta^{15}\text{N}$ values than both chick-rearing adults (difference = 0.72%, $p < 0.001$) and pre-laying females (difference = 0.91%, $p < 0.001$), and lower $\delta^{13}\text{C}$ values (chicks vs. chick-rearing adults difference = -0.54%, $p < 0.001$; chicks vs. pre-laying females difference = -0.58%, $p < 0.001$) (Table 1).

When we compared chick diets including the $\delta^{18}\text{O}$ signatures (MANOVA, $\delta^{13}\text{C} + \delta^{15}\text{N} + \delta^{18}\text{O} \sim \text{species}$), we found significant differences between the species (Wilks' Lambda, $F_{3,34} = 29.14$, $p < 0.001$) in isotopic signatures for $\delta^{18}\text{O}$ values ($F_{1,36} = 5.370$, $p = 0.026$) and $\delta^{15}\text{N}$ values ($F_{1,26} = 72.66$, $p < 0.001$) but not $\delta^{13}\text{C}$ ($F_{1,36} = 0.774$, $p = 0.385$). Further *post hoc* analyses showed the difference in $\delta^{18}\text{O}$ values to be just not significant ($t_{8,027} = 2.071$, $p = 0.072$), and $\delta^{15}\text{N}$ values to be higher in BBSP than in WSP ($t_{29,27} = 14.841$, $p < 0.001$) (Table 1).

The Bayesian Estimate 95% Prediction Ellipse Area (BEPEA) overlap analyses revealed that between species the chicks showed least overlap in $\delta^{13}\text{C}$ and $\delta^{15}\text{N}$ (BBSP vs. WSP mean overlap 5.9%; WSP vs. BBSP mean overlap 1.2%) (Table 2; Fig. 1A). Both chick-rearing adults (BBSP vs. WSP mean overlap 31.0%; WSP vs. BBSP mean overlap 7.96%) (Fig. 1C) and pre-laying females (BBSP vs. WSP mean overlap 54.6%; WSP vs. BBSP mean overlap 25.6%) (Fig. 1E) showed considerable overlap (Table 2). The overlap values were higher for BBSP than for WSP (Table 2;

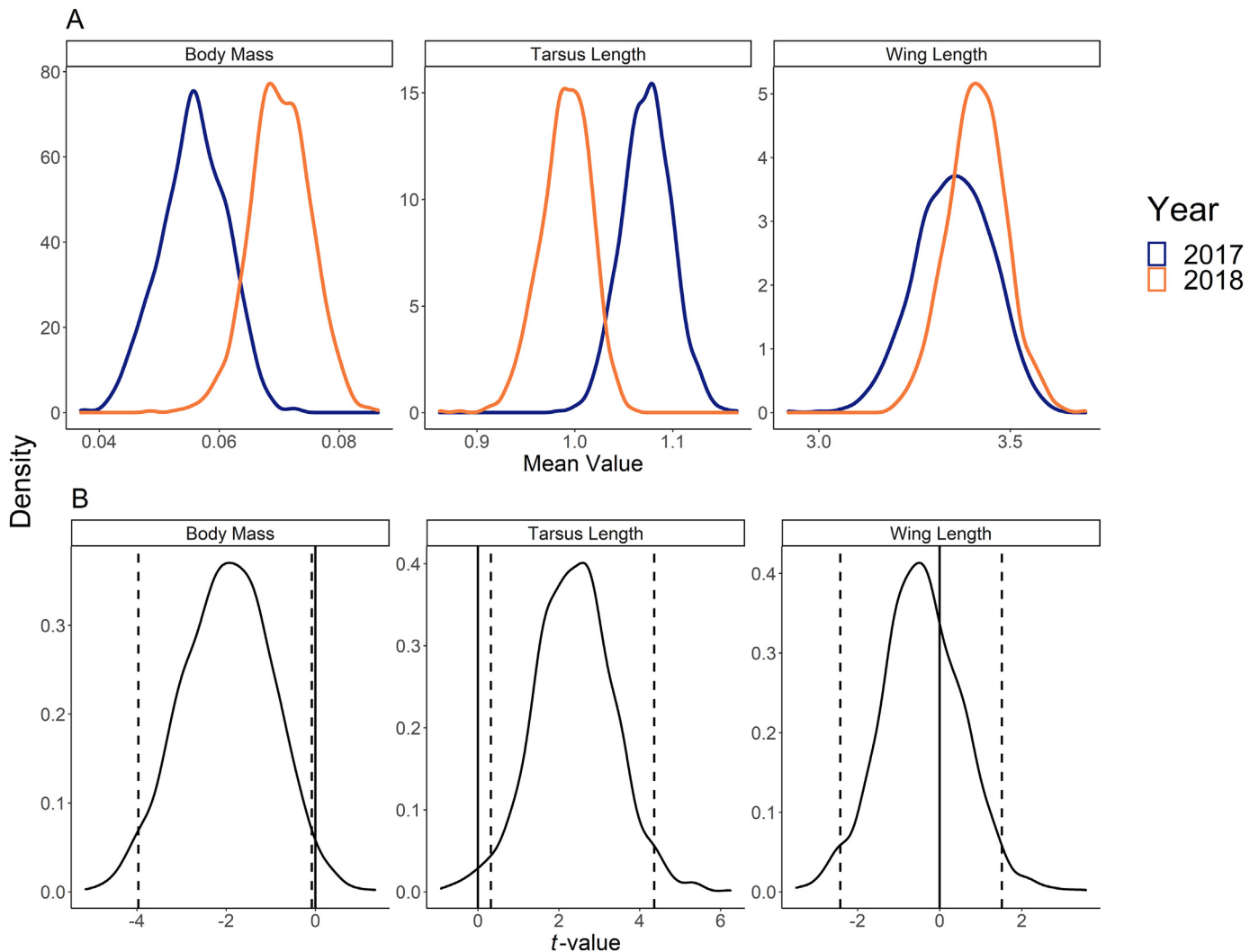


Fig. 6. Bootstrapped ($N = 1000$) chick growth parameters for the Wilson's storm-petrels; Mean and t -values for the chick growth parameters were extracted from Welch's two-sample t -tests comparing 2017 and 2018. A - mean chick growth parameter values between the years; B - t -values inter-annual differences in chick growth parameters. The dashed vertical lines show the 95% range (i.e. 2.5% and 97.5% quantiles); the solid vertical lines $t = 0.0$. We assumed significance if $t = 0.0$ fell outside of the 95% range.

Fig. 1A), as their niches were smaller than those of WSP for all three sampled life stages (Table 3; Fig. 2A), which meant that a similar overlapping area comprised a larger portion of BBSP BEPEA than of WSP BEPEA.

At the intra-specific level for BBSP, we found the least overlap in the Bayesian 95% Prediction Ellipses of chicks with either chick-rearing adults (chick-rearing adults vs. chicks mean overlap 4.71%; chicks vs. chick-rearing adults mean overlap 5.34%) or pre-laying females (pre-

laying females vs. chicks mean overlap 0.59%; chicks vs. pre-laying females mean overlap 2.76%) (Table 2; Fig. 1F). In contrast, chick-rearing adults and pre-laying females showed substantial overlap (chick-rearing adults vs. pre-laying females mean overlap 59.5%; pre-laying females vs. chick-rearing adults mean overlap 19.1%) (Table 2; Fig. 1F). All three life stages were overlapping in WSP (mean overlap range 36.8–93.8%) (Table 2; Fig. 1G). In both species, the maternal pre-laying diet signatures showed the largest niche widths (Table 3;

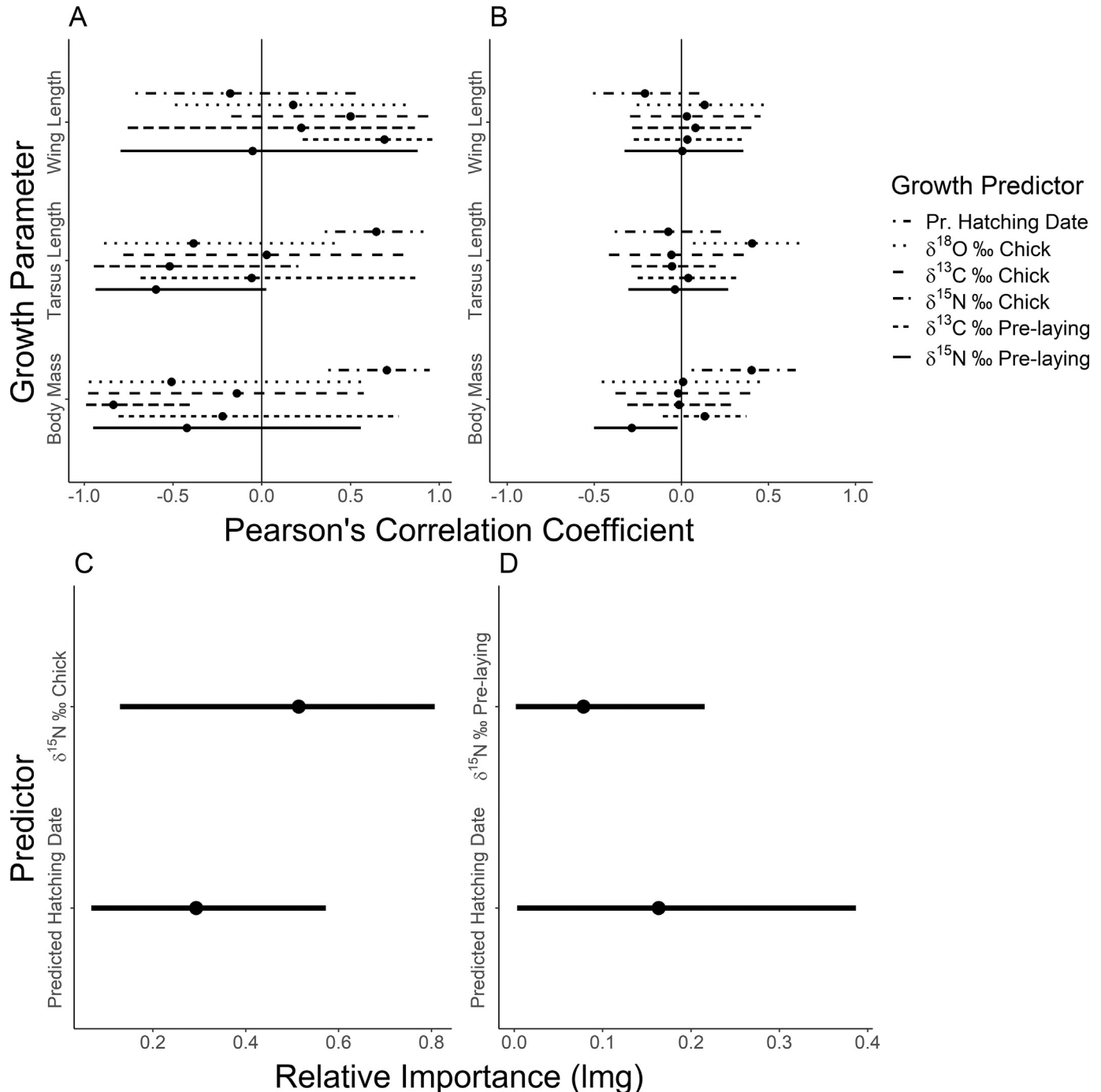


Fig. 7. Bootstrapped ($N = 1000$) Pearson's correlations between chick growth parameters and predictors and relative importance of multiple significant predictors for both studied storm-petrel species: A – pairwise Pearson's correlations for the black-bellied storm-petrels for both years; B – pairwise Pearson's correlations for the Wilson's storm-petrels for both years; C – relative importance (lmg) of both significant predictors for body mass growth in an OLS regression model for the black-bellied storm-petrels; D – relative importance of both significant predictors for body mass growth for the Wilson's storm-petrels. Pr. Hatching Date – predicted hatching date. The results are shown as mean (dot) \pm 95% range (i.e. 2.5% and 97.5% quantiles; solid horizontal line). Solid vertical line shows Pearson's correlation coefficient = 0.0. We assumed significance the 95% range of the Pearson's correlation coefficient did not overlap 0.0.

Fig. 2A). In WSP the niche widths of chick-rearing adults and chicks were similar, while in BBSP the niche width of chick diet was narrower than either pre-laying diet or chick-rearing adult diet (Table 3; Fig. 2A).

When including $\delta^{18}\text{O}_{\text{chick}}$ into the analyses, we found negligible inter-specific overlap in Bayesian Estimate 95% Prediction Ellipsoid Volumes (mean overlap <0.001%) for the studied species (Fig. 3). Conversely to the $\delta^{13}\text{C}$ and $\delta^{15}\text{N}$ niche widths, we found that the niche widths including $\delta^{18}\text{O}_{\text{chick}}$ were wider for BBSP than for WSP (Table 4; Fig. 4).

Although we found $\delta^{15}\text{N}_{\text{pre-laying}}$ to be significantly higher in 2017 than in 2018 for WSP (Fig. 5), BEPEAs showed considerable overlap between the years for both pre-laying females and chicks (mean overlap range 32.8–67.7%) (Table 2; Fig. 1B). Additionally, the niche widths were similar between the years for both pre-laying females and chicks (Fig. 2B). We found no significant differences in $\delta^{13}\text{C}_{\text{pre-laying}}$, $\delta^{13}\text{C}_{\text{chick}}$ or $\delta^{15}\text{N}_{\text{chick}}$ between the years (Fig. 5).

3.2. Factors affecting chick growth

We found no significant interspecific differences in growth rates for tarsus length ($t_{32,19} = -0.897$, $p = 0.376$, BBSP mean \pm SD = 1.01 ± 0.05 , WSP mean \pm SD = 1.04 ± 0.11), wing length ($t_{36,21} = 0.916$, $p = 0.366$, BBSP mean \pm SD = 3.48 ± 0.14 , WSP mean \pm SD = 3.36 ± 0.42) or body mass ($t_{9,53} = 1.220$, $p = 0.251$, BBSP mean \pm SD = 0.08 ± 0.04 , WSP mean \pm SD = 0.06 ± 0.02). For the WSP chicks we found significant inter-annual differences in body mass growth rate (higher in 2018), tarsus growth rate (higher in 2017) and predicted hatching dates (earlier in 2017) (Fig. 6).

For the BBSP chicks the bootstrapped Pearson's correlation analyses showed a significant positive relationship between tarsus growth and predicted hatching date for both years combined, and a significant positive relationship between $\delta^{13}\text{C}_{\text{pre-laying}}$ and wing growth (Fig. 7A). Additionally, we found a significant positive effect of predicted hatching date and a significant negative effect of $\delta^{15}\text{N}_{\text{chick}}$ on body mass growth (Fig. 7A). The relative importance of predicted hatching date was lower (mean \pm SD lmg = 0.293 ± 0.124) than that of $\delta^{15}\text{N}_{\text{chick}}$ (mean \pm SD lmg = 0.514 ± 0.176) (Fig. 7C). For the WSPs we found a significant positive correlation between $\delta^{18}\text{O}_{\text{chick}}$ and tarsus growth rate (Fig. 7B), and a significant positive effect of predicted hatching date and a

significant negative effect of $\delta^{15}\text{N}_{\text{pre-laying}}$ on body mass growth for both years combined (Fig. 7B). The relative importance of predicted hatching date was higher (mean \pm SD lmg = 0.163 ± 0.108) than that of $\delta^{15}\text{N}_{\text{pre-laying}}$ (mean \pm SD lmg = 0.078 ± 0.058) (Fig. 7D). However, when separating the data for the WSPs between the years, we found a significant positive effect of predicted hatching date on body mass only in 2017 (Fig. 8A) and a significant negative effect of $\delta^{15}\text{N}_{\text{chick}}$ on body mass growth in 2018 (Fig. 8B).

3.3. Environmental conditions in potential foraging areas

We found significant differences between the years in SST4 from November through February (Wilcoxon test, all $p < 0.05$), with sea surface temperatures from November through February being higher in 2016/17 than in 2017/18 (Table 5; Fig. 9). In March and April temperatures did not significantly differ between the years. Chl-*a* was significantly different from November through March; for April there was not enough data available due to high cloud cover (Fig. 10). Chl-*a* concentrations were higher in 2016/17 than in 2017/18 in November and December, but lower from January through March (Table 5).

4. Discussion

Our results indicate that BBSPs forage at a higher trophic level than WSPs. All studied life stages (especially chicks) of BBSP were characterised by higher $\delta^{15}\text{N}$ values than WSP. This observation is consistent with earlier studies suggesting such interspecific differences in trophic levels based on dietary data collected from regurgitations (Furness and Baillie, 1981; Hahn, 1998a; Quillfeldt, 2002). Regurgitation studies may not be fully representative for species' diet, as regurgitated food is supposed to be intended as chick food only (Furness and Baillie, 1981). Thus, our study, based on stable isotope analyses of samples collected from both chicks and adults provides a more complete picture of the foraging niches of the two species. Interestingly, we found considerable overlap between adult BBSP and WSP isotopic niches, both during the pre-laying period (chick down values) and the chick-rearing period (adult blood values), though in both instances BBSP had on average higher $\delta^{15}\text{N}$ values. This large degree of overlap may be explained by the importance of Antarctic krill (*Euphausia*

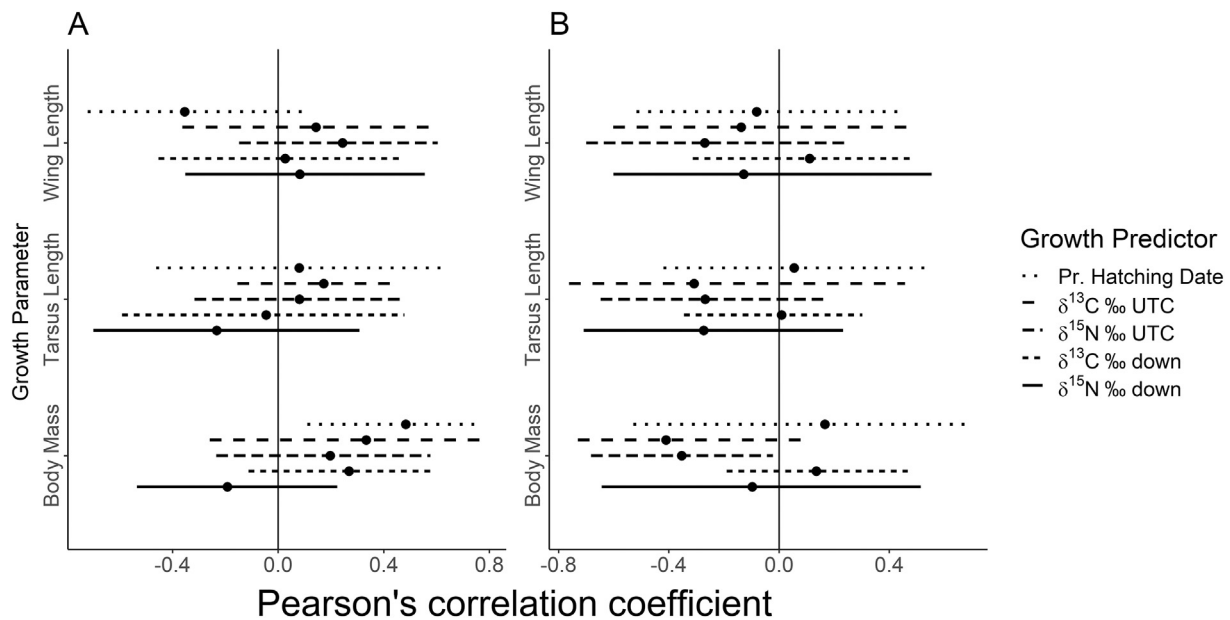


Fig. 8. Bootstrapped ($N = 1000$) Pearson's correlations between chick growth parameters and predictors and relative importance of multiple significant predictors for both years for the Wilson's storm-petrels: A – pairwise Pearson's correlations for 2017; B – pairwise Pearson's correlations for 2018. Pr. Hatching Date – predicted hatching date. The results are shown as mean (dot) \pm the 95% range (i.e. 2.5% and 97.5% quantiles; solid horizontal line). Solid vertical line shows Pearson's correlation coefficient = 0.0. We assumed significance the 95% range of the Pearson's correlation coefficient did not overlap 0.0.

Table 5
Environmental conditions [chlorophyll-*a* concentrations (chl-*a*) and sea surface temperatures (SST4)] in potential foraging areas of the studied storm-petrels: Environmental conditions (chl-*a* and SST4) as obtained from randomly selected points in a buffer of 200 km around the colonies. Significant (paired Wilcoxon Signed Rank test with continuity correction) *p*-values (<0.05) are bolded. See also Fig. 8. SD – standard deviation; n – sample size; NA – not available.

Month	Chl- <i>a</i> (mg m ⁻³)				SST4 (°C)			
	Mean ± SD		n	p	Mean ± SD		n	p
	2016/17	2017/18			2016/17	2017/18		
Nov	0.348 ± 0.146	0.303 ± 0.111	423	<0.001	-0.200 ± 0.193	-0.772 ± 0.114	15	<0.001
Dec	0.464 ± 0.302	0.426 ± 0.265	425	<0.001	0.951 ± 0.598	0.316 ± 0.368	186	<0.001
Jan	0.303 ± 0.181	0.325 ± 0.186	358	0.001	1.479 ± 0.777	1.241 ± 0.746	382	<0.001
Feb	0.313 ± 0.199	0.387 ± 0.272	398	<0.001	1.882 ± 0.960	1.357 ± 0.747	372	<0.001
Mar	0.222 ± 0.081	0.894 ± 0.933	323	<0.001	1.217 ± 0.828	1.285 ± 0.654	351	0.674
Apr	0.261 ± NA	0.415 ± NA	1	NA	0.823 ± 0.797	0.870 ± 0.510	309	0.408

superba) in the diet of both studied storm-petrel species (Beck and Brown, 1971; Hahn, 1998a; Ridoux, 1994). Foraging on this superabundant (Siegel et al., 2013; Trathan and Hill, 2016), readily available prey

may reduce stable isotope niche partitioning, although it does not necessarily eliminate the possibility of interspecific competition (Barlow et al., 2002; Dimitrijević et al., 2018). A study on three closely related

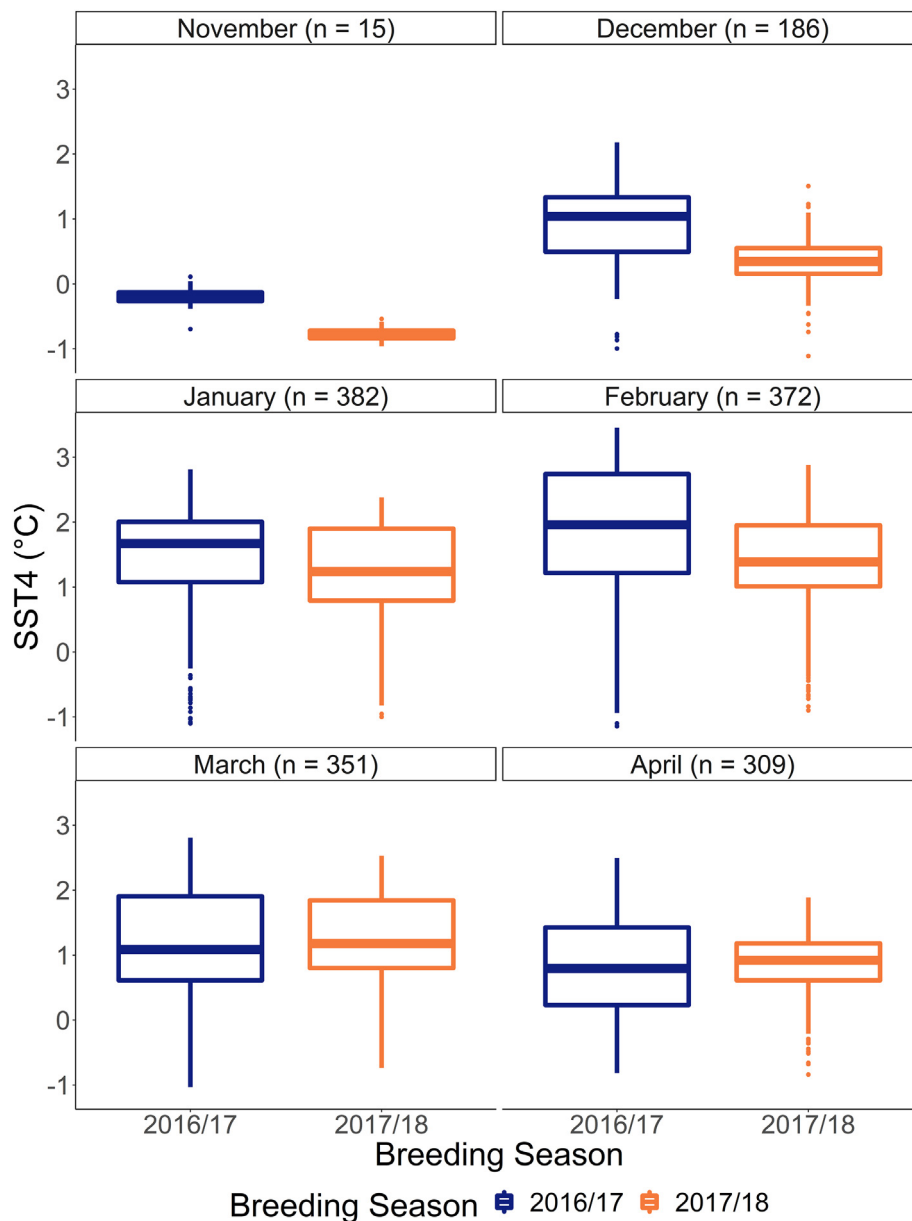


Fig. 9. Sea surface temperatures in potential foraging areas for both studied storm-petrel species. Pairwise sea surface temperature (SST4) comparisons between years per sampled month. Sample sizes are shown in brackets. For more details see Table 4 and Fig. A1.

fulmarine petrels breeding sympatrically in Antarctica revealed no significant stable isotope niche segregation between at least two species for feathers and egg membranes, and among all species during incubation as reflected by blood (Dehnhard et al., 2019). Of four species of sympatric planktivorous petrels breeding on Bird Island, South Georgia, two showed partial stable isotope niche overlap (Navarro et al., 2013). The lack of considerable stable isotope niche partitioning in sympatrically breeding species sharing the same guild may be explained by foraging behaviour differences [e.g. diving behaviour (Navarro et al., 2013)], or because the species' diets truly overlap due to generalist diets (Dehnhard et al., 2019) or focusing on superabundant prey (this study).

To increase the fitness of their current offspring seabird parents may provision their chicks at a higher trophic level than they consume themselves (Forero et al., 2002; Hodum and Hobson, 2000; Rosciano et al., 2019), by selectively foraging for higher quality prey (Kwasniewski et al., 2012) or reserving high quality prey for chick provisioning (Dänhardt et al., 2011). We found that $\delta^{15}\text{N}$ values of BBSP chicks

were higher than those of adults, which may suggest a fish-richer diet. Fish prey has been shown to have higher caloric values than crustaceans (Ruck et al., 2014), and a higher calcium content (Clarke and Prince, 1980), a mineral that is especially important for rapidly growing chicks (Hurwitz et al., 1995). In contrast, WSP chick diet showed considerable overlap with adult diets. Instead of differences in diet causing differences in $\delta^{15}\text{N}$ values, BBSP chick $\delta^{15}\text{N}$ values might have been inflated due to nutritional stress in the chicks. Nutritional stress can lead to the use endogenous instead of dietary amino acids in protein synthesis (Hobson et al., 1993), increasing the $\delta^{15}\text{N}$ values due to nitrogen fractionation. Nutritional stress may be caused by periods of fasting and facultative hypothermia (Beck and Brown, 1971; Cruz et al., 2012; Hobson et al., 1993; Kuepper et al., 2018; Polito et al., 2011).

We suggest that the overlap in diet between adults and chicks might be an effect of prioritising food security over its nutritional value. WSP preferring to forage on the readily available superabundant Antarctic krill over fish might mean higher food security, such that a higher trophic level diet does not induce a higher chick fitness if it means more

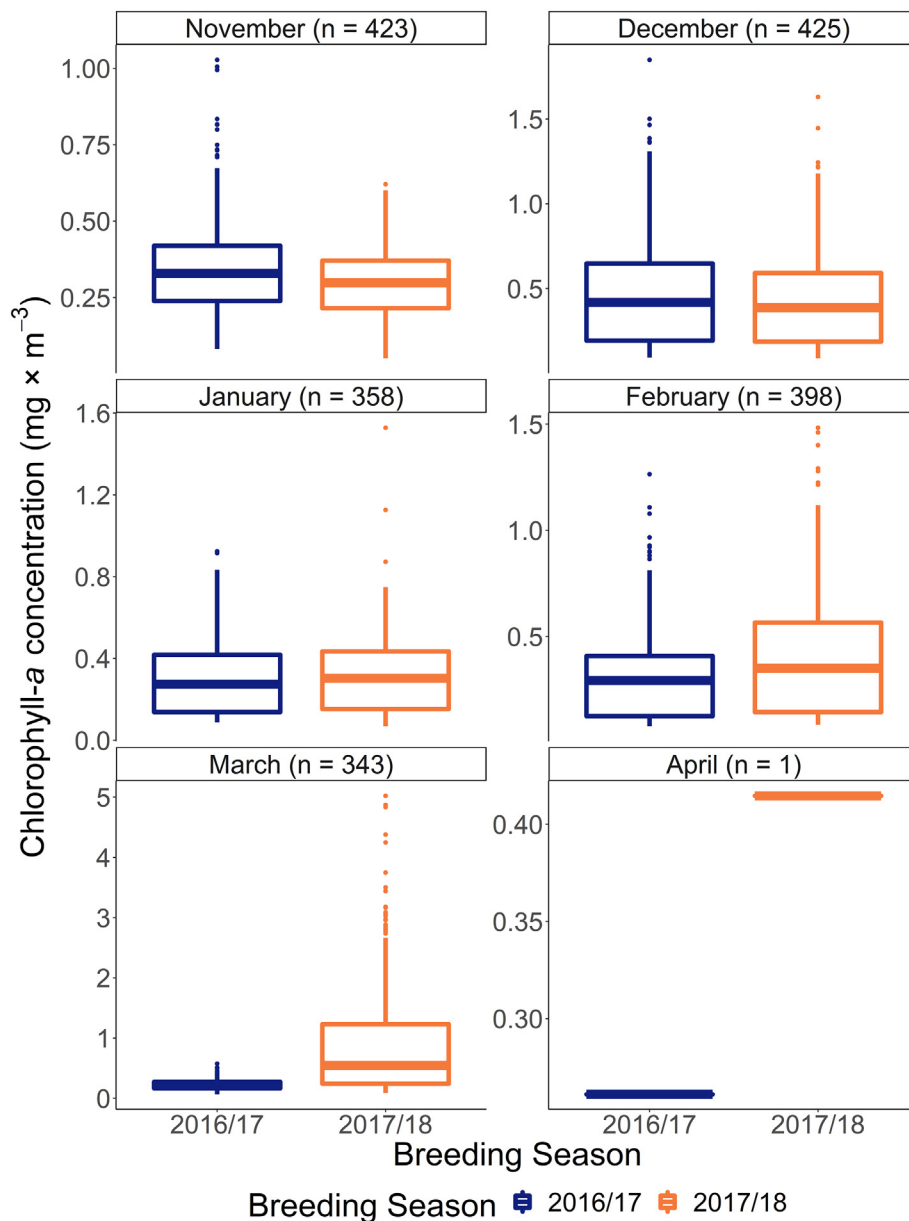


Fig. 10. Chlorophyll-*a* concentrations in potential foraging areas for both studied storm-petrel species. Pairwise chlorophyll-*a* (chl-*a*) concentration comparisons between years per sampled month. Sample sizes are shown in brackets. For more details see Table 4 and Fig. A1.

a frequent, and stable food supply (Morrison et al., 2014). The smaller WSPs may also be less adapted to catch and handle fish prey than the larger BBSPs. Storm-petrel fish prey is often larger than krill (Ruck et al., 2014), and WSP have smaller culmen (mean 12.6 mm) (Beck and Brown, 1972) than BBSP (mean 15.3 and 15.1 mm for males and females respectively) (Beck and Brown, 1971). There may thus be a threshold size for chicks before they are able to handle fish prey. Our study and previous research (Hahn, 1998a; Quillfeldt, 2002; Ridoux, 1994) do not allow us to distinguish why exactly WSP prefers provisioning their chicks with krill over fish, but their foraging strategies seem heavily reliant on krill. Indeed, WSP change their provisioning strategy based on actual krill abundance (Gladbach et al., 2009; Quillfeldt and Peter, 2000), and breeding success decreases in years with low krill abundance (Büßer et al., 2004).

The difference in nutritional demands between the chicks of both species, such that BBSP parents forage at different trophic levels for their chicks than themselves but WSP parents do not, might stem from the difference in body size and thus metabolic rates between both species (Dunn et al., 2019; Warham, 1996); a higher metabolic rate at sea is expected for heavier seabirds, here for BBSP compared to WSP (Birt-Friesen et al., 1989). While we did not find differences in chick growth rates between the chicks of both species, BBSP chicks do stay in the nest for a longer period of time than WSP chicks and consequently have a longer growth period especially considering body mass gain (Fig. A4). BBSP chicks might have been fed at a higher trophic level than WSP chicks level due to higher nutritional demands, like in black-legged kittiwakes (*Rissa tridactyla*) (Merkling et al., 2012). BBSP chicks have to grow relatively more from hatching [e.g. the mean body mass upon hatching was 10.7 g for WSP ($n = 19$) and 14.8 g for BBSP ($n = 4$), while the maximum observed chicks masses were 48.7 g for WSP and 127.8 g for BBSP, a gain of 5.4 times the initial mass for WSP and 8.6 times the initial mass for BBSP]. This difference in mass gain could explain the inclination for a bigger shift in trophic level from adults to chicks in BBSP compared to WSP. Additionally, chick feather isotope composition reflects the diet input during the whole growth period, and the effect of a shift in prey types later in the season may thus be confounded for WSP. BBSP may have been provisioning their chicks at a higher trophic level from hatching, thus showing a clearer distinction in trophic level between adults and chicks.

In the adults of both BBSP and WSP we found that the pre-laying female (i.e. chick down) stable isotope niches were widest compared to the other measured life stages, confirming our hypothesis that free roaming adults have wider isotopic niches (Pratte et al., 2018). BBSP showed no difference in $\delta^{13}\text{C}$ in adult-derived samples (i.e. blood and chick down), but did have higher $\delta^{15}\text{N}$ values in chick-rearing diets compared to pre-laying diets. This may indicate a shift in the trophic level of the diet (Minagawa and Wada, 1984) but not in foraging area locations (Cherel and Hobson, 2007; Quillfeldt et al., 2005). Both WSP adult-derived samples however, showed no significant difference in isotopic signatures, indicating both similar diets and foraging locations throughout the breeding season. Additionally, we found that chick diet niche widths were narrower than adult niche widths, which may indicate that parents were more selective about prey items they feed their chicks than prey they forage for themselves. Alternatively, many central-place foraging seabirds, including Procellariiformes and likely European storm-petrels (*Hydrobates pelagicus*) (Bolton, 1996) and its sub-species the Mediterranean storm-petrel (*H. p. melitensis*) (Albores-Barajas et al., 2011), alternate long foraging trips for self-maintenance and short foraging trips for chick provisioning visiting different foraging areas (e.g. Chaurand and Weimerskirch, 1994; Jakubas et al., 2012). The difference in the duration and distance of the foraging flights, could also explain the difference in foraging niche widths between adults and chicks as the shorter trips would cover a smaller range of stable isotope values that change with foraging area, and a smaller range of potential prey types.

Interestingly, while the BBSP isotopic niches were narrower than the WSP niches when considering the $\delta^{13}\text{C}:\delta^{15}\text{N}$ space, they were wider when including $\delta^{18}\text{O}$. This is likely due to the low sample size (BBSP $n = 8$), but alternatively may indicate that BBSP parents forage in a wider range of areas from shore to off-shore locations (Bigg and Rohling, 2000). BBSPs breeding on the South Shetland Islands have been shown to prefer foraging further off-shore than WSPs (Santora et al., 2017), which is confirmed by the tendency for higher $\delta^{18}\text{O}_{\text{chick}}$ values in BBSP than in WSP. Conversely, $\delta^{13}\text{C}$ did not differ between BBSP and WSP, reinforcing the suggestion that the difference in stable isotope niche widths was due to low sample size. However, BBSP might have been foraging in the same water mass (similar $\delta^{13}\text{C}$) but further from shore. Additionally, the scale at which changes in $\delta^{13}\text{C}$ and $\delta^{18}\text{O}$ occur was not necessarily the same, and could explain why differences in one were picked up by statistical analyses but not in the other.

We found a positive correlation between hatching date and body mass and tarsus growth for the BBSP chicks, and a positive correlation between hatching date and body mass growth for the WSP chicks. In WSP the effect of hatching date on chick growth was much stronger than any other significant effect when analysed together (Fig. 7B & D). Due to the short Antarctic summer and subsequent crash in food availability (Biggs et al., 2019), chicks have a strict deadline for fledging and late chicks may have to grow faster to be ready to leave the nest in time (VanHeezik et al., 1993). The positive correlation between BBSP wing growth and $\delta^{13}\text{C}_{\text{pre-laying}}$ may be explained in context of carry-over effects from maternal nutrients in eggs to chick isotopic signatures. Lower $\delta^{13}\text{C}$ have been correlated with lower body conditions in blue-footed booby (*Sula nebouxii*) chicks (Cruz et al., 2012). If this relationship is also present in pre-laying females, then pre-laying females with lower body conditions might have had chicks slower growing wings. Alternatively, as lipids are depleted in $\delta^{13}\text{C}$, pre-laying females foraging on high lipid prey [e.g. fish over krill (Clarke and Prince, 1980)] might have had chicks with slower growing wings. However, we have no data on pre-laying diets or its lipid contents, and thus can only speculate on the reason for the positive relationship between $\delta^{13}\text{C}_{\text{pre-laying}}$ and chick wing growth for BBSP, as the issue is apparently understudied and requires further investigation (Bond and Jones, 2009).

Similar to other studies on chick growth (Cruz et al., 2012; Trueman et al., 2005), we found that higher $\delta^{15}\text{N}_{\text{chick}}$ values were correlated with lower body mass growth rates in BBSP. This correlation was stronger than the significant effect of hatching date when analysed together (Fig. 7A & C). For WSP we also found a significant negative correlation between body mass growth and $\delta^{15}\text{N}_{\text{chick}}$ but only in 2018. Those negative correlations may be due to nutritional stress in the chicks (Hobson et al., 1993), increasing the $\delta^{15}\text{N}$ values due to nitrogen fractionation. However, in most species $\delta^{15}\text{N}$ goes up with age and size, including Antarctic krill (Polito et al., 2013) and fish (Pinkerton et al., 2013), suggesting a correlation between prey age and chick growth rate. Additionally, in Antarctic krill, the relative lipid content in immatures is higher than in adults (Clarke, 1984), implying that juvenile krill should be preferred over adults in terms of nutritional quality. Krill size decreases closer to shore (Siegel et al., 2013), possibly indicating a preference for larger krill and thus older krill, contradicting the positive effect of juvenile krill. However, in WSP we found a positive correlation between $\delta^{18}\text{O}_{\text{chick}}$ and tarsus growth rate. Sea water $\delta^{18}\text{O}$ generally decreases closer to shore, especially in bays and estuaries, due to fresh water input which has lower $\delta^{18}\text{O}$ values than ocean water, indicating a positive effect of foraging further off-shore. However, locally we found that in Admiralty bay ocean $\delta^{18}\text{O}$ values were higher than in the surrounding open ocean of the Bransfield Strait (Fig. A1D), likely caused by local currents and upwelling zones pushing $\delta^{18}\text{O}$ richer water masses up along the shore line (Campos et al., 2013; Rakusa-Suszczewski, 1980). These findings show that while $\delta^{18}\text{O}$ may be useful when studying potentially large (foraging) areas, local systems might be more complex.

When separating the effects on chick growth rates per year for the WSPs, we found significantly earlier hatching dates in 2017 compared to 2018. Additionally, we found significantly higher body mass growth rates in 2018 than in 2017, but lower tarsus growth rates. We found no significant differences in isotopic values during the breeding period, but pre-laying $\delta^{15}\text{N}$ values were higher in 2017 than in 2018. These differences in chick growth rates and hatching dates might be due to the inter-annual environmental differences in sea surface temperature and chlorophyll-*a* concentrations (Figs. 9 & 10), which likely had an effect on krill abundance (Hill et al., 2013; Loeb et al., 1997; Marrari et al., 2008). Looking at the factors affecting chick growth rate, we found that the significant negative correlation between $\delta^{15}\text{N}_{\text{pre-laying}}$ and body mass growth observed in the pooled WSP dataset disappeared when separating the years. As there were also significant inter-annual differences in $\delta^{15}\text{N}_{\text{pre-laying}}$ and body mass growth, we assume those to be the base for the significant effect in the pooled dataset. Additionally, we found a significant positive effect of hatching date on body mass growth, which disappeared in 2018 though not in 2017, indicating that this effect is not solely due to inter-annual differences in body mass growth and hatching dates. In 2018 we found a significant negative effect of $\delta^{15}\text{N}_{\text{chick}}$ on body mass growth, which was not apparent in 2017. These differences in significant effects between the years could be connected with the inter-annual differences in hatching dates, weather conditions or food availability; possibly due to the later hatching dates in 2018 (longer snow cover retention spring blocking access to the nest burrows) all chicks were restricted by the short summer so that hatching date did not affect body mass growth as strongly as in 2017. The higher SST4 and chl-*a* concentrations early in the season in 2016/17 compared to 2017/18 (Figs. 9 & 10) and their subsequent effect on krill abundance (Hill et al., 2013; Marrari et al., 2008) may have had lasting effects through the breeding seasons. Moreover, the increased precipitation in 2018 (Michielsen et al., 2019) caused increased snow blocking of the nests throughout the season, which in turn lead to more nutritional stress due to fasting and facultative hypothermia (Beck and Brown, 1971; Cruz et al., 2012; Hobson et al., 1993; Kuepper et al., 2018; Polito et al., 2011) and thus higher $\delta^{15}\text{N}_{\text{chick}}$ in chicks with higher stress levels and lower growth rates (Hobson et al., 1993). This effect may not have been apparent in 2017 as nutritional stress levels may have been lower and more similar between the chicks.

5. Conclusions

Our study is one of the first to show the differences in stable isotope niches between species and life stages in seabirds (Gladbach et al., 2007; Pratte et al., 2018). In contrast to WSPs, we found that the trophic level of BBSP chicks differed from adults, likely as a result of the specific requirements of growing and developing nestlings. The results revealed some limitations of regurgitation studies as the diet of chicks may be different from adults. Additionally, combining stable isotope data with chick growth rate data allowed us to better understand inter-specific and inter-annual differences in the relationship between diet and chick growth. Despite the expected niche partitioning driven by sympatric breeding and sharing the same guild, the studied storm-petrel species showed, similarly to some other Antarctic predators, considerable isotopic niche overlap during the breeding season. The large overlap is likely due to their reliance on similar prey types, most notably the superabundant Antarctic krill. Its high availability may have reduced interspecific isotopic niche partitioning, though interspecific competition may still play an important role in the Antarctic food web (Barlow et al., 2002; Dimitrijević et al., 2018), especially if krill abundance decreases due to global climate change (Hill et al., 2013; Loeb et al., 1997). Our study revealed dietary shifts in BBSPs that are absent in the WSPs, showing different chick provisioning strategies, and shows that the high productivity of the Antarctic marine ecosystem may facilitate foraging niche overlap of sympatrically living species.

CRediT authorship contribution statement

Anne N.M.A. Ausems: Conceptualization, Methodology, Validation, Formal analysis, Investigation, Data curation, Writing - original draft, Visualization, Project administration. **Grzegorz Skrzypek:** Formal analysis, Resources, Writing - review & editing. **Katarzyna Wojczulanis-Jakubas:** Methodology, Investigation, Writing - review & editing. **Dariusz Jakubas:** Conceptualization, Methodology, Validation, Investigation, Writing - review & editing, Supervision, Project administration, Funding acquisition.

Declaration of competing interest

The authors declare that they have no known competing financial interests or personal relationships that could have appeared to influence the work reported in this paper.

Acknowledgements

This work was supported by a grant from the Polish National Science Centre, Poland (2015/19/B/NZ8/01981). The study was conducted under the permission of the Polish National SCAR, Institute of Biochemistry and Biophysics (permit for entering the Antarctic Specially Protected Area No. 3/2016 & No. 08/2017). We would like to thank the Henryk Arctowski Polish Antarctic Station and the Department of Antarctic Biology of the Polish Academy of Sciences for their hospitality and logistic support during our stay on King George Island. We are grateful to Rosanne Michielsen for her support in the field. Lastly, we would like to thank two anonymous reviewers for their constructive on earlier versions of the manuscript.

Appendix A. Supplementary data

Supplementary data to this article can be found online at <https://doi.org/10.1016/j.scitotenv.2020.138768>.

References

- Albores-Barajas, Y.V., Riccato, F., Fiorini, R., Massa, B., Torricelli, P., Soldatini, C., 2011. Diet and diving behaviour of European Storm Petrels *Hydrobates pelagicus* in the Mediterranean (ssp. *melitensis*). *Bird Study* 58, 208–212. <https://doi.org/10.1080/00063657.2011.560244>.
- Barger, C.P., Young, R.C., Will, A., Ito, M., Kitaysky, A.S., 2016. Resource partitioning between sympatric seabird species increases during chick-rearing. *Ecosphere* 7, 1–15. <https://doi.org/10.1002/ecs2.1447>.
- Barlow, K.E., Boyd, I.L., Croxall, J.P., Reid, K., Staniland, I.J., Brierley, A.S., 2002. Are penguins and seals in competition for Antarctic krill at South Georgia? *Mar. Biol.* 140, 205–213. <https://doi.org/10.1007/s00227-001-0691-7>.
- Beck, J.R., Brown, D.W., 1971. Breeding biology of the black-bellied storm-petrel. *Ibis* (Lond. 1859), 113, 73–90.
- Beck, J.R., Brown, D.W., 1972. The biology of Wilson's storm petrel, *Oceanites oceanicus* (Kuhl), at Signy Island, South Orkney Islands. *Br. Antarct. Surv. Sci. Reports* 69, 1–54.
- Bigg, G.R., Rohling, E.J., 2000. An oxygen isotope data set for marine waters. *J. Geophys. Res. Ocean.* 105, 8527–8535. <https://doi.org/10.1029/2000JC900005>.
- Biggs, T.E.G., Alvarez-Fernandez, S., Evans, C., Mojica, K.D.A., Rozema, P.D., Venables, H.J., Pond, D.W., Brussaard, C.P.D., 2019. Antarctic phytoplankton community composition and size structure: importance of ice type and temperature as regulatory factors. *Polar Biol.* 42, 1997–2015. <https://doi.org/10.1007/s00300-019-02576-3>.
- Birt-Friesen, V.L., Montevecchi, W.A., Cairns, D.K., Macko, S.A., 1989. Activity-specific metabolic rates of free-living Northern Gannets and other seabirds. *Ecology* 70, 357–367.
- Bolton, M., 1996. Energy expenditure, body-weight and foraging performance of storm petrels *Hydrobates pelagicus* breeding in artificial nesting chambers. *Ibis* (Lond. 1859), 138, 405–409. <https://doi.org/10.1111/j.1474-919X.1996.tb08058.x>.
- Bond, A.L., Jones, I.L., 2009. A practical introduction to stable-isotope analysis for seabird biologists: approaches, cautions and caveats. *Mar. Ornithol.* 37, 183–188.
- Booth, J.M., McQuaid, C.D., 2013. Northern rockhopper penguins prioritise future reproduction over chick provisioning. *Mar. Ecol. Prog. Ser.* 486, 289–304. <https://doi.org/10.3354/meps10371>.
- Büßer, C., Kahles, A., Quillfeldt, P., 2004. Breeding success and chick provisioning in Wilson's storm-petrels *Oceanites oceanicus* over seven years: frequent failures due to food shortage and entombment. *Polar Biol.* 27, 613–622. <https://doi.org/10.1007/s00300-004-0627-z>.
- Büßer, C., Hahn, S., Gladbach, A., Lorenz, S., 2008. A decade of fundamental ecological research on storm-petrels at the Tres Hermanos colony, Potter Peninsula, King George Island. *Reports Polar Mar. Res.* 571, 168–175.

- Campos, L.S., Barboza, C.A.M., Bassoi, M., Bernardes, M., Bromberg, S., Corbisier, T.N., Fontes, R.F.C., Gheller, P.F., Hajdu, E., Kawall, H.G., Lange, P.K., Lanna, A.M., Lavrado, H.P., Monteiro, G.C.S., Montone, R.C., Morales, T., Moura, R.B., Nakayama, C.R., Oackes, T., Paranhos, R., Passos, F.D., Petti, M.A.V., Pellizari, V.H., Rezende, C.E., Rodrigues, M., Rosa, L.H., Secchi, E., Tenenbaum, D.R., Yoneshigue-Valentin, Y., 2013. Environmental processes, biodiversity and changes in Admiralty Bay, King George Island, Antarctica. In: C., V., di Prisco, G. (Eds.), *Adaptation and Evolution in Marine Environments*. Springer-Verlag, Berlin Heidelberg, pp. 127–156. <https://doi.org/10.1007/978-3-642-27349-0>.
- Carboneras, C., Jutglar, F., Kirwan, G.M., Christie, D.A., Jutglar, F., Kirwan, G.M., Sharpe, C.J., 2017. Order Procellariiformes. In: del Hoyo, J., Elliot, A., Sargatal, J., Christie, D.A., de Juana, E. (Eds.), *Handbook of the Birds of the World Alive*. Lynx Edicions, Barcelona, pp. 197–278.
- Carvalho, P.C., Davoren, G.K., 2019. Niche dynamics of sympatric non-breeding shearwaters under varying prey availability. *Ibis* (Lond. 1859) <https://doi.org/10.1111/ibi.12783>.
- Chaurand, T., Weimerskirch, H., 1994. The regular alternation of short and long foraging trips in the blue petrel *Halobaena caerulea*: a previously undescribed strategy of food provisioning in a pelagic seabird. *J. Anim. Ecol.* 63, 275–282.
- Cherel, Y., Hobson, K.A., 2007. Geographical variation in carbon stable isotope signatures of marine predators: a tool to investigate their foraging areas in the Southern Ocean. *Mar. Ecol. Prog. Ser.* 329, 281–287. <https://doi.org/10.3354/meps329281>.
- Cherel, Y., Hobson, K.A., Guinet, C., Vanpe, C., 2007. Stable isotopes document seasonal changes in trophic niches and winter foraging individual specialization in diving predators from the Southern Ocean. *J. Anim. Ecol.* 76, 826–836. <https://doi.org/10.1111/j.1365-2656.2007.01238.x>.
- Cherel, Y., Connan, M., Jaeger, A., Richard, P., 2014. Seabird year-round and historical feeding ecology: blood and feather $\delta^{13}\text{C}$ and $\delta^{15}\text{N}$ values document foraging plasticity of small sympatric petrels. *Mar. Ecol. Prog. Ser.* 505, 267–280. <https://doi.org/10.3354/meps10795>.
- Clarke, A., 1984. Lipid content and composition of Antarctic krill, *Euphausia superba* Dana. *J. Crustac. Biol.* 4, 285–294.
- Clarke, A., Prince, P.A., 1980. Chemical composition and calorific value of food fed to mollymawk chicks *Diomedea melanophris* and *D. chrysostoma* at Bird Island, South Georgia. *Ibis* (Lond. 1859). 122, 488–494.
- Clewlow, H.L., Takahashi, A., Watanabe, S., Votier, S.C., Downie, R., Ratcliffe, N., 2019. Niche partitioning of sympatric penguins by leapfrog foraging appears to be resilient to climate change. *J. Anim. Ecol.* 88, 223–235. <https://doi.org/10.1111/1365-2656.12919>.
- Coplen, T.B., 1996. New guidelines for reporting stable hydrogen, carbon, and oxygen isotope-ratio data. *Geochim. Cosmochim. Acta* 60, 3359–3360. [https://doi.org/10.1016/0016-7037\(96\)00263-3](https://doi.org/10.1016/0016-7037(96)00263-3).
- Coplen, T.B., Qi, H., 2012. USGS42 and USGS43: human-hair stable hydrogen and oxygen isotopic reference materials and analytical methods for forensic science and implications for published measurement results. *Forensic Sci. Int.* 214, 135–141. <https://doi.org/10.1016/j.forsciint.2011.07.035>.
- Corman, A.M., Mendel, B., Voigt, C.C., Garthe, S., 2016. Varying foraging patterns in response to competition? A multicollinearity approach in a generalist seabird. *Ecol. Evol.* 6, 974–986. <https://doi.org/10.1002/ece3.1884>.
- Croxall, J.P., Prince, P.A., 1980. Food, feeding ecology and segregation of seabirds at South Georgia. *Biol. J. Linn. Soc.* 103–131.
- Cruz, L.L., McGill, R.A.R., Goodman, S.J., Hamer, K.C., 2012. Stable isotope ratios of a tropical marine predator: confounding effects of nutritional status during growth. *Mar. Biol.* 159, 873–880. <https://doi.org/10.1007/s00227-011-1864-7>.
- Dänhardt, A., Fresemann, T., Becker, P.H., 2011. To eat or to feed? Prey utilization of common terns *Sterna hirundo* in the Wadden Sea. *J. Ornithol.* 152, 347–357. <https://doi.org/10.1007/s10336-010-0590-0>.
- Davies, W.E., Hipfner, J.M., Hobson, K.A., Ydenberg, R.C., 2009. Seabird seasonal trophodynamics: isotopic patterns in a community of Pacific alcid. *Mar. Ecol. Prog. Ser.* 382, 211–219. <https://doi.org/10.3354/meps07997>.
- Dehnhardt, N., Achurch, H., Clarke, J., Michel, L.N., Southwell, C., Sumner, M.D., Eens, M., Emmerson, L., 2019. High inter- and intraspecific niche overlap among three sympatrically breeding, closely-related seabird species: generalist foraging as an adaptation to a highly variable environment? *J. Anim. Ecol.* <https://doi.org/10.1111/1365-2656.13078>.
- Dimitrijević, D., Paiva, V.H., Ramos, J.A., Seco, J., Ceia, F.R., Chipev, N., Valente, T., Barbosa, A., Xavier, J.C., 2018. Isotopic niches of sympatric Gentoo and Chinstrap penguins: evidence of competition for Antarctic krill? *Polar Biol.* 41, 1655–1669. <https://doi.org/10.1007/s00300-018-2306-5>.
- Dunn, R.E., Wanless, S., Green, J.A., Harris, M.P., Daunt, F., 2019. Effects of body size, sex, parental care and moult strategies on auk diving behaviour outside the breeding season. *J. Avian Biol.* 50, 1–14. <https://doi.org/10.1111/jav.02012>.
- ESRI, 2014. *ArcMap 10.3.1*.
- Force, M.P., Santora, J.A., Reiss, C.S., Loeb, V.J., 2015. Seabird species assemblages reflect hydrographic and biogeographic zones within Drake Passage. *Polar Biol.* 38, 381–392. <https://doi.org/10.1007/s00300-014-1594-7>.
- Forero, M.G., Hobson, K.A., Bortolotti, G.R., Donazar, J.A., Bertelotti, M., Blanco, G., 2002. Food resource utilization by the Magellanic penguin evaluated through stable-isotope analysis: segregation by sex and age and influence on offspring quality. *Mar. Ecol. Prog. Ser.* 234, 289–299. <https://doi.org/10.3354/meps234289>.
- Fox, J., Weisberg, S., 2011. *An R Companion to Applied Regression*. Second. ed. Sage, Thousand Oaks CA.
- Furness, R.W., Baillie, S.R., 1981. Factors affecting capture rate and biometrics of storm petrels on St Kilda. *Ring. Migr.* 3, 137–148. <https://doi.org/10.1080/03078698.1981.9673772>.
- Furness, R.W., Camphuysen, C.J., 1997. Seabirds as monitors of the marine environment. *ICES J. Mar. Sci.* 54, 726–737. <https://doi.org/10.1006/jmsc.1997.0243>.
- Glabach, A., McGill, R.A.R., Quillfeldt, P., 2007. Foraging areas of Wilson's storm-petrel *Oceanites oceanicus* in the breeding and inter-breeding period determined by stable isotope analysis. *Polar Biol.* 30, 1005–1012. <https://doi.org/10.1007/s00300-007-0258-2>.
- Glabach, A., Braun, C., Nordt, A., Peter, H.U., Quillfeldt, P., 2009. Chick provisioning and nest attendance of male and female Wilson's storm petrels *Oceanites oceanicus*. *Polar Biol.* 32, 1315–1321. <https://doi.org/10.1007/s00300-009-0628-z>.
- Grömpig, U., 2006. Relative importance for linear regression in R: the package relaimpo. *J. Stat. Softw.* 17, 1–27.
- Hahn, S., 1998a. The food and chick feeding of blackbellied stormpetrel (*Fregatta tropica*) at King George Island, South Shetlands. *Polar Biol.* 19, 354–357. <https://doi.org/10.1007/s003000050258>.
- Hahn, S., 1998b. Brutphänologie und Morphometrie des Schwarzbauchmeerläufers (*Fregatta tropica*) auf King George Island, Antarktis. *J. für Ornithol.* 139, 149–156.
- Hatch, S.A., Hatch, M.A., 1990. Breeding seasons of oceanic birds in a subarctic colony. *Can. J. Zool.* 68, 1664–1679. <https://doi.org/10.1139/z90-247>.
- Henley, S.F., Schofield, O.M., Hendry, K.R., Schloss, I.R., Steinberg, D.K., Moffat, C., Peck, L.S., Costa, D.P., Bakker, D.C.E., Hughes, C., Rozema, P.D., Ducklow, H.W., Abele, D., Stefels, J., Van Leeuwe, M.A., Brussaard, C.P.D., Buma, A.G.J., Kohut, J., Sahade, R., Friedlaender, A.S., Stammerjohn, S.E., Venables, H.J., Meredith, M.P., 2019. Variability and change in the west Antarctic Peninsula marine system: research priorities and opportunities. *Prog. Oceanogr.* 173, 208–237. <https://doi.org/10.1016/j.pocean.2019.03.003>.
- Hill, S.L., Phillips, T., Atkinson, A., 2013. Potential climate change effects on the habitat of Antarctic krill in the Weddell quadrant of the Southern Ocean. *PLoS One* 8. <https://doi.org/10.1371/journal.pone.0072246>.
- Hobson, K.A., Welch, H.E., 1992. Determination of trophic relationships within a high Arctic marine food web using $\delta^{13}\text{C}$ and $\delta^{15}\text{N}$ analysis. *Mar. Ecol. Prog. Ser.* 84, 9–18. <https://doi.org/10.3354/meps084009>.
- Hobson, K.A., Alisauskas, R.T., Clark, R.G., 1993. Stable-nitrogen isotope enrichment in avian tissues due to fasting and nutritional stress: implications for isotopic analyses of diet. *Condor* 95, 388. <https://doi.org/10.2307/1369361>.
- Hodum, P.J., Hobson, K.A., 2000. Trophic relationships among Antarctic fulmarine petrels: insights into dietary overlap and chick provisioning strategies inferred from stable-isotope ($\delta^{15}\text{N}$ and $\delta^{13}\text{C}$) analyses. *Mar. Ecol. Prog. Ser.* 198, 273–281. <https://doi.org/10.3354/meps198273>.
- Hurwitz, S., Plavnik, I., Shapiro, A., Wax, E., Talpaz, H., Bar, A., 1995. Calcium metabolism and requirements of chickens are affected by growth. *J. Nutr.* 125, 2679–2686. <https://doi.org/10.1093/jn/125.10.2679>.
- Hutchinson, G.E., 1957. Concluding remarks. *Cold Spring Harb. Symp. Quantitative Biol.* 22, 415–427. <https://doi.org/10.1101/SQB.1957.022.01.039>.
- Jabłoński, B., 1986. Distribution, abundance and biomass of a summer community of birds in the region of the Admiralty Bay (King George Island, South Shetland Islands, Antarctica) in 1978/1979. *Polish Polar Res* 7, 217–260.
- Jackson, A.L., Inger, R., Parnell, A.C., Bearhop, S., 2011. Comparing isotopic niche widths among and within communities: SIBER - Stable Isotope Bayesian Ellipses in R. *J. Anim. Ecol.* 80, 595–602. <https://doi.org/10.1111/j.1365-2656.2011.01806.x>.
- Jaeger, A., Connan, M., Richard, P., Cherel, Y., 2010. Use of stable isotopes to quantify seasonal changes of trophic niche and levels of population and individual specialisation in seabirds. *Mar. Ecol. Prog. Ser.* 401, 269–277. <https://doi.org/10.3354/meps08380>.
- Jakubas, D., Iliżko, L., Wojczulanis-Jakubas, K., Stempniewicz, L., 2012. Foraging by little auks in the distant marginal sea ice zone during the chick-rearing period. *Polar Biol.* 35, 73–81. <https://doi.org/10.1007/s00300-011-1034-x>.
- Krüger, L., 2019. Spatio-temporal trends of the krill fisheries in the Western Antarctic Peninsula and Southern Scotia Arc. *Fish. Manag. Ecol.* 26, 327–333. <https://doi.org/10.1111/fme.12363>.
- Kuepper, N.D., Marek, C., Coria, N., Libertelli, M.M., Quillfeldt, P., 2018. Facultative hypothermia as a survival strategy during snowstorm induced food shortages in Antarctic storm-petrel chicks. *Comp. Biochem. Physiol. Part A* 224, 76–83. <https://doi.org/10.1016/j.cbpa.2018.06.018>.
- Kwasniewski, S., Gluchowska, M., Walkusz, W., Karnovsky, N.J., Jakubas, D., Wojczulanis-Jakubas, K., Harding, A.M.A., Goszczko, I., Cisek, M., Bieszczynska-Möller, A., Walczowski, W., Weslowski, J.M., Stempniewicz, L., 2012. Interannual changes in zooplankton on the West Spitsbergen Shelf in relation to hydrography and their consequences for the diet of planktivorous seabirds. *ICES J. Mar. Sci.* 69, 890–901.
- LeGrande, A.N., Schmidt, G.A., 2006. Global Gridded Data Set of the Oxygen Isotopic Composition in Seawater. 33, pp. 1–5. <https://doi.org/10.1029/2006GL026011>.
- Lindeman, R.L., 1942. The trophic-dynamic aspect of ecology. *Ecology* 23, 399–417.
- Lindeman, R.H., Merenda, P.F., Gold, R.H., 1980. *Introduction to Bivariate and Multivariate Analysis*. Scott Foresman, Glenview, IL.
- Loeb, V., Siegel, V., Holm-Hansen, O., Hewitt, R.P., Fraser, W.R., Trivelpiece, W., Trivelpiece, S., 1997. Effects of sea-ice extent and krill or salp dominance on the Antarctic food web. *Nature* 387, 897–900. <https://doi.org/10.1038/43174>.
- Marinao, C., Suárez, N., Gatto, A., Yorio, P., 2019. Forage fish to growing chicks: shared food resources between two closely related tern species. *Mar. Biol.* 166, 1–12. <https://doi.org/10.1007/s00227-019-3570-9>.
- Marrari, M., Daly, K.L., Hu, C., 2008. Spatial and temporal variability of SeaWiFS chlorophyll a distributions west of the Antarctic Peninsula: implications for krill production. *Deep. Res. II* 55, 377–392. <https://doi.org/10.1016/j.dsr2.2007.11.011>.
- Masello, J.F., Mundry, R., Poisbleau, M., Demongin, L., Voigt, C.C., Wikelski, M., Quillfeldt, P., 2010. Diving seabirds share foraging space and time within and among species. *Ecosphere* 1. <https://doi.org/10.1890/ES10-00103.1>.
- Merkling, T., Leclaire, S., Danchin, E., Lhuillier, E., Wagner, R.H., White, J., Hatch, S.A., Blanchard, P., 2012. Food availability and offspring sex in a monogamous seabird:

- insights from an experimental approach. *Behav. Ecol.* 23, 751–758. <https://doi.org/10.1093/beheco/ars023>.
- Michielsen, R.J., Aulsems, A.N.M.A., Jakubas, D., Petlicki, M., Plenzler, J., Shamoun-Baranes, J., Jakubas, K.W., 2019. Nest characteristics determine nest microclimate and affect breeding output in an Antarctic seabird, the Wilson's storm-petrel. *PLoS One* 14. <https://doi.org/10.1371/journal.pone.0217708>.
- Miller, M.G.R., Silva, F.R.O., Machovsky-Capuska, G.E., Congdon, B.C., 2018. Sexual segregation in tropical seabirds: drivers of sex-specific foraging in the brown booby *Sula leucogaster*. *J. Ornithol.* 159, 425–437. <https://doi.org/10.1007/s10336-017-1512-1>.
- Minagawa, M., Wada, E., 1984. Stepwise enrichment of ^{15}N along food chains: further evidence and the relation between $\delta^{15}\text{N}$ and animal age. *Geochim. Cosmochim. Acta* 48, 1135–1140. [https://doi.org/10.1016/0016-7037\(84\)90204-7](https://doi.org/10.1016/0016-7037(84)90204-7).
- Minnett, P.J., 2010. The validation of sea surface temperature retrievals from spaceborne infrared radiometers. In: Barale, V., Gower, J.F.R., Alberotanza, L. (Eds.), *Oceanography from Space: Revisited*. Springer, Dordrecht, pp. 237–295. <https://doi.org/10.1007/978-90-481-8681-5>.
- Moody, A.T., Hobson, K.A., Gaston, A.J., 2012. High-arctic seabird trophic variation revealed through long-term isotopic monitoring. *J. Ornithol.* 153, 1067–1078. <https://doi.org/10.1007/s10336-012-0836-0>.
- Morrison, K.W., Bury, S.J., Thompson, D.R., 2014. Higher trophic level prey does not represent a higher quality diet in a threatened seabird: implications for relating population dynamics to diet shifts inferred from stable isotopes. *Mar. Biol.* 161, 2243–2255. <https://doi.org/10.1007/s00227-014-2502-y>.
- Namgail, T., Mishra, C., De Jong, C.B., Van Wieren, S.E., Prins, H.H.T., 2009. Effects of herbivore species richness on the niche dynamics and distribution of blue sheep in the Trans-Himalaya. *Divers. Distrib.* 15, 940–947. <https://doi.org/10.1111/j.1472-4642.2009.00611.x>.
- Navarro, J., Votier, S.C., Aguzzi, J., Chiesa, J.J., Forero, M.G., Phillips, R.A., 2013. Ecological segregation in space, time and trophic niche of sympatric planktivorous petrels. *PLoS One* 8. <https://doi.org/10.1371/journal.pone.0062897>.
- Neter, J., Wasserman, W., Kupner, M.H., 1989. *Applied Linear Regression Models*. Irwin, Homewood, IL.
- Newsome, S.D., Rio Martinez del, C., Bearhop, S., Phillips, D.L., 2007. A niche for isotope ecology. *Front. Ecol. Environ.* 5, 429–436. <https://doi.org/10.1890/060150.01>.
- Obst, B.S., Nagy, K.A., 1993. Stomach oil and the energy budget of Wilson's storm-petrel nestlings. *Condor* 95, 792–805.
- Pauly, D., Christensen, V., Dalsgaard, J., Froese, R., Torres, F., 1998. Fishing down marine food webs. *Science* (80-) 279, 860–863. <https://doi.org/10.1126/science.279.5352.860>.
- Pelletier, L., Chiaradia, A., Kato, A., Ropert-Coudert, Y., 2014. Fine-scale spatial age segregation in the limited foraging area of an inshore seabird species, the little penguin. *Oecologia* 176, 399–408. <https://doi.org/10.1007/s00442-014-3018-3>.
- Pennycook, A.C.J., Croxall, J.P., Prince, P.A., 1984. Scaling of foraging radius and growth rate in petrels and albatrosses (Procellariiformes). *Ornis Scand.* 15, 145–154.
- Phillips, R.A., Silk, J.R.D., Phalan, B., Catry, P., Croxall, J.P., 2004. Seasonal sexual segregation in two Thalassarche albatross species: competitive exclusion, reproductive role specialization or foraging niche divergence? *Proc. R. Soc. B Biol. Sci.* 271, 1283–1291. <https://doi.org/10.1098/rspb.2004.2718>.
- Pinkerton, M.H., Forman, J., Bury, S.J., Brown, J., Horn, P., O'Driscoll, R.L., 2013. Diet and trophic niche of Antarctic silverfish *Pleuragramma antarcticum* in the Ross Sea, Antarctica. *J. Fish Biol.* 82, 141–164. <https://doi.org/10.1111/j.1095-8649.2012.03476.x>.
- Pol, M. van de, Ens, B.J., Oosterbeek, K., Brouwer, L., Verhulst, S., Tinbergen, J.M., Rutten, A.L., Jong, M. De, 2009. Oystercatchers' bill shapes as a proxy for diet specialization: more differentiation than meets the eye. *Ardea* 97, 335–347. <https://doi.org/10.5253/078.097.0309>.
- Polito, M.J., Abel, S., Tobias, C.R., Emslie, S.D., 2011. Dietary isotopic discrimination in gentoo penguin (*Pygoscelis papua*) feathers. *Polar Biol.* 34, 1057–1063. <https://doi.org/10.1007/s00300-011-0966-5>.
- Polito, M.J., Reiss, C.S., Trivelpiece, W.Z., Patterson, W.P., Emslie, S.D., 2013. Stable isotopes identify an ontogenetic niche expansion in Antarctic krill (*Euphausia superba*) from the South Shetland Islands, Antarctica. *Mar. Biol.* 160, 1311–1323. <https://doi.org/10.1007/s00227-013-2182-z>.
- Polito, M.J., Trivelpiece, W.Z., Patterson, W.P., Karnovsky, N.J., Reiss, C.S., Emslie, S.D., 2015. Contrasting specialist and generalist patterns facilitate foraging niche partitioning in sympatric populations of Pygoscelis penguins. *Mar. Ecol. Prog. Ser.* 519, 221–237. <https://doi.org/10.3354/meps11095>.
- Post, D.M., Layman, C.A., Arrington, D.A., Takimoto, G., Quattrochi, J., Montaña, C.G., 2007. Getting to the fat of the matter: models, methods and assumptions for dealing with lipids in stable isotope analyses. *Oecologia* 152, 179–189. <https://doi.org/10.1007/s00442-006-0630-x>.
- Pratte, I., Boadway, K.A., Diamond, A.W., Mallory, M.L., 2018. Changes in isotopic niches across stages of the annual cycle in the Arctic tern (*Sterna paradisaea*). *Arctic* 71, 259–268.
- Quillfeldt, P., 2002. Seasonal and annual variation in the diet of breeding and non-breeding Wilson's storm-petrels on King George Island, South Shetland Islands. *Polar Biol.* 25, 216–221. <https://doi.org/10.1007/s00300-001-0332-0>.
- Quillfeldt, P., Peter, H.-U., 2000. Provisioning and growth in chicks of Wilson's storm-petrels (*Oceanites oceanicus*) on King George Island, South Shetland Islands. *Polar Biol.* 23, 817–824.
- Quillfeldt, P., McGill, R.A.R., Furness, R.W., 2005. Diet and foraging areas of Southern Ocean seabirds and their prey inferred from stable isotopes: review and case study of Wilson's storm-petrel. *Mar. Ecol. Prog. Ser.* 295, 295–304. <https://doi.org/10.3354/meps295295>.
- Quillfeldt, P., Bugoni, L., McGill, R.A.R., Masello, J.F., Furness, R.W., 2008. Differences in stable isotopes in blood and feathers of seabirds are consistent across species, age and latitude: implications for food web studies. *Mar. Biol.* 155, 593–598. <https://doi.org/10.1007/s00227-008-1048-2>.
- R Core Team, 2019. *R: A Language and Environment for Statistical Computing*.
- Rakusa-Suszczewski, S., 1980. Environmental conditions and the functioning of Admiralty Bay (South Shetland Islands) as a part of the near shore Antarctic ecosystem. *Polish Polar Res* 1, 11–27.
- Ridou, V., 1994. The diets and dietary segregation of seabirds at the subantarctic Crozet Islands. *Mar. Ornithol.* 22, 1–192.
- Robertson, G.S., Bolton, M., Grecian, W.J., Wilson, L.J., Davies, W., Monaghan, P., 2014. Resource partitioning in three congeneric sympatrically breeding seabirds: foraging areas and prey utilization. *Auk* 131, 434–446. <https://doi.org/10.1642/auk-13-243.1>.
- Rogerson, P.A., 2001. *Statistical Methods for Geography*. Sage, London.
- Rosciano, N.G., Polito, M.J., Raya Rey, A., 2019. What's for dinner mom? Selective provisioning in southern rockhopper penguins (*Eudyptes chrysocome*). *Polar Biol.* 42, 1529–1535. <https://doi.org/10.1007/s00300-019-02538-9>.
- Rossmann, S., Ostrom, P.H., Gordon, F., Zipkin, E.F., 2016. Beyond carbon and nitrogen: guidelines for estimating three-dimensional isotopic niche space. *Ecol. Evol.* 6, 2405–2413. <https://doi.org/10.1002/ece3.2013>.
- Roughgarden, J., 1972. Evolution of niche width. *Am. Nat.* 106, 683–718.
- Ruck, K.E., Steinberg, D.K., Canuel, E.A., 2014. Regional differences in quality of krill and fish as prey along the Western Antarctic Peninsula. *Mar. Ecol. Prog. Ser.* 509, 39–55. <https://doi.org/10.3354/meps10868>.
- Santora, J.A., Veit, R.R., Reiss, C.S., Schroeder, I.D., Mangel, M., 2017. Ecosystem oceanography of seabird hotspots: environmental determinants and relationship with Antarctic krill within an important fishing ground. *Ecosystems* 20, 885–903. <https://doi.org/10.1007/s10021-016-0078-8>.
- Siegel, V., 2012. Krill stocks in high latitudes of the Antarctic Lazarev sea: seasonal and interannual variation in distribution, abundance and demography. *Polar Biol.* 35, 1151–1177. <https://doi.org/10.1007/s00300-012-1162-y>.
- Siegel, V., Reiss, C.S., Dietrich, K.S., Haraldsson, M., Rohardt, G., 2013. Distribution and abundance of Antarctic krill (*Euphausia superba*) along the Antarctic Peninsula. *Deep. Res. I* 77, 63–74. <https://doi.org/10.1016/j.dsr.2013.02.005>.
- Sierakowski, K., 1991. Birds and mammals in the region of SSSI No. 8 in the season 1988/89 (South Shetlands, King George Island, Admiralty Bay). *Polish Polar Res.* 12, 25–54.
- Sierakowski, K., Korczak-Abshire, M., Jadwiszczak, P., 2017. Changes in bird communities of Admiralty Bay, King George Island (West Antarctic): insights from monitoring data (1977–1996). *Polish Polar Res* 38, 231–262. <https://doi.org/10.1515/popore-2017-0010>.
- Skrzypek, G., 2013. Normalization procedures and reference material selection in stable HCNOs isotope analyses: an overview. *Anal. Bioanal. Chem.* 405, 2815–2823. <https://doi.org/10.1007/s00216-012-6517-2>.
- Skrzypek, G., Ford, D., 2014. Stable isotope analysis of saline water samples on a cavity ring-down spectroscopy instrument. *Environ. Sci. Technol.* 48, 2827–2834. <https://doi.org/10.1021/es4049412>.
- Skrzypek, G., Paul, D., 2006. $\delta^{13}\text{C}$ analyses of calcium carbonate: comparison between the GasBench and elemental analyzer techniques. *Rapid Commun. Mass Spectrom.* 20, 2915–2920. <https://doi.org/10.1002/rcm.2688>.
- Svanbäck, R., Bolnick, D.I., 2007. Intraspecific competition drives increased resource use diversity within a natural population. *Proc. R. Soc. B Biol. Sci.* 274, 839–844. <https://doi.org/10.1098/rspb.2006.0198>.
- Trathan, P.N., Hill, S., 2016. The importance of krill predation in the Southern Ocean. In: Siegel, V. (Ed.), *Biology and Ecology of Antarctic Krill*. Advances in Polar Ecology. Springer, Cham. <https://doi.org/10.1007/978-3-319-29279-3>.
- Trueman, C.N., McGill, R.A.R., Guyard, P.H., 2005. The effect of growth rate on tissue-diet isotopic spacing in rapidly growing animals. An experimental study with Atlantic salmon (*Salmo salar*). *Rapid Commun. Mass Spectrom.* 19, 3239–3247. <https://doi.org/10.1002/rcm.2199>.
- VanHeezik, Y.M., Seddon, P.J., Du Plessis, C.J., Adams, N.J., 1993. Differential growth of king penguin chicks in relation to date of hatching. *Colon. Waterbirds* 16, 71–76.
- Warham, J., 1990. *The Petrels: Their Ecology and Breeding Systems*. A&C Black, London.
- Warham, J., 1996. *The Behaviour, Population Biology and Physiology of the Petrels*. Academic Press, London.
- Warham, J., Watts, R., Dainty, R.J., 1976. The composition, energy content and function of the stomach oils of petrels (order, Procellariiformes). *J. Exp. Mar. Biol. Ecol.* 23, 1–13. [https://doi.org/10.1016/0022-0981\(76\)90081-2](https://doi.org/10.1016/0022-0981(76)90081-2).
- Wasilewski, A., 1986. Ecological aspects of the breeding cycle in the Wilson's storm petrel, *Oceanites oceanicus* (Kuhl), at King George Island (South Shetland Islands, Antarctica). *Polish Polar Res* 7, 173–216.
- Wilson, R.P., 2010. Resource partitioning and niche hyper-volume overlap in free-living Pygoscelid penguins. *Funct. Ecol.* 24, 646–657. <https://doi.org/10.1111/j.1365-2435.2009.01654.x>.

Sharing menus or kids' specials? Inter- and intraspecific differences in isotopic niches between sympatrically breeding storm-petrels

Anne N.M.A. Ausems¹, Grzegorz Skrzypek², Katarzyna Wojczulanis-Jakubas¹, Dariusz Jakubas¹

¹The University of Gdańsk, Faculty of Biology, Department of Vertebrate Ecology and Zoology, ul. Wita Stwosza 59, 80-308, Poland

²The University of Western Australia, School of Biological Sciences, West Australian Biogeochemistry Centre, 35 Stirling Highway, Crawley WA 6009, Australia

Appendix 1

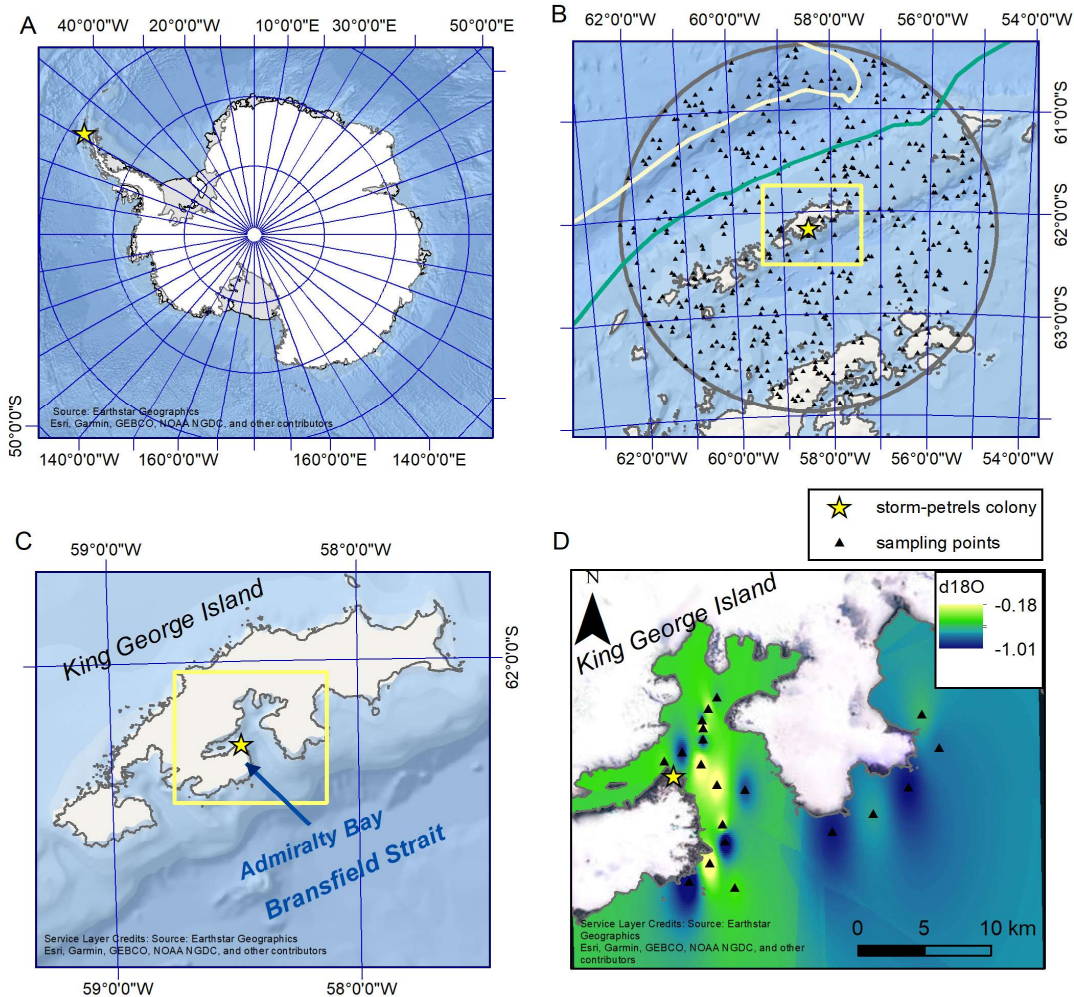


Figure A1. Study Area

The location of the black-bellied and Wilson's storm-petrel colony is shown with a yellow star. A – location of the colony relative to the entirety of Antarctica, including the bathymetry of the Southern Ocean; B – the 500 randomly selected points (black triangles) in a 200 km buffer (grey circle) around the colony, with lines showing the Southern boundary of the Antarctic Circumpolar current (green line) and the Southern Antarctic Circumpolar Current Front (off-white); C – the location of the storm-petrel colony on King George Island; D – the $\delta^{18}\text{O}$ ocean water sampling points (black triangles) and the IDW interpolation of the $\delta^{18}\text{O}$ ocean water gradient in Admiralty Bay and part of the Bransfield Strait.

Chick age prediction

We calculated the age of chicks with an unknown hatching date based on a Non-linear Least Squares model (NLS) fitted to the age and the tarsus length of chicks with known hatching dates (1), according to the following formula:

$$TL \sim \frac{\varphi_1}{(1 + e^{\varphi_2 + \varphi_3 \times Age})}$$

where TL is tarsus length and Age is the observed age in days from January 1st. NLS models were fitted to the known age chicks of the black-bellied storm-petrels pooled between both studied years and to the known age chicks of the Wilson's storm-petrels separately for each studied year. The starting parameters were φ_1 = maximum observed TL + 5, φ_2 = intercept of linear model

$$\text{logit}\left(\frac{TL}{\varphi_1}\right) \sim Age$$

φ_3 = slope of the same linear model. We used the R (2) function *nls* (package *stats*) to fit the NLS model, for which we found it performed better when adding an arbitrary +5 to the maximum observed TL for φ_1 . See also Fig. S2 and S3 for the plotted model and efficiency in predicting chick age.

Table A1: Non-linear Least Squares model (NLS) results for age prediction of the studied species. BBSP – black-bellied storm-petrel; WSP – Wilson's storm-petrel; Est – estimate; SE – standard error; φ_{1-3} – First through third fitted NLS model parameters; It – iterations; CL – convergence level.

	BBSP _{pooled}				WSP ₂₀₁₇				WSP ₂₀₁₈			
	Est	SE	t	p	Est	SE	t	p	Est	SE	t	p
φ_1	42.61	0.565	75.40	<0.001	35.74	0.634	56.36	<0.001	36.27	0.277	130.9	<0.001
φ_2	-0.960	0.057	-16.71	<0.001	-0.815	0.157	-5.794	<0.001	-1.015	0.044	-23.30	<0.001
φ_3	0.105	0.006	17.89	<0.001	0.128	0.016	8.175	<0.001	0.120	0.004	27.13	<0.001
It	8				8				9			
CL	3.32e ⁻⁶				3.89e ⁻⁶				2.19e ⁻⁶			

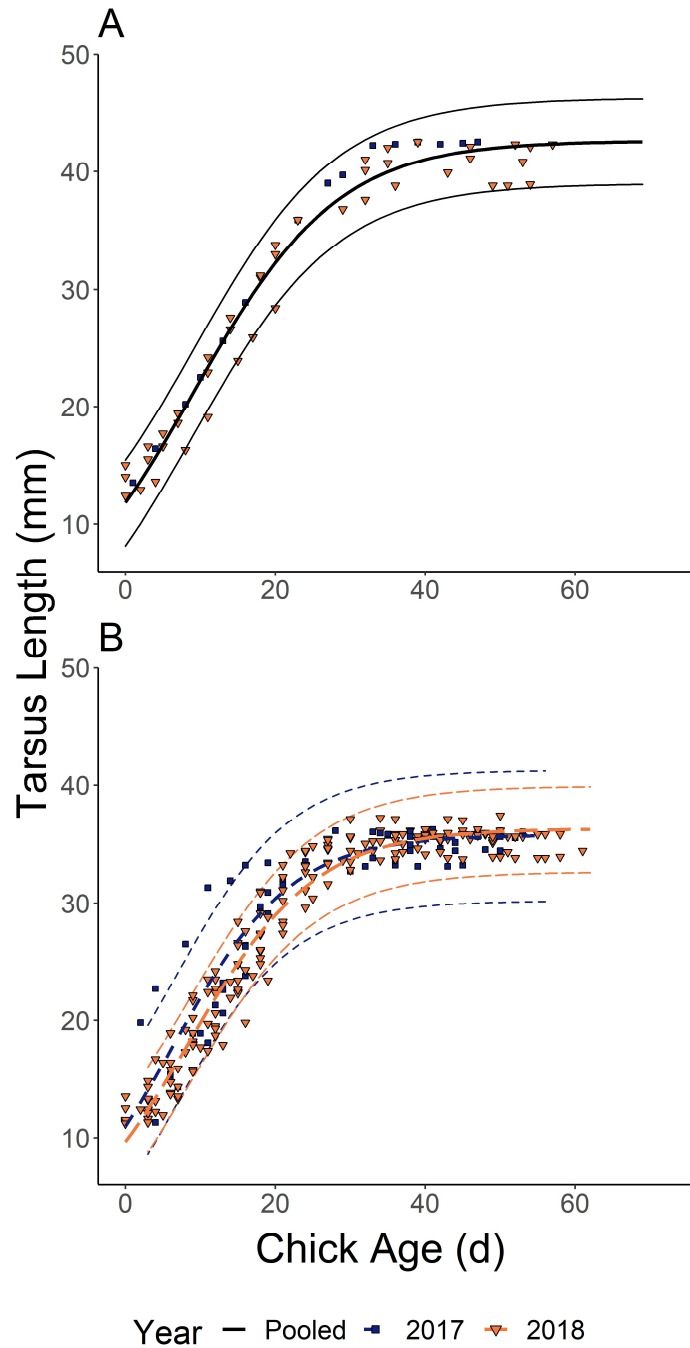


Figure A2. Non-linear Least Squares model (NLS) for tarsus length and chick age in days from January 1st: A – the model for the black-bellied storm-petrels based on data pooled between both studied years due to the low sample size ($n = 4$); B – the models for the Wilson's storm-petrels separated per year. The model-fit is shown by the solid line \pm 95 % confidence intervals in dashed lines. See also table S1.

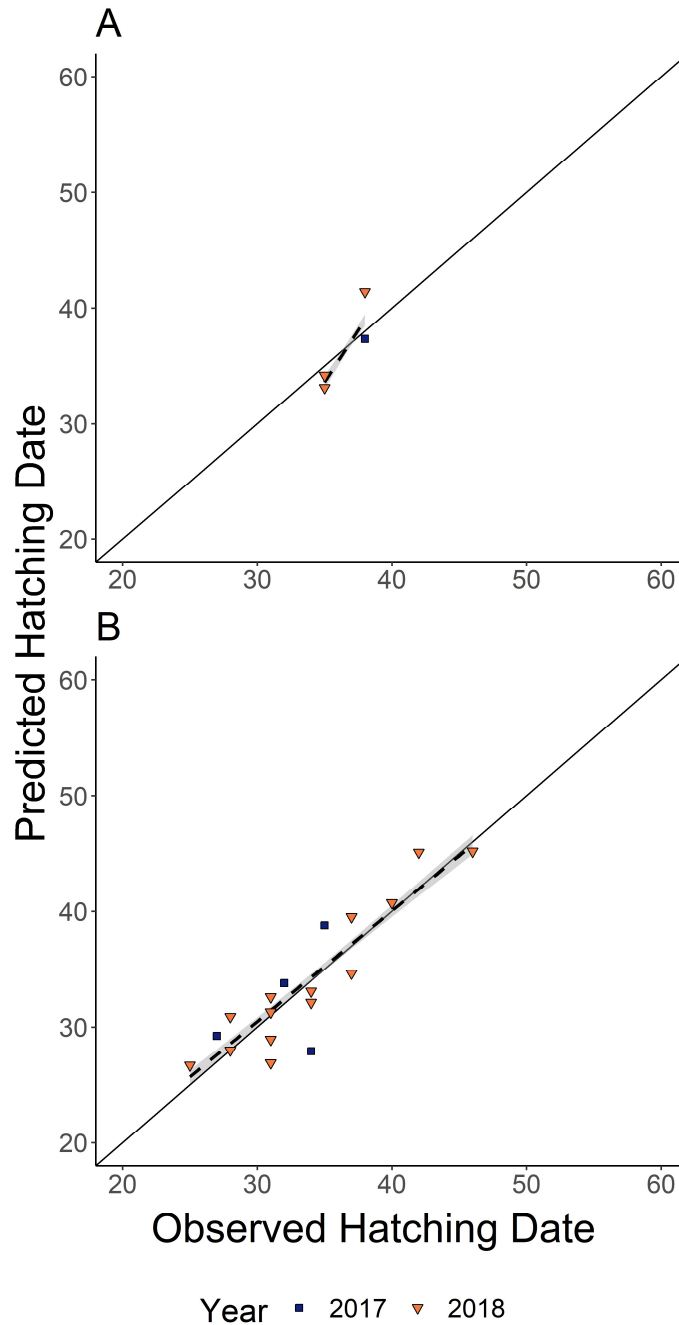


Figure A3. Correlation between observed hatching date and hatching date predicted by a Non-linear Least Squares model (NLS): A – correlation for the black-bellied storm-petrels; B – correlation for the Wilson’s storm-petrels. Observations are shown per year, but the model was fitted to both years pooled. The solid line shows a relationship of 1:1. The dashed lines show the OLS estimate \pm shaded 95 % confidence intervals.

Periods of linear growth

We determined the periods of linear growth visually based on scatter plots of the growth parameter against predicted age for both the black-bellied and Wilson’s storm-petrels. These limits were then used to select data points within the range to calculate the slope of a linear model of the growth parameter against predicted age as a proxy of growth rate. For the Wilson’s storm-petrels these ranges were determined for both years separately as age prediction was done per year as well.

Table A2 Periods of Linear Growth

BBSP – black-bellied storm-petrel; WSP – Wilson’s storm-petrel; Min – minimum age in days since January 1st; max – maximum age in days.

Parameter	BBSP _{pooled}		WSP ₂₀₁₇		WSP ₂₀₁₈	
	Min (d)	Max (d)	Min (d)	Max (d)	Min (d)	Max (d)
Tarsus Length	3.5	23.5	3	19.5	4	24
Wing Length	22	48	15	40	15	40
Body Mass	0	13	0	20	3	20

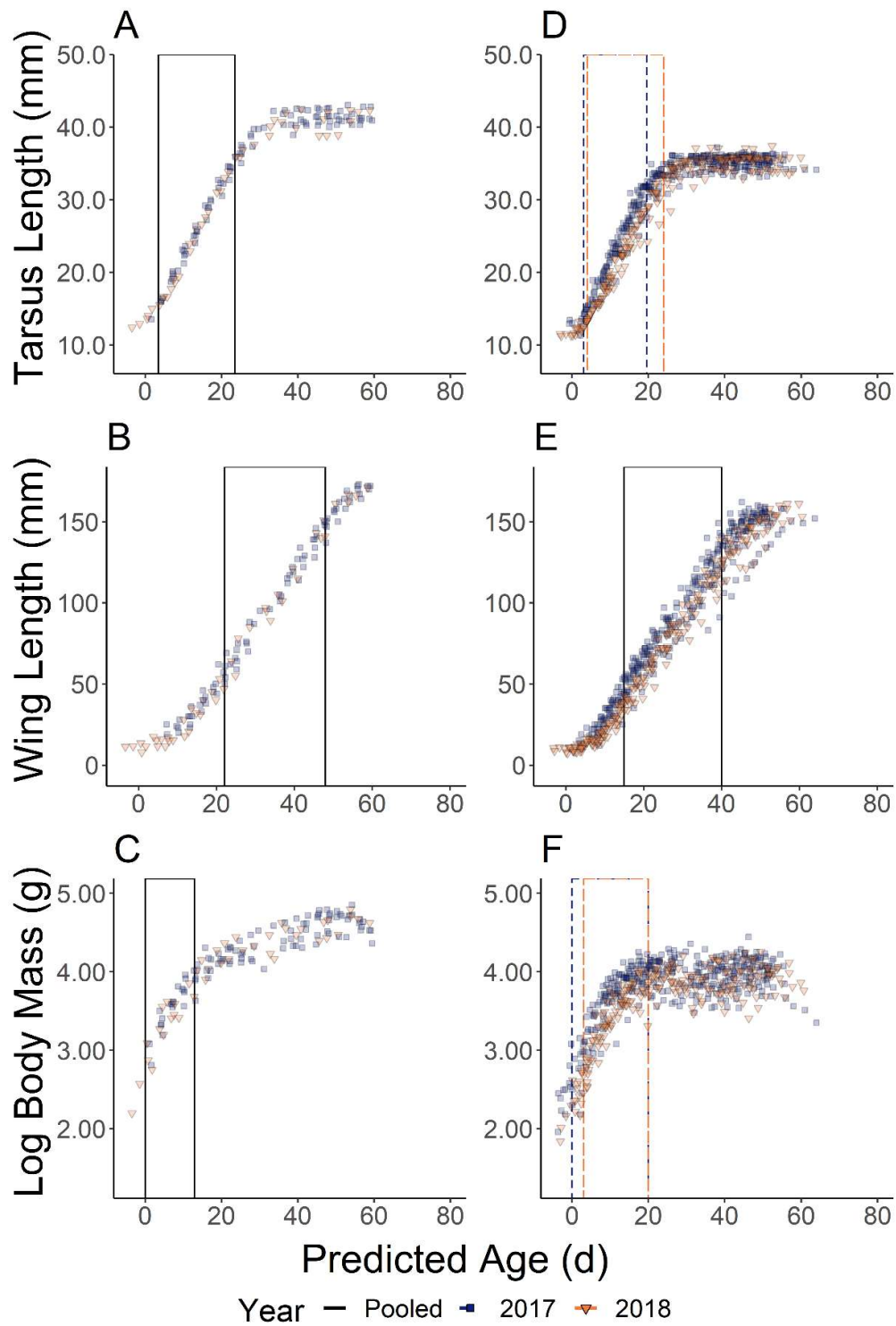


Figure A4. Periods of linear growth for the chicks of both studied storm-petrel species: A-C – chick growth for the black-bellied storm-petrels; D-F – chick growth for the Wilson’s storm-petrels. The periods of linear growth are shown with shaded rectangles and solid lines. For the Wilson’s storm-petrels linear growth was determined for each year separately, unless it was the same (i.e. for wing length). See also table S2.

5. Research Paper no. 3

Ausems, A.N.M.A., Skrzypek, G., Wojczulanis-Jakubas, K., Jakubas, D. 2021
Birds of a feather moult together: differences in moulting distribution of four
species of storm-petrels, PLOS ONE 16(1):e0245756.

<https://doi.org/10.1371/journal.pone.0245756>

RESEARCH ARTICLE

Birds of a feather moult together: Differences in moulting distribution of four species of storm-petrels

Anne N. M. A. Ausems^{1*}, Grzegorz Skrzypek², Katarzyna Wojczulanis-Jakubas¹, Dariusz Jakubas¹

1 Department of Vertebrate Ecology and Zoology, Faculty of Biology, The University of Gdańsk, Gdańsk, Poland, **2** West Australian Biogeochemistry Centre, The University of Western Australia, Crawley, WA, Australia

* anne.ausems@gmail.com



OPEN ACCESS

Citation: Ausems ANMA, Skrzypek G, Wojczulanis-Jakubas K, Jakubas D (2021) Birds of a feather moult together: Differences in moulting distribution of four species of storm-petrels. PLoS ONE 16(1): e0245756. <https://doi.org/10.1371/journal.pone.0245756>

Editor: Vitor Hugo Rodrigues Paiva, MARE – Marine and Environmental Sciences Centre, PORTUGAL

Received: October 14, 2020

Accepted: January 6, 2021

Published: January 22, 2021

Peer Review History: PLOS recognizes the benefits of transparency in the peer review process; therefore, we enable the publication of all of the content of peer review and author responses alongside final, published articles. The editorial history of this article is available here: <https://doi.org/10.1371/journal.pone.0245756>

Copyright: © 2021 Ausems et al. This is an open access article distributed under the terms of the [Creative Commons Attribution License](https://creativecommons.org/licenses/by/4.0/), which permits unrestricted use, distribution, and reproduction in any medium, provided the original author and source are credited.

Data Availability Statement: All relevant data are within the manuscript and its [Supporting Information](#) files.

Abstract

The non-breeding period of pelagic seabirds, and particularly the moulting stage, is an important, but understudied part of their annual cycle as they are hardly accessible outside of the breeding period. Knowledge about the moulting ecology of seabirds is important to understand the challenges they face outside and within the breeding season. Here, we combined stable carbon ($\delta^{13}\text{C}$) and oxygen ($\delta^{18}\text{O}$) signatures of rectrices grown during the non-breeding period of two pairs of storm-petrel species breeding in the northern (European storm-petrel, *Hydrobates pelagicus*, ESP; Leach's storm-petrel, *Hydrobates leucorhous*, LSP) and southern (black-bellied storm-petrel, *Fregetta tropica*, BBSP; Wilson's storm-petrel, *Oceanites oceanicus*, WSP) hemispheres to determine differences in moulting ranges within and between species. To understand clustering patterns in $\delta^{13}\text{C}$ and $\delta^{18}\text{O}$ moulting signatures, we examined various variables: species, sexes, years, morphologies (feather growth rate, body mass, tarsus length, wing length) and $\delta^{15}\text{N}$. We found that different factors could explain the differences within and between the four species. We additionally employed a geographical distribution prediction model based on oceanic $\delta^{13}\text{C}$ and $\delta^{18}\text{O}$ isoscapes, combined with chlorophyll-*a* concentrations and observational data to predict potential moulting areas of the sampled feather type. The northern species were predicted to moult in temperate and tropical Atlantic zones. BBSP was predicted to moult on the southern hemisphere north of the Southern Ocean, while WSP was predicted to moult further North, including in the Arctic and northern Pacific. While moulting distribution can only be estimated on large geographical scales using $\delta^{13}\text{C}$ and $\delta^{18}\text{O}$, validating predictive outcomes with food availability proxies and observational data may provide valuable insights into important moulting grounds. Establishing those, in turn, is important for conservation management of elusive pelagic seabirds.

Funding: The study was funded by a grant of the National Science Centre, Poland to Dr. Dariusz Jakubas (2015/19/B/NZ8/01981; <https://www.ncn.gov.pl/?language=en>). The funders had no role in study design, data collection and analysis, decision to publish, or preparation of the manuscript.

Competing interests: The authors have declared that no competing interests exist.

Introduction

The non-breeding period is an important part of the avian annual cycle, and it often spans the majority of the year in pelagic seabirds. Knowledge about seabird non-breeding ecology is crucial to understand the entire annual avian cycle as events on the non-breeding grounds may carry-over into the breeding period. Differences in non-breeding distribution and food availability [1], diet quality [2] or diet composition [3] at the non-breeding area may affect survival [4] and breeding success [5] during the subsequent breeding season. Additionally, contaminant accumulation during one stage of the annual cycle may be carried over to other stages, such as maternal transfer of contaminants to eggs and chicks [6, 7]. Nevertheless, the non-breeding period is understudied in many pelagic seabird species due to the inaccessibility of the birds beyond the breeding period.

An important stage in the non-breeding period of many pelagic seabird species is the moulting stage. Moulting is an energetically costly process [8], and plumage gaps caused by missing feathers increase flight costs through lowered flight efficiency [9], and reduced aerodynamic performance through lowered manoeuvrability [10, 11]. In pelagic seabirds moulting individuals may spend more time floating on the water than outside of the moulting period [12], affecting foraging effectiveness. Many pelagic seabirds, therefore, spread the impact of moult by reducing the number of feathers moulting at once [13], thus increasing the length of the moulting period. The extended moulting period thus covers a large part of the non-breeding period, and may even overlap with the end of the breeding period [14].

Studying the non-breeding distribution of small pelagic seabirds, such as storm-petrels, is still a challenge, resulting in a considerable knowledge gap. Although progress is being made with the miniaturisation of devices enabling whole year tracking [15–17], sample sizes remain relatively small due to low retrieval rates and incomplete tracks [15–17]. Additionally, these devices, while not proven detrimental [15–17], may be considered a relatively invasive method to study year-round movements.

Stable carbon isotope analysis in various avian tissues is a well-established method to determine seabird trophic level and foraging distribution during the moulting period [18, 19]. Stable isotope compositions of feathers remain inert after formation and thus represent the isotopic signatures of the prey eaten during feather synthesis [20], following the principle “you are what you eat” [21]. Since many seabird species complete their moulting during the non-breeding period, feather stable isotope analysis can be used to examine some of the ecological aspects of this part of the avian annual cycle.

Storm-petrels are typical pelagic seabirds, as they are highly mobile [15] and with feather growth taking up to several weeks [22]. Hence, isotope analysis applied to reconstruct birds' migratory movements provides a summary value for the feather growth period. However, combining multiple isotopes considerably increases the resolution to a more regional scale.

In this study, we aimed to characterise isotopic niches and use them to predict differences in moulting distribution of two species pairs of migratory storm-petrels, breeding sympatrically in both the northern (European storm-petrel, *Hydrobates pelagicus*, ESP; Leach's storm-petrel, *Hydrobates leucorhous*, LSP) and southern (black-bellied storm-petrel, *Fregetta tropica*, BBSP; Wilson's storm-petrel, *Oceanites oceanicus*, WSP) hemispheres. The latter species is considered the world's most abundant seabird species. However, relatively little is known about storm-petrel ecology during the non-breeding period. Due to their abundance, they may play an important role in global marine ecosystems, significantly influencing marine food webs. Additionally, due to their prevalence, and small size, they may be affected by anthropological disturbances and pollution differently than larger species. As such, they could be used as valuable sentinel species [23], but for that more knowledge is needed about their ecological niches during the non-breeding period.

To characterise stable isotopic niches and determine differences in ecological range during moult, we used the stable isotope composition of two elements: $\delta^{13}\text{C}$ and $\delta^{18}\text{O}$ of tail feathers moulted during the non-breeding period, largely simultaneously with other flight feathers [14, 24]. Stable isotope compositions of both elements vary spatially in marine ecosystems; $\delta^{13}\text{C}$ values are correlated with phytoplankton distribution [25, 26] while $\delta^{18}\text{O}$ values are correlated with salinity and fresh water input [27]. Both marine isotope values follow inshore/offshore gradients [26–28]. To our knowledge, this study is the first to combine $\delta^{13}\text{C}$ and $\delta^{18}\text{O}$ analyses to determine differences in moult distributions of storm-petrels breeding sympatrically in both hemispheres. Traditionally, $\delta^{13}\text{C}$ is combined with $\delta^{15}\text{N}$ to study species' trophic and isotopic niches as nitrogen isotopic compositions serve as an important proxy for trophic level. However, this can only be used at local scales, e.g. during the breeding period when seabirds act as central place foragers having a restricted foraging range. During the non-breeding period pelagic seabirds roam freely through the vast oceans with spatially variable $\delta^{15}\text{N}$ values. Specific predator trophic positions can only be inferred from bulk $\delta^{15}\text{N}$ values if bulk $\delta^{15}\text{N}$ values of lower trophic positions is known [29, 30].

As different moulting areas may vary in food availability, we tested whether moulting distribution differed in feather growth rate, a proxy for nutritional status during moulting [31]. Furthermore, we explored differences in feather $\delta^{15}\text{N}$ between moulting niches as an additional, but cautious measurement for food availability and foraging location, as $\delta^{15}\text{N}$ values are heavily dependent on trophic level, food source and foraging location [32]. Moreover, we expected that differences in stable isotopic niches and moulting distribution may be linked to differences in body size and sex within species. A study on several Procellariiformes species showed that in larger, size-dimorphic, species $\delta^{13}\text{C}$ values in females were higher than in males, suggesting a more northerly distribution, while no isotopic differences were found in species not displaying sexual dimorphism [33]. In storm-petrels, sexual isotopic segregation was previously found in several species [34, 35], but not all [36].

To visualise and further interpret the differences in moulting niches, we used a predictive model to estimate moulting locations based on oceanic $\delta^{13}\text{C}$ and $\delta^{18}\text{O}$ gradients [37]. We verified these predictions using observations of storm-petrels recorded in online databases, and placed their predicted moulting grounds in established ecoregions [38]. Additionally, we used oceanic chlorophyll-*a* concentrations from the non-breeding period to validate predicted moulting areas, as high chlorophyll-*a* concentrations (a proxy of high primary productivity) have been linked to areas with high seabird abundance [39], and highly productive marine areas are preferred moulting grounds [40].

Materials and methods

Study species and location

We captured ESP and LSP adults in August of 2018 ($n = 52$; $n = 56$, respectively) and 2019 ($n = 40$; $n = 37$, respectively) on the island of Mykines, Faroe Islands ($62^{\circ}05' \text{N}$, $07^{\circ}39' \text{W}$), and BBSP and WSP adults during the austral summer of 2017 ($n = 15$; $n = 100$, respectively) and 2018 ($n = 19$; $n = 126$, respectively) around the Henryk Arctowski Polish Antarctic Station, on King George Island, South Shetland Islands, Antarctica ($62^{\circ}09' \text{S}$, $58^{\circ}27' \text{W}$). ESP are the world's second smallest seabirds, while WSP is the smallest endotherms breeding on Antarctica. The northern (*Hydrobatidae*) and southern (*Oceanitidae*) species represent two different subfamilies [41, 42] differing in morphology and breeding ranges. The species name of LSP was therefore recently changed by BirdLife from *Oceanodroma leucorhoa* to *Hydrobates leucorhous* [43] though the old nomenclature is still widely used as well. BBSP and LSP have similar body sizes, except for tarsus length, and are larger than both ESP and WSP [44].

Both northern storm-petrel species have been observed along the west coast of Africa during their non-breeding season, generally as far south as the Cape of Good Hope [16, 17, 45], and LSP has been observed close to the Antarctic Peninsula [46]. A study based on stable $\delta^{13}\text{C}$ and $\delta^{15}\text{N}$ isotopes suggests that ESP from different Atlantic breeding colonies share moult grounds as feathers grown during their non-breeding periods had similar stable isotope compositions. Contrastingly, feathers grown during their breeding periods had different stable isotope signatures [47]. A study on GLS-tracked LSP from Canadian colonies revealed that they moult in several geographically distinct areas [16]. WSPs can be observed around the British Isles [48, 49], though most are expected to moult south of the Subtropical Front [50]. The non-breeding distribution of BBSP is vastly understudied, but they are assumed not to cross the equator [44], though they have been sporadically observed in the North Atlantic [48], and likely moult in different oceanic zones than WSP [51].

The period from egg-laying to fledging takes on average 3.5 months in all four studied species [44, 52, 53]. All breeding activities take place during the summer (boreal and austral for the northern and southern hemisphere species, respectively), and though chicks generally fledge in late summer, in the northern hemisphere occasional late breeding attempts may be observed until autumn [54]. WSPs and BBSPs moult their flight feathers fully outside of the breeding period [24], while both ESPs and LSPs have been observed to overlap the start of flight feather moult with the last stages of chick-rearing [14, 55–57]. LSP rectrix moult overlaps more extensively with the breeding season than ESP rectrix moult [14, 55, 57]. Additionally, while in both species tail feather moult is irregular, ESPs seem to start tail moult with the central rectrix pair while LSP is more likely to start from the outer pair [14, 58]. However, the order in which tail feathers are moulted and the position of the start of tail moult is not conclusive [1/3 of observed LSP did not start tail moult at the outer rectrix pair; [14]].

Data collection

Field study. We captured adults of all studied species using mist-nets in the colony at night and by taking incubating BBSP and WSP birds from their nest. From each individual, we collected the right outer rectrix expected to be grown during the non-breeding season. For each sampled individual we measured body mass to the nearest 0.1 g using a digital scale (Pesola PTS3000, Switzerland), tarsus to the nearest 0.1 mm using callipers and folded wing length to the nearest 1 mm using a wing ruler. We determined the feather growth rate for the outermost rectrix by measuring growth bar width to the nearest $0.1 \text{ mm} \times \text{d}^{-1}$. Feather growth bars are visible as alternating light and dark bands, formed during feather synthesis, but see Ausems et al. 2019 [59] for a detailed description of the method used.

It took several weeks for the sampled rectrices to be fully grown (ESP 30.6 ± 8.5 d; LSP 40.8 ± 13.0 d; BBSP 18.5 ± 2.5 d; WSP 18.7 ± 3.0 d; [59]). Thus, the rectrix formation period, overlapping to a considerable extent with flight feather moult [14, 24], includes a considerable part of the non-breeding period, even if feather growth started at the end of the breeding season. Although sampling tail-feathers increases the chance of sampling a feather moulted during the breeding period in LSP, we considered the uncertainty around the location of the start of tail moult too great to justify adding the negative effect of increasing feather gaps by sampling a more central feather.

Molecular sexing. For molecular sexing, we collected several body feathers from the back of the neck from each individual from WSP and BBSP, and a drop of blood, stored in 70% ethanol, from ESP and LSP. We extracted DNA from the feathers and the blood after evaporation of the ethanol using the Sherlock AX (feathers) and Blood Mini kit (blood; A&A Biotechnology, Gdynia, Poland). We followed Griffiths et al. 1998 [60] to perform molecular sexing with

primer pair 2550F and 2718R but adapted the protocol by using 50°C for the annealing temperature in the polymerase chain reaction (PCR). The primer pair amplifies introns on the CHD-W and CDH-Z genes located on the Wand Z avian sex chromosomes that vary in length [60]. The difference between the two fragments (~200 bp) was clearly visible in UV-light when separating on 2% agarose gel, stained with Midori Green. Some of the samples did not give reliable PCR products, thus for the southern species, we tested the sex of a total of 3 BBSP (2 females; 1 male) and 76 WSP (29 females; 47 males). In BBSP and WSP we additionally assigned sexes to 1 BBSP male, 7 WSP females and 2 WSP males based on the sex of the partner caught in the same nest. For the northern species, we successfully determined sex in 2018 and 2019 for 77 ESP (23 females; 54 males) and 52 LSP (9 females, 43 males).

Ethics statement. The Antarctic part of the study was conducted under the permission of the Polish National Standing Committee on Agricultural Research, Institute of Biochemistry and Biophysics (permit for entering the Antarctic Specially Protected Area No. 3/2016 & No. 08/2017). All birds captured on the Faroe Islands were handled under licenses of the Statens Naturhistoriske Museum, Københavns Universitet issued to AA (C 1012). All tissue samples on the Faroe Islands were taken with the permission of the Faroese Food and Veterinary Authority (19/01411-9) issued to AA. The study sites on the Faroe Islands was on privately owned land the local landowners gave permission to enter the study sites.

Stable isotope analyses

Before analyses, all collected feather samples were washed in a 2:1 chloroform:methanol solution and twice in methanol, then air-dried for 24 h. The samples were then cut up into sub-millimetre sections using stainless steel scalpel blades. The $\delta^{15}\text{N}$ and $\delta^{13}\text{C}$ compositions were analysed using a continuous flow system consisting of a Delta V Plus mass spectrometer connected with a Thermo Flush 1112 Elemental Analyser via Conflo IV (Thermo-Finnigan/Germany; [61]). Raw values were reduced to the international scale using multi-point normalisation [62], based on international standards provided by IAEA: $\delta^{13}\text{C}$ –NBS22, USGS24, NBS19, LSVEC [63]; and for $\delta^{15}\text{N}$ –N1, N2, USGS32 and laboratory standards. Stable $\delta^{18}\text{O}$ composition was analysed using a TC/EA coupled with Delta XL Mass Spectrometer in continuous flow mode (Thermo-Fisher Scientific). The $\delta^{18}\text{O}$ results were normalised to the VSMOW scale based on USGS42 and USGS43 and the equilibration method [64]. All $\delta^{13}\text{C}$ results are reported in ‰ on VPDB, $\delta^{15}\text{N}$ in ‰ on Air and $\delta^{18}\text{O}$ in ‰ on VSMOW scale [62], with an external analytical uncertainty (one standard deviation) of 0.10 ‰ for $\delta^{13}\text{C}$ and $\delta^{15}\text{N}$, and 0.50 ‰ for $\delta^{18}\text{O}$.

Statistical analyses

All statistical analyses were done in R version 3.6.3. [65]. Individuals missing $\delta^{13}\text{C}$ or $\delta^{18}\text{O}$ values were removed from further analyses. From ESP two apparent outliers with $\delta^{13}\text{C} < -23$ ‰ were removed for further analyses, as we could not determine whether these values were caused by biological processes (i.e. different moulting ranges or ages) or were due to measurement errors. The results for the analyses including the outliers are reported in the (S2 File).

Factors correlated with moult distribution differences. We determined whether differences in $\delta^{13}\text{C}$ and $\delta^{18}\text{O}$ values were correlated with $\delta^{15}\text{N}$, feather growth rate, body mass, tarsus length, wing length, sex, and sample year with a conditional inference tree (CIT; function *ctree*; package *partykit*; [66, 67]). The CIT is a non-parametric regression tree, examining the relationship between multiple explanatory variables and one or multiple response variables. The *ctree* function estimates a regression relationship by binary recursive partitioning in a conditional inference framework. CIT outputs are in the form of an ‘inverted tree’, such that the

root at the top of the tree contains all observations, which is then divided into two branches, and again at each subsequent node. The aim of splitting the data at each step is to establish groups with a between-variation as large as possible and a within-variation as small as possible. Each node contains information about the explanatory variable name, its probability value, and the cut-off value in case of continuous explanatory variables [68]. CIT uses a machine learning algorithm to determine when splitting into further branches is no longer valid using a statistically determined stopping criterion; an *a priori* p-value [66]. CIT is robust against typical regression violations, such as over-fitting, (multi-) collinearity, and biases with regard to the types of explanatory variables used. To perform the CIT analysis we defined a multivariate response model for both $\delta^{13}\text{C}$ and $\delta^{18}\text{O}$ for both hemispheres separately adding species as an explanatory factor along with the aforementioned explanatory variables (i.e. $\delta^{13}\text{C} + \delta^{18}\text{O} \sim \delta^{15}\text{N} + \text{year} + \text{species} + \text{sex} + \text{feather growth rate} + \text{body mass} + \text{tarsus length} + \text{wing length}$).

We used a Welch's two sample t-tests (function *t.test*) to further explore the differences in $\delta^{13}\text{C}$ and $\delta^{18}\text{O}$ for each node. Additionally, for species with more than two terminal CIT nodes, we used a MANOVA (function *manova*) to further explore differences in $\delta^{13}\text{C}$ and $\delta^{18}\text{O}$ between terminal nodes, followed by a univariate ANOVA (function *aov*) when the MANOVA results were significant. Significant ANOVA results were followed by a Tukey HSD *post hoc* test (function *TukeyHSD*). Both $\delta^{13}\text{C}$ and $\delta^{18}\text{O}$ can be reasonably assumed to be normally distributed within the populations with homogenous variances, though the sample sizes within terminal CIT nodes were often too low to test these assumptions. We used the terminal nodes defined by the CIT model to group individuals for further analyses.

Predicted moulting areas. We created probability-of-origin raster maps for each storm-petrel species terminal CIT node (also called groups) based on both $\delta^{13}\text{C}$ and $\delta^{18}\text{O}$ signatures with the *isocat* package [69]. The probability-of-origin values produced by *isocat* range from 0 to 1, with low values indicating a low probability that the sample originated from that area, and high values indicating a high probability of origin (i.e. they should not be confused with p-values where a low value is generally preferred). Probability-of-origin values were calculated for each $1 \times 1^\circ$ (Latitude \times Longitude) oceanic grid cell for $\delta^{13}\text{C}$ and $\delta^{18}\text{O}$ separately. As we did not necessarily expect each stable isotope to have similar probability-of-origin values for each cell, we summed the two values to generate one, combined probability-of-origin value per grid cell. The values presented here qualitatively, but not quantitatively, present the likelihood of bird presence during moulting within each species' subgroup partitioned using the CIT tree method. The expected primary spatial bird species distribution is in the regions $> 95\%$ quantile but these do not reflect bird population density. We used seasonally averaged plankton $\delta^{13}\text{C}$ prediction isoscapes provided by C. Trueman from models described in Magozzi et al. 2017 [25], for the core non-breeding periods of the northern (November to March) and southern (May to October) species separately. For $\delta^{18}\text{O}$ we used an annual averaged gridded dataset for Global Seawater Oxygen-18 Database isoscape obtained from LeGrande and Smith 2006 ([70]; <https://data.giss.nasa.gov/o18data/>) and visualized in ArcMap 10.3.1 [71]. For the two northern species, we only used data from the Atlantic Ocean as the studied populations do not migrate to other oceans and thus, we restricted the rasters to the area between 75°W and 52°E . For $\delta^{13}\text{C}$ and $\delta^{18}\text{O}$ isoscape maps see the (S1 File).

The calculated probability-of-origin values in all studied species differed by an order of magnitude (i.e. $P \times 10^{-5}$ for $\delta^{13}\text{C}$ and $P \times 10^{-4}$ for $\delta^{18}\text{O}$). As we could not rule out this difference was due to artefacts caused by inappropriate discrimination factors, we centered and scaled both $\delta^{13}\text{C}$ and $\delta^{18}\text{O}$ probability-of-origin maps for each individual using the *scale* function (package *raster*; [72]) before summing the scaled probability-of-origin values in each cell. Before scaling, the probability-of-origin values were centered by subtracting the raster mean from each individual cell value. Scaling was then done by dividing the raster layers (i.e. all

probability-of-origin maps were grouped for both the northern and southern hemisphere separately) by their standard deviations. Due to the scaling procedure and summing the probability-of-origin values of both $\delta^{13}\text{C}$ and $\delta^{18}\text{O}$, the probability-of-origin values reported in this study are thus factors reflecting probability and no longer range from 0 to 1. The reported probability-of-origin values are only meaningful in relation to the other probability-of-origin values within a hemisphere, such that a value can only be interpreted based on the distribution and range within each examined group (e.g. a value of 1 may be considered high if the values within the group range from -2 to 3, but may be considered low if the values range from 0 to 4). Therefore, in further analyses, values are compared to specific quantiles of the entire contemplated group to determine their meaning, and comparing values with values outside of the group is meaningless. We calculated the difference in predicted moult distribution maps using the Jaccard index (function *jaccard*; package *zonator*; [73]).

We corrected for differences in feather $\delta^{13}\text{C}$ and $\delta^{18}\text{O}$ compared to the source material (i.e. phytoplankton for $\delta^{13}\text{C}$ and ocean water for $\delta^{18}\text{O}$) by subtracting trophic enrichment factors from the observed values. For seabirds, $\delta^{13}\text{C}$ increases with trophic level, with trophic enrichment factors varying between species, sampled tissues and diet [74]. In storm-petrels, a trophic enrichment factor of 0.8 ‰ per trophic level has been used in previous studies [75, 76]. Although the exact trophic level of the studied storm-petrels during the non-breeding period is unknown, they consume mostly zooplankton [53, 77–87] and thus are at least two trophic levels higher than the source material. We, therefore, subtracted 1.6 ‰ from the observed $\delta^{13}\text{C}$ values before starting the statistical analyses. As the discrimination factor between oceanic $\delta^{18}\text{O}$ and feather $\delta^{18}\text{O}$ were unknown, we calculated that based on 8 feathers known to be growing at the breeding site and the mean $\delta^{18}\text{O}$ values of water samples taken within 5–120 km of the study site for each hemisphere. These rectrices were either actively growing when sampled or replaced a previously pulled feather (LSP $n = 5$, BBSP $n = 1$, WSP $n = 2$). We found discrimination factors of 10.4 ‰ & 13.0 ‰ between $\delta^{18}\text{O}$ of ocean water and feathers grown during the breeding period, for the northern and southern species respectively.

Moult area verification. We validated the predicted moulting areas using chlorophyll-*a* concentrations as a proxy for food abundance which may serve as moulting areas [40], and observational data. We used chlorophyll-*a* concentrations at the surface layer from remote sensing MODIS Aqua satellite data (NASA Ocean Color Web, <https://oceancolor.gsfc.nasa.gov/>). We created concentration rasters for the corresponding core non-breeding periods for the species from the northern (November to March 2003–2018) and southern (May to October 2003–2018) hemispheres (S1). We averaged monthly maps in ArcMap 10.3.1 [71]. For the two northern species, we only used data from the Atlantic Ocean as the studied populations do not migrate to other oceans and thus restricted the rasters to the area between 75°W and 52°E. To find whether the predicted moulting areas were located in areas with increased primary productivity we firstly grouped the areas with lower 75% quantile of the scaled probability-of-origin values (i.e. 0–75% of the scaled probability-of-origin values) and the higher 25% quantile of the scaled probability-of-origin values (i.e. 76–100% of the scaled probability-of-origin values), and compared those two area categories using a Welch two sample *t*-test (function *t.test*).

For the southern species we also predicted the latitude at which the birds moulted for each terminal CIT node group using the equation from Quillfeldt et al. 2005 [76]: $\delta^{13}\text{C} = -8.52 - (0.26 \times \text{latitude})$. We calculated the mean latitude for each terminal CIT node group, then extracted the scaled probability-of-origin values within the predicted latitude range (i.e. mean \pm SD). If the predicted latitude was $> -44^\circ$, we referred to the estimated moulting area as north of the Subtropical Front, as the equation used is only accurate for predictions $< -44^\circ$ [50]. To determine the likelihood of the individuals moulting close to the predicted latitude we compared the maximum and mean \pm standard deviation of the scaled probability-of-origin

values along the latitude range to the 95% quantile of scaled probability-of-origin values per terminal CIT node.

We grouped observations per species recorded in two online repositories from January 1990 until May 2020 [88, 89] in each 10° latitude \times 10° longitude cell and calculated the average latitude and longitude for the observations within each cell. Not all species were consistently observed between years and areas due to differences in observation effort (e.g. the chance of observing an individual flying close to the shore in the Northern Atlantic is much higher than observing an individual flying in the pelagic waters of the Southern Atlantic due to an absence of observers), thus the observational data must be interpreted with caution.

We extracted the scaled probability-of-origin values within a buffer of 1.1×10^6 m (approximately 10°) around each observation point (average latitude and longitude) for each terminal CIT node group. For each terminal CIT node, we calculated the mean scaled probability-of-origin value per observation point, and the 50% and 95% quantiles for the entire map. We then compared the mean extracted scaled probability-of-origin value with the 50% and 95% quantile of the scaled probability-of-origin values for the whole raster map. Similarly, for each species, we extracted the chlorophyll-*a* concentration around each observation point and compared its mean with the 50% and 95% quantile of the chlorophyll-*a* raster for each hemisphere. Additionally, for each terminal CIT node for all species, we calculated the mean scaled probability-of-origin value in each marine eco-realm as defined in Spalding et al. 2007 [38], and compared those to the previously defined 50% and 95% scaled probability-of-origin quantiles.

Results

Stable isotopic moulting niches

The CIT for both hemispheres showed that carbon and oxygen isotopic signatures differed significantly between species (Node 1; $p < 0.001$; Fig 1, Table 1), but not between sexes. ESP had significantly higher $\delta^{13}\text{C}$ values compared to LSP but lower $\delta^{18}\text{O}$ values (Table 1), with $\delta^{18}\text{O}$ being lower in 2019 than 2018 for both species and $\delta^{13}\text{C}$ being lower in 2019 than 2018 for LSP but not differing for ESP (Table 2). Furthermore, within ESP individuals with tarsus length ≤ 23.5 mm differed significantly in moult distribution from individuals with tarsus length > 23.5 (Fig 1A), with individuals with shorter legs having significantly lower $\delta^{18}\text{O}$ values than individuals with longer legs while $\delta^{13}\text{C}$ did not differ (Table 1).

The CIT model for ESP including wing length and sex revealed confounding results, such that the significant dividing effect of tarsus length disappeared when including both wing length and sex, but not when including either one separately. Wing length is known to differ between sexes in storm-petrels [90, 91] and it was significantly longer in females than in males for LSP (Welch two-sample *t*-test; $t_{13,0} = 2.23$, $p = 0.044$) and WSP ($t_{57,2} = 2.63$; $p = 0.011$) in our study, but it did not differ significantly between males and females in ESP (Welch two-sample *t*-test: $t_{40,8} = 1.61$, $p = 0.116$; BBSP had too few sexed individuals to test). Therefore, we included either wing length or sex in the ESP CIT model. In both models, the CIT results were the same (Fig 1A), neither of which included wing length or sex.

The MANOVA results for the ESP terminal CIT nodes showed significant differences but this effect was only significant for $\delta^{18}\text{O}$ and not for $\delta^{13}\text{C}$ (Table 3). Terminal CIT node 3 had significantly higher $\delta^{18}\text{O}$ values than terminal CIT node 5 (Tables 2 and 3).

In the southern hemisphere storm-petrel species the CIT revealed that BBSP had higher $\delta^{13}\text{C}$ values and $\delta^{18}\text{O}$ than WSP (Table 1). No further differences in moult distribution within BBSP were detected. In WSP nitrogen signatures significantly split studied birds into groups with $\delta^{15}\text{N}$ values cut-off at 14.79 ‰ (Fig 1B); individuals with $\delta^{15}\text{N}$ values lower or equal to the cut-off point had significantly lower $\delta^{13}\text{C}$ values and higher $\delta^{18}\text{O}$ values (Table 1) than

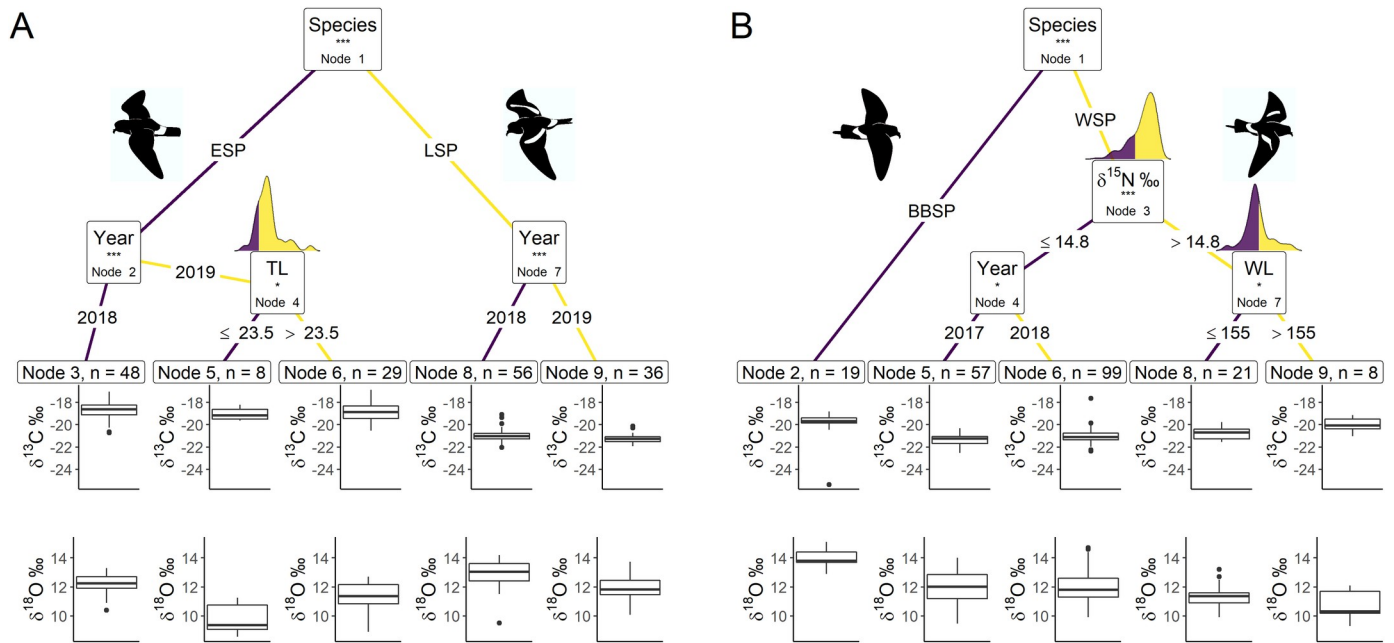


Fig 1. Conditional inference trees characterising factors affecting the stable carbon ($\delta^{13}\text{C}$) and oxygen ($\delta^{18}\text{O}$) isotopic signatures. We used Species, Year, $\delta^{15}\text{N}$ (stable nitrogen isotope ratio), FGR (feather growth rate), BM (body mass), TL (tarsus length), and WL (wing length) as initial predictors. Body morphometrics (i.e. BM, TL and WL) were measured during the breeding season after moulting. Only variables with a significant dividing effect are shown in order of importance from the top down. At each node the dividing variable and corresponding p-value sign are listed in the box. These significance levels represent the test of independence between the listed variable and the response variables. Terminal CIT nodes indicate variable levels characterizing the response variable. Density plots above node boxes show the distribution of the continuous divisive variables, with the cut-off point dividing the colours. Boxplots show the median (band inside the box), the first (25%) and third (75%) quartile (box), the lowest and the highest values within 1.5 interquartile range (whiskers) and outliers (circles). (A) Northern hemisphere species; ESP–European storm-petrel; LSP–Leach’s storm-petrel; (B) Southern hemisphere species; BBSP–black-bellied storm-petrel; WSP–Wilson’s storm-petrel; n–number of individuals in each terminal CIT node group. P-values < 0.001 are shown with ***, p-values < 0.01 are shown with ** and p-values < 0.05 are shown with *.

<https://doi.org/10.1371/journal.pone.0245756.g001>

individuals with higher $\delta^{15}\text{N}$ values. The individuals with $\delta^{15}\text{N}$ values ≤ 14.79 ‰ could be further split significantly by year (Fig 1B), with $\delta^{13}\text{C}$ being significantly lower in 2017 than 2018, while $\delta^{18}\text{O}$ did not differ (Table 1). The individuals with higher $\delta^{15}\text{N}$ values could be further

Table 1. Welch’s two-sample *t*-test results for $\delta^{13}\text{C}$ and $\delta^{18}\text{O}$ values of the CIT internal nodes.

Hemisphere	Node	Variable	$\delta^{13}\text{C}$			$\delta^{18}\text{O}$		
			<i>df</i>	<i>t</i>	<i>p</i>	<i>df</i>	<i>t</i>	<i>p</i>
Northern	1	Species	139.8	22.4	< 0.001	167.1	-5.76	0.001
	2	Year	77.7	0.949	0.346	49.8	5.93	< 0.001
	4	Tarsus Length	18.8	-0.633	0.534	11.6	-3.69	0.003
	7	Year	88.6	3.24	0.002	78.6	6.12	< 0.001
Southern	1	Species	18.7	3.64	0.002	30.5	13.5	< 0.001
	3	$\delta^{15}\text{N}$	37.0	- 4.56,	< 0.001	42.2	4.20	< 0.001
	4	Year	136.8	-3.55	< 0.001	102.7	-0.104	0.917
	7	Wing Length	10.4	-3.13	0.010	10.1	1.65	0.130

We tested the differences in stable carbon isotope ratios ($\delta^{13}\text{C}$) and stable oxygen isotope ratios ($\delta^{18}\text{O}$) between the child nodes of the conditional inference tree (CIT) analyses. Variable codes: Species, Year, $\delta^{15}\text{N}$ (stable nitrogen isotope ratio), FGR (feather growth rate), BM (body mass), TL (tarsus length), and WL (wing length) as initial predictors. Body morphometrics (i.e. BM, TL and WL) were measured during the breeding season after moulting. Welch’s two-sample *t*-test results: *df*–degrees of freedom; *t*–*t* value. P-values < 0.05 are shown in bold.

<https://doi.org/10.1371/journal.pone.0245756.t001>

Table 2. Mean±SD $\delta^{13}\text{C}$ and $\delta^{18}\text{O}$ values of subgroups distinguished based on conditional inference tree terminal nodes.

Species	Terminal node	N	$\delta^{13}\text{C}_{\text{VPDB}}$ (‰)	$\delta^{18}\text{O}_{\text{VSMOW}}$ (‰)
ESP	3	48	-18.8 ± 0.8	12.2 ± 0.6
	5	8	-19.1 ± 0.5	9.8 ± 1.0
	6	29	-18.9 ± 0.8	11.3 ± 1.0
	Total	85	-18.8 ± 0.8 (-20.7; -16.7)	11.7 ± 1.1 (8.6; 13.3)
LSP	8	56	-21.0 ± 0.5	13.0 ± 0.8
	9	36	-21.3 ± 0.4	11.9 ± 0.8
	Total	92	-21.1 ± 0.5 (-22.0; -19.1)	12.6 ± 1.0 (9.5; 14.2)
BBSP	Total	19	-19.9 ± 1.4 (-25.4; -18.8)	14.0 ± 0.6 (12.9; 15.1)
WSP	5	57	-21.3 ± 0.5	12.0 ± 1.1
	6	99	-21.0 ± 0.6	12.0 ± 0.9
	8	21	-20.8 ± 0.5	11.4 ± 0.8
	9	8	-20.0 ± 0.6	10.7 ± 1.0
	Total	185	-21.1 ± 0.6 (-22.5; -17.6)	11.9 ± 1.0 (9.3; 14.7)

The species were split into groups with differing $\delta^{13}\text{C}$ and $\delta^{18}\text{O}$ values, based on variables described in the text. ESP–European storm-petrel; LSP–Leach’s storm-petrel; BBSP–black-bellied storm-petrel; WSP–Wilson’s storm-petrel; Terminal node–terminal CIT node number; n–sample size. Minimum and maximum values are provided at the species level in parentheses. See also Fig 1 for CIT results.

<https://doi.org/10.1371/journal.pone.0245756.t002>

divided by wing length (Fig 1B). Individuals with wing lengths ≤ 155 mm had significantly lower $\delta^{13}\text{C}$ values than individuals with wing lengths > 155 mm, while they did not differ in $\delta^{18}\text{O}$ values (Table 1).

The WSP terminal CIT nodes groups differed significantly in both $\delta^{13}\text{C}$ and $\delta^{18}\text{O}$ (Table 3). Terminal CIT node 5 had significantly lower in $\delta^{13}\text{C}$ values than terminal CIT node 8 and terminal CIT node 9 (Table 3). Terminal CIT node 5 $\delta^{18}\text{O}$ values did not differ significantly from

Table 3. Comparison of $\delta^{13}\text{C}$ and $\delta^{18}\text{O}$ values for species with > 2 CIT terminal nodes.

Species	MANOVA			SI	ANOVA			Tukey HSD		
	df	F	p		df	F	p	Pair	Dif	p
ESP	2, 82	12.5	< 0.001	$\delta^{13}\text{C}$	2, 82	0.56	0.572			
				$\delta^{18}\text{O}$				5–3	-2.45	< 0.001
								6–3	-0.95	< 0.001
WSP	3, 181	10.8	< 0.001	$\delta^{13}\text{C}$	3, 181	16.5	< 0.001	8–5	0.56	< 0.001
								9–5	1.34	< 0.001
								8–6	0.25	0.246
				9–6				1.03	< 0.001	
				$\delta^{18}\text{O}$				8–5	-0.58	0.101
								9–5	-1.26	0.005
								8–6	-0.60	0.060
								9–6	-1.27	0.003

MANOVA followed by ANOVA and *post hoc* Tukey HSD tests were used to determine the differences in $\delta^{13}\text{C}$ and $\delta^{18}\text{O}$ between non-related terminal nodes. ESP–European storm-petrel; WSP–Wilson’s storm-petrel; SI–tested stable isotope; df–degrees of freedom; F–F-value; pair–tested terminal node pair; dif–difference. P-values < 0.05 are in bold.

<https://doi.org/10.1371/journal.pone.0245756.t003>

terminal CIT node 8 but did differ from terminal CIT node 9 (Table 3). Group 6 did not differ significantly from terminal CIT node 8, but did differ significantly from terminal CIT node 9 (Table 3).

Predicted moult distribution

Based on CIT terminal nodes groups, ESP was split into three groups, LSP into two groups and WSP into four groups, differing in $\delta^{13}\text{C}$ and $\delta^{18}\text{O}$ (Table 2). BBSP was not split at all.

The similarity in scaled probability-of-origin distribution maps for ESP groups was very low (Jaccard index; terminal CIT node 3–5, $J = 0.066$; terminal CIT node 3–6, $J = 0.041$; terminal CIT node 5–6, $J = 0.027$). For LSP the similarity was higher than for ESP, but still relatively low (terminal CIT node 8–9, $J = 0.181$). WSP terminal CIT node 5 and 6 were nearly identical ($J = 0.957$), terminal CIT node 8 and 9 were fairly similar ($J = 0.613$). WSP terminal CIT node group 5 and 8, and group 6 and 8 shared approximately half of the same probability-of-origin value distributions ($J = 0.502$; $J = 0.485$, respectively), while terminal CIT node group 5 and 9, and group 6 and 9 shared approximately one-third of the scaled probability-of-origin value distributions ($J = 0.299$; $J = 0.288$, respectively). As BBSP was not separated into different terminal nodes, and thus did not have multiple scaled probability-of-origin maps, we did not calculate a Jaccard index.

Within the northern hemisphere species, we found significantly lower chlorophyll-*a* concentrations in the areas with the 76%–100% highest scaled probability-of-origin values than in the lower 0%–75% value areas for all groups for all terminal CIT node groups (*t*-test; ESP group 3 $t_{215.9} = 9.32$, $p < 0.001$; ESP group 6 $t_{255.1} = 3.05$, $p = 0.003$; LSP group 8 $t_{230.5} = 9.80$, $p < 0.001$; LSP group 9 $t_{221.9} = 6.90$, $p < 0.001$; Figs 2 and 3) except for ESP group 5 ($t_{244.5} = -6.68$, $p < 0.001$; Fig 2). For BBSP we found no significant difference in chlorophyll-*a* concentrations between higher and lower scaled probability-of-origin areas ($t_{841.2} = 1.36$, $p = 0.174$; Fig 4). In WSP we found significantly higher chlorophyll-*a* concentrations in the areas with the 76%–100% highest scaled probability-of-origin values than in the lower 0%–75% value areas for all groups for all four terminal CIT nodes (group 5 $t_{615.2} = -15.8$, $p < 0.001$; group 6 $t_{614.0} = -15.4$, $p < 0.001$; group 8 $t_{621.1} = -17.0$, $p < 0.001$; group 9 $t_{643.8} = -12.1$, $p < 0.001$; Fig 5).

BBSP and WSP individuals in terminal CIT node group 9 were predicted to moult north of -44° (Table 4), and we thus did not analyse scaled probability-of-origin values around their predicted moulting latitudes. The mean \pm SD of the scaled probability-of-origin values around the predicted moulting latitude for the other three WSP terminal CIT nodes were lower than the 95% quantile of the entire scaled probability-of-origin maps, although the maximum values of WSP terminal CIT nodes 5 and 6 were higher (Table 4; Fig 5).

In none of the marine eco-realms mean scaled probability-of-origin values for ESP individuals from terminal CIT node 3 were higher than the 95% quantile of the entire considered area (Tables 5 and 6; Fig 2); though only the Southern Ocean and the Arctic had mean scaled probability-of-origin values lower than the 50% quantile. Individuals from ESP terminal CIT node 5 had higher than the 95% quantile scaled probability-of-origin values for the Temperate Southern America eco-realm, while individuals from ESP terminal CIT node 6 had mean scaled probability-of-origin values higher than the 95% quantile for Temperate Southern Africa (Tables 5 and 6; Fig 2). In LSP neither terminal CIT nodes had mean scaled probability-of-origin values higher than the 95% quantile for any of the eco-realms. However, all eco-realms besides the Southern Ocean and Arctic had mean values higher than the 50% quantile (Tables 5 and 6; Fig 3). Similarly, for BBSP no eco-realms had mean scaled probability-of-origin values higher than the 95% quantile, but the Temperate Southern Africa, Western Indo-Pacific,

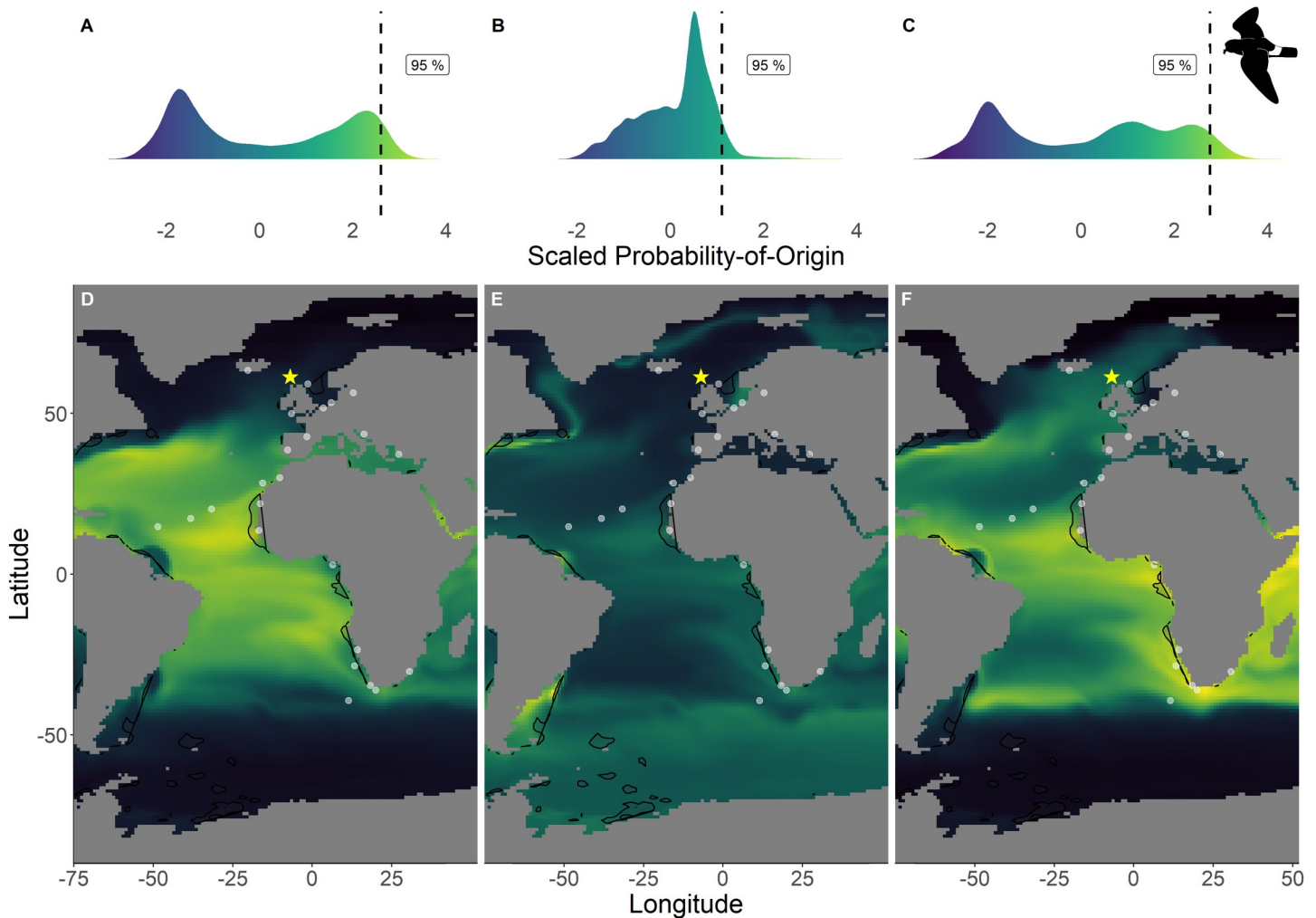


Fig 2. Scaled probability-of-origin maps based on $\delta^{13}\text{C}$ and $\delta^{18}\text{O}$ for each group for the European storm-petrel. Terminal nodes from a conditional inference tree (CIT) based on differences between years, and correlated to body morphology (Fig 1A) were treated as groups. (A) Scaled probability-of-origin value distribution for terminal CIT node 3; (B) scaled probability-of-origin value distribution for terminal CIT node 5; (C) scaled probability-of-origin value distribution for terminal CIT node 6; (D) scaled probability-of-origin map for terminal CIT node 3; (E) scaled probability-of-origin map for terminal CIT node 5; (F) scaled probability-of-origin map for terminal CIT node 6. Scaled probability-of-origin values are shown on a relative high (yellow)–low (black) gradient in both the density plots and maps. The 95% quantile of the scaled probability-of-origin values per terminal CIT node are shown with the dashed line. Shaded contours show high chlorophyll-*a* concentration areas (upper 95% of the data), and white dots show observation locations [88, 89]. The yellow star indicates the location of the breeding colony where birds were sampled.

<https://doi.org/10.1371/journal.pone.0245756.g002>

Tropical Atlantic, Eastern Indo-Pacific, Central Indo-Pacific, Temperate Australasia and Tropical Eastern Pacific eco-realms had mean scaled probability-of-origin values higher than the 50% quantile (Tables 5 and 6; Fig 4). WSP terminal CIT nodes 5, 6 and 8 had mean scaled probability-of-origin values higher than the respective 95% quantiles for the Temperate Northern Pacific eco-realm (Tables 5 and 6; Fig 5). For terminal CIT nodes 5 and 6 the Southern Ocean, Temperate Northern Atlantic and Temperate Australasia eco-realms had mean scaled probability-of-origin values lower than the 50% quantiles, while the remaining eco-realms had mean scaled probability-of-origin values between the 50% and 95% quantiles (Tables 5 and 6, Fig 5). For WSP terminal CIT node 8 Temperate Australasia and the Southern Ocean had mean scaled probability-of-origin values lower than the 50% quantiles (Tables 5 and 6, Fig 5). WSP terminal CIT node 9 had mean scaled probability-of-origin values higher than the 95% quantile for the Arctic and Temperate Northern Pacific eco-realms (Tables 5 and 6, Fig 5). The

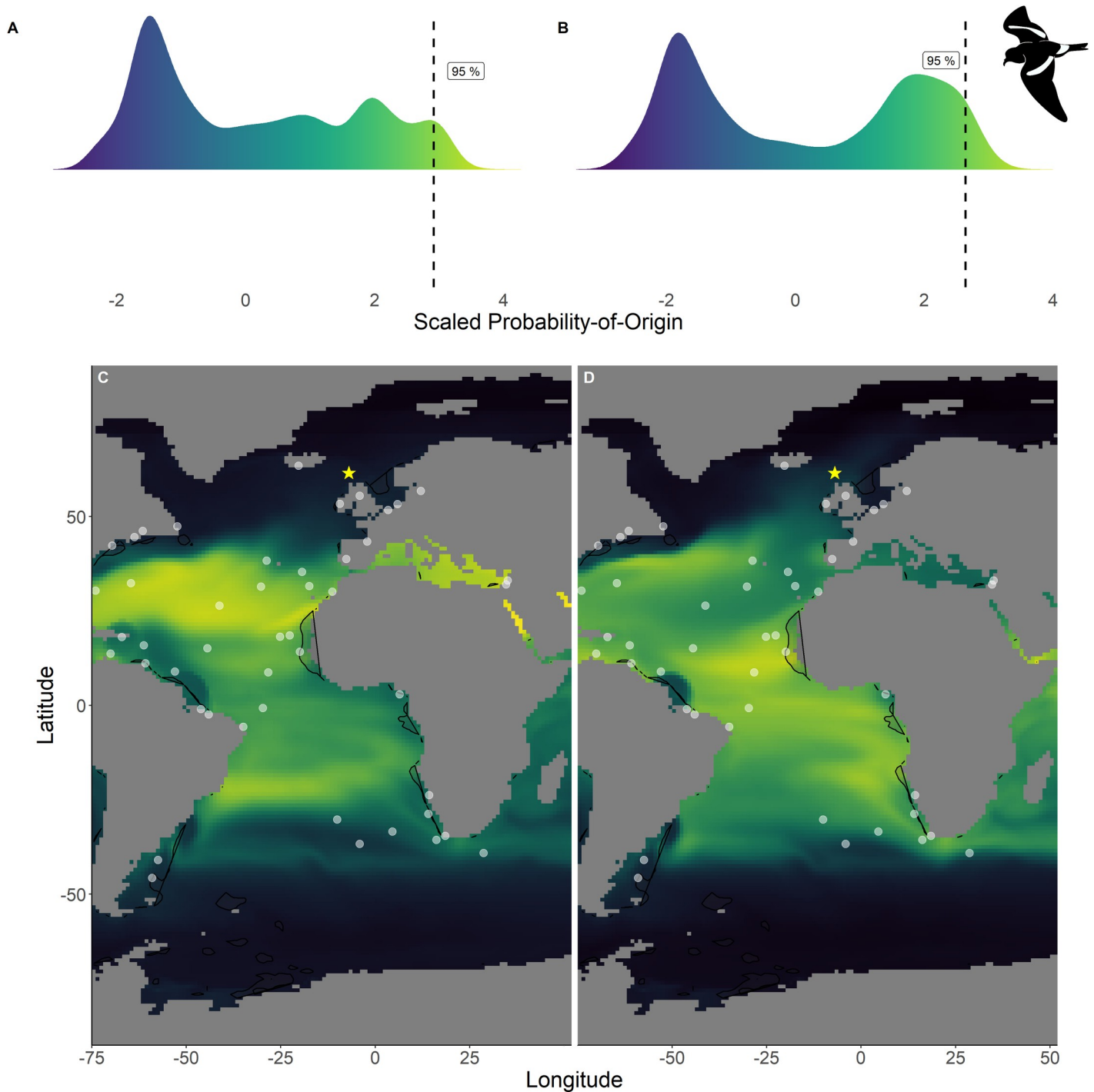


Fig 3. Scaled probability-of-origin maps based on $\delta^{13}\text{C}$ and $\delta^{18}\text{O}$ for each group of the Leach's storm-petrel. Terminal nodes from a conditional inference tree (CIT) based on differences between years, and correlated to body morphology (Fig 1A) were treated as groups. (A) Scaled probability-of-origin value distribution for terminal CIT node 8; (B) scaled probability-of-origin value distribution for terminal CIT node 9; (C) scaled probability-of-origin map for terminal CIT node 8; (D) scaled probability-of-origin map for terminal CIT node 9. Scaled probability-of-origin values are shown on a relative high (yellow)–low (black) gradient in both the density plots and maps. The 95% quantile of the scaled probability-of-origin values per terminal CIT node are shown with the dashed line. Shaded contours show high chlorophyll-*a* concentration areas (upper 95% of the data), and white dots show observation locations [88, 89]. The yellow star indicates the location of the breeding colony where birds were sampled.

<https://doi.org/10.1371/journal.pone.0245756.g003>

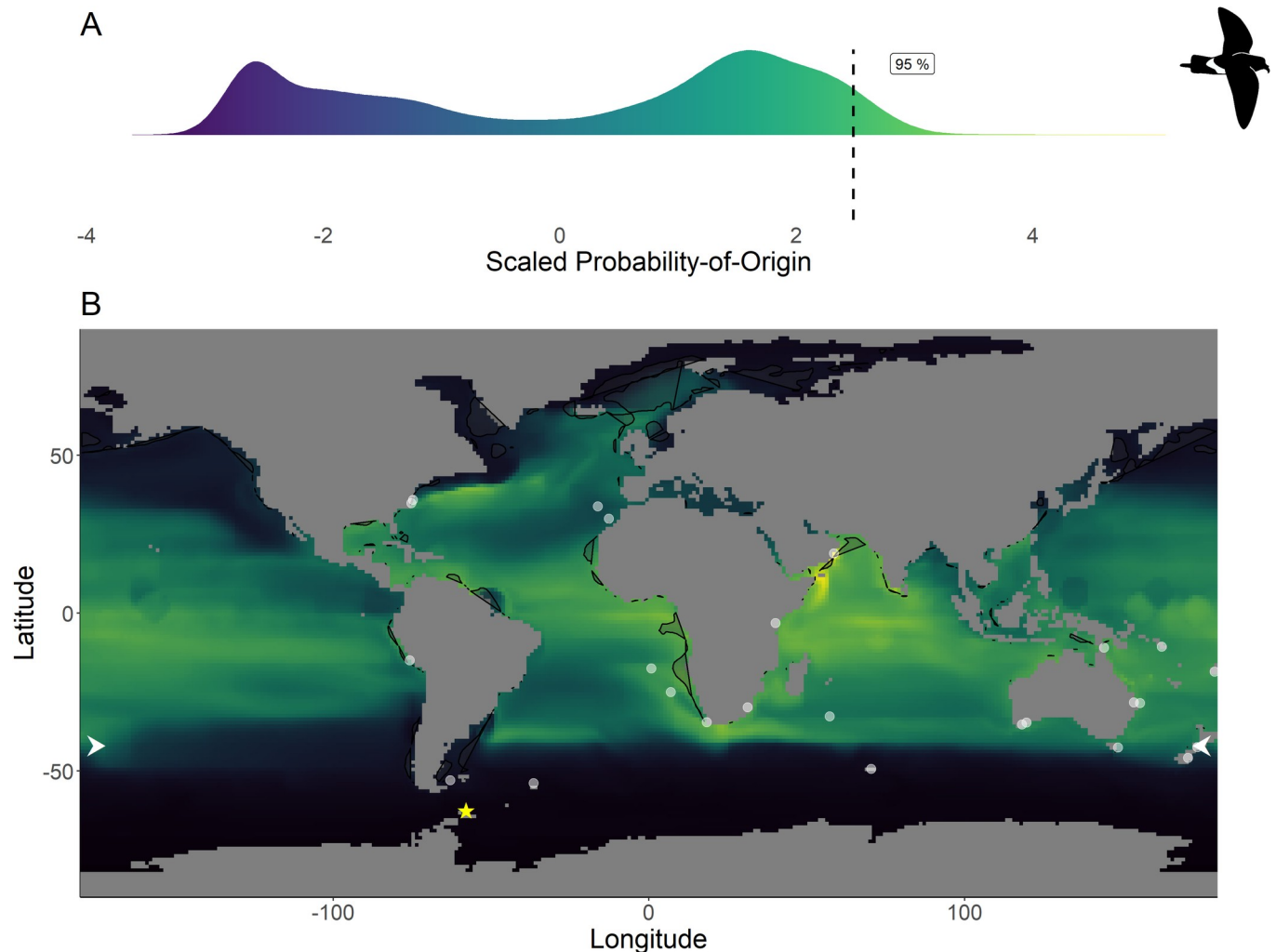


Fig 4. Scaled probability-of-origin map based on $\delta^{13}\text{C}$ and $\delta^{18}\text{O}$ for the black-bellied storm-petrel. (A) Scaled probability-of-origin value distribution; (B) scaled probability-of-origin map. Scaled probability-of-origin values are shown on a relative high (yellow)–low (black) gradient in both the density plot and map. The 95% quantile of the scaled probability-of-origin values is shown with the dashed line. Shaded contours show high chlorophyll-*a* concentration areas (upper 95% of the data), and white dots show observation locations [88, 89]. The white arrows at the edge of the plot show the predicted mouling latitude based on the equation from Quillfeldt et al. 2005([76]; Table 4). The yellow star indicates the location of the breeding colony where birds were sampled.

<https://doi.org/10.1371/journal.pone.0245756.g004>

Temperate South America, Temperate Australasia and Southern Ocean eco-realm mean scaled probability-of-origin values for WSP terminal CIT node 9 were lower than the 50% quantiles, while the remaining eco-realms had mean scaled probability-of-origin values between the 50% and 95% quantiles (Tables 5 and 6, Fig 5).

Observational data

The locations at which the species were observed during the non-breeding period were generally outside of the 95% quantile of the scaled probability-of-origin areas, although for all species except BBSP they were on average observed in the 75% quantile of the scaled probability-of-origin areas (Table 5). For all species the mean \pm SD of the chlorophyll-*a* concentrations around the observation locations overlapped with the 95% quantile of the chlorophyll-*a* concentration for the entire area in which the species could be expected to moult, with the ESP mean being closest to the 95% quantile for the northern hemisphere species (Table 5).

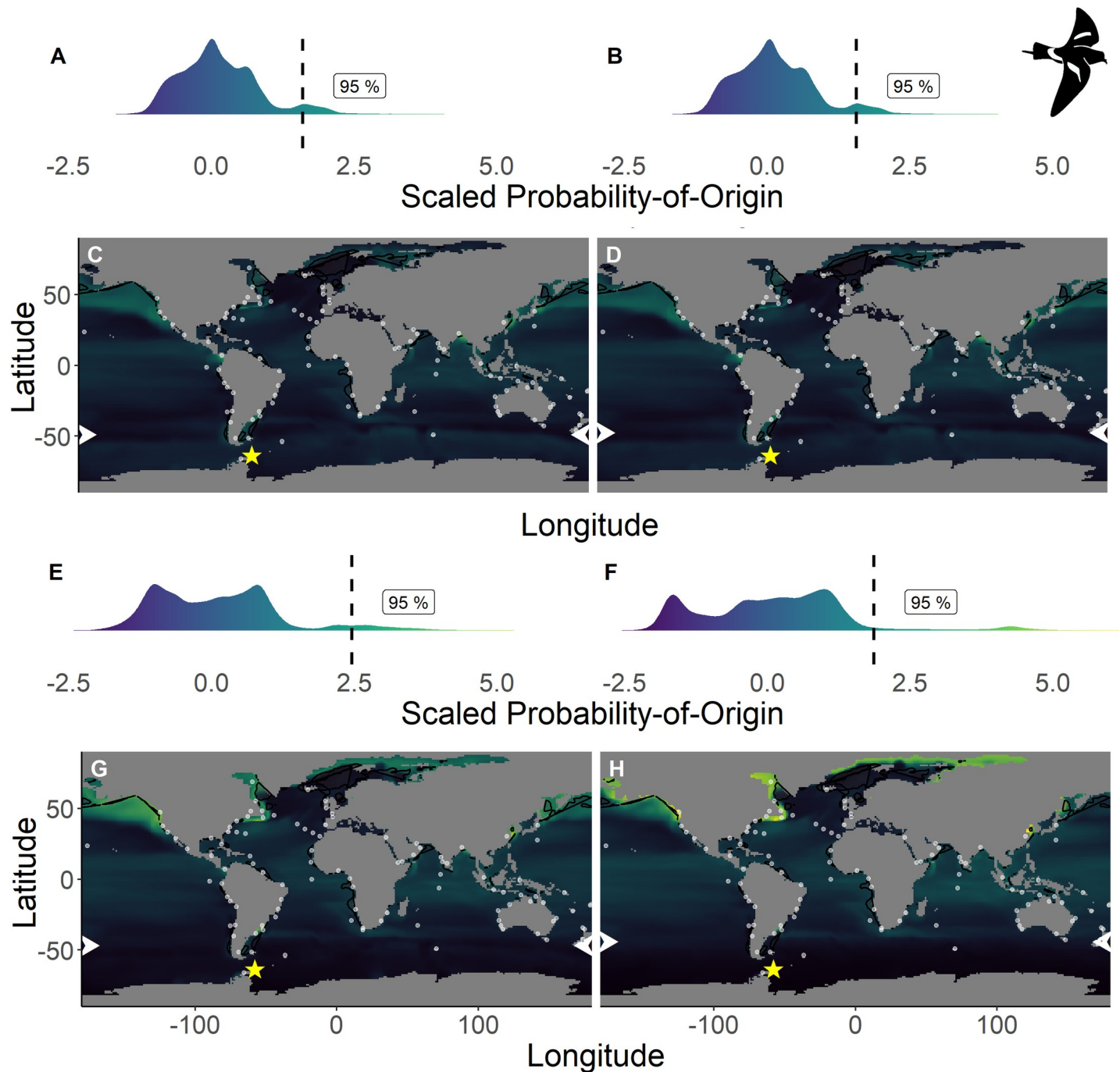


Fig 5. Scaled probability-of-origin maps based on $\delta^{13}\text{C}$ and $\delta^{18}\text{O}$ for each group for the Wilson's storm-petrel. Terminal nodes from a conditional inference tree (CIT) based on differences between years, and correlated to body morphology (Fig 1B) were treated as groups. (A) Scaled probability-of-origin value distribution for terminal CIT node 5; (B) scaled probability-of-origin value distribution for terminal CIT node 6; (C) scaled probability-of-origin map for terminal CIT node 5; (D) scaled probability-of-origin map for terminal CIT node 6; (E) scaled probability-of-origin value distribution for terminal CIT node 8; (F) scaled probability-of-origin value distribution for terminal CIT node 9; (G) scaled probability-of-origin map for terminal CIT node 8; (H) scaled probability-of-origin map for terminal CIT node 9. Scaled probability-of-origin values are shown on a relative high (yellow)–low (black) gradient in both the density plots and maps. The 95% quantile of the scaled probability-of-origin values per terminal CIT node are shown with the dashed line. Shaded contours show high chlorophyll-*a* concentration areas (upper 95% of the data), and white dots show observation locations [88, 89]. The white arrows at the edge of the plot show the predicted moulting latitude based on the equation from Quillfeldt et al. 2005 ([76]; Table 4). The yellow star indicates the location of the breeding colony where birds were sampled.

<https://doi.org/10.1371/journal.pone.0245756.g005>

Table 4. Scaled probability-of-origin values in the predicted moulting latitude range for the southern hemisphere species.

Species	Terminal Node	Latitude (°)	Scaled probability-of-origin		
			Maximum	Mean ± SD	95% Quantile
BBSP	2	-41.3 ± 5.4	NA	NA	NA
WSP	5	-47.1 ± 1.8	2.17	-0.32 ± 0.60	1.57
	6	-46.0 ± 2.2	2.14	-0.37 ± 0.58	1.53
	8	-45.0 ± 1.8	1.69	-0.74 ± 0.29	2.45
	9	-42.3 ± 2.4	NA	NA	NA

The latitude at which the species were expected to moult was predicted using the equation from Quillfeldt et al. 2005 [76]. Predicted maximum, mean and SD of the scaled probability-of-origin values were extracted from the SD latitude wide buffer around the predicted mean latitude for each terminal CIT node group. The 95% quantile of the scaled probability-of-origin values was calculated for the entire probability-of-origin map. We did not compare scaled probability-of-origin values for groups predicted to moult at < 44°S as the equation used was not accurate further north (41). Terminal node–terminal CIT node; Latitude–predicted moulting latitude; BBSP–black-bellied storm-petrel; WSP–Wilson’s storm-petrel. See also Figs 4 and 5 for the scaled probability-of-origin distributions. Note: the scaled probability-of-origin values are relative, i.e. not comparable between species from both hemispheres.

<https://doi.org/10.1371/journal.pone.0245756.t004>

Discussion

Our study combining stable carbon and oxygen isotopes ($\delta^{13}\text{C}$ and $\delta^{18}\text{O}$), revealed that for both hemispheres the storm-petrel species moulted their rectrices in different areas, as they differed significantly in both isotopic signatures (Fig 1). ESP had significantly higher $\delta^{13}\text{C}$ values and lower $\delta^{18}\text{O}$ values than LSP, suggesting less pelagic moulting ranges for the former [92], while BBSP had both higher $\delta^{13}\text{C}$ and higher $\delta^{18}\text{O}$ values than WSP indicating a more pelagic lifestyle and moulting grounds further north for BBSP [76, 92]. The lack of any division into subgroups in BBSP is likely due to the relatively small sample size ($n = 19$). However, BBSP also generally has a more pelagic lifestyle [44, 52] with larger foraging areas where stable isotope ratios differ over larger areas, and as such the feather isotopic signatures may vary less between individuals as they are averaged over a wider range of sources.

Table 5. Scaled probability-of-origin and chlorophyll-*a* concentration values around each observation location per terminal CIT node.

Species	Terminal node	Scaled probability-of-origin			Chlorophyll- <i>a</i>		
		Mean ± SD	50%	95%	Mean ± SD	50%	95%
ESP	3	1.85 ± 0.38	-0.17	2.60	1.33 ± 4.23	0.24	1.34
	5	0.75 ± 0.32	0.37	1.11			
	6	1.93 ± 0.60	0.45	2.76			
LSP	8	0.51 ± 0.32	-0.19	2.92	0.55 ± 2.23		
	9	0.52 ± 0.37	-0.06	2.64			
BBSP	2	0.02 ± 0.51	0.76	2.48	0.96 ± 3.43	0.17	1.45
WSP	5	-0.30 ± 0.47	0.02	1.57	0.78 ± 2.55		
	6	-0.26 ± 0.43	0.03	1.53			
	8	-0.26 ± 0.46	0.04	2.45			
	9	-0.29 ± 0.55	0.15	1.86			

Scaled probability-of-origin and chlorophyll-*a* concentration values were averaged for a buffer of approximately 10° around the average latitude and longitude for each observation location. The 50% and 95% quantiles were calculated for the entire raster, for both the scaled probability-of-origin maps and the chlorophyll-*a* concentration maps. ESP–European storm-petrel; LSP–Leach’s storm-petrel; BBSP–black-bellied storm-petrel; WSP–Wilson’s storm-petrel; Terminal node–terminal CIT node. See also Figs 2–5 for scaled probability-of-origin distributions. Note: the scaled probability-of-origin values are relative, i.e. not comparable between species from both hemispheres.

<https://doi.org/10.1371/journal.pone.0245756.t005>

Table 6. Mean±SD of the scaled probability-of-origin values per marine eco-realm per terminal CIT node.

Eco-realm	Species									
	ESP			LSP			BBSP		WSP	
	Terminal node									
	3	5	6	8	9	2	5	6	8	9
Arctic	-1.86 ± 0.16	-0.77 ± 0.50	-2.07 ± 0.44	-1.69 ± 0.16	-1.94 ± 0.18	-1.65 ± 0.34	0.45 ± 0.54	0.40 ± 0.53	1.87 ± 0.78	2.50 ± 1.13
Central Indo-Pacific	NA ± NA	NA ± NA	NA ± NA	NA ± NA	NA ± NA	1.85 ± 0.15	0.63 ± 0.14	0.64 ± 0.15	0.85 ± 0.13	1.10 ± 0.13
Eastern Indo-Pacific	NA ± NA	NA ± NA	NA ± NA	NA ± NA	NA ± NA	1.97 ± 0.17	0.15 ± 0.15	0.14 ± 0.15	0.42 ± 0.15	0.62 ± 0.15
Southern Ocean	-1.58 ± 0.11	0.68 ± 0.11	-1.85 ± 0.12	-1.35 ± 0.12	-1.68 ± 0.12	-2.35 ± 0.16	-0.11 ± 0.21	-0.09 ± 0.21	-1.01 ± 0.25	-1.45 ± 0.15
Temperate Australasia	NA ± NA	NA ± NA	NA ± NA	NA ± NA	NA ± NA	1.32 ± 0.43	-0.36 ± 0.13	-0.37 ± 0.13	-0.12 ± 0.15	0.08 ± 0.15
Temperate Northern Atlantic	0.36 ± 0.28	-0.50 ± 0.48	0.07 ± 0.42	0.76 ± 0.34	0.27 ± 0.28	0.28 ± 0.47	-0.12 ± 0.47	-0.14 ± 0.47	0.42 ± 0.51	0.63 ± 0.71
Temperate Northern Pacific	NA ± NA	NA ± NA	NA ± NA	NA ± NA	NA ± NA	-0.52 ± 0.26	1.61 ± 0.41	1.58 ± 0.41	2.28 ± 0.50	2.00 ± 0.61
Temperate South America	-0.04 ± 0.28	1.19 ± 0.41	0.02 ± 0.43	0.11 ± 0.26	-0.07 ± 0.31	-0.5 ± 0.46	0.48 ± 0.55	0.47 ± 0.54	0.33 ± 0.71	0.09 ± 0.54
Temperate Southern Africa	1.61 ± 0.32	0.80 ± 0.15	2.88 ± 0.17	1.08 ± 0.25	1.98 ± 0.27	2.26 ± 0.24	0.29 ± 0.18	0.29 ± 0.18	0.57 ± 0.18	0.78 ± 0.18
Tropical Atlantic	2.17 ± 0.31	0.41 ± 0.23	2.09 ± 0.33	1.76 ± 0.27	2.25 ± 0.33	2.00 ± 0.30	0.37 ± 0.14	0.36 ± 0.15	0.68 ± 0.12	0.82 ± 0.12
Tropical Eastern Pacific	NA ± NA	NA ± NA	NA ± NA	NA ± NA	NA ± NA	0.83 ± 0.27	0.86 ± 0.38	0.88 ± 0.39	0.78 ± 0.25	0.96 ± 0.18
Western Indo-Pacific	NA ± NA	NA ± NA	NA ± NA	NA ± NA	NA ± NA	2.11 ± 0.25	0.75 ± 0.25	0.75 ± 0.25	0.98 ± 0.25	1.17 ± 0.21

Marine eco-realms were defined in Spalding et al. 2007 [38]. Mean scaled probability-of-origin values were compared to the respective 50% and 95% scaled probability-of-origin quantiles per terminal CIT node per species (Table 5). ESP—European storm-petrel; LSP—Leach's storm-petrel; BBSP—black-bellied storm-petrel; WSP—Wilson's storm-petrel; Terminal node—terminal CIT node. Mean scaled probability-of-origin values > 50% and < 95% quantiles of the corresponding terminal CIT node are italicised and mean scaled probability-of-origin values > 95% quantile of the corresponding terminal CIT node are **bolded**. NA—no data available as it was outside of the species distribution extent. See also Figs 2–5 for scaled probability-of-origin distributions. Note: the scaled probability-of-origin values are relative, i.e. not comparable between species from both hemispheres.

<https://doi.org/10.1371/journal.pone.0245756.t006>

Factors affecting moult distribution

As the breeding seasons of the northern and southern species are at opposite times of the year, and fieldwork in the two hemispheres was carried out sequentially, the interannual difference in $\delta^{13}\text{C}$ and $\delta^{18}\text{O}$ differed for both hemispheres and that not necessarily had to be related to species characteristics. For example, an El Niño event was observed between the two studied breeding seasons in the northern hemisphere (2018–2019) but not between the two studied breeding seasons in the southern hemisphere (2017–2018) (e.g. <https://www.climate.gov/news-features/blogs/enso/february-2019-enso-update-el-ni%C3%B1o-conditions-are-here>, accessed 04-09-2020). El Niño events in the Pacific Ocean generally lead to lower sea surface temperatures and more stable weather conditions in the Atlantic Ocean [93]. Nevertheless, interannual variability in weather conditions is higher for the North Atlantic than the South, and in the first half of the year compared to the second [93]. As such, a stronger interannual variability in $\delta^{13}\text{C}$ and $\delta^{18}\text{O}$ during the non-breeding period could be expected for the studied northern hemisphere species than for the southern hemisphere species [28]. Indeed, year was only a significant factor in the CIT dividing WSP into groups predicted to have moult ranges extending further South (Table 5).

For WSP $\delta^{15}\text{N}$ was the first dividing factor in the CIT (Fig 1B). Individuals from the lower $\delta^{15}\text{N}$ group had lower $\delta^{13}\text{C}$ but higher $\delta^{18}\text{O}$ values (Table 2) and were predicted to moult further South compared to individuals higher $\delta^{15}\text{N}$ group (Table 4; Fig 5). As $\delta^{15}\text{N}$ is linked both to trophic level [94] and foraging location [28] at wide geographical scales, we could not distinguish whether these differences were due to differences in foraging range, diet or a combination of both. However, areas around Alaska, Nova Scotia and the Labrador Sea show relatively high plankton $\delta^{15}\text{N}$ values [28, 92], and were also highlighted as high scaled probability-of-

origin areas for these two moult groups, after correcting for trophic enrichment factors (Fig 5). Additionally, WSP has been observed in high quantities close to some of these areas [88, 89], and individuals breeding on King George Island have been predicted to moult north of the Subtropical Front before [50, 76]. The Temperate Northern Pacific eco-realm was characterized by high scaled probability-of-origin values for all four groups of WSP distinguished in our study; for one of the WSP groups with high $\delta^{15}\text{N}$ values the Arctic was designated as an important moult region as well (Table 6). For both high $\delta^{15}\text{N}$ values WSP groups (8 and 9), the temperate Northern Atlantic was shown to have relatively high scaled probability-of-origin values, but this region had relatively low scaled probability-of-origin values in the other two terminal CIT nodes (5 and 6; Table 6). Therefore, although $\delta^{15}\text{N}$ may still be affected by differences in trophic level, we assume at least part of the variation in this variable may be explained by differences in moult distribution.

We found some morphological differences between individuals differing in moult distributions for ESP and WSP. These differences may be caused by a trade-off between foraging ability and flight costs during migration [95], and may be linked to sexual dimorphism [33]. In ESP we found that individuals with shorter tarsi had lower $\delta^{18}\text{O}$ values than individuals with longer tarsi (Fig 1A; Table 2), and in WSP we found that individuals with shorter wings had significantly lower $\delta^{13}\text{C}$ values than individuals with longer wings (Fig 1B; Table 2). As $\delta^{18}\text{O}$ values in coastal zones close to large river mouths are lower compared to the open ocean due to increased freshwater input [27], this may indicate that ESP individuals with shorter legs forage closer to estuaries such as the Banc d'Arguin [96]. Additionally, $\delta^{18}\text{O}$ values differ over a latitudinal gradient with $\delta^{18}\text{O}$ being considerably lower closer to the polar regions than the Equator and tropical zones. ESP differs in migratory behaviour between sexes [97], and shows sexual dimorphism for several body measurements but not tarsus length [90]. WSP females are slightly larger than males [98], with wings being approximately 2.8% longer in females than males [91]. However, we did not find a significant effect of sex in CIT analyses.

Stable isotopic signatures of secondary feathers (S8) of the Monteiro's storm-petrel (*Hydrobates monteiroi*) moulted during the previous non-breeding period showed an evident isotopic niche segregation between sexes. Males exhibited higher $\delta^{13}\text{C}$ and $\delta^{15}\text{N}$ values, and larger isotopic niches compared to females, presumably caused by spatial sexual segregation and exploitation of areas of contrasting environmental conditions [34]. In the Madeiran storm-petrel (*Hydrobates castro*) $\delta^{15}\text{N}$ values differed between sexes during the non-breeding period, with females having lower $\delta^{15}\text{N}$ values than males, possibly caused by intersexual differences in distribution during the non-breeding season, or as a result of differences in diet between sexes or differences in the relative amount of different prey taken [35]. However, in Canadian LSP populations, no sexual isotopic segregation was found [86]. Our results thus suggest that the different moulting distributions are probably not caused by sexual segregation in ESP, LSP or WSP.

Thus, the dividing effect of tarsus length and wing length in ESP and WSP may be correlated with differences in foraging behaviour between individuals, rather than sexual segregation during the non-breeding period. Storm-petrel species with shorter tarsi show less pattering behaviour [99], and species with shorter wings are better adapted to the strong winds in polar regions to exploit less mobile, highly abundant prey [100]. Additionally, these effects were only present in a part of the studied individuals, indicating that differences in behaviour only arise under specific circumstances such as differences in prey availability between areas or years [101].

Predicted moulting areas

Chlorophyll-*a* concentration being a proxy for primary production may be used to locate seabirds foraging hotspots [39], as high concentrations indicate high food availability. Therefore,

we expected predicted moult areas to overlap with high chlorophyll-*a* concentrations. We found this to be true for WSP (Fig 5). For BBSP chlorophyll-*a* concentration did not differ between areas with high and low scaled probability-of-origin values (Fig 4), and for the northern hemisphere species, the high scaled probability-of-origin areas had relatively low chlorophyll-*a* concentrations (Figs 2 and 3). These contrasting findings may be due to large areas being designated as high scaled probability-of-origin areas for the northern species, as the considered possible moulting areas were smaller than those of the southern species, and thus included a smaller range of oceanic $\delta^{13}\text{C}$ and $\delta^{18}\text{O}$ values. Indeed, the locations at which the species were observed during the non-breeding period were generally in areas with high chlorophyll-*a* concentrations (Table 5).

For both northern hemisphere species, the predicted moulting areas (Figs 2 and 3) differed considerably from each other, while the predicted WSP moulting areas (Fig 5) were relatively similar. However, the differences in the similarity between scaled probability-of-origin maps may be due to differences in considered possible moulting areas between northern and southern hemisphere species, or an artefact of the scaling procedure. The locations at which the species were observed were generally located within the areas with the 25% highest scaled probability-of-origin values (Table 5). We hypothesised that ESP would moult close to the African West coast, which our predictions of moult locations in the eco-realms also reiterate (Table 6). However, our model also predicted ESP to moult close to Temperate South America (Table 6), where they have not been observed (Fig 2). The other three species were expected to be more widespread, and could be more easily assigned to eco-realms. These findings imply that although predicting moult distribution based on $\delta^{13}\text{C}$ and $\delta^{18}\text{O}$ can only be performed at a large geographical scale, and while observation likelihood is highly affected by differences in observation effort, combining both approaches may give an approximate estimate of important moulting areas.

Context of the study

Stable isotope analyses can only provide large scale movement information, which is one of the study limitations. Stable carbon isotope ($\delta^{13}\text{C}$) signatures in seabirds vary depending on phytoplankton distribution [25] and could be a subject of seasonal changes. Phytoplankton distribution varies between years and seasons, and is affected by multiple inorganic processes, such as sea surface temperature, nutrient levels linked to the stratification of the water column (in itself affected by upwelling and turmoil due to waves breaking), CO_2 uptake [32], and El Niño events [102]. Due to the striation of water masses around Antarctica, $\delta^{13}\text{C}$ can be used to predict moulting latitudes in the southern species [76], but only up to the Subtropical Front [50]. Oceanic stable oxygen isotope ratios ($\delta^{18}\text{O}$) generally decrease closer to shore in estuarine environments such as the Amazon river mouth and Rio de la Plata area [27], due to a combination of increased freshwater input closer to shore (e.g. river mouths and precipitation) and differences in evaporation rates, creating stark differences with neighbouring marine areas (S1).

Due to these limitations in resolution, while we were able to show inter- and intra-specific differences in moulting distributions, we could only show estimates of predicted moulting areas and assign them to eco-realms close to the shore, while the vast pelagic areas are not included in eco-realms classification [38]. We based our prediction of moulting areas on multi-year isoscapes of stable carbon and oxygen isotopes, instead of isoscapes generated for particular non-breeding periods. While there is a trophic component to the observed $\delta^{13}\text{C}$ in seabird tissues of approximately 0.8‰ per trophic level [103], this can be controlled for, and therefore $\delta^{13}\text{C}$ can be used to predict differences in moulting distribution [25]. The trophic

component of $\delta^{18}\text{O}$ in wild animals is complex and may vary depending on diet and location [104]. We did not know the enrichment factors for $\delta^{18}\text{O}$, and could only base those on a very small sample size of regrowing feathers [105]. We could only calculate those enrichment factors between feather and water samples, instead of between feather, different prey items and seawater samples. Calculating enrichment factors between prey and predator, and prey and seawater masses may have provided a deeper understanding of $\delta^{18}\text{O}$ assimilation [104]. Additionally, while rectrix feathers are often moulted simultaneously with other flight feathers [14, 24], storm-petrels also limit the number of feathers moulted at once [13]. Therefore, while the feathers sampled for our study have grown over a period of several weeks [59], they only represent part of the moulting period.

Nevertheless, our study is the first trying to discover differences in moulting distributions and reconstruct the location of moulting areas of the small storm-petrels breeding in north and south hemispheres based on multiple isotopes. It has filled an evident gap in knowledge about isotopic niches of moulting pelagic storm-petrels. Effective conservation actions and assessments require well-documented knowledge on species' biology and habitat use. While such information is often available for the breeding period, it is frequently lacking for the non-breeding period, especially in pelagic species. Studies such as ours, to better identify important moulting grounds, are therefore needed to properly delineate key conservation areas, and to decide where to direct protection efforts and form conservation planning in the vast marine ecosystem [106]. Combining the large-scale estimates for moulting areas based on $\delta^{13}\text{C}$ and $\delta^{18}\text{O}$ with chlorophyll-*a* concentrations and long-term observation data may provide valuable insights into potential moulting areas. Thus, our study may help to comprehend the year-round feeding ecology of small storm-petrels and understand possible pathways of contaminant (e.g. pollution, microplastics) transfer to breeding areas.

Conclusions

We found both inter- and intra-specific differences in isotopic moulting ranges for the four studied storm-petrel species. Within ESP, LSP and WSP individuals could be grouped into different moulting niches as the $\delta^{13}\text{C}$ and $\delta^{18}\text{O}$ signatures of their tail feathers differed between groups. These divisions were linked to interannual differences in all three species, but also to morphological and $\delta^{15}\text{N}$ differences in ESP and WSP. These morphological differences were likely caused by differences in foraging ecology and prey availability, rather than sexual segregation. Our results suggest that predicting moult distribution based on $\delta^{13}\text{C}$ and $\delta^{18}\text{O}$ can be performed at large geographical scales, but combining these predictions with observational data can be effective to better determine important moulting areas.

Our findings indicate the importance of a large array of different marine regions as moulting areas for the storm-petrel species from both hemispheres because individuals breeding at the same location may adopt different migration strategies, spending the moulting period in different areas. Future studies combining GPS or GLS-tracking and stable isotope analyses based on individuals sampled in multiple locations, including the non-breeding period and multiple feather types, are required to more accurately define moulting areas and further comprehend the foraging ecology at this phase of the annual cycle.

Supporting information

S1 File. Base maps for stable oxygen and carbon ocean isoscapes and chlorophyll-*a* concentrations.

(DOCX)

S2 File. European storm-petrel results including two outliers.
(DOCX)

S3 File. Data collected by the authors and used in this study.
(XLSX)

Acknowledgments

C. Trueman gracefully provided $\delta^{13}\text{C}$ prediction isoscapes. We would like to thank the Henryk Arctowski Polish Antarctic Station and the Department of Antarctic Biology, the Polish Academy of Sciences for their hospitality and logistic support during our stay on King George Island. We would like to thank Jens-Kjeld Jensen and Marita Gulkklett for their hospitality and support for the project on the Faroe Islands. We are grateful to Rosanne Michielsen for her support in the field on King George Island, and Rachel Shepherd, Jessica Hey, Jón Aldará and Katherine Keogan for their support in the field on the Faroe Islands.

Author Contributions

Conceptualization: Anne N. M. A. Ausems, Dariusz Jakubas.

Data curation: Anne N. M. A. Ausems.

Formal analysis: Anne N. M. A. Ausems, Grzegorz Skrzypek, Katarzyna Wojczulanis-Jakubas.

Funding acquisition: Dariusz Jakubas.

Investigation: Anne N. M. A. Ausems, Katarzyna Wojczulanis-Jakubas, Dariusz Jakubas.

Methodology: Anne N. M. A. Ausems, Katarzyna Wojczulanis-Jakubas, Dariusz Jakubas.

Project administration: Anne N. M. A. Ausems, Dariusz Jakubas.

Resources: Grzegorz Skrzypek.

Supervision: Dariusz Jakubas.

Validation: Anne N. M. A. Ausems, Dariusz Jakubas.

Visualization: Anne N. M. A. Ausems.

Writing – original draft: Anne N. M. A. Ausems.

Writing – review & editing: Grzegorz Skrzypek, Katarzyna Wojczulanis-Jakubas, Dariusz Jakubas.

References

1. Carroll MJ, Bolton M, Owen E, Anderson GQA, Mackley EK, Dunn EK, et al. Kittiwake breeding success in the southern North Sea correlates with prior sandeel fishing mortality. *Aquat Conserv Mar Freshw Ecosyst.* 2017; 27(6):1164–1175.
2. Sorensen MC, Hipfner JM, Kyser TK, Norris DR. Carry-over effects in a Pacific seabird: Stable isotope evidence that pre-breeding diet quality influences reproductive success. *J Anim Ecol.* 2009; 78:460–467. <https://doi.org/10.1111/j.1365-2656.2008.01492.x> PMID: 19021778
3. Hovinen JEH, Tarroux A, Ramírez F, Forero M, Descamps S. Relationships between isotopic ratios, body condition and breeding success in a high arctic seabird community. *Mar Ecol Prog Ser.* 2019; 613:183–195.
4. Reiertsen TK, Erikstad KE, Anker-Nilssen T, Barrett RT, Boulinier T, Frederiksen M, et al. Prey density in non-breeding areas affects adult survival of black-legged kittiwakes *Rissa tridactyla*. *Mar Ecol Prog Ser.* 2014; 509:289–302.

5. Bogdanova MI, Butler A, Wanless S, Moe B, Anker-Nilssen T, Frederiksen M, et al. Multi-colony tracking reveals spatio-temporal variation in carry-over effects between breeding success and winter movements in a pelagic seabird. *Mar Ecol Prog Ser*. 2017; 578:167–181.
6. Pacyna AD, Jakubas D, Ausems ANMA, Frankowski M, Polkowska, Wojczulanis-Jakubas K. Storm petrels as indicators of pelagic seabird exposure to chemical elements in the Antarctic marine ecosystem. *Sci Total Environ*. 2019; 692:382–392. <https://doi.org/10.1016/j.scitotenv.2019.07.137> PMID: 31351282
7. Pacyna-Kuchta AD, Jakubas D, Frankowski M, Polkowska Ż, Wojczulanis-Jakubas K. Exposure of a small Arctic seabird, the little auk (*Alle alle*) breeding in Svalbard, to selected elements throughout the course of a year. *Sci Total Environ*. 2020; 732:139103. <https://doi.org/10.1016/j.scitotenv.2020.139103> PMID: 32428770
8. Lindström Å, Visser GH, Daan S. The energetic cost of feather synthesis to basal metabolic rate is proportional. *Physiol Zool*. 1993; 66(4):490–510.
9. Edwards AE. Large-scale variation in flight feather molt as a mechanism enabling biennial breeding in albatrosses. *J Avian Biol*. 2008; 39:144–151.
10. Hedenström A, Sunada S. On the aerodynamics of moult gaps in birds. *J Exp Biol*. 1999; 202:67–76. PMID: 9841896
11. Slagsvold T, Dale S. Disappearance of female pied flycatchers in relation to breeding stage and experimentally induced molt. *Ecology*. 1996; 77(2):461–471.
12. Chérel Y, Quillfeldt P, Delord K, Weimerskirch H. Combination of at-sea activity, geolocation and feather stable isotopes documents where and when seabirds molt. *Front Ecol Evol*. 2016; 4:3.
13. Bridge ES. Influences of morphology and behavior on wing-molt strategies in seabirds. *Mar Ornithol*. 2006; 34:7–19.
14. Ainley DG, Lewis J, Morrell S. Molt in Leach's and Ashy storm-petrels. *Wilson Bull*. 1976; 88(1):76–95.
15. Halpin LR, Pollet IL, Lee C, Morgan KH, Carter HR. Year-round movements of sympatric Fork-tailed (*Oceanodroma furcata*) and Leach's (*O. leucorhoa*) storm-petrels. *J F Ornithol*. 2018; 0(0):1–14.
16. Pollet IL, Ronconi RA, Leonard ML, Shutler D. Migration routes and stopover areas of Leach's storm petrels *Oceanodroma leucorhoa*. *Mar Ornithol*. 2019; 47:53–63.
17. Pollet IL, Hedd A, Taylor PD, Montevecchi WA, Shutler D. Migratory movements and wintering areas of Leach's storm-petrels tracked using geolocators. *J F Ornithol*. 2014; 85(3):321–328.
18. Hobson KA. Isotopic ornithology: A perspective. *J Ornithol*. 2011; 152(Suppl 1):S49–66.
19. Chérel Y, Hobson KA, Weimerskirch H. Using stable-isotope analysis of feathers to distinguish moulting and breeding origins of seabirds. *Oecologia*. 2000; 122:155–162. <https://doi.org/10.1007/PL00008843> PMID: 28308369
20. Mizutani H, Fukuda M, Kabaya Y. ¹³C and ¹⁵N enrichment factors of feathers of 11 species of adult birds. *Ecology*. 1992; 73(4):1391–1395.
21. Wada E, Hattori A. Nitrogen in the Sea: Forms, Abundance, and Rate Processes. CRC Press; 1990.
22. Rohwer S, Ricklefs RE, Rohwer VG, Copple MM. Allometry of the duration of flight feather molt in birds. *PLoS Biol*. 2009; 7(6):e1000132. <https://doi.org/10.1371/journal.pbio.1000132> PMID: 19529759
23. Furness RW, Camphuysen CJ. Seabirds as monitors of the marine environment. *ICES J Mar Sci*. 1997; 54:726–737.
24. Beck JR, Brown DW. The biology of Wilson's storm petrel, *Oceanites oceanicus* (Kuhl), at Signy Island, South Orkney Islands. *Br Antarct Surv Sci Reports*. 1972; 69:1–54.
25. Magozzi S, Yool A, Vander Zanden HB, Wunder MB, Trueman CN. Using ocean models to predict spatial and temporal variation in marine carbon isotopes. *Ecosphere*. 2017; 8(5):e01763.
26. Ceia FR, Chérel Y, Paiva VH, Ramos JA. Stable isotope dynamics ($\delta^{13}\text{C}$ and $\delta^{15}\text{N}$) in neritic and oceanic waters of the North Atlantic inferred from GPS-tracked Cory's shearwaters. *Front Mar Sci*. 2018; 5:377.
27. Bowen GJ. Isoscapes: Spatial Pattern in Isotopic Biogeochemistry. *Annu Rev Earth Planet Sci*. 2010; 38:161–187.
28. McMahon KW, Hamady LL, Thorrold SR. Ocean ecogeochemistry: A review. *Oceanogr Mar Biol An Annu Rev*. 2013; 51:327–374.
29. Weiss F, Furness RW, McGill RAR, Strange IJ, Masello JF, Quillfeldt P. Trophic segregation of Falkland Islands seabirds: insights from stable isotope analysis. *Polar Biol*. 2009; 32:1753–1763.
30. Post DM. Using stable isotopes to estimate trophic position: Models, methods, and assumptions. *Ecology*. 2002; 83(3):703–718.

31. Grubb TC. Ptilochronology: feather growth bars as indicators of nutritional-status. *The Auk*. 1989; 106(2):314–320.
32. Graham BS, Koch PL, Newsome SD, McMahon KW, Auriolos D. Using isoscapes to trace the movements and foraging behavior of top predators in oceanic ecosystems. In: West JB, editor. *Isoscapes: Understanding Movement, Pattern, and Process on Earth Through Isotope Mapping*. 2010. p. 299–318.
33. Phillips RA, Bearhop S, McGill RAR, Dawson DA. Stable isotopes reveal individual variation in migration strategies and habitat preferences in a suite of seabirds during the nonbreeding period. *Oecologia*. 2009; 160:795–806. <https://doi.org/10.1007/s00442-009-1342-9> PMID: 19377898
34. Paiva VH, Ramos JA, Nava C, Neves V, Bried J, Magalhães M. Inter-sexual habitat and isotopic niche segregation of the endangered Monteiro's storm-petrel during breeding. *Zoology*. 2018; 126:29–35. <https://doi.org/10.1016/j.zool.2017.12.006> PMID: 29352679
35. Carreiro AR, Paiva VH, Medeiros R, Franklin KA, Oliveira N, Fagundes AI, et al. Metabarcoding, stable isotopes, and tracking: unraveling the trophic ecology of a winter-breeding storm petrel (*Hydrobates castro*) with a multimethod approach. *Mar Biol*. 2020; 167:14.
36. Hedd A, Montevecchi WA, Davoren GK, Fifield DA. Diets and distributions of Leach's storm-petrel (*Oceanodroma leucorhoa*) before and after an ecosystem shift in the Northwest Atlantic. *Can J Zool*. 2009; 87:787–801.
37. Campbell CJ, Fitzpatrick MC, Vander Zanden HB, Nelson DM. Advancing interpretation of stable isotope assignment maps: comparing and summarizing origins of known-provenance migratory bats. *Anim Migr*. 2020; 7:27–41.
38. Spalding MD, Fox HE, Allen GR, Davidson N, Ferdaña ZA, Finlayson M, et al. Marine ecoregions of the world: A bioregionalization of coastal and shelf areas. *Bioscience*. 2007; 57(7):573–583.
39. Suryan RM, Santora JA, Sydeman WJ. New approach for using remotely sensed chlorophyll *a* to identify seabird hotspots. *Mar Ecol Prog Ser*. 2012; 451:213–225.
40. Hedd A, Montevecchi WA, Otley H, Phillips RA, Fifield DA. Trans-equatorial migration and habitat use by sooty shearwaters *Puffinus griseus* from the South Atlantic during the nonbreeding season. *Mar Ecol Prog Ser*. 2012; 449:277–290.
41. Penhallurick J, Wink M. Analysis of the taxonomy and nomenclature of the Procellariiformes based on complete nucleotide sequences of the mitochondrial cytochrome *b* gene. *Emu*. 2004; 104:125–147.
42. Prum RO, Berv JS, Dornburg A, Field DJ, Townsend JP, Lemmon EM, et al. A comprehensive phylogeny of birds (Aves) using targeted next-generation DNA sequencing. *Nature*. 2015; 526:569–573. <https://doi.org/10.1038/nature15697> PMID: 26444237
43. BirdLife International. IUCN Red List for birds. 2020 [cited 2020 Sep 30]. Available from: <http://www.birdlife.org>
44. Carboneras C, Jutglar F, Kirwan GM, Christie DA, Jutglar F, Kirwan GM, et al. Order Procellariiformes. In: del Hoyo J, Elliot A, Sargatal J, Christie DA, de Juana E, editors. *Handbook of the Birds of the World Alive*. Barcelona: Lynx Edicions; 2017. p. 197–278.
45. Griffiths AM. European stormpetrels *Hydrobates pelagicus* feeding by diving off South Africa. *Cormorant*. 1981; 9:47.
46. Hahn S, Quillfeldt P. First record of Leach's stormpetrel *Oceanodroma leucorhoa* at King George Island, South Shetland Islands, Antarctica. *Mar Ornithol*. 1998; 26:80.
47. Martínez C, Roscales JL, Sanz-Aguilar A, González-Solís J. Inferring the Wintering Distribution of the Mediterranean Populations of European Storm-Petrels *Hydrobates pelagicus melitensis* from Stable Isotope Analysis and Observational Field Data. *Ardeola*. 2018; 66(1):13–32.
48. Flood RL, Thomas B. Identification of "black-and-white" storm-petrels of the North Atlantic. *Br Birds*. 2007;(100):407–442.
49. Flood RL, Fisher A. Wilson's storm-petrels off the Isles of Scilly: a ten-year analysis, 2000–09. *Br Birds*. 2010;(103):396–404.
50. Gladbach A, McGill RAR, Quillfeldt P. Foraging areas of Wilson's storm-petrel *Oceanites oceanicus* in the breeding and inter-breeding period determined by stable isotope analysis. *Polar Biol*. 2007; 30:1005–1012.
51. Quillfeldt P, Thorn S, Richter B, Nabte M, Coria N, Masello JF, et al. Testing the usefulness of hydrogen and compound-specific stable isotope analyses in seabird feathers: a case study in two sympatric Antarctic storm-petrels. *Mar Biol*. 2017; 164:192.
52. Cramp S, Simmons KEL, Ferguson-Lees IJ, Gillmor R, Hollom PAD, Hudson R, et al. Family *Hydrobatidae* storm-petrels. In: *Handbook of the Birds of Europe and the Middle East and North Africa The Birds of the Western Palearctic Volume 1*. Oxford: Oxford University Press; 1977. p. 155–178.

53. Wasilewski A. Ecological aspects of the breeding cycle in the Wilson's storm petrel, *Oceanites oceanicus* (Kuhl), at King George Island (South Shetland Islands, Antarctica). *Polish Polar Res.* 1986; 7(3):173–216.
54. Cadiou B. The breeding biology of the European Storm-petrel *Hydrobates pelagicus* in Brittany, France. *Atl Seabirds.* 2001; 3(4):149–164.
55. Amengual JF, Gargallo G, Suárez M, Bonnin J, González JM, Rebassa M, et al. The Mediterranean storm petrel *Hydrobates pelagicus melitensis* at Cabrera archipelago (Balearic Islands, Spain): Breeding moult, biometry and evaluation of the population size by mark and recapture techniques. *Ringing Migr.* 1999; 19(3):181–190.
56. Arroyo B, Mínguez E, Palomares L, Pinilla J. The timing and pattern of moult of flight feathers of European storm-petrel *Hydrobates pelagicus* in Atlantic and Mediterranean breeding areas. *Ardeola.* 2004; 51(2):365–373.
57. Bolton M, Thomas R. Moult and ageing of storm petrels *Hydrobates pelagicus*. *Ringing Migr.* 2001; 23(3):193–201.
58. Mayaud N. Nouvelles précisions sur la mue des Procellariiformes. *Alauda.* 1949; 17/18:144–55, 222–233.
59. Ausems ANMA, Wojczulanis-Jakubas K, Jakubas D. Differences in tail feather growth rate in storm-petrels breeding in the Northern and Southern hemisphere: a ptilochronological approach. *PeerJ.* 2019; 7:e7807. <https://doi.org/10.7717/peerj.7807> PMID: 31637118
60. Griffiths R, Double MC, Orr K, Dawson RJG. A DNA test to sex most birds. *Mol Ecol.* 1998; 7:1071–1075. <https://doi.org/10.1046/j.1365-294x.1998.00389.x> PMID: 9711866
61. Skrzypek G, Paul D. $\delta^{13}\text{C}$ analyses of calcium carbonate: Comparison between the GasBench and elemental analyzer techniques. *Rapid Commun Mass Spectrom.* 2006; 20:2915–2920. <https://doi.org/10.1002/rcm.2688> PMID: 16941549
62. Skrzypek G. Normalization procedures and reference material selection in stable HCNOS isotope analyses: An overview. *Anal Bioanal Chem.* 2013; 405:2815–2823. <https://doi.org/10.1007/s00216-012-6517-2> PMID: 23135627
63. Coplen TB. New guidelines for reporting stable hydrogen, carbon, and oxygen isotope-ratio data. *Geochim Cosmochim Acta.* 1996; 60(17):3359–3360.
64. Coplen TB, Qi H. USGS42 and USGS43: Human-hair stable hydrogen and oxygen isotopic reference materials and analytical methods for forensic science and implications for published measurement results. *Forensic Sci Int.* 2012; 214:135–141. <https://doi.org/10.1016/j.forsciint.2011.07.035> PMID: 21852055
65. R Core Team. R: A language and environment for statistical computing. Vienna, Austria: R Foundation for Statistical Computing; 2020. Available from: <https://www.r-project.org>
66. Hothorn T, Hornik K, Zeileis A. Unbiased recursive partitioning: a conditional inference framework. *J Comput Graph Stat.* 2006; 15(3):651–674.
67. Hothorn T, Zeileis A. *partykit*: A modular toolkit for recursive partytioning in R. *J Mach Learn Res.* 2015; 16:3905–3909.
68. Quinn GP, Keough MJ. *Experimental design and data analysis for biologists.* Cambridge University Press; 2002.
69. Campbell C. *isocat*: Isotope Origin Clustering and Assignment Tools. 2020. Available from: <https://cran.r-project.org/package=isocat>
70. LeGrande AN, Schmidt GA. Global gridded data set of the oxygen isotopic composition in seawater. *Geophys Res Lett.* 2006; 33:L12604.
71. ESRI. ArcMap 10.3.1. Redlands, CA: Environmental Systems Research Institute; 2014.
72. Hijmans RJ. *raster*: Geographich Data Analysis and Modeling. 2020. Available from: <https://cran.r-project.org/package=raster>
73. Lehtomaki J. *zonator*: R package. 2018. Available from: <https://cran.r-project.org/package=zonator>
74. Meier RE, Votier SC, Wynn RB, Guilford T, McMinn Grivé M, Rodríguez A, et al. Tracking, feather moult and stable isotopes reveal foraging behaviour of a critically endangered seabird during the non-breeding season. *Divers Distrib.* 2017; 23:130–145.
75. Michener RH, Schell DM. Stable isotopes as tracers in marine aquatic food webs. In: Lajtha K, Michener RH, editors. *Stable isotopes in ecology and environmental science.* Oxford, UK: Blackwell Scientific Publications; 1994. p. 138–157.
76. Quillfeldt P, McGill RAR, Furness RW. Diet and foraging areas of Southern Ocean seabirds and their prey inferred from stable isotopes: Review and case study of Wilson's storm-petrel. *Mar Ecol Prog Ser.* 2005; 295:295–304.

77. Ainley DG, O'Connor EF, Boekelheide RJ. The marine ecology of birds in the Ross Sea, Antarctica. *Ornithol Monogr.* 1984; 32:1–97.
78. Ridoux V. The diets and dietary segregation of seabirds at the subantarctic Crozet Islands. *Mar Ornithol.* 1994; 22:1–192.
79. Frith R, Krug D, Ronconi RA, Wong SNP, Mallory ML, Tranquilla LAM, et al. Diet of Leach's storm-petrels (*Hydrobates leucorhous*) among three colonies in Atlantic Canada. *Northeast Nat.* 2020; 27(4):612–630.
80. Ainslie JA, Atkinson R. On the breeding habits of Leach's fork-tailed petrel. *Br Birds.* 1936;(30):234–249.
81. Büßer C, Kahles A, Quillfeldt P. Breeding success and chick provisioning in Wilson's storm-petrels *Oceanites oceanicus* over seven years: Frequent failures due to food shortage and entombment. *Polar Biol.* 2004; 27(10):613–622.
82. Croxall JP, Hill HJ, Connell MJO, Prince PA. Food and feeding ecology of Wilson's storm petrel *Oceanites oceanicus* at South Georgia. *J Zool.* 1988; 216:83–102.
83. Croxall JP, Prince PA. Food, feeding ecology and segregation of seabirds at South Georgia. *Biol J Linn Soc.* 1980;(14):103–131.
84. D'Elbée J, Hémerly G. Diet and foraging behaviour of the British storm petrel *Hydrobates pelagicus* in the Bay of Biscay during summer. *Ardea.* 1998; 86:1–10.
85. Hahn S. The food and chick feeding of blackbellied stormpetrel (*Fregatta tropica*) at King George Island, South Shetlands. *Polar Biol.* 1998; 19:354–357.
86. Hedd A, Montevecchi WA. Diet and trophic position of Leach's storm-petrel *Oceanodroma leucorhoa* during breeding and moult, inferred from stable isotope analysis of feathers. *Mar Ecol Prog Ser.* 2006; 322:291–301.
87. Quillfeldt P. Seasonal and annual variation in the diet of breeding and non-breeding Wilson's storm-petrels on King George Island, South Shetland Islands. *Polar Biol.* 2002; 25:216–221.
88. ebird.com. eBird Basic Dataset May 2020. Ithaca, New York: Cornell Lab of Ornithology; 2020.
89. Observation.org. Stichting Observation International and local partners. 2020. Available from: <https://www.observation.org>
90. Jakubas D, Wojczulanis-Jakubas K, Jensen J. Body size variation of European storm petrels *Hydrobates pelagicus* in relation to environmental variables. *Acta Ornithol.* 2014; 49(1):71–82.
91. Büßer C. Elterliche Investition und Morphometrie der Buntfußsturmschwalbe, *Oceanites oceanicus*, auf King George Island, Südshetland-Inseln, Antarktis (Diploma Thesis). Friedrich-Schiller-University, Jena; 2003.
92. McMahon KW, Hamady LL, Thorrold SR. A review of ecogeochemistry approaches to estimating movements of marine animals. *Limnol Oceanogr.* 2013; 58(2):697–714.
93. Enfield DB, Mayer DA. Tropical atlantic sea surface temperature variability and its relation to El Niño-Southern Oscillation. *J Geophys Res C Ocean.* 1997; 102(C1):929–945.
94. Minagawa M, Wada E. Stepwise enrichment of ^{15}N along food chains: Further evidence and the relation between $\delta^{15}\text{N}$ and animal age. *Geochim Cosmochim Acta.* 1984; 48:1135–1140.
95. Orben RA, Paredes R, Roby DD, Irons DB, Shaffer SA. Body size affects individual winter foraging strategies of thick-billed murrelets in the Bering Sea. *J Anim Ecol.* 2015; 84:1589–1599. <https://doi.org/10.1111/1365-2656.12410> PMID: 26095664
96. Leopold MF. Seabirds in the shelf edge waters bordering the Banc d'Arguin, Mauritania, in May. *Hydrobiologia.* 1993; 258:197–210.
97. Medeiros RJ, King RA, Symondson WOC, Cadiou B, Zonfrillo B, Bolton M, et al. Molecular evidence for gender differences in the migratory behaviour of a small seabird. *PLoS One.* 2012; 7(9):e46330. <https://doi.org/10.1371/journal.pone.0046330> PMID: 23029481
98. Quillfeldt P, Masello JF, Lubjuhn T. Variation in the adult body mass of Wilson's storm petrels *Oceanites oceanicus* during breeding. *Polar Biol.* 2006; 29:372–378.
99. Sausner J, Torres-Mura JC, Robertson J, Hertel F. Ecomorphological differences in foraging and patting behavior among storm-petrels in the eastern Pacific Ocean. *Auk.* 2016; 133:397–414.
100. Spear LB, Ainley DG. Morphological differences relative to ecological segregation in petrels (Family: Procellariidae) of the Southern Ocean and tropical Pacific. *Auk.* 1998; 115(4):1017–1033.
101. Gladbach A, Braun C, Nordt A, Peter HU, Quillfeldt P. Chick provisioning and nest attendance of male and female Wilson's storm petrels *Oceanites oceanicus*. *Polar Biol.* 2009; 32:1315–1321.
102. Conde A, Prado M. Changes in phytoplankton vertical distribution during an El Niño event. *Ecol Indic.* 2018; 90:201–205.

103. Ceia FR, Paiva VH, Fidalgo V, Morais L, Baeta A, Crisóstomo P, et al. Annual and seasonal consistency in the feeding ecology of an opportunistic species, the yellow-legged gull *Larus michahellis*. *Mar Ecol Prog Ser*. 2014; 497:273–284.
104. Magozzi S, Vander Zanden HB, Wunder MB, Bowen GJ. Mechanistic model predicts tissue–environment relationships and trophic shifts in animal hydrogen and oxygen isotope ratios. *Oecologia*. 2019; 191:777–789. <https://doi.org/10.1007/s00442-019-04532-8> PMID: 31642988
105. Ausems ANMA, Skrzypek G, Wojczulanis-Jakubas K, Jakubas D. Sharing menus and kids' specials: Inter- and intraspecific differences in stable isotope niches between sympatrically breeding storm-petrels. *Sci Total Environ*. 2020; 728:138768. <https://doi.org/10.1016/j.scitotenv.2020.138768> PMID: 32339838
106. Rodríguez A, Arcos JM, Bretagnolle V, Dias MP, Holmes ND, Louzao M, et al. Future directions in conservation research on petrels and shearwaters. *Front Mar Sci*. 2019; 6:94.

Birds of a feather moult together: differences in moulting distribution of four species of storm-petrels

Anne N.M.A. Ausems¹, Grzegorz Skrzypek², Katarzyna Wojczulanis-Jakubas¹, Dariusz Jakubas¹

¹The University of Gdańsk, Faculty of Biology, Department of Vertebrate Ecology and Zoology, ul. Wita Stwosza 59, 80-308 Gdańsk, Poland

²The University of Western Australia, West Australian Biogeochemistry Centre, 35 Stirling Highway, Crawley WA 6009, Australia

Corresponding author: Anne N.M.A. Ausems, anne.ausems@gmail.com

Supporting Information 1: Base maps for stable oxygen and carbon ocean isoscapes and chlorophyll-*a* concentrations

For the *isocat* analyses (Campbell, 2020) we used prediction isoscapes for both $\delta^{18}\text{O}$ and $\delta^{13}\text{C}$ (Fig. S1). We used seasonally averaged plankton $\delta^{13}\text{C}$ prediction isoscapes provided by C. Trueman from models described in Magozzi et al. (2017), for the core non-breeding periods of the northern (November to March) and southern (May to October) species separately. For $\delta^{18}\text{O}$ we used an annually averaged gridded dataset for Global Seawater Oxygen-18 Database isoscape obtained from LeGrande and Schmidt (2006; <https://data.giss.nasa.gov/o18data/>) and visualized in ArcMap 10.3.1 (ESRI, 2014). For the two northern species, we only used data from the Atlantic Ocean as the studied populations do not migrate to other oceans and thus, we restricted the rasters to the area between 75 °W and 52 °E.

To validate the moulting areas predicted by the *isocat* analyses, we used chlorophyll-*a* concentrations as a proxy for food abundance. We used chlorophyll-*a* concentrations at the surface layer from remote sensing MODIS Aqua satellite data (NASA Ocean Color Web, <https://oceancolor.gsfc.nasa.gov/>). We created concentration rasters for the corresponding core non-breeding periods for the species from the northern (November to March 2003-2018) and southern (May to October 2003-2018) hemispheres (Fig. S1). We averaged monthly maps in ArcMap 10.3.1 (ESRI, 2014).

References

- Campbell, C., 2020. *isocat*: Isotope Origin Clustering and Assignment Tools.
- ESRI, 2014. ArcMap 10.3.1.
- LeGrande, A.N., Schmidt, G.A., 2006. Global gridded data set of the oxygen isotopic composition in seawater 33, 1–5. <https://doi.org/10.1029/2006GL026011>
- Magozzi, S., Yool, A., Vander Zanden, H.B., Wunder, M.B., Trueman, C.N., 2017. Using ocean models to predict spatial and temporal variation in marine carbon isotopes. *Ecosphere* 8. <https://doi.org/10.1002/ecs2.1763>

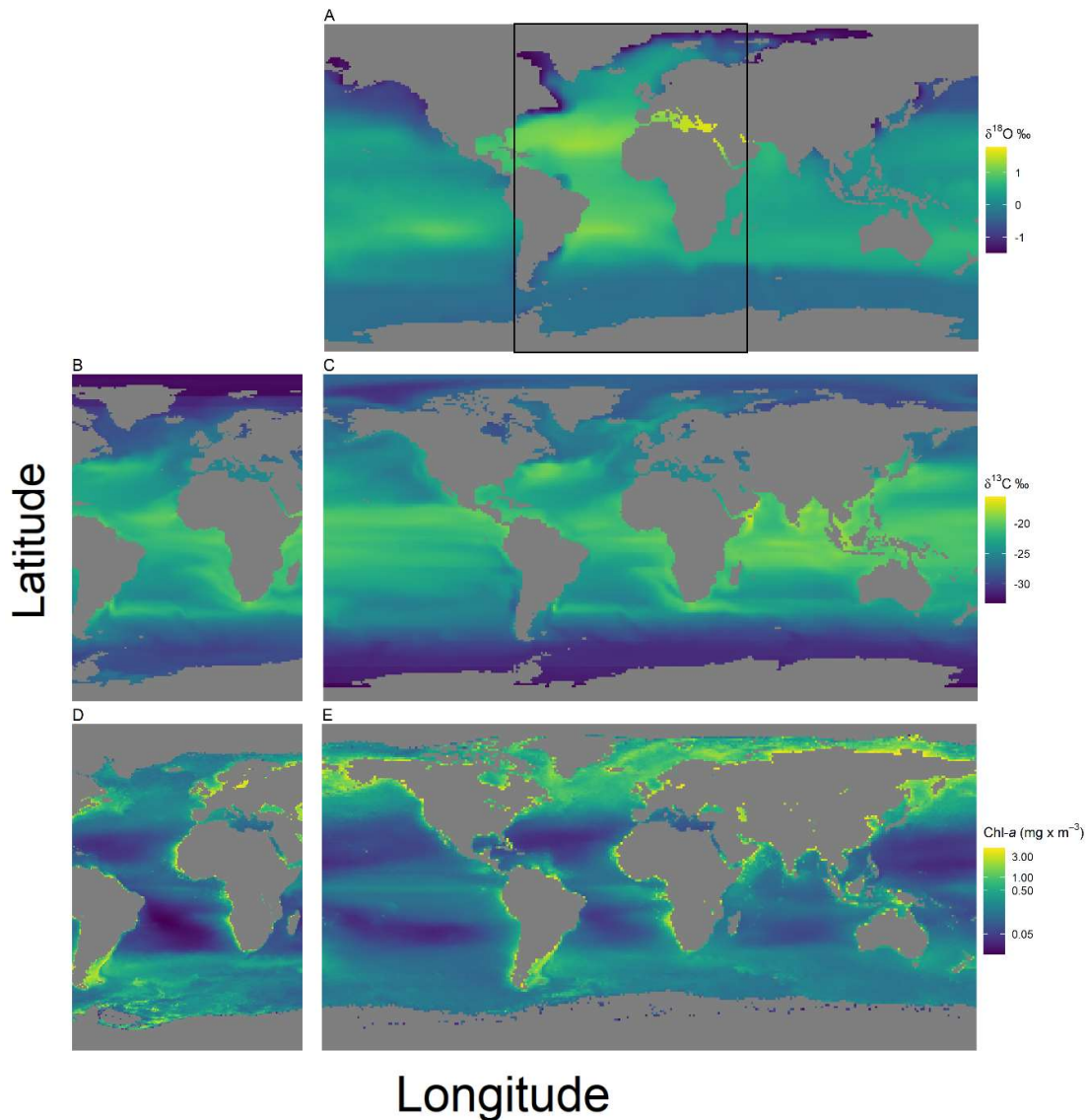


Figure S1 Base maps for stable oxygen and carbon ocean isoscapes and chlorophyll-*a* concentrations: Panel A – Annually averaged $\delta^{18}\text{O}$ isoscape; panel B – Seasonally averaged plankton $\delta^{13}\text{C}$ isoscape for the Northern species (non-breeding; November – March); panel C – Seasonally averaged plankton $\delta^{13}\text{C}$ isoscape for the Southern species (non-breeding; May – October); panel D – Chlorophyll-*a* concentrations for the non-breeding period of the Northern species (non-breeding; November – March); panel E – Chlorophyll-*a* concentrations for the non-breeding period of the Southern species (non-breeding; May – October). The black rectangle panel A shows the area between 75 °W and 52 °E used for the Northern species. Panel B and D are restricted to the same area.

Birds of a feather moult together: differences in moulting distribution of four species of storm-petrels

Anne N.M.A. Ausems¹, Grzegorz Skrzypek², Katarzyna Wojczulanis-Jakubas¹, Dariusz Jakubas¹

¹The University of Gdańsk, Faculty of Biology, Department of Vertebrate Ecology and Zoology, ul. Wita Stwosza 59, 80-308 Gdańsk, Poland

²The University of Western Australia, West Australian Biogeochemistry Centre, 35 Stirling Highway, Crawley WA 6009, Australia

Corresponding author: Anne N.M.A. Ausems, anne.ausems@gmail.com

Supporting Information 2: European storm-petrel results including two outliers

The CIT terminal nodes did not differ significantly in $\delta^{13}\text{C}$ (Welch two-sample *t*-test; $t_{62.8} = 1.68$, $p = 0.097$) but CIT node 2 had significantly higher $\delta^{18}\text{O}$ values than CIT node 3 ($t_{52.6} = 5.57$, $p < 0.001$; Fig. S2.1; Table S2.1).

The similarity in the scaled probability-of-origin distribution maps was very low (Jaccard index; $J = 0.050$; Fig. S2.2).

Chlorophyll-*a* concentrations in CIT node 2 were significantly lower in the areas with the 76 % – 100 % highest scaled probability-of-origin values than in the lower 0 % – 75 % value areas (Welch two sample *t*-test; $t_{215.9} = 9.32$, $p < 0.001$), but did not differ between scaled probability-of-origin areas in CIT node 3 ($t_{254.5} = 1.13$, $p = 0.260$).

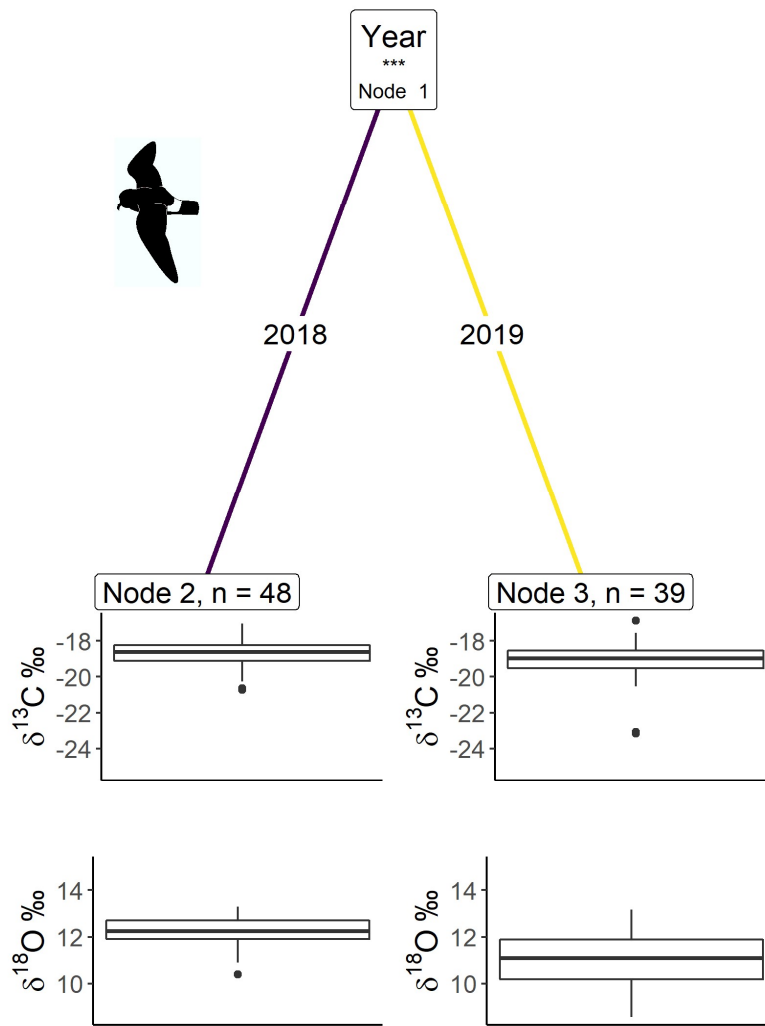


Figure S2.1 Conditional inference trees (CIT) characterizing factors affecting the stable carbon ($\delta^{13}\text{C}$) and oxygen ($\delta^{18}\text{O}$) isotopic signatures for the European storm-petrel including outliers during the moulting period. We used Species, Year, $\delta^{15}\text{N}$ (stable nitrogen isotope composition), FGR (feather growth rate), BM (body mass), TL (tarsus length), and WL (wing length) as initial predictors. Body morphometrics (i.e. BM, TL and WL) were measured during the breeding season after moulting. Only variables with a significant dividing effect are shown in order of importance from the top down. At each node the dividing variable and corresponding p-value sign are listed in the box. These significance levels represent the test of independence between the listed variable and the response variables. Terminal CIT nodes indicate variable levels characterizing the response variable. Density plots above node boxes show the distribution of the continuous divisive variables, with the cut-off point dividing the colours. Boxplots show the median (band inside the box), the first (25%) and third (75%) quartile (box), the lowest and the highest values within 1.5 interquartile range (whiskers) and outliers (circles). ESP – European storm-petrel; n – number of individuals in each terminal CIT node group. P-values < 0.001 are shown with ***, p-values < 0.01 are shown with ** and p-values < 0.05 are shown with *.

Table S2.1 The mean \pm SD $\delta^{13}\text{C}$ and $\delta^{18}\text{O}$ values of the subgroups distinguished based on the conditional inference tree (CIT) terminal nodes for the European storm-petrel including outliers. The individuals were divided into groups with differing $\delta^{13}\text{C}$ and $\delta^{18}\text{O}$ values, based on variables described in the text. Terminal node – terminal CIT node number; n – sample size. See also Fig. S2.1 for tree results.

Terminal node	n	$\delta^{13}\text{C}_{\text{VPDB}}$ (‰)	$\delta^{18}\text{O}_{\text{VSMOW}}$ (‰)
2	48	-18.8 ± 0.8	12.2 ± 0.6
3	39	-19.1 ± 1.2	11.0 ± 1.2
Total	87	-18.9 ± 1.0	11.7 ± 1.1

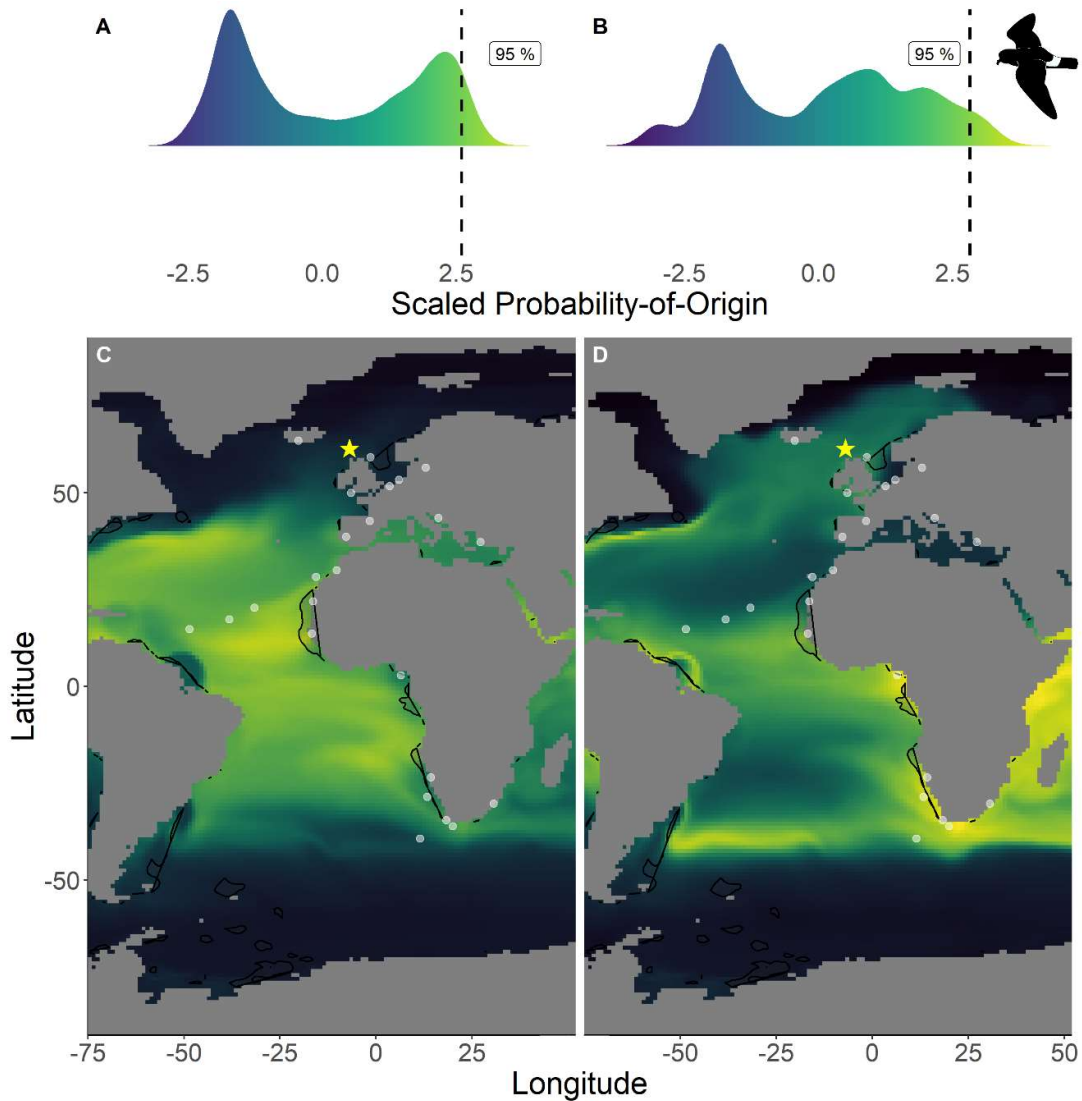


Figure S2.2 Scaled probability-of-origin maps based on $\delta^{13}\text{C}$ and $\delta^{18}\text{O}$ for each group for the European storm-petrel (ESP) including outliers. Terminal nodes from a conditional inference tree (CIT) based on differences between years, and correlated to body morphology (Fig. S2.1) were treated as groups. Panel A – Scaled probability-of-origin value distribution for terminal CIT node 2; panel B – scaled probability-of-origin value distribution for terminal CIT node 3; panel C – scaled probability-of-origin map for terminal CIT node 2; panel D – scaled probability-of-origin map for terminal CIT node 3. Scaled probability-of-origin values are shown on a relative high (yellow) – low (black) gradient in both the density plots and maps. The 95 % quantile of the scaled probability-of-origin values per terminal CIT node are shown with the dashed line. Shaded contours show high chlorophyll-a concentration areas (upper 95 % of the data), and white dots show observation locations (ebird.com, 2020; Observation.org, 2020). The yellow star indicates the location of the breeding colony where birds were sampled.

Table S2.2 Scaled probability-of-origin and chlorophyll-a concentration values around each observation location per terminal CIT node for the European storm-petrel including outliers. Scaled probability-of-origin and chlorophyll-a concentration values were averaged for a buffer of approximately 10 ° around the average latitude and longitude for each observation location. The 50 % and 95 % quantiles were calculated for the entire raster, for both the scaled probability-of-origin maps and the chlorophyll-a concentration maps. See also Fig. S2.2 for scaled probability-of-origin distributions. Note: the scaled probability-of-origin values are relative, i.e. not comparable between species from both hemispheres.

Terminal node	Scaled probability-of-origin			Chlorophyll- <i>a</i>		
	Mean ± SD	50 %	95 %	Mean ± SD	50 %	95 %
2	1.85 ± 0.38	-0.17	2.60	1.33 ± 4.23	0.24	1.34
3	1.99 ± 0.64	0.33	2.82			

Table S2.3 Mean ± SD of the scaled probability-of-origin values per marine eco-realm per terminal CIT node for the European storm-petrel including outliers. Marine eco-realms were defined in Spalding et al. (2007). Mean scaled probability-of-origin values were compared to the respective 50 % and 95 % scaled probability-of-origin quantiles per terminal CIT node per species (Table S2.2). Mean scaled probability-of-origin values > 50 % and < 95 % quantiles of the corresponding terminal CIT node are *italicised* and mean scaled probability-of-origin values > 95 % quantile of the corresponding terminal CIT node are **bolded**. See also Fig. S2.2 for scaled probability-of-origin distributions. Note: the scaled probability-of-origin values are relative.

Eco-realm	Terminal node	
	2	3
Arctic	-2.02 ± 0.29	-2.02 ± 1.06
Central Indo-Pacific	NA ± NA	NA ± NA
Eastern Indo-Pacific	NA ± NA	NA ± NA
Southern Ocean	-1.61 ± 0.24	-1.70 ± 0.29
Temperate Australasia	NA ± NA	NA ± NA
Temperate Northern Atlantic	<i>0.30 ± 1.36</i>	0.18 ± 0.95
Temperate Northern Pacific	NA ± NA	NA ± NA

Temperate South America	-0.17 ± 0.78	0.33 ± 1.24
Temperate Southern Africa	1.61 ± 0.40	2.93 ± 0.37
Tropical Atlantic	2.17 ± 0.51	1.65 ± 0.82
Tropical Eastern Pacific	NA \pm NA	NA \pm NA
Western Indo-Pacific	NA \pm NA	NA \pm NA

References

ebird.com, 2020. eBird Basic Dataset May 2020.

Observation.org, 2020. Stichting Observation International and local partners.
<https://www.observation.org>

Spalding, M.D., Fox, H.E., Allen, G.R., Davidson, N., Ferdaña, Z.A., Finlayson, M., Halpern, B.S., Jorge, M.A., Lombana, A., Lourie, S.A., Martin, K.D., McManus, E., Molnar, J., Recchia, C.A., Robertson, J., 2007. Marine ecoregions of the world: A bioregionalization of coastal and shelf areas. *Bioscience* 57, 573–583.
<https://doi.org/10.1641/B570707>

6. Other publications in the project

1. Pacyna, A.D., Jakubas, D., **Ausems, A.N.M.A.**, Frankowski, M., Polkowska, Ż., Wojczulanis-Jakubas, K. 2019 Storm petrels as indicators of pelagic seabird exposure to chemical elements in the Antarctic marine ecosystem, *Science of the Total Environment*, 692: 382—392. <https://doi.org/10.1016/j.scitotenv.2019.07.137>



Storm petrels as indicators of pelagic seabird exposure to chemical elements in the Antarctic marine ecosystem

Aneta Dorota Pacyna^{a,*}, Dariusz Jakubas^b, Anne N.M.A. Ausems^b, Marcin Frankowski^c,
Żaneta Polkowska^{a,*}, Katarzyna Wojczulanis-Jakubas^b

^a Gdańsk University of Technology, Faculty of Chemistry, Department of Analytical Chemistry, Gdańsk, Poland

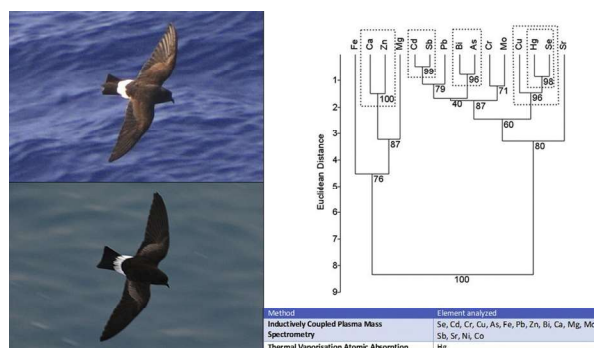
^b University of Gdańsk, Faculty of Biology, Department of Vertebrate Ecology and Zoology, Gdańsk, Poland

^c Adam Mickiewicz University Poznań, Faculty of Chemistry, Poznań, Poland

HIGHLIGHTS

- We examined 17 element levels in adults and chicks feathers of two storm petrel species.
- We found interspecies differences, between black-bellied and Wilson's storm petrel.
- Hg accumulation in black-bellied storm petrel could be classified as intermediate.
- The contaminant profile was different for adults and young.
- There was also evidence on maternal transfer of Hg in both species.

GRAPHICAL ABSTRACT



ARTICLE INFO

Article history:

Received 15 March 2019

Received in revised form 26 June 2019

Accepted 9 July 2019

Available online 10 July 2019

Editor: Daniel Wunderlin

Keywords:

Contamination

Feather

Toxic metals

ICP-MS

Mercury

Procellariiformes

ABSTRACT

Data on trace element bioavailability in the south-polar marine ecosystem is still scarce, compared to that relating to temperate zones. Seabirds can be used as indicators of ecosystem health and sentinels of environmental pollution, constituting a link between marine and terrestrial environments. Here, we analysed the concentration of 17 elements (with special emphasis on mercury, Hg) in feathers of adults and chicks of two pelagic seabirds – the Wilson's storm petrel *Oceanites oceanicus* and the black-bellied storm petrel *Fregetta tropica* – breeding sympatrically in the maritime Antarctic. Since adult feathers are formed during the non-breeding period away from the breeding grounds, but down and body feathers of chicks grow at the breeding sites, we were able to evaluate the birds' exposure to contaminants at various stages of their annual life cycle and in various marine zones. We found that of the two studied species, adult black-bellied storm petrels had significantly higher mercury, selenium and copper levels (5.47 ± 1.61 ; 5.19 ± 1.18 ; $8.20 \pm 0.56 \mu\text{g g}^{-1}$ dw, respectively) than Wilson's storm petrels (2.38 ± 1.47 ; 1.81 ± 0.98 ; $2.52 \pm 2.35 \mu\text{g g}^{-1}$ dw, respectively). We found that Wilson's storm petrel chicks had a significantly different contaminant profile than adults. Arsenic, bismuth and antimony were detected exclusively in the chick feathers, and the Se:Hg molar ratio was higher in chicks than in adults. Our study also suggests considerable maternal transfer of Hg (to down feathers) in both species. As global contaminant emissions are expected to increase, birds inhabiting remote areas with sparse anthropogenic pollution can indicate the temporal trends in global contamination.

© 2019 Elsevier B.V. All rights reserved.

* Corresponding authors.

E-mail addresses: an.pacyna90@gmail.com (A.D. Pacyna), zanpolko@pg.edu.pl (Ż. Polkowska).

2. Michielsen, R.J., **Ausems, A.N.M.A.**, Jakubas, D., Pełlicki, M., Plenzler, J., Shamoun-Branes, J., Wojczulanis-Jakubas, K. 2019 Nest characteristics determine nest microclimate and affect breeding output in an Antarctic seabird, the Wilson's storm-petrel, PLoS ONE 14(6): e0217708. <https://doi.org/10.1371/journal.pone.0217708>

RESEARCH ARTICLE

Nest characteristics determine nest microclimate and affect breeding output in an Antarctic seabird, the Wilson's storm-petrel

Rosanne J. Michielsen^{1,2*}, Anne N. M. A. Ausems², Dariusz Jakubas², Michał Pełlicki³, Joanna Plenzler⁴, Judy Shamoun-Baranes¹, Katarzyna Wojczulanis-Jakubas²

1 Institute for Biodiversity and Ecosystem Dynamics, University of Amsterdam, Amsterdam, The Netherlands, **2** Department of Vertebrate Ecology and Zoology, University of Gdańsk, Gdańsk, Poland, **3** Centro de Estudios Científicos, Valdivia, Chile, **4** Institute of Biochemistry and Biophysics, Polish Academy of Sciences, Warsaw, Poland

* r.j.michielsen@gmail.com



OPEN ACCESS

Citation: Michielsen RJ, Ausems ANMA, Jakubas D, Pełlicki M, Plenzler J, Shamoun-Baranes J, et al. (2019) Nest characteristics determine nest microclimate and affect breeding output in an Antarctic seabird, the Wilson's storm-petrel. PLoS ONE 14(6): e0217708. <https://doi.org/10.1371/journal.pone.0217708>

Editor: Brian G. Palestis, Wagner College, UNITED STATES

Received: February 13, 2019

Accepted: May 16, 2019

Published: June 13, 2019

Copyright: © 2019 Michielsen et al. This is an open access article distributed under the terms of the [Creative Commons Attribution License](https://creativecommons.org/licenses/by/4.0/), which permits unrestricted use, distribution, and reproduction in any medium, provided the original author and source are credited.

Data Availability Statement: All relevant data are within the manuscript and Supporting Information files.

Funding: DJ, KWJ, AA received funding from 2015/19/B/NZ8/01981, National Science Centre, Poland, <https://www.ncn.gov.pl/?language=en>. MP received funding from Centers of Excellence Base Financing Program, Comisión Nacional de Investigación Científica y Tecnológica (CONICYT-Chile), <https://www.conicyt.cl/RM> received funding

Abstract

The importance of nest characteristics for birds breeding in the extreme climate conditions of polar regions, has been greatly understudied. Nest parameters, like nest orientation, exposure and insulation, could strongly influence microclimate and protection against precipitation of the nest, thereby affecting breeding success. A burrow nesting seabird, the Wilson's storm-petrel (*Oceanites oceanicus*) is an excellent model species to investigate the importance of nest characteristics, as it is the smallest endotherm breeding in the Antarctic. Here, we investigated the effects of nest parameters such as internal nest dimensions, nest micro-topography and thermal properties of the nest burrow and the influence of weather conditions on breeding output, measured as hatching success, chick survival, and chick growth. We collected data during the austral summers of 2017 and 2018, on King George Island, maritime Antarctica. Our results showed that the thermal microclimate of the nest burrow was significantly improved by a small entrance size, a low nest height, and insulation and tended to be enhanced by a low wind exposition index and an eastern nest site orientation. In addition, an eastern nest site orientation significantly reduced the chance of snow blocking. However, the relationships between nest characteristics and breeding output were complex and might be affected by other parameters like food availability and parental quality. The relation between chick growth and nest air temperature remained especially indistinct. Nevertheless, our results indicate that nest characteristics that enhance the thermal microclimate and reduce the risk of snow blocking favoured both hatching success and chick survival. Due to climate change in the Antarctic, snowfall is expected to increase in the future, which will likely enhance the importance of nest characteristics that determine snow blocking. Additionally, despite global warming, thermally favourable nest burrows will likely still be advantageous in the highly variable and challenging Antarctic climate.

7. Acknowledgements

Completing my Ph.D. with this dissertation, would never have been possible without the help and support of many people to whom I am eternally grateful. Firstly, I would like to thank my family; my father Jan-Willem, for teaching me my opinion matters and how to be assertive, my mother, Margo, for keeping me grounded and supporting me no matter what, and my sister, Carlijn, for being my personal cheerleader. Without their input I would either not have believed myself capable of pursuing a Ph.D., would have had a hard time listening to other opinions, or would not have realised the magnitude of the feat. I am grateful for the friends I made along the way, and the ones I already had, for their support, but also their distractions whenever needed showing me there is more besides work and keeping me sane. Annelies, Floor and Patricia stayed virtually by my side, showing me friendships can last even across borders, decades and careers. Ania Z made me feel welcome in Poland and often helped me overcome several of the challenges I faced living in this foreign country. I would like to acknowledge C.J. Kees Camphuysen, not only for handing me the application for this project, but more importantly for being the first supervisor to believe I should aim higher and not settle for anything. He made me fall in love with seabirds. For their hospitality and belief in me and our project, I am indebted to Jens-Kjeld Jensen and Marita Gulckett. Without them I would not have been able to find my way on the Faroe Islands. I am thankful to Rosanne, Rachel, Jessica, Kat and Jón for all the help I got during the fieldwork for this project, without them, I would not have been able to collect nearly as much data or had such a good time collecting it. I would like to thank Greg Skrzypek, my only co-author not based in Gdańsk, for generally responding fast and with useful feedback on our shared manuscripts. Our research group welcomed me into their midst, even though the language barrier sometimes made it difficult to fully understand each other. Lastly, but definitely not least, I would like to thank my supervisor and colleagues, Dariusz Jakubas and Katarzyna Wojczulanis-Jakubas. Firstly for taking me on as their student, but also for their continued support. They showed me very different ways of approaching research, from asking a thousand questions about everything and anything, to diving as deep as possible in one project (even if we sometimes got a little lost). Kasia saved my computer numerous times from defenestration whenever R was a little too gReat for me. Darek let me follow my own path but was always ready to help me find my way, not only within the project, but also by helping me navigate the bureaucracy of the University and the Polish government, or by helping me find or translate anything else I might need.